Diet and Aging Influence the Dynamic of the Gut Microbiome and Health in Mice

Zhen Bao

A thesis submitted in fulfilment of the requirement for the degree of
Doctor of Philosophy

School of Life and Environmental Science
Faculty of Science
The University of Sydney
2024

Statement of originality

This is to certify that to the best of my knowledge, the content of this thesis is my own work. This thesis has not been submitted for any degree or other purposes.

I certify that the intellectual content of this thesis is the product of my own work and that all the assistance received in preparing this thesis and sources have been acknowledged.

Zhen Bao Date

Acknowledgements

This is it! I finally finished this! There have been ups and downs. I feel grateful for all the help I received over the past years.

First and foremost, I want to thank my parents. Thank you for supporting my decision to be a PhD candidate. I wouldn't have the courage to transfer to a different school and start over if it were not for you. I'm so lucky to have your unconditioned love and sponsor for the whole time.

Thank you so much to my supervisor, Andy, for giving me this opportunity and for guidance in getting me through my candidature. I learnt how to do a study design, and how to convey the message better via presentation and writing. Thank you for your understanding of my using English as a second language and for being patient with all my writing.

Thank you to all the Holmes and Shanahan lab members. Thank you to Alison for being an awesome neighbour and answering all my questions even during your maternity leave. Thank you to Erin, for helping me with my bioinformatics analysis and the study design. Thank you to Yubin and Mark for your codes to get me started with bioinformatics. Thank you to Reem, for all the well-documented protocols and arranging the training sessions. You prepared me well for my mice cull day. Knowing you were in the same situation made me feel not alone. Thank you to Miguel for teaching me how to do flow cytometry from scratch to analysis and picking up my anti-body staining panic call during your party time. Thank you to Marie and Louise for helping me prepare the single-cell suspension.

Thanks to the Simpson's lab for letting me join the project grant and longevity study. Thank you to the Alyssa and Sophie for helping in the animal house. Thank you to Teshi for introducing me to animal work and teaching me how to do one of the most important techniques for my study, faecal collection. Thank you to Saiful for helping me with the mice cull with last-minute notice. Thank you to Amanda, for helping me with my animal ethics. And, there are not enough words to express my gratitude to Tamara. You helped me in all aspects of my study. Without your help, I would not have been able to complete my animal study, especially the mice cull. Thank you for all the extra training sessions for my animal-handling skills. Thank you for always being patient with all my questions.

Thank you to my friends Sally and Miumiu. Sally, I first met you when we both transferring and about to start our PhD in CPC. I'm glad that we've been through this journey together. Thank you for the company and wish you all the best for the future. Thank you to Miumiu for delivering all the food and keeping me company in the lab. Nice food always made me feel better on a fully packed day.

Thank you to the Beauty Chef for the generous donation to support me as a researcher. This research reported in this thesis was supported by the award of a Research Training Program scholarship to the PhD Candidate.

Thank you to the University of Sydney facilities that contributed to this thesis: Joshua Hawkey, the Germ-free facility and the Laboratory Animal Services at the Charles Perkins Centre for animal services; Dr Georgia Teasdale-Twyford, Dr Shaun Miller and the Animal Welfare Veterinarian for training and vet advise; the Sydney Informatic Hub for providing bioinformatic training and high-performance computing resources, Artemis; the Sydney Imaging at Charles Perkins Centre for animal imaging facilities; the Sydney Cytometry at Charles Perkins Centre for flow cytometry facilities.

Finally, I would like to thank all the mice that were sacrificed in the experiments, making this thesis possible. R.I.P.

Abstract

Increasing in the aged population and age-related diseases had become an issue in Australia. Promoting healthy aging delays the onset of age-related diseases, thus improving the quality of life and reducing healthcare costs. Diet profoundly impacts animals' metabolic health and life span through mechanisms mediated by the gut microbiota. Diets that are known to promote longevity were associated with facilitating fermentative microbes in the gut and reducing systemic inflammation of the host. The "tipping point" for age-related decline is closely related to chronic inflammation and immunity. This "inflammaging" and "immuno-senescence" can only be understood by considering diet, and microbiome in conjunction with immuno-metabolic health. However, aging studies about gut microbiome often overlook dietary effects. Meanwhile, the commonly used cross-sectional settings are limited by microbiome's individualism when comparing old to young cohorts. In this thesis, I aimed to investigate the diet, microbiome and host interactional impact on immune-senescence.

This thesis incorporates material from a large cohort of cross-sectional animal models, a life-long longitudinal animal model and a small cohort gnotobiotic mice model to examine the interactions among diet, gut microbiome and host physiological outcomes. Diet was simplified into three macronutrient categories, carbohydrate, protein and fat. Previous studies demonstrated that dietary macronutrient compositions and eating behaviour had an impact on the mice's longevity and gut microbial composition. Therefore, I tested the hypothesis that diet macronutrient composition together with energy intake and microbiome change can modulate the rate of progression to Immuno-senescence. I used a geometric framework to systematically investigate average microbiota status and individual gut microbial behaviours under different nutrient environments during aging. Mechanistic linkage of age-related interactions among diet, microbiome and host was evaluated via the gnotobiotic model.

The common finding across these studies was that aging did have an impact on gut microbial composition. I identified two microbial types, type I level, 2 was enriched with *Bacterodiota* and *Verrucomicrobiota (Akkermansia)* while type II was high in *Firmicutes* and *Actinobacteriota*. Both microbial types were associated with dietary macronutrient intake, with type I associated with fat intake and type II correlated with carbohydrate intake. At the global community level, age-related microbial type shift from type II to type I was observed with

different rates under different nutrient environments. Within the individual distinct microbial state transitions were observed with varied onset ages subject to diet. Delaying the microbial state transition and microbial type drift might keep the health state of the microbiome and prolong the lifespan. Transferring aged gut microbiome to young germ-free mice microbiome associated aging phenotype. However, the age's impact was marginal compared to the diet, where the food component had the largest impact followed by the macronutrient composition. Altering diet in the recipient mice also showed changes in microbial composition compared to the donor mice.

Overall, my research presented the possibility of dietary intervention in slowing/reducing age-related decline and promoting healthy aging.

Table of Contents

List of Figures

List of Tables

1 Gut microbiome, immune response and aging (literature review)

1.1 Introduction

Population aging has been becoming an issue in developed countries. Australia has 16% of its population aged 65 or older. And, it was estimated that by 2066, the aged population will increase by another 4.7% (Health and Welfare 2021). Aged people are more susceptible to certain diseases, like COVID-19, cardiovascular disease, Alzheimer, impaired vision and sarcopenia. More than 80% of aged people (65 and above) suffered from at least 1 long-term health disorder, and also have a higher hospital administration rate compared to younger generations (Statistics 2017, Statistics 2018). At least 50% of the aged population were also reported to have mild to severe disabilities and need assistance with daily activities. (Statistics 2017, Statistics 2018) Consequently, these health conditions significantly impact the functional independence and well-being of older individuals. Moreover, it puts pressure on the healthcare system and the national budgeting. Given the challenge, there is a need for developing effective interventions to promote "healthy aging", thus improving the quality of life and reducing the health care costs.

Aging can be broadly separated into primary and secondary aging (Anstey, Stankov et al. 1993, Holloszy 2000) (Figure 1-1). Primary aging involves the degeneration of cell and organ, thus the decline of the functional system. This impacts the maximum lifespan of a healthy individual. Secondary aging, on the other hand, is independent from genetic changes and is affected by extrinsic factors, which are associated with average lifespan (Anstey, Stankov et al. 1993). Illness and disease are the primary factors that impact the secondary aging, causing body function declines like physical ability, frailty and recognition (Anstey, Stankov et al. 1993). Promoting healthy aging is not to extend the maximum lifespan. Rather, it is to delay/stop the development of diseases, thus to largely maintain the functionality of an individual and prolonging the average lifespan of the population. Most importantly, to improve the quality of life.

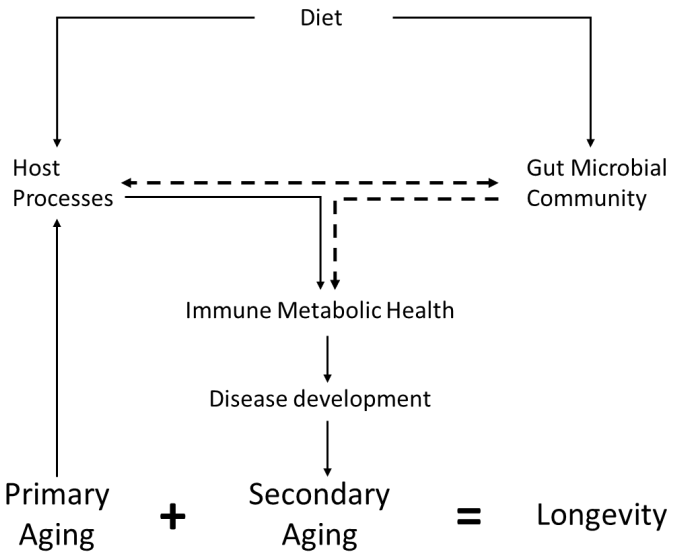

Figure 1-1. Longevity is affected by the interaction among host, gut microbiome and diet. The solid line indicates the impact caused by host and nutritional signals; the dash line indicates the microbial signals.

Currently, we are also experiencing an epidemic of nutrient-related metabolic chronic diseases like obesity, type 2 diabetes, mental disorders etc. More than 60% of Australian adults were obese, and the proportion was even higher in older adults (78%) (Health and Welfare 2023). Obesity causes more health complications which affects the physical activity and the longevity of the elderly (Amarya, Singh et al. 2014). Therefore, preventing metabolic diseases can effectively reduce the risk of related illnesses and slow down secondary aging, thereby promoting healthy aging in a greater population (Figure 1-1). The development of metabolic diseases was closely linked to the interactions among host, dietary intake and gut microbiome (Turnbaugh, Ley et al. 2006, Fan and Pedersen 2021, Wali, Milner et al. 2021). Thus, interventions have been mainly targeted at diet and gut microbiome to improve overall health and well-being. However, due to the high individualism, outcomes varied (Wali, Milner et al. 2021). Thus, it is becoming increasingly important to understand how diet interacts with the microbiome. A better understanding of how aberrant interactions contribute to aging and biological function will aid in developing universally applicable diet- and microbiome-based interventions.

1.2 Human are a holobiont

Human are a holobiont (Bordenstein and Theis 2015). It is a biological unit of the host and the surrounding environment. The holobiont contains broadly two biological component categories, the human cells and the microbial cells. This concept challenges traditional views of individuality and organismal boundaries, highlighting the interconnection between hosts and

their microbiota (Bordenstein and Theis 2015). Altogether, the human body and the gut microbiome share a symbiotic relationship, collectively overseeing health regulation upon encountering environment stimuli.

1.2.1 The human component of the holobiont

The physical compartment of the human holobiont is a complex functional system that is built from a collection of differentiated cells. These cells share the same genome, but acquire change through developmental differentiation, genetic mutation and epigenetic modification, which result in different functional roles and, ultimately the human organism. To sustain the function of this multicellular organism and to respond to extrinsic environmental cues, it is essential to have intercellular communication networks that coordinate different biological processes.

Adaptive responses are complex but can be broadly categorized into three levels, network control (primary), topological control (secondary) and cell dynamic toning (tertiary) (Figure 1-2). The primary mechanism involves the inherent capability encoded in the genome to modify transcriptional processes or modulate protein activity. Upon encountering environmental stimuli, it binds to a specific receptor, thereby initiating a signalling cascade within the cellular network (Rasheed and Rayner 2021). This primary mechanism is complex and vital for all types of cells. The secondary mechanism is determined by the topological organization of cellular components, which influences the primary responses. This level involves epigenetic modifications to the DNA structure, such as methylation, or modifications to DNA-interacting proteins, like histone acetylation, which serve to restrict the access of transcription factors (Issa 2003, Agrawal, Tay et al. 2010). This secondary mechanism is particularly important in animal cells and serves as a foundation for cellular differentiation. The tertiary mechanism is dictated by the composition of cells within a given system, resulting in a constraint on the response toning. This mechanism happens within certain mammalian systems, notably the lymphoid compartment, changes in cell populations play a crucial role in modulating immune tone (Janeway, Travers et al. 2001). The three levels of adaptive are in a one-way direction and happen in an accumulative manner.

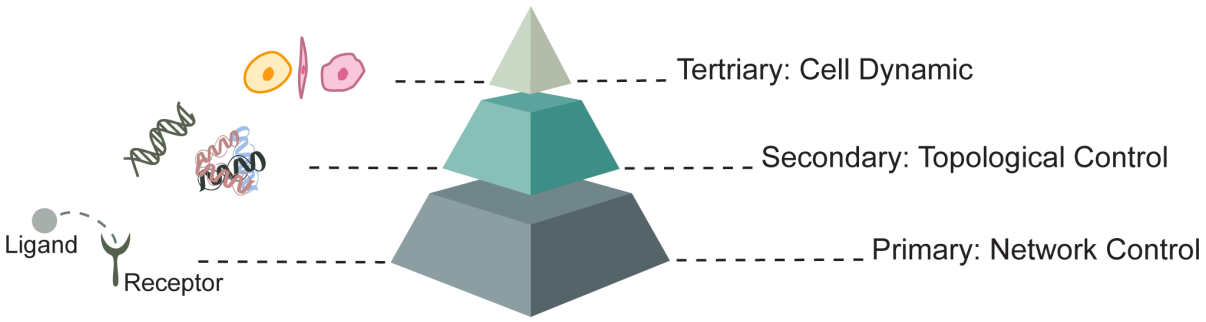

Figure 1-2. The animal compartment responds to environmental stimuli at four different levels.

1.2.2 The gut microbiome component of the holobiont

Unlike the cell component, microbe cells are mainly bacterial and consist of hundreds of different species- each with a unique 'species genome' and each occupying a distinct ecological niche within the human body (Turnbaugh, Ley et al. 2007). The microbial component is acquired postnatal and initially from the mother during the delivery (Gomez de Agüero, Ganal-Vonarburg et al. 2016, Ferretti, Pasolli et al. 2018). Then, it is differentiated by adapting to and selecting by the local body site, forming unique communities (Gomez de Agüero, Ganal-Vonarburg et al. 2016). By far, the gut microbiome is the largest microbial compartment, which can be defined as the microbial community occupying the intestinal tract between pyloric and anal sphincters. What makes the gut microbiome unique is that its initial colonization and assembly is influenced not only by the specific body site but also by the types of food a person consumes.

Since the gastrointestinal tract is the main site for food digestion, diet plays a crucial role as a selective factor in determining the composition and function of the gut microbiome (Figure 1-3). After the birth, the gut microbiome is developed to acclimate to the intestine environment and the nutrients provided by the milk (Koenig, Spor et al. 2011, Bäckhed, Roswall et al. 2015). Thus, the baby's microbial composition was affected by the nutrient content of milk, breastfeeding vs baby formula and brand of baby formula (Vatanen, Jabbar et al. 2022). During the initial 3 years, the gut microbiome of a baby shifted dramatically, changing from lactate utilization dominant species to carbohydrate metabolism and vitamin biosynthesis species, with an increase in Bacteroidetes abundance (Koenig, Spor et al. 2011, Yatsunenko, Rey et al. 2012, Bäckhed, Roswall et al. 2015, Gomez de Agüero, Ganal-Vonarburg et al. 2016). This was associated with the diet changes gradually from milk to solid table food (Bäckhed, Roswall et al. 2015, Janiak, Montague et al. 2021). With the introduction of plant-based food (plant polysaccharide degradation), microbial functional succession favoring the growth of complex-

carbohydrate-degrading microbes (Shafquat, Joice et al. 2014). Moreover, from toddler to adult, there is an increase in energy and nutrient consumption, thus requiring more energy harvesting bacteria (Faizan and Rouster 2020). One of the signature of transition from infant microbiome to adult like microbiome was the increasing of butyrate production bacteria, with butyrate being a preferred energy source of the intestine epithelial cell (Roswall, Olsson et al. 2021). Overall, by the age of about 3, the gut microbiome reached a stable state and close to that composition of adults (Koenig, Spor et al. 2011, Yatsunenko, Rey et al. 2012). Due to the different solid food intake after weaning, differences in microbial composition, thus, observed among different species (Koenig, Spor et al. 2011, Bäckhed, Roswall et al. 2015, Janiak, Montague et al. 2021) From this point onward, the development of the gut microbial community is complete.

The established community is relatively stable and resilient. It was able to recover its composition after rapid diet change or antibiotic deletion treatment. (Thaiss, Itav et al. 2016, Wang, Tang et al. 2022) Despite its composition being consistent, the relative abundance of microbes fluctuates from day to day and at different times of the day (Thaiss, Zeevi et al. 2014, Johnson, Vangay et al. 2019, Risely, Wilhelm et al. 2021, Wang, Tang et al. 2022). These changes are closely related to the body's activities, including diet alteration, food digestion, gut motility, immune activity etc. For adults, the nutrient requirements are stable. However, consuming different diets from time to time, and changing dieting frequencies can affect the microbial activities. Although the microbial response to diet is rapid (Wu, Chen et al. 2011, David, Maurice et al. 2014), the diet has a prolonged effect on the microbiome (Thaiss, Itav et al. 2016). Therefore, dietary intake may exhibit cumulative impacts on microbial structure.

The established microbial community remains stable until old age, when changes in composition are observed. This will be discussed in a later section.

1.2.3 Symbiotic interactions between the two components

Considering the holobiont is a unified entity, the cell compartment, the microbial compartment and the interactions between them, altogether are essential to maintain the overall health and well-being. The development of the gut microbiome and the immune system occurs in parallel, starting at birth and continuing throughout an individual's life (Figure 1-3). This process establishes a complex, symbiotic relationship that is vital for sustaining health.

Infants were born with immature immune system and underdeveloped microbiome. Microbiome colonization is generally believed initially happen during delivery, during which the microbiome from the mother was passed to the baby (Gomez de Agüero, Ganal-Vonarburg et al. 2016, Ferretti, Pasolli et al. 2018). Mothers can also pass immunoglobulins like SIgA to the babies via breastfeeding together with the microbes (Suzuki, Meek et al. 2004, Guo, Ren et al. 2021, Rio-Aige, Azagra-Boronat et al. 2021). These immunoglobulins can select for microbes for colonization, thus help to shape the gut microbiome and the immune system (Guo, Ren et al. 2021). Microbial colonization also facilitates the immune system development and immune activities (Huang, Zhu et al. 2013). Microbial assembly can produce cytokines like transforming growth factor-β (TGF-β) to suppress pathogens and induce regulatory T-cell proliferation, providing early protection to the baby (Rautava and Isolauri 2002).

Moreover, both breast milk and baby formula contain large amounts of oligosaccharides, which facilitate the growth of microbes (Ghisolfi 2003, Çavdar, Papich et al. 2019). In return, the microbe produces a series of small molecules like short-chain fatty acids, which provide energy and support the immune response (Priyadarshini, Kotlo et al. 2018, Hou, Huang et al. 2023). Introducing solid food, plant-based food in particular, results in more diversified microbial-derived metabolites, further enhancing the gut microbiota's composition and promoting overall digestive health.

The relationship between the matured gut microbiome and the immune response is often studied in the germ-free (GF) mice model (Hrncir, Stepankova et al. 2008, Hapfelmeier, Lawson et al. 2010, Fransen, Van Beek et al. 2017, Kundu, Lee et al. 2019). Germ-free mice were mice that lack of any form of microbiome. Comparing to the conventional mice, the GF mice were having an immature immune system with impaired T cell regulation and fewer B cells for immune response (Ohwaki, Yasutake et al. 1977, Östman, Rask et al. 2006, Hrncir, Stepankova et al. 2008, Hapfelmeier, Lawson et al. 2010). By transferring the gut microbiome to the germ free mice, enables us to understand process of the microbial colonization, microbial primary succession and secondary succession with additional interventions like altering diet. By comparing the changes in immune response, allowing to study the microbial derived immune response and phenotypical changes. Therefore, understand how the microbiome effects the immune activities and vice versa.

However, there are limitations. First of all, the viability of the bacteria cells that for colonization was low. Fecal matter transplant was the most widely used method for conventionalizing the germ-free mice. As the gut microbes are primarily anaerobic, inevitably, some of these bacteria die during fecal collection and fecal slurry preparation when encounter oxygen. Even when samples were processed under strict anaerobic conditions, the death rate was still as high as 50% (Papanicolas, Choo et al. 2019). This means that these fecal transplant studies did not transfer the whole microbiome to the recipients to start with. Meanwhile, microbes that were survived may not necessarily colonize the new gut environment, especially for the humanized germ-free mice, who received gut microbiome from human. Differences between human and mice physiology may result in different microbes to colonize and differentiate. Thus, the correlation results were strongly biased towards certain species. However, as the fecal transplant was still able to transfer the main microbes to the recipient mice (Wang, Zhang et al. 2022), making it a good model for study.

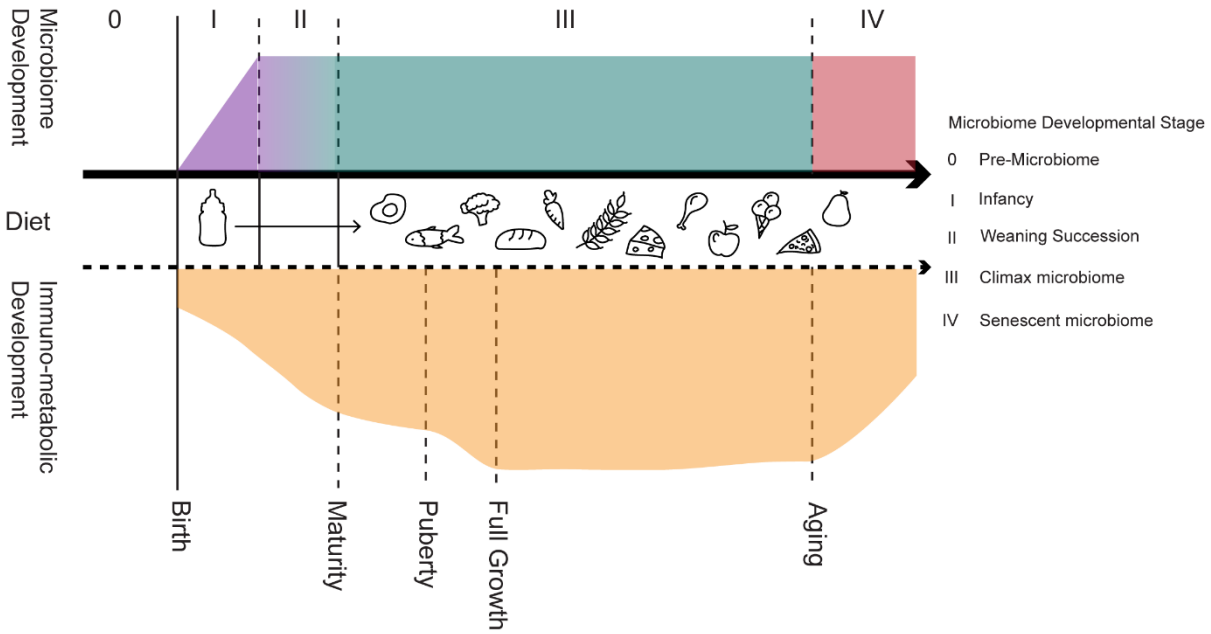

Figure 1-3. The development of the immune system and the gut microbiome happen head to head and are associated with diet.
Purple: gut microbiome development; Green: matured gut microbiome; Red: aged gut microbiome; Orange: development of immune system

1.3 Dimension of diet and the impact of diet

To ensure proper growth and maintenance, the holobiont requires nutrients and energy, which are primarily obtained from the food. The terms “food”, “diet” and nutrients were often used as synonyms. However, they have distinct meanings. Food is the source of different nutrients and energy. The consumption of a variety of foods in different amounts and at various times

becomes a diet. Thus, diet refers to the parts that reach the gut. After reaching the gut, majority of the food components are digested and absorbed in small intestine, which become nutrients and used by the cells. The part that resists to digestion, like dietary fibre, passes to the large intestine. Microbial fermentation can also turn them into nutrients used by the host and microbes (Figure 1-4D). Therefore, what is supplied in the food is not equivalent to what is used by the host and microbes.

To better understand the effect of diet on the holobiont, it can be simplified into 3 macronutrients categories, carbohydrate, protein and fat (Figure 1-4A and D). Different foods in a diet supply varying amounts of macronutrients, resulting in differences in overall energy intake. These macronutrients can come from both animal and plant-based sources, except for carbohydrates, which are solely derived from plant-based foods. Together with macronutrients, other nutrients are also consumed from food. Therefore, the quality of macronutrients varies depending on the food source. Considering taking carbohydrate and fat from a donut vs a nut. Unlike the latter, the former contains barely any other vitamins and minerals, thus has a lower nutrient quality. Moreover, food can contain dietary fibres which are resistant to digestion, resulting in different amounts of energy being absorbed from the same quantity of food. This indicates that the food source also determines the energy density of the nutrient and the total energy intake. Taken together, the study of dietary effect essentially becomes the study of the macronutrient distribution, caloric intake and nutrient quality.

As the nutrients are not stand-alone factors, modern nutritional studies use a geometric framework approach (Simpson and Raubenheimer 1997). Geometric framework, is one of such tools, which maps macronutrient ratio, energy and food intake into the same space (Figure 1-4 B). The physiological trait of interest, then can be added as a response surface on the map. In this way, we can easily see how this particular trait varies with different macronutrient ratios. The geometric framework can be used to find the optimal food composition for the given trait, and better, to predict the physical outcomes individually. (Solon-Biet, McMahon et al. 2014, Holmes, Chew et al. 2017, Wali, Milner et al. 2021)

However, the nutritional geometry does not take dietary fiber and gut microbiome into account (Figure 1-4D). Dietary fiber is resistant to digestion in the small intestine, and usually does not include in calculating the energy intake as part of the diet. However, when passing to the large intestine, the gut microbes, are able to break down these complex compounds and harvest

energy from them (Bäckhed, Ding et al. 2004). It encountered up to 10% of the energy requirement of human (McNeil 1984). Moreover, the gut microbes are able to provide extra nutrients and bio-active molecules for the host and supplement nutrients that were deficient in the diet (Koay, Wali et al. 2019, Koay, Chen et al. 2021).

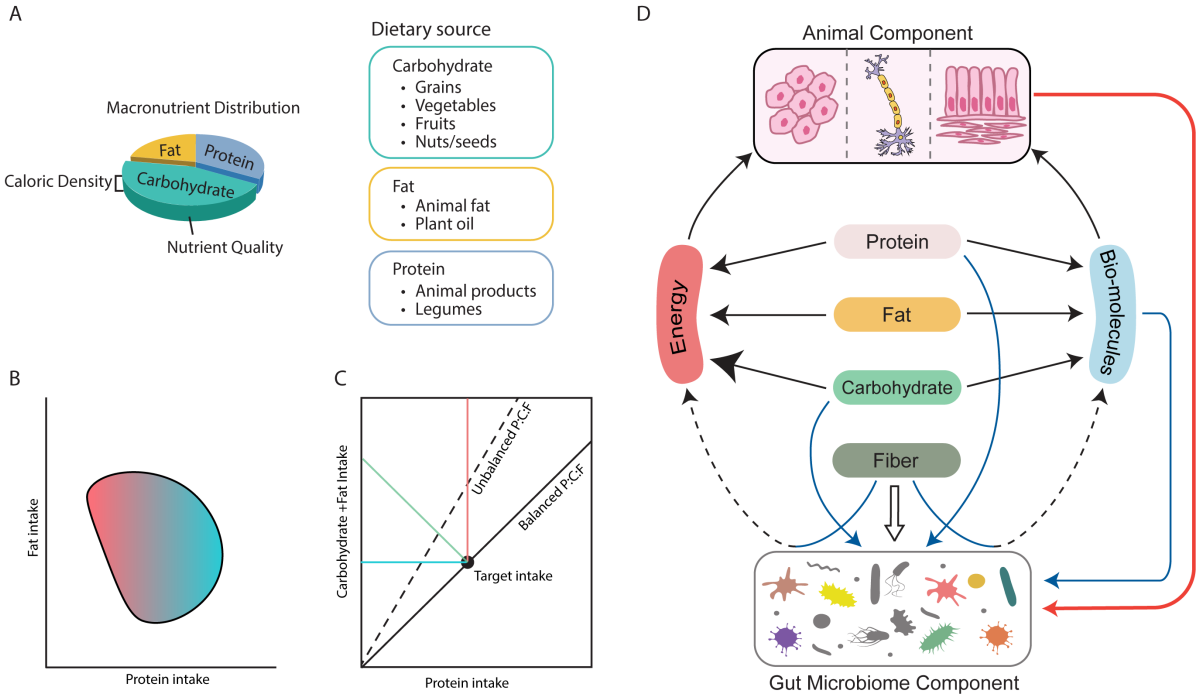

Figure 1-4. Diet influences the human holobiont.
A. Diet can be simplified into three macronutrients, carbohydrate, protein and fat. Different dietary sources contribute to varied macronutrient ratios, caloric density and nutrient quality in diet. B) Geometric framework maps multiple dietary factors into the same space. The area in the middle is a combination of diets with different macronutrient compositions. The color indicates the energy density, with red being high and blue being low. C) Geometric framework can be used to analyse the nutrient requirement for the host. Unbalanced diets are indicated by red (protein leverage situation), green (satisfied with energy intake only) and blue line (satisfied with nutrient intake only). D) Dietary nutrient intake for the host and the microbes. The black arrow is the diet-derived molecules directly used by the host. The blue arrow is the diet-derived molecules directly used by the microbes. Dash lines are the microbial derived molecular used by the host.

1.3.1 Nutrient requirement for the cell component

Having balanced nutrients and energy are essential for health and well-being. The host is capable of self-regulating the food intake when the nutrient requirement is not satisfied Figure 1-4C) (Simpson and Raubenheimer 2005, Raubenheimer and Simpson 2016). Each individual has a target intake for macronutrients and energy. An unbalanced diet can result in a protein leverage situation (red line), where people tend to consume more food to meet the desirable protein intake. Consequently, they overconsume other nutrients and energy. Alternatively, they stay in a tipping balance (green line) to meet the energy intake requirement or in a non-protein leverage (blue line) situation to meet the carbon and fat requirement.

1.3.2 Nutrient requirements for the gut microbiome

Like the host, the microbes also require nutrients for their daily activities, which include obtaining energy, maintaining redox balance as well as gathering for carbon and nitrogen. The microbes have access to nutrients from 3 sources, the undigested food passing from the small intestine, the end products from microbial active and the host secretion (Holmes, Chew et al. 2017).

Diet is a preferred nutrient source for the microbes. When enough of it can be obtained from the diet, diet-forging microbes thrive (Holmes, Chew et al. 2017). With a balanced macronutrient ratio, increasing energy harvesting was observed with ob/ob mice when they were having excessive food intake (Turnbaugh, Ley et al. 2006). When having an unbalanced diet, in particular with the ratio between protein and carbohydrate, the microbial response is affected by whoever gets limited (Holmes, Chew et al. 2017). In this case, they will seek alternative nutrient sources, like the endogenous nitrogen waste and mucin layer. As microbes have a preference in obtaining endogenous carbon or nitrogen, limiting one of the nutrients drives the microbial community by selecting for specific phylum (Zeng, Xing et al. 2022). Significant changes are often observed between Bacteroides and Firmicutes. Thus the ratio between these two phylum was usually reported in nutrient studies (Turnbaugh, Ley et al. 2006, Magne, Gotteland et al. 2020). Fat, in contrast, was believed to have the least effect on the microbiome, but it can dilute the nutrient density when added into a diet. When supplied with a high fat diet, however, increased bile acid secretion was observed which select against bile-sensitive species (Sayin, Wahlström et al. 2013).

Moreover, as microbes live in a confined environment, they are inevitable to interact with each other. Despite competing for limited nutrients, they also cooperate to forge nutrients, like breaking down complex carbohydrate (Flint, Scott et al. 2012, Ostrem Loss, Thompson et al. 2023). Fermenting carbohydrate produces small molecules like short chain fatty acids and vitamins (Flint, Scott et al. 2012). Some of the readily fermented products were directly used by other microbes before feeding back to the host (Zeng, Xing et al. 2022, Beyhan and Yıldız 2023). Therefore, for parasite microbes, they gain nutrients and energy from the byproduct of other microbes.

1.4 The aging process

The aging process affects both the host and the gut microbiome (Figure 1-1). Aging can be affected by a series of different extrinsic factors like diet, lifestyle choices, the surrounding environment and diseases. These factors concurrently exert an impact on the gut microbiome. Consequently, an association arises between the gut microbiome and the aging process, establishing a reciprocal relationship between these two entities. From the perspective of my thesis, I will overlook at the disease factor and only consider the impact of diet on healthy aging.

1.4.1 Aging is associated with cell senescence and systematic inflammation

The host is a complex biological system. To maintain the functionality of this system, animals try to balance among survival, growth and repair damages. Daily activity and environmental cues lead to the production of free radicals, known as reactive oxygen species (ROS) (Liguori, Russo et al. 2018). Although the self-defence mechanism releases anti-oxidants to neutralize ROS, accumulation of ROS was found during aging (Liguori, Russo et al. 2018). Increasing in ROS causes damage to the cells and DNA (Liguori, Russo et al. 2018).

As animals have limited access to metabolic resources, with the increasing in the demand for repairing, there is a requirement for redirecting nutrient resources. According to the disposable soma theory, animals only do the bare minimum to maintain the overall functionality rather than fully repair the damage (Kirkwood 1977, Kirkwood and Holliday 1979). Prolonged cellular and DNA damage eventually leads to cell senescence. Cell apoptosis and T cell exhaustion marker, programmed cell death protein 1 (PD-1) and its receptor PD-L1, were found to increase in aged individuals (McClanahan, Riches et al. 2015, Onorati, Havas et al. 2022). Meanwhile, damage causes immune response immune, thus a low-grade systematic inflammation was observed in aged individuals, known as inflammaging (Franceschi, Garagnani et al. 2018). Increasing in activated T cells, B cells, macrophages and natural killing cells, were found in multiples organs in aged mice (McClanahan, Riches et al. 2015, Elyahu, Hekselman et al. 2019, Mogilenko, Shpynov et al. 2021) Inflammaging was associated with the gut microbiome and nutrient intake as a similarity in mechanism between the inflammaging and metabolic inflammation (Franceschi, Garagnani et al. 2018, Prattichizzo, De Nigris et al. 2018).

1.4.2 Age-related change in gut microbiome

Age-related research in microbiome faced many obstacles, particularly with humans. Inevitably, aged people often suffered from one or multiple diseases (Statistics 2017, Statistics 2018). Thus, they received varies medical treatments, which affected their microbial compositions (Leite, Pimentel et al. 2021). Medicine altered microbial composition was distinguished from the aged associated microbiome (Leite, Pimentel et al. 2021). Moreover, microbiome is highly personalized. Graphic differences, dietary history, ethnic background (diet culture background) and living environment can all affect the microbial composition (de la Cuesta-Zuluaga, Kelley et al. 2019, Zhang, Zhong et al. 2021). Even in the controlled lab setting, the gut microbiome is hypervariable among individuals (Langille, Meehan et al. 2014, Ke, Mitchell et al. 2021). Thus, it was not possible to separate the age related changed from all the other factors. It's also hard to compare the results across studies, as the results can sometimes even contradict to each other (addressed later).

However, there are still some common findings from both animal and human studies. All studies have shown that aged individuals had a distinguished gut microbial composition compared to young ones. Table 1-1 and Table 1-2 give a summary of how the aged microbial structures were different from the young ones. Overall, the aged gut microbiome tends to have more unique and rare species, with increased richness in the colon (Ke, Mitchell et al. 2021, Wilmanski, Diener et al. 2021, Wu, Muthyala et al. 2021). This was observed in both human and mice. Moreover, the uniqueness of the gut microbiome was also associated with the longevity in humans (Wilmanski, Diener et al. 2021, Wang, Qie et al. 2022).

The aged gut microbiome also showed distinctive characteristics. Comparing to young adults, the gut microbiome of aged individuals reduced its dynamic and resilience properties. Therefore, they were less likely to respond to the daily environment turbulence or recover from antibiotic microbial depletion (Kim, Moon et al. 2021, Wang, Tang et al. 2022). Moreover, the aged gut microbiome exhibited a proinflammatory phenotype, similar to obese people (Binyamin, Werbner et al. 2020). Transferring the old gut microbiome to germ-free mice, results in systematic inflammation in recipient mice (Fransen, Van Beek et al. 2017, Binyamin, Werbner et al. 2020, D'Amato, Di Cesare Mannelli et al. 2020, Parker, Romano et al. 2022). This indicates that the gut microbiome over an animal's lifetime, adapted to the proinflammatory environment due to aging.

Microbial function analysis shows that the aged gut microbes have changes in macronutrient utilization. It has shifted its focus from amino acid utilization to amino acid synthesis (Rampelli, Candela et al. 2013, Chen, Wang et al. 2022). Increasing in amino acid auxotrophic bacteria was associated with long-term microbial stability and higher diversity in healthy individuals. (Starke, Harris et al. 2023) Meanwhile, carbohydrate metabolism is increased, especially the monosaccharide (Langille, Meehan et al. 2014, You, Dadwal et al. 2022). Changing in the amount of hydrolyse congregate bile acid also indicated the fat metabolism was varied during aging (Qiu, Yu et al. 2022).

However, the age-related change of the specific microbes varies across studies, some even conflict with each other (Table 1-2). For example, *Prevotellaceae* was found to increase with aging in Langille, Meehan et al. (2014)'s study but decrease in Wu, Muthyala et al. (2021)'s study. This is due to the large inter-individual variations (Langille, Meehan et al. 2014, Ke, Mitchell et al. 2021, Wang, Qie et al. 2022). In particular, for the human studies, diets were not controlled across participants in different studies. Also, people in different areas tend to have different food choices and living environments, both have an impact on the microbiome. Even the difference in diet, with living in cared facility or not, can make a difference (Claesson, Jeffery et al. 2012). Therefore, conclusion from such human studies was limited, as the aging effects were masked by the dietary effects.

Furthermore, most studies used cross-sectional experimental setting. Such method was good to obtain tissue and blood samples for multi-omic analysis, particularly in animal studies. It was also early to include more study subjects to have meaning results. However, in cross-sectional studies, only one snapshot of the microbiome profile was taken at one-time point for each experimental group. Therefore, it is hard to differentiate age associated changes from individual variations. Longitudinal studies, in contrast, track microbial behaviour of the same individuals across different age periods. Such studies are necessary to understand the interactive relationship between the gut microbiome and aging biology as the induvial variance was kept the same. However, currently, not many longitudinal studies were available that systematically analyse the gut microbiome throughout an individual's lifetime. Yet, no study looked at the microbiome and diet interactions under such setting.

Table 1-1. Summary of aged gut microbiome characteristic and functional change.

Yong microbiome	Old microbiome
Characteristic: • Resilience • Dynamic	Characteristic: • Proinflammatory • Obesogenic
Functional: • Amino acid utilization	Functional: • Amino acid synthesis • Increasing carbohydrate metabolism (Mono-carbohydrate) • Altered fat metabolism

Table 1-2. Summary of aged gut microbiome compositional change.

	Species	Study type	Gender	Age	n	Characteristic of aged gut microbial composition	Diet
(Wilmanski, Diener et al. 2021)	Human	Cross-sectional	Both	18-98 yr	4,560	Number of species ↑ Bacteroidetes ↓	Uncontrolled diet
(Pang, Chen et al. 2023)	Human	Cross-sectional	Both	20-44yr, 45-65yr, 66-85yr, 90-99yr, 100-117yr	1,575	Number of species highest in 90-99yr Bacteroidetes ↓ (age >66 yr) Firmicutes highest in 66-85yr	Uncontrolled diet
(Langille, Meehan et al. 2014)	C57BL/6	Cross-sectional	Female	6-7mo, 19-20mo, 28-29mo	10	Prevotellaceae↑ Akkermansia, Porphyromonadaceae ↓	Lab diet (P/C/F=26/59/14)
(Wu, Muthyala et al. 2021)	C57BL/6	Cross-sectional	Male	3mo, 6mo, 18mo, 28mo	33	Number of species ↑ Preoteobacteria, Parabacterodies, Clostridiales ↑ Firmicutes/Bacteroidetes ↓ (Firmicutes ↓) Porphyromonadaceae, Prevotellaceae ↓	Lab diet (P/C/F=24/60/16)
(Ma, Hong et al. 2020)	C57BL/6	Cross-sectional	Both	3mo, 26mo	5-9 per group	Gender specific difference Male: Actinobacteria, Erysipelotrichaceae, Faecalibaculum, Ruminococcaceae, Bifidobacterium↓	Lab diet (unknown composition)

						Shannon index, Lachnospiraceae, Oscillibacter, Blautia ↑ Female: Firmicutes, Actinobacteria, Erysipelotrichaceae ↑ Shannon index, Proteobacteria, Desulfovibrio, Lachnospiraceae↓	
(Borsom, Conn et al. 2023)	B6129F2/J	Longitudinal study	Female	2mo – 13mo	31	Lactobacillus salvarius↓ Bacterodies acidifaciens↑	Lab diet (unknown composition)
(Nakanishi, Nozu et al. 2020) (pre-print)	C57BL/6	Longitudinal study	Male	<1mo -18mo	6	Number of species ↓ Allobaculum, Turicibacter↑ Lachnospiraceae, Ruminococcus , Clostridiales ↓	Lab diet (CA1, CLEA)

1.5 Potential mechanism to drive age-related microbial alternation

Although the gut microbiome of elderly individuals is commonly referred to as the "old" or "senescence" microbiome, the gut microbiome itself does not age as we grow older. Instead, it changes its community structures to accommodate the nutrient and physiology changes due to aging. Age related decline in body function alters the nutrient environment for the microbes and initiating microbial activities to adapt to the new environment. Adaption takes time and the change of the microbiome is a continuous process. However, most aging studies are cross-sectional, thus they were not able to capture this process. Such studies often directly comparing young and old individuals. The result can only demonstrate distinct differences between their microbiomes, which the latter was then referred to as the "old microbiome." Little was known if such “old microbiome” was just a snap shoot during the on-going adapting process. Or, it was the end results of after adaptation.

Multiple factors can effects the nutrient environment to the microbes. As people age, there was a natural reduction in appetite and decrease in the amount of food consumed on a regular basis (Zhu, Devine et al. 2010, Otsuka, Kato et al. 2016, Cox, Bowyer et al. 2021). This is due to the reduction in taste and smell sensitivity, and slowing in food empty rate (especially after big meals). (Roth 1979, Lamberts, Van den Beld et al. 1997, Morley 2001, Boyce and Shone 2006, Lehallier, Gate et al. 2019) As a result, older individuals may experience a diminished desire for food, leading to a decreased motivation to eat. Moreover, age-related alterations in the structure and function of the gastrointestinal tract can impact digestion and nutrient absorption. The thinning of the mucosal lining decreased blood flow to the intestines, and changes in the structure of intestinal villi can all contribute to nutrient deficiencies in the elderly (Dangin, Guillet et al. 2003, Milan, D’Souza et al. 2015, Moorefield, Andres et al. 2017, Tremblay, Côté et al. 2017, Sovran, Hugenholtz et al. 2019) Therefore, reducing in overall food, nutrient and energy intake was observed in aged individuals.

The reduction in nutrient availability over time caused microbes to modify their nutrient metabolism. From microbes’ point of view, this means less nutrients and energy can be obtained from the diet. Under a starvation mode urged them to increase energy harvesting. Therefore, the aged microbiome showed obesogenic characteristics (Binyamin, Werbner et al. 2020). A similar trend was also observed with an increase in *Firmicutes* at the expense of *Bacteroidetes* in aged individuals and obese people (Ley, Bäckhed et al. 2005, Turnbaugh, Ley et al. 2006). In the meantime, limited dietary nutrients forced microbes to seek for alternative

nutrient sources like the endogenous carbohydrate and nitrogen (Holmes, Chew et al. 2017). As a result, mucus layer degrading Therefore, reduced mucus layer thickness was found in old animals (Elderman, Sovran et al. 2017).

Due to the reduction in epithelial barrier integrity, microbial associated molecular patterns (MAMPs) are easier to pass through the epithelial barrier adding to age-related inflammation. (Elderman, Sovran et al. 2017, Parker, Romano et al. 2022) Meanwhile, during the inflammation response, pro-inflammation cytokines like IL-6 and TNFα were released altering the microbial population and metabolic pathways (Schirmer, Smeekens et al. 2016). Therefore, creating a cascade loop of inflammation response in aged individuals.

A healthy adult's gut microbiome has more than one stable state. The microbiome constantly shifts among different stable states to maintain the overall homeostasis of the gut environment (Chang, VanInsberghe et al. 2020). During aging, microbes experience long-term exposure to nutrient deficiency, hormone and immune cytokine shift due to systematic inflammation. Chronically stressed by the environmental cues, the microbiome gradually shifted from a healthy state to a disease state. However, no data so far suggests at what stage such a transition will happen and how this progress is affected by different environmental factors.

1.6 Research aims

In this thesis, my overall aim was to understand how diet macronutrient composition, dietary source and energy density influence the interaction among microbes, host system and physiology outcomes during aging. This study improves the understanding of personalized modulation of the gut microbiome contributes towards promoting health and healthy aging.

Aim 1: To identify if aging alters the average gut microbiota and individual gut microbiome stability.

My hypothesis is that the individual gut microbiome and overall gut microbiota of a population are impacted by aging and aging biological. I compared changes in gut microbial compositions of mice at 4 different age groups to see if there were differences in the compositions among these age groups (Chapter 3). In Chapter 4, I further examined the gut microbial behaviour over time by following individual mice through their lifespan. Furthermore, I studied how the gut microbial daily temporal stability changed over aging.

Aim 2: To evaluate the weight of different factors (food components, macronutrient compositions, energy density and gender) on average gut microbiota over aging.

I predict that food components, macronutrient composition, energy density, gender and age all have an impact on the gut microbiome. However, the impact levels were different among these factors. To test this, I compared the extent of microbial compositional change among these different factors in Chapter 3 and Chapter 4.

Aim 3: To understand the microbial composition evolutionary change during aging.

My hypothesis is that aging-induced functional decline alters the microbial nutrient availability and accessibility thus causing microbes to undergo evolutionary change. Therefore, I examined the microbial response towards 3 dietary macronutrients at 4 different time points (Chapter 3). I identified two microbial compositional types that were associated with dietary macronutrient intake and aging (Chapter 3 and Chapter 4). Furthermore, I examined the microbial behaviour of individual ASVs during aging under different nutrient environments (macronutrient composition, feeding behaviour and energy density) (Chapter 3 and Chapter 4).

Aim 4: To identify the potential mechanism of aging biology modulating the microbiome.

I hypothesise that age-related diseases are caused by the interaction of gut microbiome, dietary component and immune senescence during aging (Chapter 5). I characterized the aged phenotype specifically associated with aged gut microbiome under 3 different nutrient environments. I examined the effect of different nutrient and gut microbiome interactions on biological outcomes.

In order to address these aims, I engaged in 2 collaborative studies in which I performed the gut microbial analysis (Chapters 3-4); and designed one faecal matter transplant study (Chapter 5). These studies promote the understanding of dietary, microbial and host factors on immune-senescence and inform further research for potential interventions like faecal matter transplant and personalized nutrient therapy in improving elder health conditions.

2 General Materials and Methods

This chapter contains the general methods used for animal maintenance, fecal/caecal DNA extraction and microbial analysis. Variation and extra methods used are noted in each chapter separately.

2.1 Materials

The chemical and reagents used were molecular biology grade unless otherwise stated.

2.2 Methods

2.2.1 Animal maintenance

All mice were housed in the Laboratory Animal Services facilities at the Charles Perkins Centre (The University of Sydney, NSW, Australia), under conditions of 24-26^{o}C, 44-46% humidity, with 12hr light/ 12hr dark cycle settings. Food and water were provided to mice ad libitum, except for the caloric restriction mice (Chapter 4 and Chapter 5). Caloric restriction mice had unlimited access to water, while 80% caloric matched to Diet 5 was provided every day in the afternoon.

2.2.2 Water and food intake

Water and food intake was recorded as 24h water and food consumption. After a 24h period, the remaining food in the hopper and the water bottle were weighed. The difference in weight was then averaged among the mice per cage to determine the average food and water consumption per mouse per day.

2.2.3 DNA extraction

Total DNA was extracted from fecal/caecal samples using FastDNA™ SPIN Kit for Feces (MP Biomedicals Australasia) according to the manufacturer's manual with modifications. Briefly, stool or caecal content (~50mg) was added to sodium phosphate buffer (825 µL) in a lysing matrix E tube (2mL), then topped up with PLS solution (275 µL). The mixture was homogenized (MP FastPrep^{TM}-24, 4m/s,15s), and centrifuged (14,000 xg, 5min) to remove the supernatant. After this, sodium phosphate buffer (978 µL) and MT buffer (122 µL) were added. The mixture was homogenized (6m/s, 40s), rest for 5 min and homogenized again (6m/s, 40s). The supernatant was transferred to a clean 2mL centrifuge tube after centrifuge (14,000 xg, 5min). To the same tube, added PPS solution (250 µL), shake vigorously to mix and incubated in the cold room (4^{o}C, 10min). After centrifuge (14,000 xg, 2min, 1x repeat if suspended particle was observed), the supernatant was transferred to a conical tube (15mL) with pre-added Binding Matrix Solution (1mL) and mixed by a tube roller (ISG® , 5min) every 6 samples. The supernatant was discarded after centrifuge (1,400 xg, 2min). The binding mixture pellet was washed with Wash Buffer #1 (1mL), and transferred to a SPIN^{TM} Filter tube. The washed pellet was separated by centrifuge (Thermo Scientific Heraeus Pico21, 14,000 xg, 1min), followed by another two washes by Wash Buffer #2 with pre-added ethanol. After being separated by centrifuge (14,000 xg, 2min), the pellet was centrifuged (14,000 xg, 4min) again to remove the

remaining ethanol. The residue was, then, air dried in a bio-safety cabinet for 20min. The DNA was eluted with TES solution (60uL-100uL) and collected in a catch tube by centrifuge (14,000g, 2min). DNA concentration was determined by a fluorometer (Qubit™ 2.0). A portion of stock DNA was diluted to 10ng/uL using Milli-Q water. Samples with a concentration less than 10ng/uL remained undiluted. Both the stock and diluted DNA solution were stored at -30ºC until further use.

2.2.4 16S rRNA gene sequencing

2.2.4.1 DNA qualification

For amplicon detection and product size estimation, DNA was assessed using conventional PCR and electrophoresis in agarose gel electrophoresis.

2.2.4.2 Polymerase chain reaction (PCR)

Each reaction contained 1x OneTaq Quick-load (New England Biolab), 5pmol of 27F forward primer (Sigma-Aldrich), 5pmol 1492R-long reverse primer (Sigma-Aldrich), 5nmol dNTP mix(New England Biolab), 1.25 unit OneTaq polymerase (New England Biolab) and 20ng template DNA. The program used was as follows: initial denaturation at 94°C for 30 secs, then 25 cycles of denaturation (94°C, 30 secs), annealing (60°C, 30 secs) and extension (68°C, 1 min 30 secs), with a final extension at 68°C for 5 mins.

2.2.4.3 Gel electrophoresis

PCR product from section 2.2.4.2 was first dyed by mixing 5µl PCR product with 1µl BBS Gel Loading Dye (MP Biomedicals Australasia). The agarose gel was made with agarose power (Bioline) in 1x TBE buffer (Sigma-Aldrich) (1% w/v), and stained with Gel Red (0.02% v/v, Biotium). 5 µl pre-dyed PCR products and 1 ng 1kb DNA ladder (New England Biolabs) were run in parallel in 1x TBE buffer (Sigma-Aldrich) at 100V for 40 min. Gels were visualised using the GelDoc system (Bio-Rad Laboratories, USA).

2.2.4.4 16S rRNA gene sequencing

20uL of diluted DNA of each sample was collected in 96-well plates and sent to the Ramaciotti Centre for Genomics at University of New South Wales. The bacterial community was profiled using the 16S rRNA gene V4 region (515F/806R) by Illumina MiSeq (Chapter 3) or Illumina NextSeq 1000 (Chapter 4 and 5).

2.2.5 Gut microbial analysis

Microbial analysis was performed in R v.4.2.2 using R studio.

2.2.5.1 16S rRNA gene profiling and ASV filtering

Sequence reads were aligned and partitioned into amplicon sequence variants (ASVs) using DADA2 v.1.24.0 (Callahan, McMurdie et al. 2016). The DADA2 algorithm uses a parametric error model to correct the amplicon errors and infer the true sample composition. As such error is learned based on the amplicon dataset, for big data sets like the one in Chapter 3 and Chapter 4, the error model was built for each sequencing run/batch. Then the different datasets from the same study were combined for downstream analysis.

For the MiSeq sequencing result, default parameters were used to learn the error. Due to its binned quality scores, modifications of the error model for the NextSeq sequencing results were done by altering the weights (log10), span (span = 0.95), and degree (degree =1) in the loess function and enforcing monotonicity. A joint convergence solution was reached after 12-16 rounds of estimating error rate and inferring sample composition.

Then, paired-end sequence reads were aligned and partitioned into amplicon sequence variants (ASVs). Taxonomy was assigned to ASVs against the SILVA database v138 (Glöckner, Yilmaz et al. 2017). Multiple sequence alignment was performed with the msa package v.1.28.0 (Bodenhofer, Bonatesta et al. 2015), phylogenetic tree construction was performed with the phangorn package v.2.9.0 (Schliep 2011) and rooted using the ape package v.5.6-2 (Paradis, Claude et al. 2004).

To remove low abundance taxa and noise, abundance and ubiquity was performed. ASVs that contained less than 0.01% of total reads, showed in less than 10% samples were filtered out. The given threshold is considered ideal as it effectively filters out uninformative reads while preserving an adequate number of ASVs (Supplementary Table 7-1). The number of sequence reads processed at each step for each study is summarized in Supplementary Table 7-1.

2.2.5.2 Diversity analysis

Microbial diversity analysis was performed with phyloseq package v.1.40.0 (McMurdie and Holmes 2013) and visualized with the ggplot2 package v.3.3.6 (Wickham, Chang et al. 2016).

Prior to perform within-sample diversity (α-diversity), the microbial data was rarefied to even the sampling depth. α-diversity was measured with 3 different metrics (the inverse Simpson index, the Shannon index and the number of observed taxa) at 4 different taxonomy resolutions

(Phylum, Family, Genus and ASV). Statistical analysis on α-diversity was performed with FSA package v.0.9.3 using Kruskal-Wallis test, and post-hoc test was done using Dunn's test. Adjust p value was calculated using Benjamini-Hochberg Procedure.

Prior to comparing between-sample diversity (β-diversity), centered log-ratio (CLR) transformation was done with the microbiome package v.1.18.0 (Lahti and Shetty 2018). A pseudo count of 0.5 was applied across the dataset to allow for the CLR transformation (Yamamura 1999). β-diversity was measured using the Bray-Curtis metric, weighted UniFrac metric and unweighted UniFrac using vegan package v.2.6-2 (Oksanen, Blanchet et al. 2019). β-diversity distances between samples was visualised with principal coordinate analysis. Pairwise permutational multivariate analysis of variance (PERMANOVA) was performed using EcolUtils package v.0.1. The p-value was adjusted using Benjamini-Hochberg Procedure.

2.2.5.3 Differential abundance analysis

Differential abundance analysis was performed with ANOVA-Like Differential Expression (ALDEx) Analysis using ALDEx2 package v.1.28.1 (Fernandes, Macklaim et al. 2013). Prior to perform ALDEx analysis, CLR transformation was done using the built-in function in ALDEx2 package. To find the significant bacteria taxa in desired groups, two selected datasets were compared using Kruskal Wallace test. The p-value was adjusted using Benjamini-Hochberg Procedure. The difference of bacterial taxa abundance was calculated DESeq2 package v.1.36.0. Bacteria taxa were considered significant if the adjusted p-value was less than 0.05 and the log2 fold change was larger than 2 (a.k.a more than 4 times larger). ALDEx2 result was visualized via either the built-in graphic tool in ALDEx2 package or via volcano plot using EnhancedVolcano package v.1.14.0.

2.2.5.4 Community typing and clustering analysis

Community typing was performed using partitioning around medoids (PAM) clustering with cluster package v. 2.1.3 and clusterSim package v. 0.51-3 (Arumugam, Raes et al. 2011). The optimal number of clusters was determined by the maximum Calinski-Harabasz (CH) index. Bray-Curtis distance at ASV level and unweighted UniFrac distance, were used to perform PAM cluster. The result was visualized using PCA plot from ade4 pack package v. 1.7-19. The predominant bacteria in each PAM cluster was determined via core microbiome analysis. The analysis was performed using microbiome package v.1.18.0. Same package was used for visualizing results.

3 Characterising Age-related Change in Gut Microbiota under Different Macronutrient Compositions and Energy Intake

This chapter is under a program grant in collaboration with Prof. Stephen Simpson at Charles Perkins Centre. The animal maintenance and sample collection were done by Dr. Amanda Brandon's team (University of Sydney, Australia). DNA extraction and microbial analysis were performed by me.

3.1 Introduction

Virtually all animals have ingestive nutrition and their diet profoundly shapes their health and ecology. In order to understand this it is useful to conceptualize animals as holobionts, which include both physiological parts and the microbes harboured inside them (Bordenstein and Theis 2015). Such organisms are very complex since, microbial cells, animal cells, and the whole animal operate at very different spatial and temporal scales. The holobiont concept is useful since it provides a framework to understand how diet shapes the interactions between the host and its microbiome that determine overall, or emergent, health. Here I aim to explore this interaction in the context of aging biology, with the aim of identifying mechanisms through which diet and gut microbiome may interact to influence healthy aging.

Aging can be viewed as the change in biological function that is associated with accumulation of damage over time. Such damage can be at the level of genes (eg. Mutations), or cells and tissues. For example, well-established changes with age are telomere shortening (genetic), immune-senescence (lymphoid cell functions), osteoporosis (bone density) and skin wrinkles (loss of connective tissue elasticity) (Uitto 1986, Demontiero, Vidal et al. 2012, McClanahan, Riches et al. 2015, Elyahu, Hekselman et al. 2019, Rossiello, Jurk et al. 2022). There can also be behavioural changes such as cognitive function and appetite decline (Kundu, Lee et al. 2019, Cox, Bowyer et al. 2021). To maintain healthy aging is to delay the accumulation of damage, thus largely preserve the biological functions of the holobiont. Diet plays a crucial role in sustaining the functionality and health of the holobiont through the interactions among genes, metabolism, the immune system, and the gut microbiome.

Diet, however, is complex. It is a collective term that describes the integrated pattern of food intake over time, which is a combination of eating behaviours, food components, nutrient and bioavailable molecules (Raubenheimer and Simpson 2016). Although diet and food were often used together and sometimes interchangeable, they are different. Food exists externally and can be ingested as source of nutrients and energy. Diet, in contrast, refers to what reaches the gut. The parts that were digested and absorbed become nutrients, and then used by the microbes and cells. It is the nutrients that mechanistically impact physiology and metabolism. Therefore, what is supplied in the food is not equivalent to what is accessible to the microbes or the body. Age-related reduction in body function affects the food digestion, thus the nutrient availability to both the host and gut microbes. To determine which nutrients are affected by aging and how

they influence the gut microbiome, it is necessary to adopt an approach that the interaction among dietary elements can be all accessed.

Taking into account of the diet complexity, modern nutrient research uses the geometric framework to capture the interactive effect of multiple dietary factors (Raubenheimer and Simpson 2016). Geometric framework is an approach that represents the total range of possible diets, such that looks at the main effect of one component and how it interacts with other components. In principle, all possible food components and diet compositions can and should be examined. However, this is not possible to do so in reality. Therefore, a simplified dimension is often used to represent useful diet information. This enables the study of dietary impact on the host holobiont in totality, while still simplifying the complexity of the diet to a certain extent.

Applying geometric framework in studying the dietary effect on aging biology and longevity was initially described by Solon-Biet, McMahon et al. (2014) in mice. Solon-Biet, McMahon et al. (2014) simplified diet into four dimensions – three macronutrients and energy density. Foods were formulated from defined sources of three macronutrients, protein (casein), carbohydrate (starch, dextrin and sucrose) and fat (soy oil), and supplemented with indigestible cellulose to create 3 energy densities (low, medium and high). Physiological measurement from aged mice were then mapped into the macronutrient energy intake space. Physiological phenotypes in aged mice, like branched chain fatty acid, body fat/lean, food intake and food intake, were found to be primarily affected by the protein-to-carbohydrate ratio available in the diet. Microbial analysis performed on these mice, later, by Holmes, Chew et al. (2017) also linked the dietary nitrogen and carbon source to the gut microbial composition. However, the nitrogen that can be accessed by the microbes in the gut environment ultimately shapes the microbial community. These studies reveal that food vary in amount and caloric intake changed the animal physiology, microbial activities and host microbial interaction. However, these studies only looked at the association between macronutrient intake, body function and microbial response at 15 months of age. Little was known if such relationship alters with younger, older mice or during the process of aging. Neither was the effect of eating behaviour and food components was tested.

Evidence suggests that nitrogen availability was a fundamental factor controlling microbiome composition and furthermore that N-driven change in microbiome would have an impact on

host physiology (Holmes, Chew et al. 2017). Here I aimed to test several questions resulting from this: Is there an age-associated microbiome as a consequence of age-related decline in host ability to regulate nitrogen availability in the gut? If so, is the onset of the age-associated shift different across diets that differ in macronutrient distribution and intake, especially nitrogen (protein) content. Furthermore, does the age-associated microbiome potentiate changes in host functions known to be microbiome-influenced such as immune, appetite and metabolic regulation? A significant challenge for exploring such questions is that some measurements require post-mortem sample collection, thus preventing a longitudinal exploration of age-related processes in individuals. To address this, a large cross-sectional study with four distinct time cohorts was designed, to investigate these questions.

The overall study aims to use the geometric frame work to test the effect of multiple different dietary factors during aging (Figure 3-1A). First of all is to study the effect of relative amount of macronutrients by setting the energy density the same. The diet is also simplified into 3 different macronutrients from defined source. 10 different macronutrient ratios were tested, which were sampled around the Australian recommended intake (Simpson and Raubenheimer 1997) (Figure 3-1B). By using the so-called "unhealthy" diet, how the imbalanced diets affect the animal holobiont during aging can be understood. To keep the animal number reasonable for long period of time, 2 energy densities was used to test the effect of total caloric intake. These two energy level was pick because they were on either side of tipping points in the pervious study (Solon-Biet, McMahon et al. 2014). The nature of the diets, differences in energy density, caused differences in food intake (Supplementary Figure 7-11 and Supplementary Figure 7-12). Although higher food intake was found with lower energy density diets, the overall energy intake was still lower compared to the higher density diets. Therefore, a caloric restriction diet was implanted to differentiate the difference caused by energy density or food intake. Due to ethic reason, two diets were aborted after 1 month. The experimental group ended up with 20 diets involving 10 different macronutrient compositions and 2 energy densities plus a caloric restriction diet (Figure 3-1B).

To capture the different age states, 4 experimental cohorts were set up to represent mice's early adulthood (4mo old/time on diet (ToD) for 1mo), mature adulthood (9mo old/time on diet for 6mo), middle age (15mo old/time on diet for 12mo) and old age (21mo old/time on diet for 18mo) (Flurkey, Currer et al. 2007, Dutta and Sengupta 2016) (Figure 3-1C). Additionally, to account for the gender difference during aging, the study included both male and female

population. As this is a cross-sectional study, mice in each ToD group were different individuals. To avoid batch effects, a stagger entry strategy was applied when assigning mice to different experimental groups (Supplementary Figure 7-6). The 1,368 mice used for this experiment were spread over 19 different birth cohorts. They were born and arrived within 5 months in 2019. Upon arrival, the mice were randomly and evenly assigned to 19 dietary groups and 2 ToD groups (1mo and 18mo were assigned together; 6mo and 12mo were assigned together). In the end, each ToD group contains at least 9 different birth cohorts.

The microbial analysis part of this study aims to look at the microbial secondary succession under different nutrient environment exposure, and how age-related animal physiology and metabolic change effects the microbial behaviour and microbial response to nutrients. For laboratory mice, the initial gut microbial colonization and assembly is expected to occur during the weaning period at the breeder facility (Guittar, Shade et al. 2019). Introducing the experimental diets, created turbulence in the gut microbiota initiating secondary succession, during which the microbiota changes its composition to adapt to the new environment.

With respect to microbial community dynamics, three factors are important in this experiment. The first is the starting microbiome state (which potentially varies across the animals). The second is the disturbance associated with the transition from the maintenance diet with complex composition complex composition (standard lab “brown chow”) to one of the set of experimental diets with defined compositions, which caused a disturbance to the gut microbiome (Figure 3-1D). The third is selection over time on the different experimental diets. It is important to note that, with all the dietary factors involved in the geometric framework, the food component was not included. Compared to the maintenance diet, the experimental diets lack the non-starch polysaccharide (i.e. typical dietary fibre). This means that the microbially accessible carbohydrate is primarily in the form of digestion resistant starch. What is accessible to the body is not always the same as what is accessible to the microbes, as differences in food components can affect nutrient availability. For animals, the difference is not obvious when comes to standard brown chow and purified experimental diet that share the same macronutrient ratio and energy density, the difference is not obvious. For microbes, however, whole food contains more dietary fibers and in different forms, thus more food, which affects the microbial activities and adaption to the surrounding environment. The disturbance associated with the diet transition may cause the microbial community to undergo a secondary succession to assemble a new community.

The manipulation is that the set of experimental diets vary in nutrient environment exposure to the microbes (Figure 3-1A). For the three aspects of nutrient environment were tested during the experimental period, macronutrient ratio, energy density and eating behaviours, the first two parameters change the nutrient availability and the amount to microbes. Caloric restriction and *ad-libtum* feeding vary when nutrients and energy are available to the microbes. Distinct nutrient environments create 'habitat filtering' for the microbiota to also undergo secondary succession to assemble as new communities.

It takes time for microbes to respond to new diets and assemble a stable new community, ranging from 1 day to 6 months (Wu, Chen et al. 2011, Claesson, Jeffery et al. 2012, Thaiss, Itav et al. 2016). Meanwhile, aging biology changes the animal physiology and metabolism, affecting the microbes' nutrient environment. As the animals used in this study are all individuals, to ensure a fair comparison and to check that the effectiveness of the stagger entrance strategy, baseline fecal samples were collected before starting the experimental diets. At the end of the experiment, ceacal samples were collected for analysis, so that the gut microbial properties can be associated with proteomics, metabolomic and other physiological parameters later to understand the host-microbial interactions during aging. Therefore, the interactive effect on microbial activity will be accessed by analyzing the baseline fecal samples and the caecal samples at the end of 4 experimental endpoints. For each time point, 1 animal was randomly chosen from each cage for microbial analysis (Figure 3-1C). Therefore, 3 males and 3 females were assessed for each diet. Since two cages failed to survive to old age, each timepoint ended up with 42-114 baseline fecal samples and 112-114 caecal samples for each timepoint.

Enterotyping is a common tool used in microbial studies both with human and mice (Arumugam, Raes et al. 2011, Hildebrand, Nguyen et al. 2013). Microbial enterotypes/ community types were associated with multiple environmental factors like dietary pattern, dietary history, cage history and host genotype (Wu, Chen et al. 2011, Hildebrand, Nguyen et al. 2013, Wang, Linnenbrink et al. 2014). It allows to simplify the complex gut microbiome while still capturing the individual variance. However, there are still some debates about the reliability of enterotypes, as it is biased to sampling frame, subject to clustering method and microbial taxonomy resolution (Knights, Ward et al. 2014, Costea, Hildebrand et al. 2018) Despite that, enterotypes were recurrently observed in multiple studies with similar microbial compositions, indicating there are underlying meaningful biological principle, in particularly

joint analyzed with other results (Costea, Hildebrand et al. 2018). Here, enterotying typing was applied on whole gut microbiota of all mice to study the microbial behavior at community level during aging. This method may allow the results to potentially applied to the human community, which includes all genders, different age groups and varied diet habits.

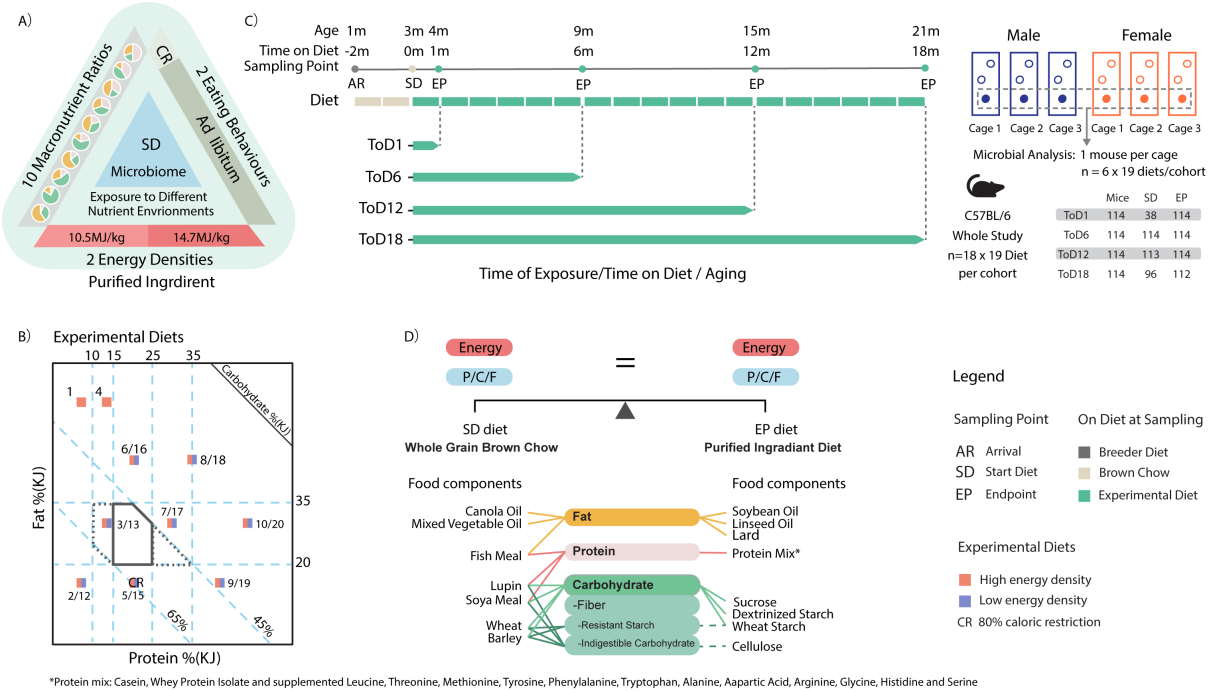

Figure 3-1. Experimental and diet design for the animal study reported in this chapter.
A) This experiment aimed to look at microbial secondary succession after exposure to different nutrient environments. Four categories of nutrient conditions were varied, food components, macronutrient ratio, diet energy density, and eating behavior. B) The experimental diets used purified ingredient and consist of 10 macronutrient ratios, at 2 different energy densities plus a caloric restriction diet (P/C/F ratio of 21/64/15). Two of the nutrient distribution formulations were only tested at high energy density, since the low energy diets L_7/33/60 and L_14/26/60 were aborted after 1 month due to excessive weight loss. C) The microbial secondary succession was examined at 4 different durations, time on experimental diet for 1mo (ToD1), 6mo (ToD6), 12mo (ToD12) and 18mo (ToD18). Each cohort contains 342 mice (3 cages of females and 3 cages of males, and 3 mice per cage) having 19 diets. For each mouse, samples were collected at baseline (fecal), when mouse was on standard brown chow, and at endpoint (ceacal) after nutrient exposures. One mouse from each cage was used for microbial analysis (n= 6 per diet per cohort). Due to sample collection issue and adverse events, end up with 361 SD samples and 454 EP samples for analysis. D) One of the main difference between the SD brown chow and the experimental diets were the nutrient sources/food components. Such difference can affect the microbial accessibility to food. The brown chow and purified diets can share the same macronutrient ratio and energy density. For animals, the difference is not obvious. For microbes, brown chow contains more dietary fibers and in different forms, thus more food, which effects the microbial activities and adaption to the surrounding environment.

3.2 Methods

3.2.1 Animal

Male and female C57BL/6 mice (4 weeks old, n=1,368) were purchased from Animal Resources Centre (Perth, Australia). To limit systematic differences between the main

experimental treatment groups (four for age and 19 for diet) the mice arrived in 19 different cohorts within 5 months in 2019 (Supplementary Figure 7-6). They were randomly separated into 4 cohorts, time on experimental diets for 1 month (ToD1), 6 months (ToD6), 12 months (ToD12) and 18 months (ToD18), as shown in Figure 3-1a. Each cohort consists of an equal number of male and female mice. They were housed three per cage in standard approved cages (Tecniplast GM500), and fed standard chow for 8 weeks before starting experiment diets (Specialty Feeds). At the end of the experiment, the mice were euthanized by CO_2.

3.2.2 Diet composition

The experiment diets consist of 18 ad libitum access diets and a calorie restriction diet, involving 10 combinations of macronutrients under two energy densities (14.7 MJ/kg and 10.5 MJ/kg). The energy density was adjusted by adding or subtracting indigestible cellulose. Mice feeding calorie restriction (CR) diet were having 20% restriction of food intake. For every 1g consumed by the diet H_21/64/15 (high energy density diet with a macronutrient composition C/P/F = 21/64/15) cohort, 0.8g of the same food was provided to CR mice. Two of the nutrient distribution formulations were only tested at high energy density, since the low energy diets L_7/33/60 and L_14/26/60 were aborted after 1 month due to excessive weight loss. Therefore, yielding a total of 19 experiment diets. The diet composition and source of nutrients are given in Figure 3-1B and D. A detailed nutrient source composition is also provided in Supplementary Table 7-2.

3.2.3 Samples collection

Baseline mice faecal samples were collected in the morning of switching standard chow to experimental diets, which were labelled as start diet (SD). Faecal samples were stored in Eppendorf tubes at -30^{o}C until further processing. A total of 1,178 mouse fecal pellets were collected and stored. Storage time before processing for DNA extraction ranged from 104 days to 762 days. At the end of the experiment, mice were culled. Caecal content was snap freezed in liquid nitrogen and labelled as endpoint (EP). Caecal content was stored in Eppendorf tubes at -80^{o}C until further processing. Matching samples (SD and EP from the same mouse) from one random mouse in each cage were selected for microbial analysis).

3.2.4 Gut microbial analysis

For one mouse per cage, DNA extraction was performed as detailed in Chapter 2.2.3. Bacterial amplicon 16S rRNA gene sequencing was performed as detailed in Chapter 2.2.4. Microbial profiling was done with DADA2 as detailed in Chapter 2.2.5 with classification at the ASV

level. Two filtering steps were applied, for abundance filtering an ASV must comprise of 0.01% of total reads, for ubiquity filtering an ASV must be present in at least 10% of samples. The number of sequence reads processed and filtered is summarised in Supplementary Table 7-1. After filtering, the reads per sample ranges from 10,146 to 109,848, with a median reads of 35,455.

3.2.4.1 Generalised additive models (GAMs)

To model the microbial abundance response to dietary macronutrient composition, GAMs model was applied using the mgcv package v.1.8.40 (Wood, Pya et al. 2016). Prior to perform GAMs modelling, centered log-ratio (CLR) transformation was done on the microbial abundance counts with the microbiome package v.1.18.0 (Lahti and Shetty 2018). A pseudo count of 0.5 was applied across the dataset to allow for the CLR transformation (Yamamura 1999)

The best model fit was determined based on a combination of Akaike information criterion (AIC) value and percentage deviance explained using the stats package v.4.2.1(R Core Team 2013). All AIC values were rounded to the nearest integer, the lowest AIC value identified the best-fitting GAM. In case, when the AIC values are the same, whoever had a higher percentage of deviance explained was picked. GAMs response surfaces were visualized using the graphic package v.4.2.1 (R Core Team 2013).

3.2.4.2 Distance-based redundancy analysis (db-RDA)

Distance-based redundancy analysis was used to identify potential drivers of microbial type (Legendre and Anderson 1999). The analysis was performed between the dietary macronutrient energy intake and the Bray-Curtis dissimilarity of CLR transform microbial abundance data (Legendre and Anderson 1999, Legendre and Gallagher 2001). Detrended correspondence analysis (DCA) was used to determine if RDA is a superior model than the canonical correspondence analysis (CCA) based on the first length of gradient (Hill and Gauch Jr 1980, Oksanen and Minchin 1997). In this data set, the value was less than 3, thus RDA was the better choice. Redundancy analysis was done using capscale() function from the vegan package v.2.6-2 (Oksanen, Blanchet et al. 2019) and visualized using ggplot2 package v.3.3.6 (Wickham, Chang et al. 2016).

3.3 Results

3.3.1 Microbial diversity at arrival had two community states

The term microbiota refers to the collective microbial composition across all animals in the study, with the individual microbial communities being referred to as microbiomes. Differences in microbial initial colonization and functional succession lead to distinctions in the microbiome (Shafquat, Joice et al. 2014). Thus, individuals with different gut microbiome contribute to a microbiota, and includes different microbial types, which are known as enterotypes (Arumugam, Raes et al. 2011). Since a microbiome is a product of community assembly from a subset of the microbiota, the potential exists in a large study such as this for confounding effects arising from assembly differences between cohorts.

To study the age related effect on the gut microbiota, the endpoint microbiota will be compared across the 4 ToD groups. Considering that the mice involved in the ToD groups were different individuals and from different birth cohorts, a stagger entrance strategy was applied when assigning mice to different experimental groups to minimize the batch effects (Supplementary Figure 7-6). Therefore, the total microbiota of SD samples was first examined to see if the stagger entrance strategy was able to even out the groups variance at baseline. To remove low abundance taxa and noise, all SD samples were filtered together with the endpoint samples. ASVs that contained less than 0.01% of total reads, showed in less than 10% of samples were filtered out. The given threshold is considered ideal as it effectively filters out uninformative reads while preserving an adequate number of ASVs. This abundance filtering was equivalent to an average of 4 reads per sample, and the ubiquity filtering was equivalent to present in at least 1 male or 1 female in each diet at one timepoint SD or EP). The abundance and ubiquity filtering resulted in 386 unique ASVs and an average of 37,508 reads per sample (Supplementary Table 7-1).

The mean relative abundance of these 386 ASVs was calculated and used for comparison across 19 birth cohorts. Due to space constraints, only the top 159 ASVs were listed and shown in the heatmap in Supplementary Figure 7-7. The results showed that although microbiomes were different among the birth cohorts, they were assembled from a ‘common’ microbiota. No birth cohort was found to contain all 159 ASVs and only 95 ASVs were shared by all birth cohorts. However, these 95 ASVs (representing 24.6% of the 386 ASVs in the microbiota), were among the most abundant ASVs and covered 50-97% of the total reads in each microbiome. *Erysipelotrichaceae Allobaculum* ASV2 was an exception. It is one of the most

abundant ASVs, but was not shared by all individuals and was missing from one outline cohort (20200213). This birth cohort was a replacement cohorts, which contains 3 cages of mice from ToD12 and ToD18. 3 of them was used for microbial analysis. *Allobaculum* together with the 95 ASVs account for more than 80% of the total reads in each microbiome. This suggests that although microbial community structure (microbiome types) upon arrival was not homogeneously distributed across all cohorts, the microbiomes were all assembled from a common set of microbes.

Beta diversity assessment and PAM clustering support two distinct community states having been adopted across the study animal microbiomes. Between-sample beta-diversity of all fecal samples at baseline was calculated. All three metrics, Bray-Curtis dissimilarity, weighted UniFrac and unweighted UniFrac distance (Figure 3-2E) were used. Statistical significance was determined by pair-wise adonis followed by the Benjamini-Hochberg procedure. Pair-wise adonis found there was no difference between dietary groups using all metric (Supplementary Table 7-3). However, differences were found between ToD groups using Bray-Curtis dissimilarity and unweighted UniFrac distance. For weighted UniFrac distance, differences were observed between ToD1 and older groups, but not between the older groups (Supplementary Table 7-4). Such difference was likely due to the uneven sample size between the ToD groups, as ToD1 only had 42 baseline samples. Dispersion analysis showed that the samples from the ToD1 group were within the dispersion of other groups (Supplementary Figure 7-8). This indicates that the ToD1 group samples were within the same range of microbial composition as other samples. At baseline, the abundance microbes had a similar in phylogenetic distance among the ToD groups, but the specific species and rate species were different.

Although the birth cohorts did not have 100% identical ASV membership, the overall microbial structure may share a similar functional type. To test this, I applied community typing to all the baseline samples to using the Partition Around Medoids (PAM) clustering algorithm with Bray-Curtis dissimilarity at ASV level (Figure 3-2A). The number of clusters, k, was determined based on the value of Calinski-Harabasz (CH) index (Supplementary Figure 7-9). An optimal cluster of k=2 was obtained when the CH index was at maximum. PAM cluster analysis resulted in two distinctive enterotypes (Figure 3-2A). Core microbiome analysis was done on both clusters, using 0.1% relative abundance as the cut-off line, to examine microbial structure in each cluster (Supplementary Figure 7-10). The analysis ranks the taxa according

to their prevalence in each cluster and presents the results in a heatmap of the prevalence at different relative abundance percentage. The results found that *Allobaculum* was the predominant taxa in cluster 1. For cluster 2, multiple ASVs were present with low relative abundance.

These data showed that staggered entry approach here was effective in normalizing the number of each community type across the experiment (Figure 3-2A) – but their prevalence varied between arrival groups (Figure 3-2B). The group allocation approach resulted in near-even prevalence of starting community types across ToD groups (Figure 3-2D), but some differences in diet treatment groups (Figure 3-2C). Please note that, for ToD1 only 42 baseline samples were available. Therefore, the sampler number for each microbial type looks uneven. Overall, the analysis in baseline samples showed that the microbiome of the mice on standard brown chow has two community types. However, our staggered recruitment 'normalised' distribution of microbiome types across the treatment groups at baseline.

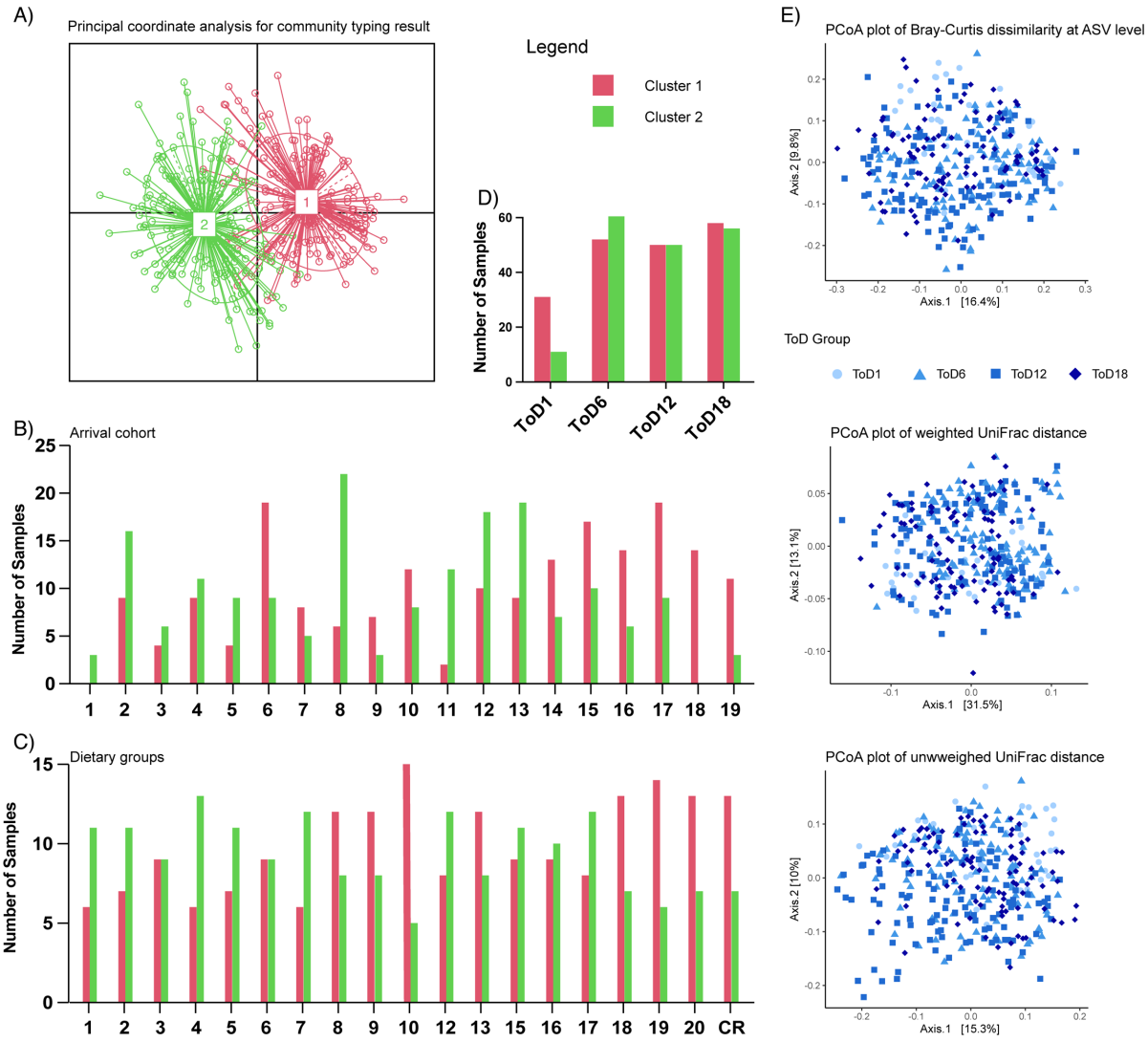

Figure 3-2. The baseline microbial structure includes two community types.
A) PAM cluster result of all baseline samples crossing 4 experimental cohorts using Bray-Curtis dissimilarity at ASV level. B – D) Number of samples in each cluster, grouped by B) Arrival cohorts, C) Dietary group and D) Time on diet group. D) PCoA plot of all baseline samples with three beta-diversity metrics, colored by ToD groups. From top to bottom are Bray-Curtis dissimilarity at ASV level, weighted UniFrac distance and unweighted UniFrac distance

3.3.2 The communities on the baseline are markedly different to all on experimental diets

Introducing of the experimental treatments changes the food component from whole grain to purified ingredients. Changing in nutrient environment initiates the gut microbial secondary succession to adopt to the new conditions. To assess whether the diet components exerted a global effect on the microbiota, between-sample beta-diversity for all samples in each ToD group was calculated. Beta-diversity was calculated using all three metrics, Bray-Curtis dissimilarity (Supplementary Figure 7-13A), weighted UniFrac (Supplementary Figure 7-13B) and unweighted UniFrac distance (Figure 3-3A). All metrics show that the samples were clustered together according to the food component, i.e. baseline (blue dots for chow) or

endpoints (red dots for purified ingrdients). This implies that mice consumed the same food component tend to have a more similar gut microbial structure. Switching from a whole grain diet to a purified ingredient diet results in a new microbial community different from the baseline community. Moreover, the beta-diversity also showed that the end-point samples were more distant from the baseline samples than the end-point samples themselves in all ToD groups (Figure 3-3A, Supplementary Figure 7-13). Given that the mice were supplied with different experimental diets, this suggests that the source of nutrients (whole grain or purified ingredients) has a larger impact on the gut microbiome than the macronutrient distribution or energy density.

As animals age, their metabolic and immune homeostatic capabilities change. Consequently, the effects of diet on the microbiome may shift due to various adaptive responses that vary with age. Therefore, the impact of duration of dietary on the gut microbial response to food components is examined next. To do so, the Bray-Curtis dissimilarity was calculated between the SD and EP samples (SD-EP) from the same mouse, as well as the difference among the EP samples (EP-EP) between two randomly chosen mice (Figure 3-3B). SD-EP difference measures the microbial composition variance between the endpoint and the baseline. Factors caused such variance include changing in the dietary nutrient source, and differences in sampling site (fecal samples vs caecal samples). EP-EP difference measures the microbial composition difference between endpoints, regardless of gender. The result showed that, on average, the SD-EP differences were larger than the EP-EP differences, except for some samples in the ToD12 group. This indicates that the combination of changes in dietary food components and differences in sampling site results in a larger discrepancy in microbial composition than the macronutrient ratio and energy density.

Comparing SD-EP differences among different ToD and gender groups shows that both age and gender have an impact on secondary succession. First, the effect of time on diet/aging on the microbial composition was examined by comparing the SD-EP difference among ToD groups using all three beta-diversity metrics (Figure 3-3C, Supplementary Figure 7-14A and C). It was assumed that the effects of difference in the dietary component (i.e. nutrient source) were not confounded by the sample types (feces vs cecum). Rather, the variance among ToD groups would be primarily due to the effects of time on diet (or aging). All three metrics found a significant difference between the microbiome from the old population (ToD18) and the young adult (ToD1). This indicates an age effect on the microbiome as more changes were

observed between the old and baseline microbiome. Both unweighted UniFrac (Figure 3-3C) and Bray-Curtis dissimilarity (Supplementary Figure 7-14A) showed no difference in microbial structure between the early ages (1mo and 6mo on diet), but not the weighted UniFrac distance (Supplementary Figure 7-14C).

This study used both male and female populations. Therefore, one of the aim is to look at if aging had the same effect on females and males. The SD-EP differences between the two genders in each ToD group was compared using all three beta-diversity metrics (Figure 3-3D, Supplementary Figure 7-14B and D). No significant difference were found between the females and males until 12mo on diet with weighted UniFrac distance (Supplementary Figure 7-14D) and until 18mo on diet with unweighted UniFrac distance (Figure 3-3D). No difference were found between these two groups with Bray-Curtis dissimilarity (Supplementary Figure 7-14B). This indicates that aging has an effect on the microbiome in females and males, such difference was likely caused by changing in rare species or shifting relative abundance of major/minor microbial populations. To examine how the two communities were different at an older age, differential abundance test of CLR-transformed ASV counts was performed between these two groups at ToD18 (Figure 3-3E). Multiple ASVs were different in abundance (green dots) but two ASVs were significantly differentiated (red dots), *Peptococcaceae Peptococcus* ASV237 and *Sutterellaceae Parasutterlla* ASV153. On average, they consisted of less than 7% bacteria population in males and less than 3% bacteria population in females. Overall, the microbial structures were similar between males and females.

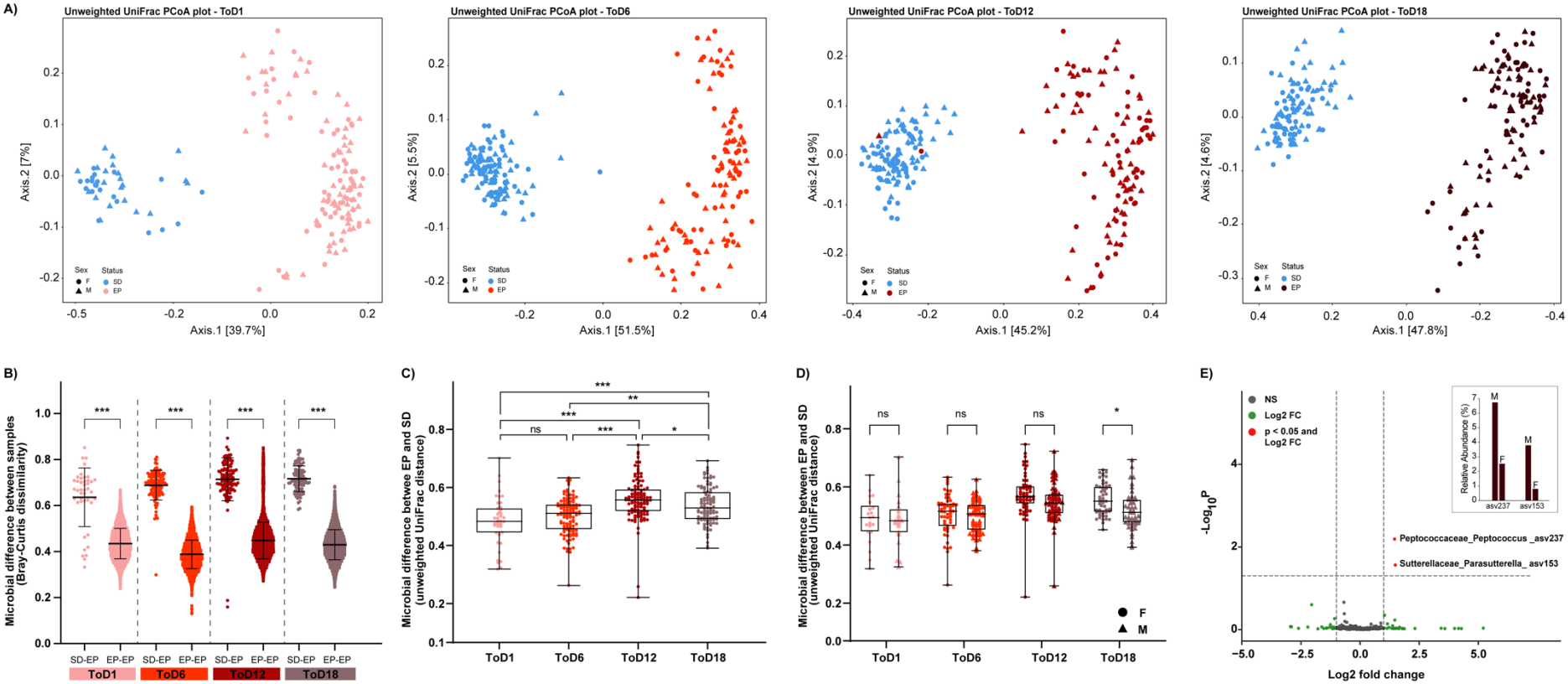

Figure 3-3. Difference in the microbial composition is associated with the source of nutrients and aging.
A) Unweighted UniFrac PCoA plot of SD fecal samples (blue) and EP cecal samples (red) for each time of diet group. From left to right are ToD1, ToD6, ToD12 and ToD18, respectively. B) Comparison of two unweighted UniFrac distance differences in the same ToD group. The difference between the SD and EP samples from the same mouse; and the difference between the EP samples. C) Comparison of the unweighted UniFrac difference between the SD and EP samples of the same mouse among ToD groups. D) Comparison of the unweighted UniFrac difference between genders in each ToD group. E) Volcano plot of ALDEx2 differential abundance testing at ASV level in the ToD18 group between male and female population. The x-axis represents the fold difference in abundance and the y-axis is the p-value adjusted using Benjamini-Hochberg procedure. Grey dots indicate ASVs are neither abundant nor significantly differentiated between groups. Green dots indicate ASVs are abundant compared to the other group but not significantly differentiate between groups. Red dots are both abundant and significant. Only two ASVs were significantly differentiated between genders for ToD18 groups. Both of them have a higher relative abundance in Males.

3.3.3 Transition to experimental diets resulted in post-disturbance assembly of new community types that was influenced by diet formulations and possibly time on diet (or cohort)

To further understand the age-related effect at the community level, the endpoint gut microbiota at each timepoint/ToD group was assessed individually. As mentioned in the previous session (3.3.1), the start microbiota is equivalent across ToD groups. Therefore, to assess community structure in the ToD groups for effects of age and nutrient availability, the endpoint samples were compared directly. As only endpoint samples were compared, to ensure capturing all meaningful ASVs, a separate abundance filtering for all the endpoint samples. After multiple sequence alignment as described in section 2.2.5.1, all the endpoint samples were subset out. ASVs with less than 0.01% of total reads were regarded as noises and filtered out, which is equivalent to about 2 reads per sample. The abundance filtering resulted in a total of 372 unique ASVs. As such number was manageable during analysis, no ubiquity filtering was performed.

At baseline, two distinct microbial community types were observed (Figure 3-2A). It is expected that switching from whole grain diets to experimental diets with purified ingredients will lead to community disturbance. Therefore, the aim was to first access if the endpoint samples had formed different community types. If so, were these types correlated to the baseline types and stable over aging. Community typing was, then, applied on the filtered endpoint samples for each ToD group (Figure 3-4) and all endpoint samples (Supplementary Figure 7-27) using the PAM clustering algorithm with Bray-Curtis dissimilarity at ASV level. The optimal number is determined by the maximum value of CH index. The community typing found 3 microbial types after 1 month on diet (Figure 3-4A). This indicates that switching dietary components from wholemeal to purified ingredients caused turbulence in the microbial community, drove a secondary succession forming 3 new community types. However, from 6 months onwards, only 2 microbial types were observed (Figure 3-4B-D). Moreover, when looking at all the EP samples together, two microbial types were also observed (Supplementary Figure 7-27). This suggests after the initial turbulence, microbiomes adapted to the new nutrient environment after more than month on diet. The newly formed community was likely also have two stable states.

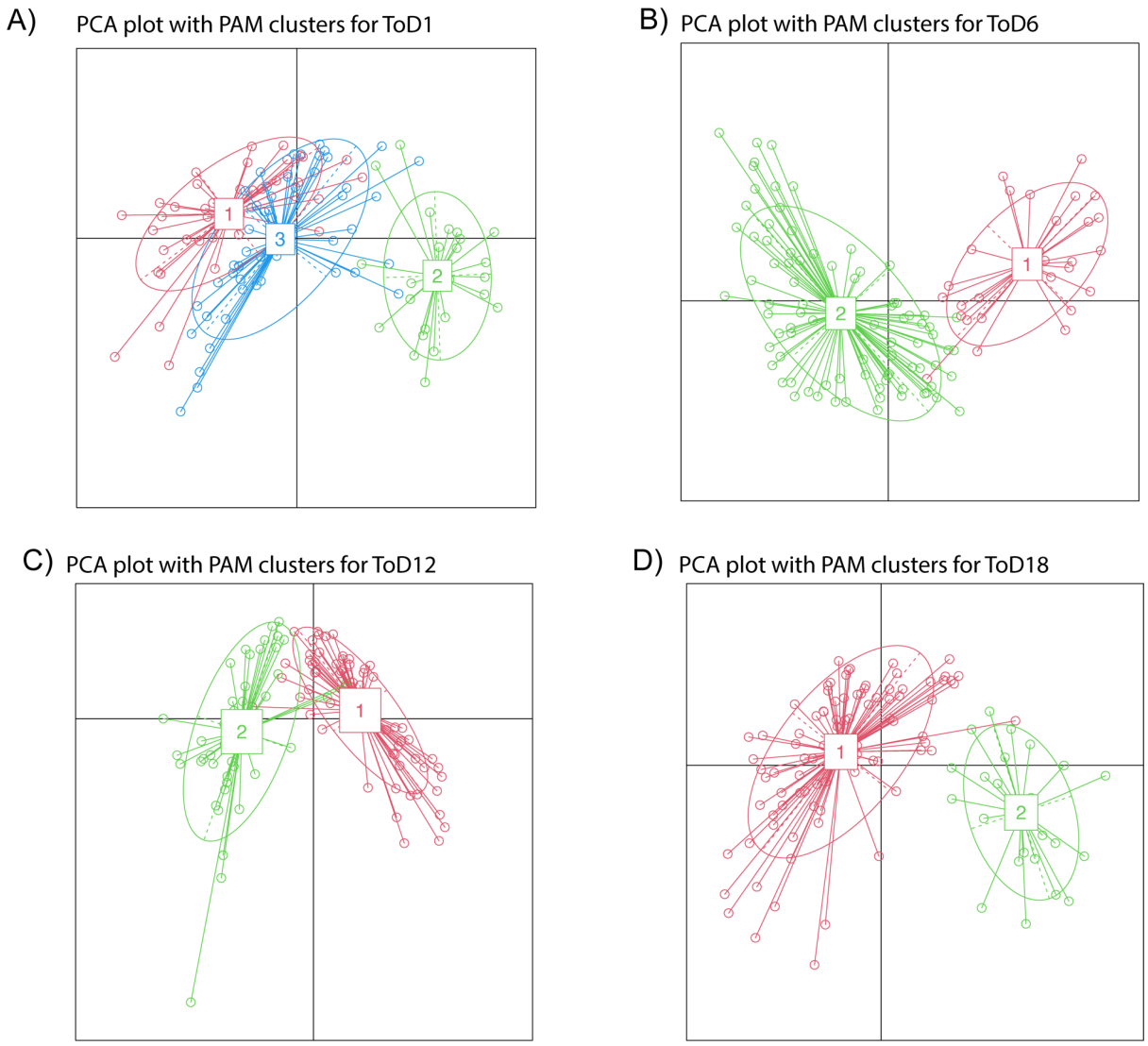

Figure 3-4.The community typing of the endpoint cecal samples found 3 microbial types after 1 month on diet, but only 2 types from 6 months onwards.
A) -D) PAM cluster for the endpoint cecal samples using Bray-Curtis dissimilarity at ASV level. A) ToD1 group, B) ToD6 group, C) ToD12 group and D) ToD 18 group.

To better characterize these newly formed microbial types, the microbial composition in each type was investigated. To do so, the relative abundance of phylum (Figure 3-5 and Supplementary Figure 7-28) and the core microbiome (Figure 3-6) as per cluster for each ToD group were examined. Figure 3-5 gives the top 5 most abundant phylum in each cluster. The phylum plot indicates showed a greater difference between cluster 1 (microbiome type ED_1) and cluster 2 (microbiome type ED_2) in all experimental groups, with ED_1 high in both *Firmicutes* and *Bacteroidota* while ED_2 dominated by *Firmicutes*. Comparing the endpoint microbial types across the 3 timepoints found that the clusters from ToD12 and ToD18 share a more similar microbial composition to each other, than to the ones from ToD6. Cluster 1 (microbiome type ED_1) in ToD6 had a lower relative abundance of *Firmicutes* in associated with more abundant *Bacteroidota.* Slight higher of *Actinobacteriota* was also observed. The

biggest difference came from *Deferribacteriota*, which was less than 0.5% of the total microbial population (Supplementary Figure 7-28). Overall, the major phylum were similar in the clusters cross these three timepoints. The data indicate that the microbiomes adopt one of two possible community types after time one diet for 6 months.

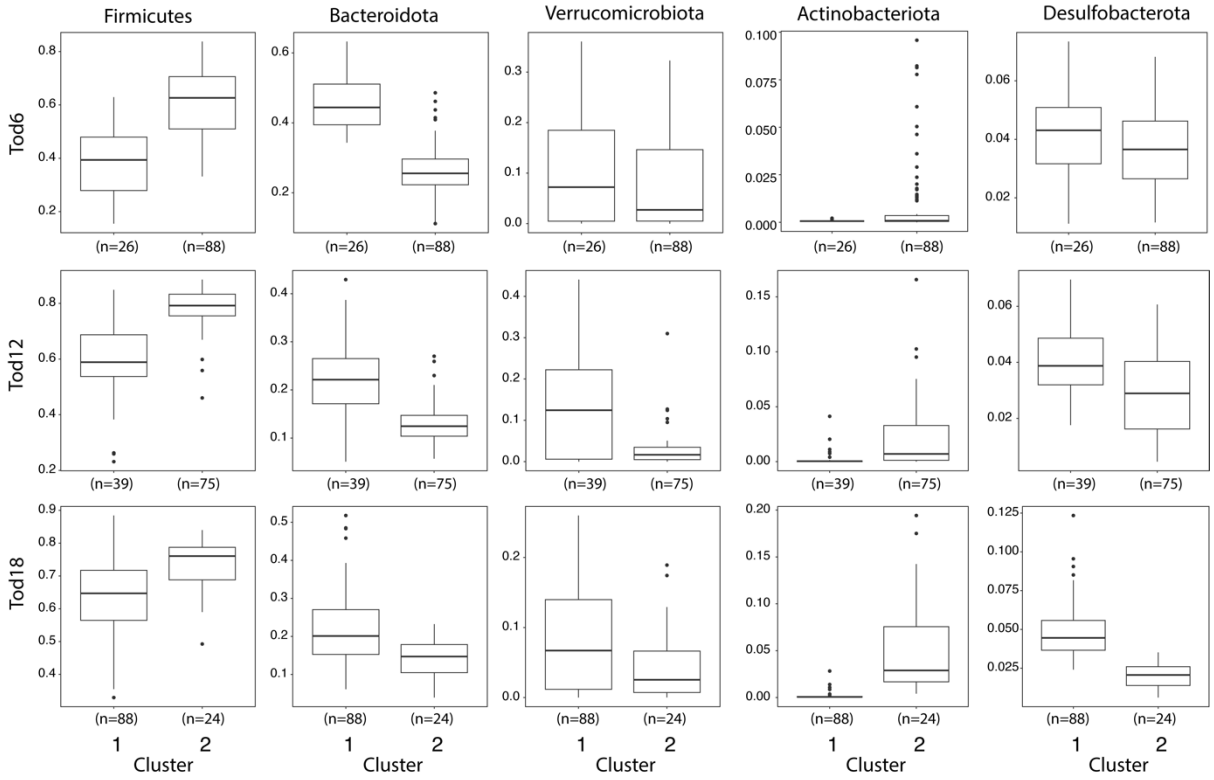

Figure 3-5. Relative abundance of the top 5 most abundant phyla in each cluster.
From top to bottom are experimental group ToD6, ToD12 and ToD18. Note, the number of samples are different for each cluster in the different ToD cohorts.

To identify signature microbes for each cluster, core microbial analysis was performed together with ALDEx2. Core microbiome looks at both the prevalence and relative abundance of each ASVs in the giving microbial community (Figure 3-6). Figure 3-6 gives the top 15 most abundant ASVs in each cluster. The prevalence of each ASV was given at different relative abundance levels. Core microbiome analysis found that the clusters were not exactly the same cross ToD groups.

After switch diet for 6 months, when the two stable microbial types were initial observed, the two clusters were close to each other. *Akkermansia_asv1* was the most abundant taxa in both clusters, although higher relative abundance was observed in cluster 1 (microbiome type ED_1). However, a greater difference was found between the two microbial types in the older groups, ToD 12 and ToD 18. For cluster 1 (microbiome type ED_1) in both groups, *Akkermansia_asv1* was the major taxa with *Desulfovibrio fairfieldensis_asv18* being the most prevalent taxa (at a lower relative abundance). For cluster 2 (microbiome type ED_1), *Faecalibaculum rodentium_asv4* was the most prevalent and predominant taxa.

ALDEx2 was used to compare the two clusters at each timepoint to identify the signature taxa for each cluster (Supplementary Table 7-5). The relative abundance of these taxa in each individual mouse was plotted in a heatmap (Figure 3-7). ASV15, 20 and 40 was found to be persistently differentially abundant in the cluster 1 in all timepoints. However, only ASV15 at ToD6 and ASV40 at ToD18 had an effective size greater than 1. This was shown in their relative abundance, which was fairly similar across all diets and in both clusters. The effective size of ASV40 was increasing from ToD6 to ToD18. This was also reflected in its relative abundance in Figure 3-7. By ToD18, ASV40 was found missing in Diet 2 and the caloric restriction diet, both of which were assigned to cluster 2. It is important to mention *Akk. muciniphila* (ASV1) was not picked by the ALDEx2 analysis as a signature taxa, as it was only differential abundant in ToD12. However, ASV1 was the most abundant taxa in cluster 1, as found in the core analysis. ASV1 was found to be present in all individuals with a higher amount in cluster 1.

In contrast, for the signature ASVs for cluster 2 was distinctively present in cluster 2, but not in cluster 1. ASV3, 4 and 6, were differential abundant and had an effective size larger than 1 from ToD6 onwards. They were enriched primarily in Diet 2, Diet3, Diet 5, Diet 9 and the caloric restriction diet. Moreover, Diet 1 and Diet 7 were also showing an selective effect for

genders, as ASV 3, ASV4 and ASV6 were found missing in males on Diet 1 and females on Diet 7. These samples were all assigned to cluster 2.

Overall, cluster 2 was better defined microbial community primarily by three ASVs. Cluster 1, however, was primarily high in *Akk. muciniphila*, but other composition was less well defined. Distinct differences was observed in the presence or absence of signature taxa for cluster 2 from different types among individuals on specific diets. This suggests that there might be associations among the microbial types, gender, dietary intake and, possibly, time on diet.

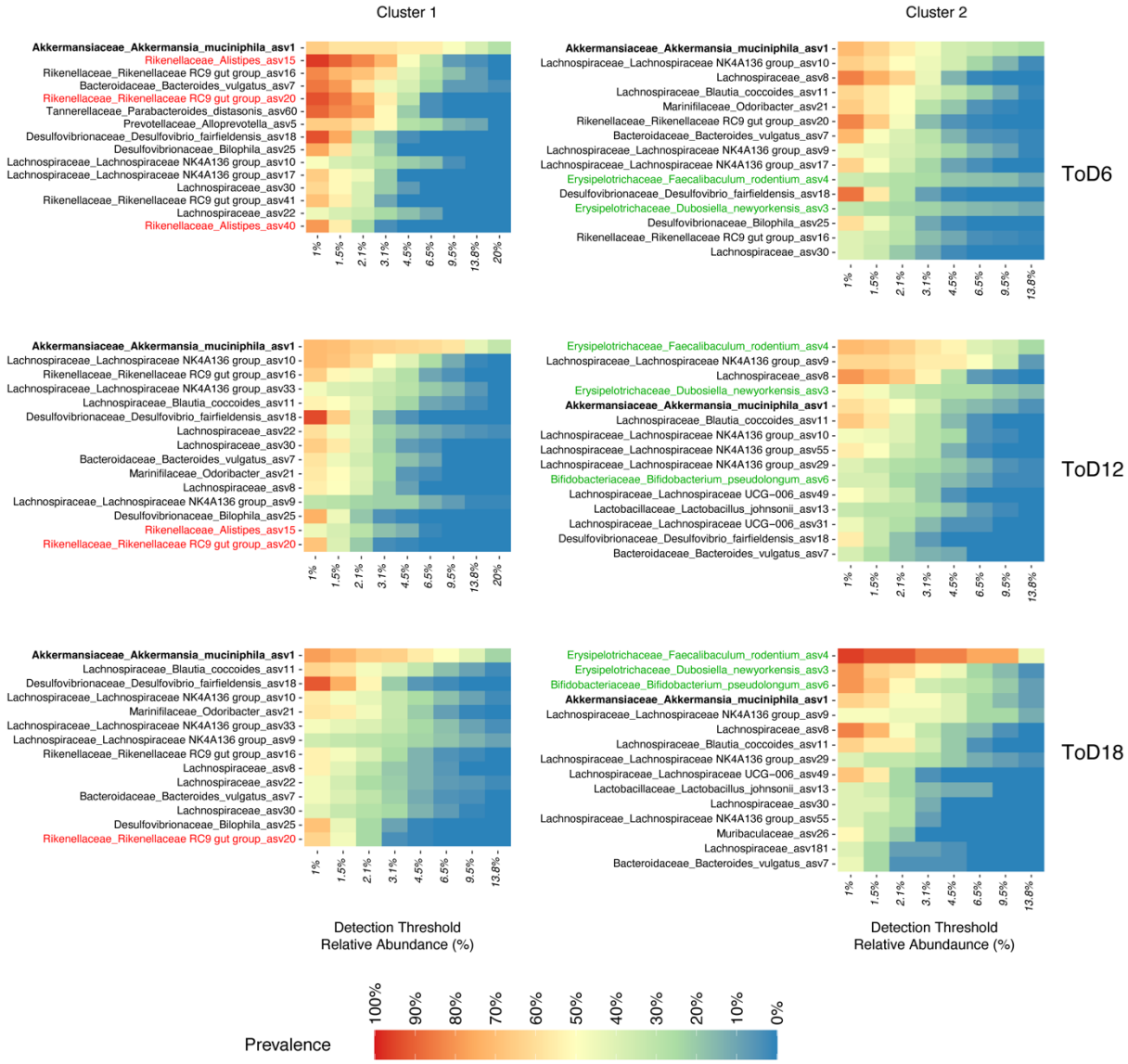

Figure 3-6. Heatmap of the core microbiome with the top 15 prevalent ASVs in each cluster. Left panel is cluster 1 and right panel is cluster 2. From top to bottom are ToD6, ToD12 and ToD18, respectively. Representative ASVs for each community type (red for community type I and green for community type II) were determined via comparing two clusters at each timepoints via ALDEx2 (results are in Supplementary Table 7-5). ASV1 were marked bold as it were enriched in cluster 1 in the core microbiome analysis but not in differentially abundant in ALDEx2 analysis.

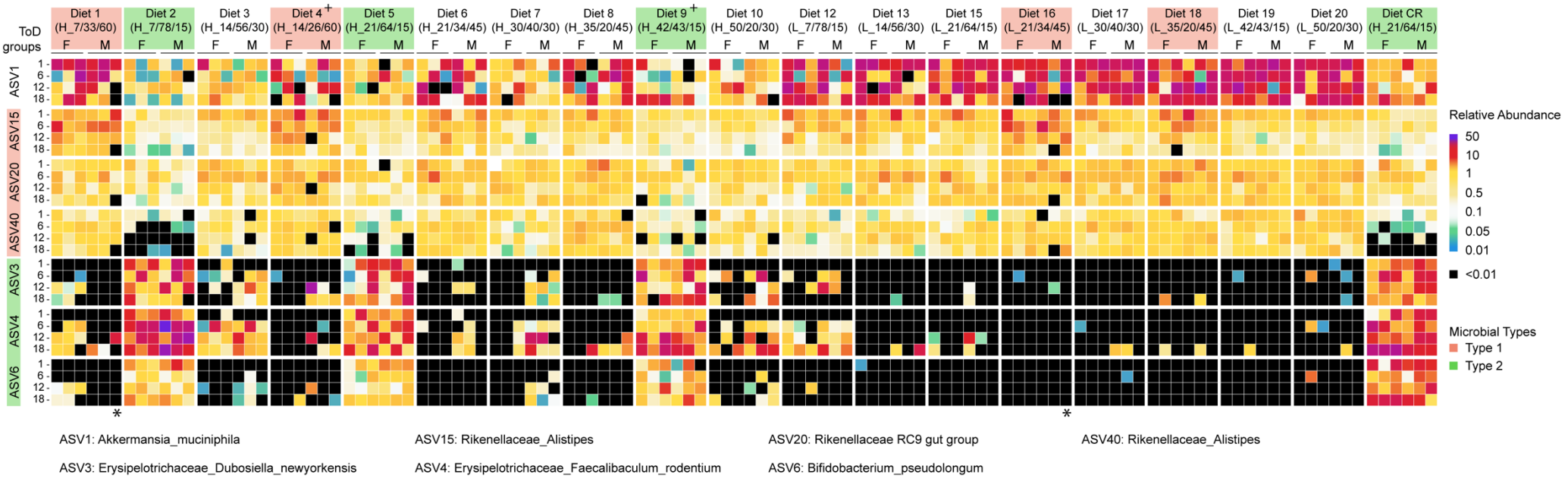

Figure 3-7. Relative abundance of selected taxa from each pam cluster.
Data are organized by diet with each set of 6 columns representing the 3 females and 3 males on that diet. The green or red highlighting indicates diets where the community type was stable from time on diet for 6 months and onwards (see also Figure 3-9). Each row in the table shows relative abundance for selected taxa that were differentially abundant (ASV1, 15, 20 and 40) or identified are discriminated taxa (ASV3, 4 and 6) for the two community types.
ASVs highlighting indicates ASVs representing each community type (red: community type I or green: community type II) based on core microbiome analysis (see also Figure 3-6) and/or ALDEx2 (see also Supplementary Table 7-5). For each ASV, data for ToD 1 (1 month on diet), ToD 6 (6 months on diet), ToD 12 (12 months on diet) and ToD 18 (18monts on diet) are shown in separate rows.
* In diet 1 and diet 9, 1 male mouse from ToD18 did not survive to expected age and died early. The black square for all ASVs represents no data available.
+ Diet 4 had one outlier in two timepoints. Diet 9 had one outlier in one timepoint (see also Figure 3-9).

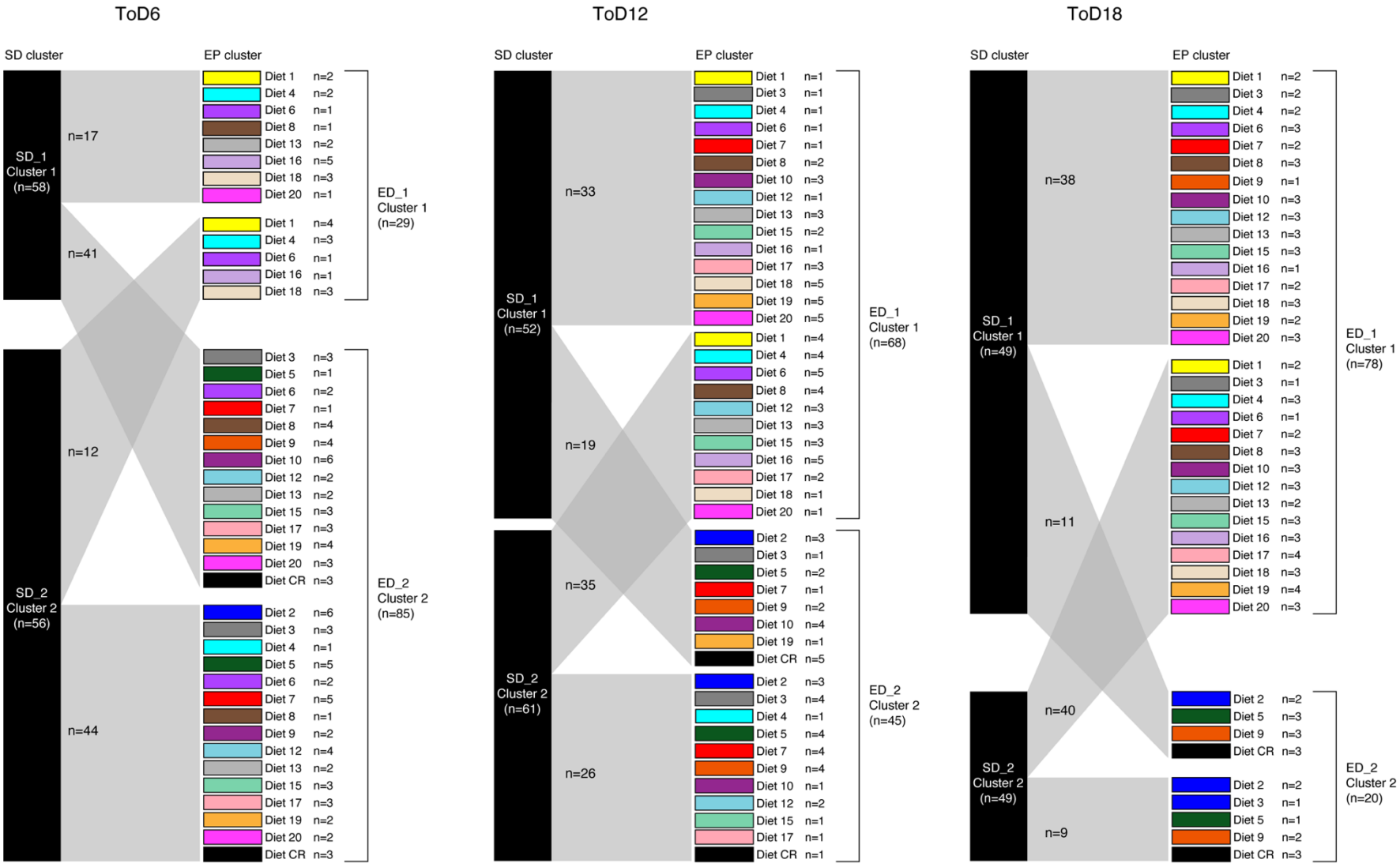

Figure 3-8. Sankey diagram of samples changes from SD cluster to EP cluster in each ToD group.
From left to right are ToD6, ToD12 and ToD18, respectively. Note that numbers of mice in SD cluster microbiomes are similar in all three ToD cohorts, but ED microbiomes are increasingly biased to cluster 1 with age – both diet and age influenced the adoption of a community type.

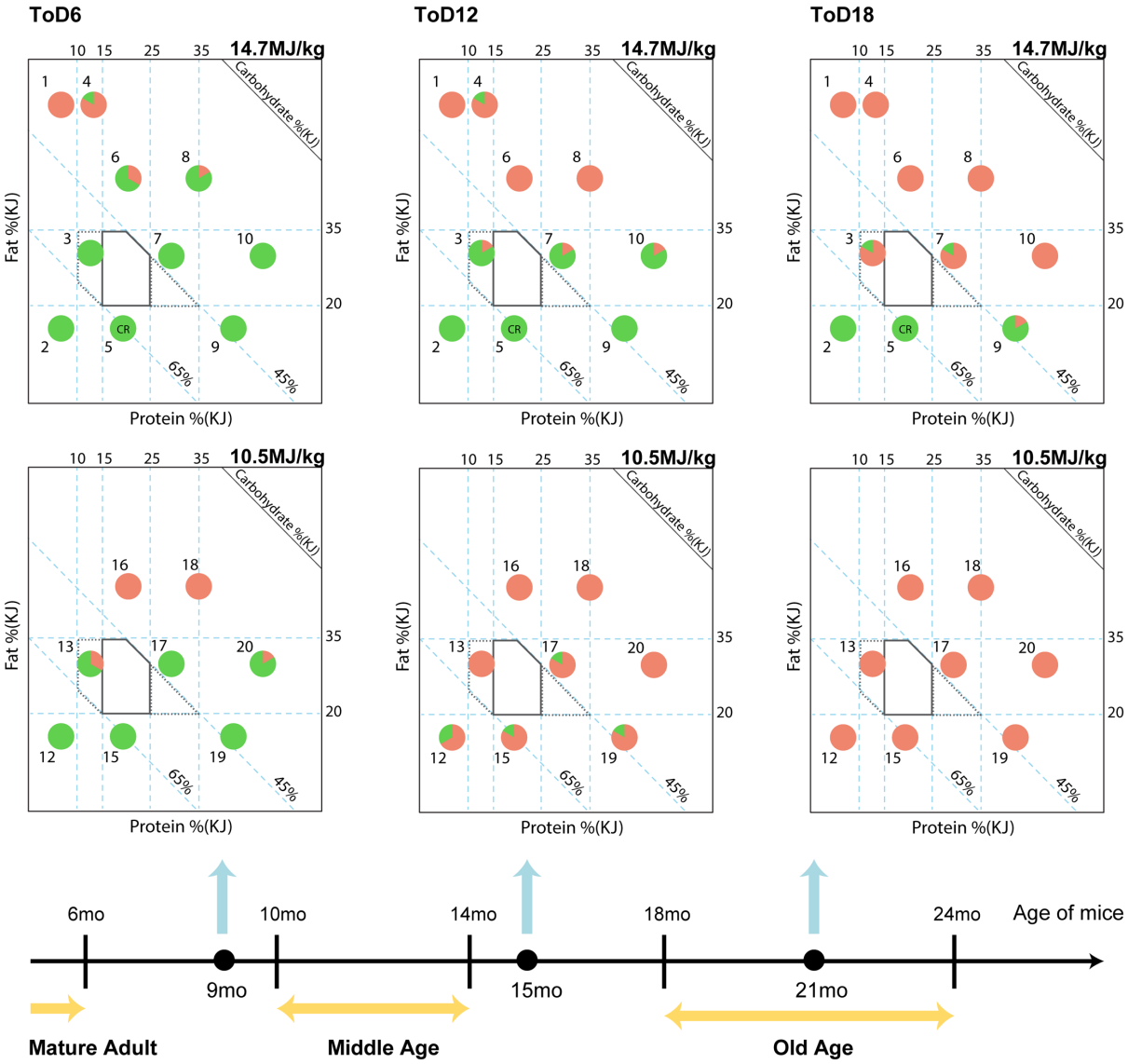

Figure 3-9. PAM EP cluster per diet in each ToD group represented on the macronutrient composition map.

Red represents cluster 1 and green represents cluster 2. Each circle represent 6 mice on that diet, regardless of gender. Microbial shift from Type 2 to Type 1 was indicated by the clockwise color shading. The timeline indicates the age of mice and its corresponding physiological age period.

3.3.4 Diet composition and time on diet/age interact such that both impact adoption of the two community states

The experimental diets differed in macronutrient ratios and energy densities, but had identical components. To explore the potential selective effect of different macronutrient distribution on the endpoint microbial types, taxa with high relative abundance or prevalence were selected from each type based on the core microbiome and ALDEx2 results. The relative abundance of these taxa in each individual mouse was plotted in a heatmap (Figure 3-7). Distinct differences were observed in the presence or absence of signature taxa from different types among individuals on specific diets. Signature taxa for microbial type1, were present in all animals, regardless which diets they were on. The selected taxa for microbial type 2, however, were

enriched primarily in Diet 2, Diet 5, Diet 9 and the caloric restriction diet. Moreover, Diet 1 and Diet 7 were also showing an selective effect for genders. ASV 3, ASV4 and ASV6 were found missing in males on Diet 1 and females on Diet 7. These results suggest that there might be associations among the microbial types, gender, dietary intake and, possibly, time on diet.

To further investigate the effect of diet and time on diet, all individuals were mapped together by diet, end-point community type (ED), ToD group and starting microbial type (Supplementary Figure 7-15, Supplementary Figure 7-16, Figure 3-8). These graph revealed that the clusters/microbial types were closely related to diet and time on diet. Samples on Diet 1, 16, and 18 were cluster together and stayed as the same microbial type (Type 1). Samples on Diet 2, 5 and CR were also clustered together but stayed as a different microbial type (Type 2). During the stabilization period (from 1mo to 6mo on diet), samples in ToD1 cluster 1 (Supplementary Figure 7-16) stayed as ED_1 (Supplementary Figure 7-15, Figure 3-8), except for Diet 8. Samples in ToD1 cluster 2 and clsuter 3 merged together and become the same type, ED_2.

When only looking at the stable period (6mo to 18mo on diet), 3 diets (Diets 2, 5 and CR) had a determinative effect on selection for ED_2. All individuals on these diets in ToD6, 12 and 18 developed a microbiome of this type irrespective of their starting diet microbiome type (Figure 3-8). 3 diets (Diets 1, 16 and 18) had a determinative effect on selection for ED_1. All individuals on these diets in ToD6, 12 and 18 developed a microbiome of this type irrespective of their starting diet microbiome type.

All other diets selected for the microbial types via a ToD/age-depended mechanism, regardless of the initial microbial type. Moreover, the microbial adoption time differs among diets. For Diet 6, 8, 13 and 20, individuals started to develop a microbiome type ED_1 from 6mo on diet. By 12mo on diets, all individuals have adapted to the new microbial type ED_1. For Diet 12, 15, 17 and 19, such process started between 6mo to 12mo on diets. More than half of its individuals became type ED_1. Diet 3 and 7 started changing of microbial types from 12mo on diet, and it took more than 6mo for them to finish the process. Finally, the adaptation didn't start in Diet 9 until 18mo on diet. In this study the mice's gut microbiome will eventually shift from type ED_2 to type ED_1 on 15 of the 19 tested diets. Diet differences in macronutrient intake pattern can delay or accelerate such process.

Figure 3-9 visualises where these diet compositions and community prevalence sit in a right-angled mixture triangle representation of macronutrient distribution. Interestingly, comparing to mice on low energy density diets, mice that were on a high energy density diets with low fat (less than 35%) content exhibited slower microbial adaptation towards diet selection. Altogether, this shows that both nutrient density and distribution interact to influence microbial community outcomes – but that the 'tipping points for adoption of a new community state shifts with either time on diet or age.

These data suggest that diet composition (or more strictly its constraint on macronutrient intake) is not the only factor that influences microbial community dynamics. Microbial community state is driven by the availability of nutrients. This is most strongly predicted by the nutrient composition of diets. A key observation here is that the association between nutrient composition of diets and microbial community type changes over time. Although, in principle, it could also be microbe evolution over time but it seems unlikely this would lead to such consistent change in association with diet. Therefore, I hypothesize that this reflects an aspect of aging biology whereby the capacity of the animal to modulate the microbiome by immune and/or nutrient control changes over time.

(i) Change in immune functions with age mean organisms whose competitive access to nutrients was suppressed in youth has been relaxed.
(ii) Change in GIT and metabolic functions with age mean nutrient sequestration by the animal is less regulated making more nutrients available to gut microbes.

3.3.5 The adoption of the two community states is associated with macronutrient energy intake

To test how the dietary composition potentially driving for the microbial type change, a distance-based redundancy analysis (db-RDA) was performed using macronutrient intake data and the CLR transformed microbiome data at ASV level. The macronutrient intake was calculated from mice 24h food intake data as a cage average. For the caloric restriction mice, the food intake was fixed as 2.8g for males and 2.7g for females. Then, the three macronutrients' energy intake was mapped onto the Bary-Curtis dissimilarity PCoA plot at each time point (Supplementary Figure 7-15). The db-RDA PCoA plot (Figure 3-10) showed that diet formulation/ macronutrient intake was the major driver of the clusters. Moreover, samples belonging to endpoint microbial type 2 (ED_2) gradually shifted to microbial type 1 (ED_1) with time on diet/aging. At 1mo on diet, cluster 1 and cluster 3 were both associated with protein and fat intake, while cluster 2 was associated with carbohydrate intake. After the microbial community became stable (6mo on diet), microbial Type 1 correlated to fat intake

only, and Type 2 was evenly affected by both carbohydrate and protein. As time went on, more samples were shifted to Type 1, and protein became more weighted in Type 1. By 18mo on Diet, Type 2 was more or less impacted by carbohydrate energy intake only. This suggests that on these simplified-defined diets, the drivers of microbiome were protein and carbohydrate intake vs fat intake as previously suggested in Holmes, Chew et al. (2017). Aged people were found altered protein metabolism (Dangin, Guillet et al. 2003, Milan, D'Souza et al. 2015), which affects the protein availability to the dietary forging microbes and causes a compositional change in the microbiome. Microbial clusters may be "artifacts" of analysis, but they also consistently reflect meaningful biological drivers.

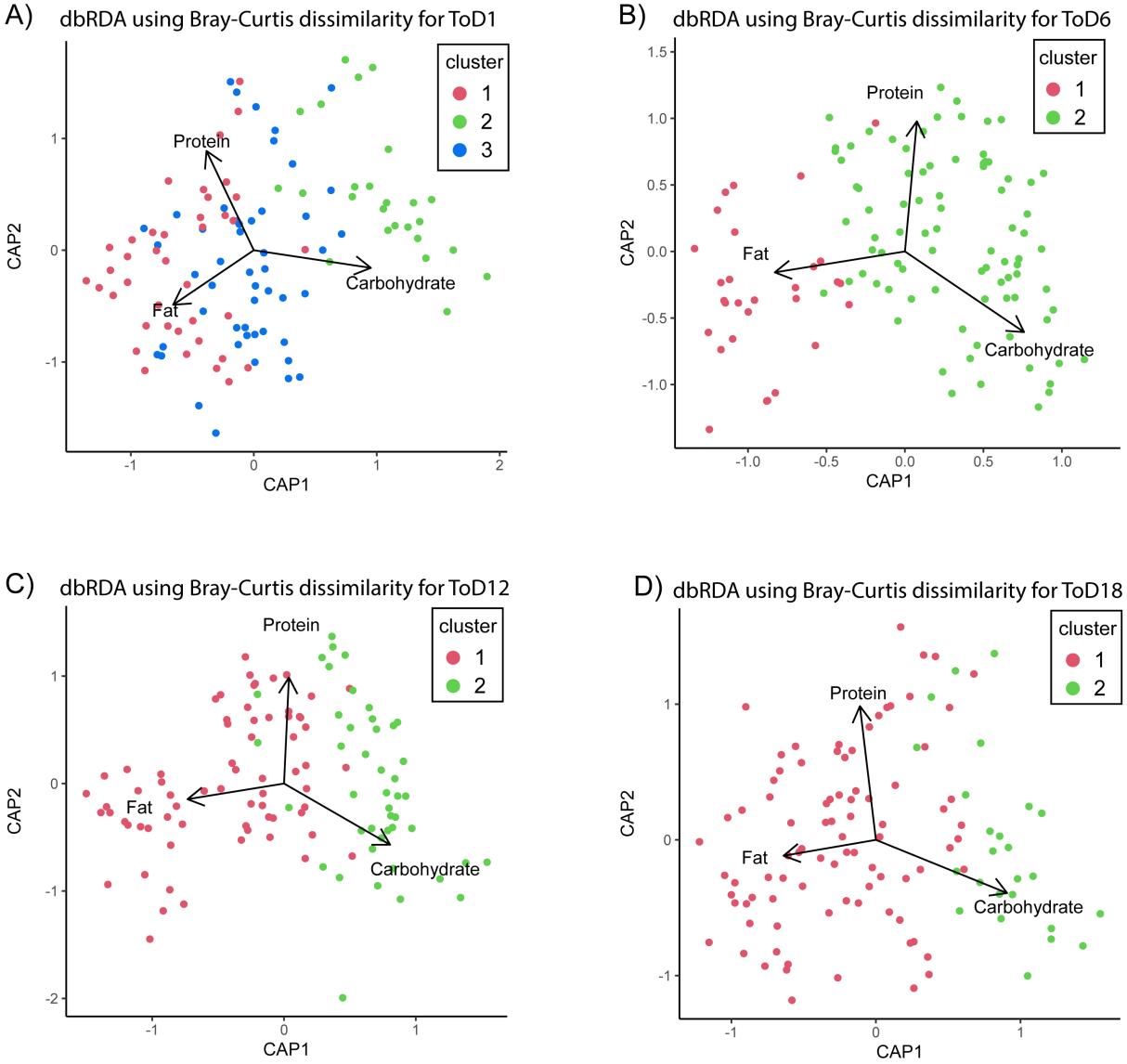

Figure 3-10. Distance-based redundancy analysis with macronutrient 24h energy intake and Bray-Curtis dissimilarly at ASV level for each ToD group.
Microbial data color coded according to the PAM clusters. A) ToD1 group, B) ToD6 group, C) ToD12 group and D) ToD 18 group.

3.3.6 Why does the effect of macronutrient intake on community structure change over time

I postulate that the community type changed over time is due to the age-related physiological changes. The changes in appetite, digestion, and nutrient absorbance alters the nutrient availability to the microbes. The generalized additive models (GAMs) was able to model the individual ASVs response to the diet over time. The GAM model assumes that each ASV has the same nutrient requirement over time. However, the nutrient available to the population has changed during aging, thus shown as change in nutrient response towards the dietary intake.

The response of individual taxa to macronutrient intake was, then, analyzed in further details using a three dimensional GAM. In this model, the macronutrient energy intake values of the mice in each ToD group were used as predictors to generate a macronutrient space. The microbial alpha diversity at ASV level (Supplementary Figure 7-19), CLR transformed microbial data at phylum level (Supplementary Figure 7-18), family level (Supplementary Figure 7-17) and ASV level (Figure 3-11) was then mapped into the nutrient space to make a response surface. It is assumed that the same microbes had the same nutrient requirement over time. However, age-related physiology change resulted in altering nutrient availability, and the microbes may need alternative nutrient source for growth. This reflects as difference in GAM response to the dietary nutrients. Therefore, looking at GAM response at different age groups can give an insight on the interactive between dietary macronutrient intake and age with adoption of distinct microbiome states. A total of seven different intake factors were modeled with GAMs, including three stand-alone macronutrients (protein, fat, and carbohydrate) and the interactions between them. This model allows for the prediction of microbial behavior in various nutrient environments. As mentioned in section 3.3.1, the microbial composition gender difference was small. Thus, the modelling did not differentiate between females and males.

GAM used the existing data points to create response surface, which then can be used for prediction. Therefore, sufficient data points were required for accurate prediction results. Due to individual variance of the microbiome, ASVs in one sample do not necessarily appear in other samples. To ensure the power of prediction, out of 372 ASVs, ASVs with less than 33.3% prevalence were removed from modelling. This is equivalent to one ASV present at least in 2 individuals in each diet, 1 male and 1 female. Such filtering step was applied separately in each ToD group. Thus, I ended up modelling 167, 222, 165 and 192 ASVs in ToD groups 1, 6, 12 and 18 respectively. After combined the results for analysis, there were 238 unique ASVs in

total. Among these 238 ASVs, 24 were unique to ToD6, 8 were unique to ToD18. For the ASVs that were not unique to certain ToD group, 11 ASVs had no significant response in any ToD group, and 31 ASVs only had significant response in 1 ToD group (non-unique ASV to that ToD group). Therefore, ending up with 164 ASVs which were used for analyzing the changing of response to nutrients over time on diet/aging. Both the lowest Akaike information criterion (AIC) value and highest deviance explained were used to identify the best-fitting GAM to determine whether dietary macronutrients had the strongest impact on each ASV. During the comparison, all AIC values were rounded to the nearest integer. In the case when the models have the same AIC values, whoever had a higher deviance explained was picked.

Macronutrient intake had a strong dominant role (GAM: >20% deviance explained) in 26.3 % ASVs at ToD1, 49.5% ASVs at ToD6, 30.3% ASVs at ToD12 and 41.7% ASVs at ToD18 (Figure 3-11). Differences in ASV response were observed in each ToD group. Among the 164 ASVs, only 44% were consistently responded in all 4 time points. In the rest of 56% ASVs, 39 of them were either filtered out (<33.3 prevalence) or did not have significant responses at an early adulthood, 3mo to 6mo on diet (32 ASVs at ToD1, 7 ASVs both at ToD1 and ToD6). However, they showed responses at older ages (12mo and 18mo diet). 21 ASVs gave the opposite effects, responses at an early age but not at older ages (12 ASVs no responses at ToD18 only, 9 ASVs no response both at ToD12 and ToD18). 12 ASVs only responses at ToD6 and ToD12. For the consistent responders (76 ASVs), 67%-87% of them responded to a combination of nutrients, rather than a single nutrient (Figure 3-11). Out of the 8 ASVs that were selected from the core microbiome analysis, 7 of them were also modelled in GAM analysis. These ASVs were marked in red in Figure 3-11.

Many taxa showed a different response surface at different timepoints. This is consistent with changes in how dietary intake influences nutrient availability to microbes with age, but could also be explained by other factors. ASV1 (*Akk. muciniphila*), one of the selected ASVs for microbial type I, was present in all samples at all time points. At ToD1, a GAM was derived revealing carbohydrate intake (18.6%), fat intake (3.9%) and a combination of all nutrients intake (15.7%) significant explained deviation with *p*-value greater than 0.05 (Figure 3-11B). The best fit model (lowest AIC) was carbohydrate intake (highlight in green in Figure 3-11B). A response surface is shown in Figure 3-12A indicating increase in ASV1 relative abundance under lower nutrient intake with the main effect due to carbohydrate intake but also an interaction with P and F. Interestingly, the model fit was much poorer at ToD6 (no model with

significance was generated) and ToD12 (low explained deviance), but significantly stronger at ToD18 (Figure 3-11 table). For ToD18, carbohydrate intake no longer showed a main effect and interactions between carbohydrate and protein were more important. A response surface in Figure 3-12A showing an negative response towards such interaction as indicated by the intensity of the response.

A consequence of the compositional nature of relative abundance data is that this outcome could reflect change in growth outcomes for ASV1 (net population size) or change in other populations. Here it is likely that a significant contributory factor was the marked increase in ASV4 (*Faecalibacterium rodentium*) and ASV3 (*Dubosiella newyorkensis*) on most of the high energy density diets especially with long ToD, but not with low energy density diets. Not enough data points were available for both ASVs to generate a GAM model at ToD1 (Figure 3-11 table). For both ASVs, stand-alone protein has the least effects, as no significant model was generated. However, when in combination with other nutrients, carbohydrate in particular, showed an effect on microbial growth. It is important to note that, carbohydrate was selected as the best model for ASV3 at ToD12 (lowest AIC value). However, the model of the interaction between P+C and fat intake was able to explain the largest deviance (36.3%) with a slight higher AIC value than the carbohydrate alone model (517 vs 513). This indicates there was a trade off when coming to selecting the best model for the data. By ToD18, both ASVs has support an interaction between P+C and F intake as a driver, which explained the deviance of 31.6% for ASV3 and 35.5% for ASV4, respectively.

Among the three single nutrients, the models reveal that fat was the strongest driver, especially at older age. In particular with ASV3, at ToD18, fat intake model showed 27.5% deviance explained, comparing to 8.8% for carbohydrate intake and no model generated for protein. For ASV4, the driving force of fat was less dramatic, with only 3.8% deviance explained higher than the carbohydrate intake model. Due to low in total sample size and uneven distribution among diets, it is not possible to generate a response surface for ASV3 and ASV4 to understand the direction of the response. Instead, direct correlation was plotted between the nutrients energy intakes and the relative abundance of ASV3 and ASV4 (Figure 3-12B and C). The scatter plot showed a trend of negative correlation between the taxa relative abundance and fat caloric intake. Such outcome was more acute with aging. This indicates the probability that fat suppress the growth of these two ASVs.

Moreover, positive correlations were found between the taxa relative abundance and both the carbohydrate and protein intake, which was the total opposite from ASV1 as indicated by the response surface (Figure 3-12A). All three ASVs had an effects on the interactive effect of protein and carbohydrate as shown in the tables in Figure 3-11. Age-related changes in nutrient availability likely affected the growth of ASV1, driven by shifts in the populations of ASV3 and ASV4. This indicates that ASV1 and ASV4 (together with ASV3) are the 'best' biomarkers for community types 1 and 2 respectively. This strongly supports the idea that dietary macronutrient intake and age interact to influence the adoption of distinct microbiome states.

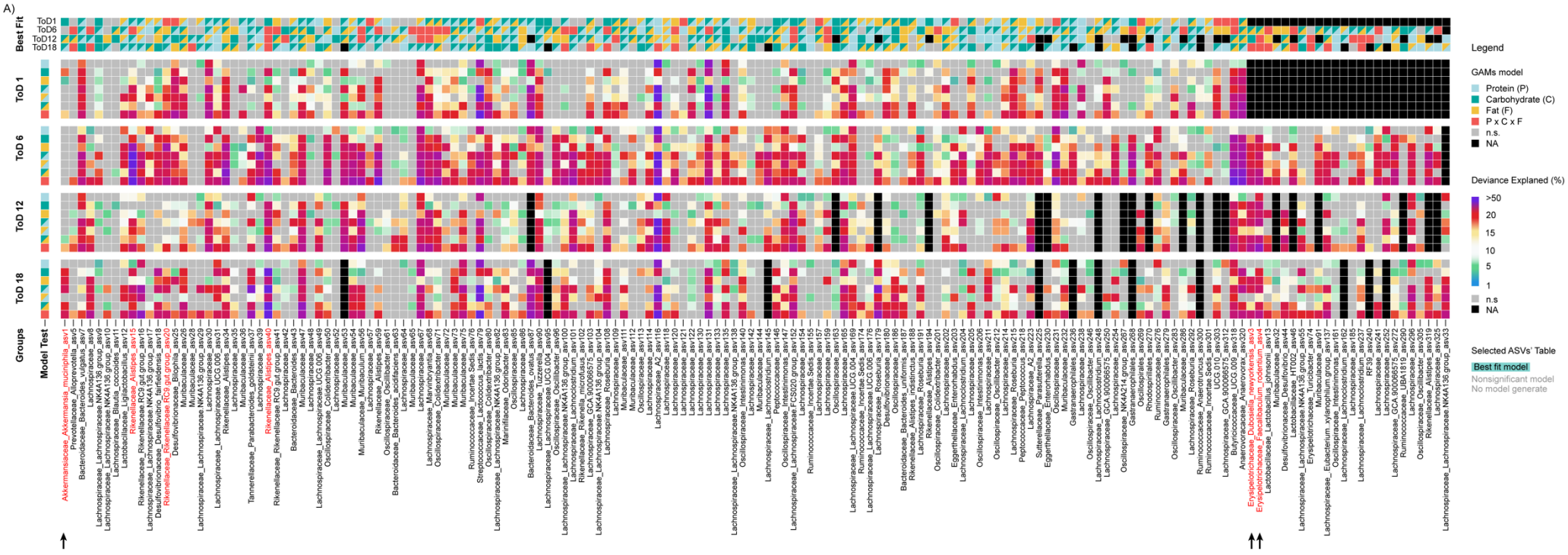

B)Akkermansiaceae_Akkermansia_muciniphila_asv1

GAM significance	ToD 1			ToD 6			ToD 12			ToD 18		
	p	AIC	*Dev (%)*	*p*	AIC	*Dev (%)*	*p*	AIC	*Dev (%)*	*p*	AIC	*Dev (%)*
Prot	n.s.	499	2.3%	n.s.	540	1.4%	n.s.	523	11.6%	n.s.	488	4.7%
Carb	0.016	489	18.6%	n.s.	539	2.5%	n.s.	524	2.2%	0.005	476	20.7%
Fat	0.035	496	3.9%	n.s.	542	0.0%	n.s.	523	7.4%	0.003	474	23.7%
P x C	n.s.	493	11.4%	n.s.	541	2.7%	n.s.	522	10.3%	0.000	468	27.6%
P x F	n.s.	497	5.9%	n.s.	542	1.4%	n.s.	524	8.5%	n.s.	486	10.2%
C x F	n.s.	495	7.7%	n.s.	540	3.2%	0.025	520	6.4%	0.000	469	20.2%
P x C X F	0.032	497	15.7%	n.s.	551	5.8%	0.023	522	16.4%	0.000	472	27.3%
N data points	111			111			108			106		

Erysipelotrichaceae_Dubosiella_newyorkensis_asv3

GAM significance	ToD 1			ToD 6			ToD 12			ToD 18		
	p	AIC	*Dev (%)*	*p*	AIC	*Dev (%)*	*p*	AIC	*Dev (%)*	*p*	AIC	*Dev (%)*
Prot	-	-	-	n.s.	552	1.8%	n.s.	546	12.8%	n.s.	535	0.5%
Carb	-	-	-	0.000	531	17.5%	0.000	513	29.0%	0.002	525	8.8%
Fat	-	-	-	0.000	524	23.5%	0.001	531	25.9%	0.000	512	27.5%
P x C	-	-	-	0.000	527	22.1%	0.000	515	29.4%	0.003	517	25.6%
P x F	-	-	-	0.000	526	24.4%	0.006	539	15.7%	n.s.	529	10.2%
C x F	-	-	-	0.000	517	30.5%	0.000	515	31.6%	0.025	524	14.9%
P x C X F	-	-	-	0.000	522	33.8%	0.000	517	36.3%	0.000	510	31.6%
N data points	27			43			45			44		

Erysipelotrichaceae_Faecalibaculum_rodentium_asv4

GAM significance	ToD 1			ToD 6			ToD 12			ToD 18		
	p	AIC	*Dev (%)*	*p*	AIC	*Dev (%)*	*p*	AIC	*Dev (%)*	*p*	AIC	*Dev (%)*
Prot	-	-	-	n.s.	559	5.6%	0.005	574	23.1%	n.s.	564	5.3%
Carb	-	-	-	0.000	524	29.8%	0.000	541	33.7%	0.000	540	22.1%
Fat	-	-	-	0.000	541	24.0%	0.000	559	30.4%	0.001	547	25.9%
P x C	-	-	-	0.000	524	30.8%	0.000	540	35.6%	0.000	536	30.3%
P x F	-	-	-	0.000	539	23.1%	0.012	577	12.5%	0.019	558	12.4%
C x F	-	-	-	0.000	520	34.6%	0.000	543	34.3%	0.000	540	25.8%
P x C X F	-	-	-	0.000	527	37.3%	0.000	538	44.2%	0.000	535	35.5%
N data points	26			52			52			68		

Figure 3-11. ASVs response to nutrients varies across difference timepoints.

A) Heat map of best model fit result from GAM modelling. Rows 1-4 were the best fitted model for each ASV at the 4 timepoints. The best model was determined based on a combination of lowest AIC values and highest deviance explained by each model. Color indicates best model fit to a single nutrient (single colored squares), an interaction of two nutrients (diagonally splitted coloured squares) or the interaction of all three nutrients (red colored single square). Not all taxa gave a significant model (grey squares, *p*-value > 0.05) or were able to generate a model at all (black squares, data points < 33). Statistic for indicates taxa (pointed by arrows) are in the tables in panel B. The direction of response is given by the intensity of response in the response surface or the correlation scatter plot in Figure 3-12. The rest of the rows are the % deviance explained by dietary nutrient dimensions. From top to bottom panels are time on diet for 1mo, 6mo, 12mo and 18mo. Within each panel, each row represent one nutrient dimension, from top to bottoms are, protein, carbohydrate, fat, interaction between two of the macronutrients and the interaction among all three nutrients. The ASVs that were marked as red were that ones that selected out from core microbiome analysis. B) GAM model statistical results for 3 picked ASVs. Model with no significance were indicated as grey, the best model pick was highlighted in green and highest deviance explained was marked in red. Full model statistics are in appendix (Supplementary Table 7-6, Supplementary Table 7-7, Supplementary Table 7-8 and Supplementary Table 7-9).

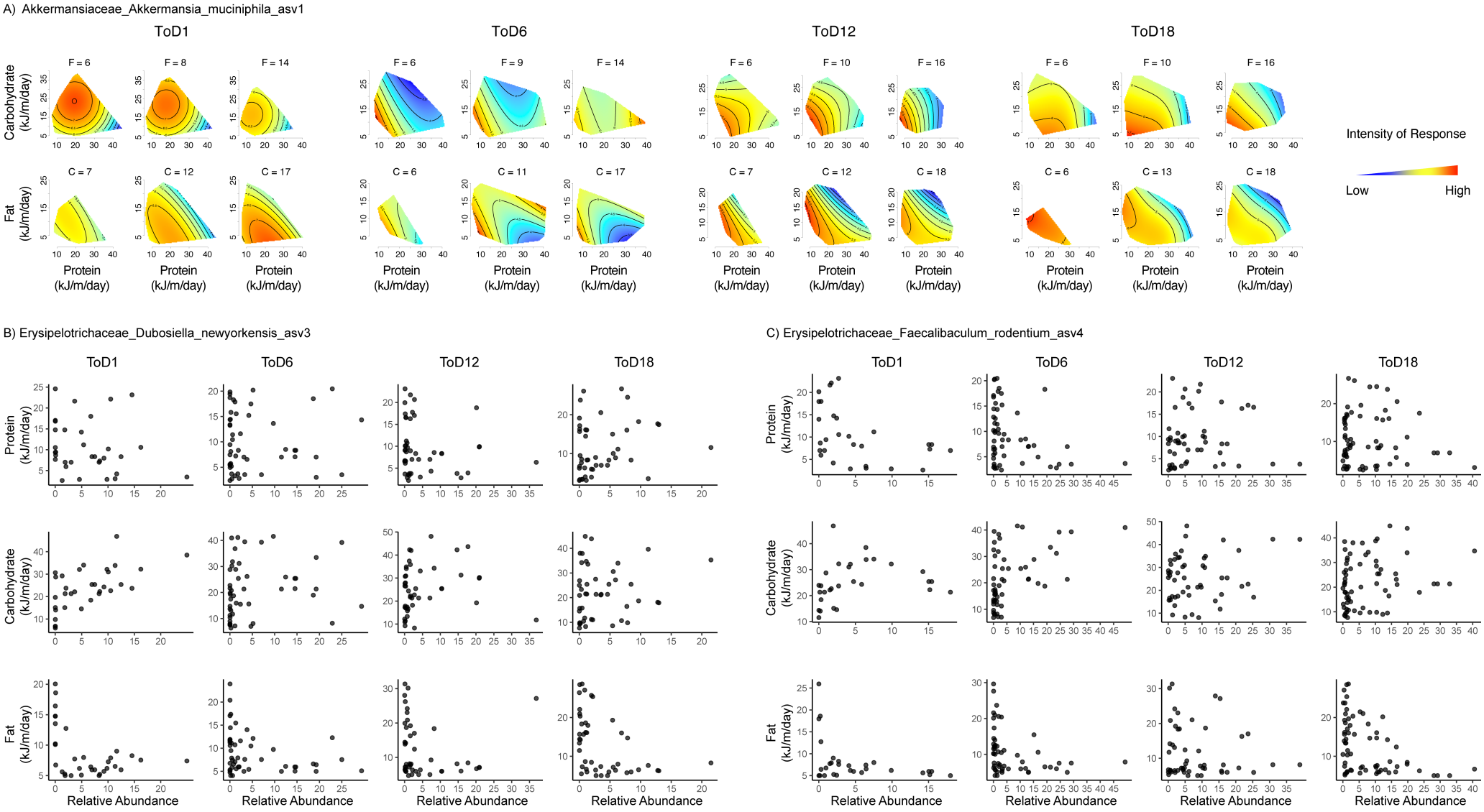

Figure 3-12. Representative ASVs of different repones profiles at different timepoints.
The nutrient response behaviors for the three ASVs marked red in Figure 3-11. A) The response surface resulted from GAM modeling for ASV1. The response surface includes six 2D response surface slices at each timepoint, three for carbohydrate vs protein and three for fat vs protein. These surface slices were visualised at the 25%, 50% and 75% quantiles of fat or carbohydrate consumption (kJ/m/day), respectively. The intensity of the response was shown as highest in red, and lowest in blue. The intensity of response surface showed the direction of the response to nutrients. B) and C) are the correlation between three nutrients intake (energy intake per mouse per day) and the relative abundance of ASV3 (B) and ASV4 (C) at four different timepoints.

3.4 Discussion

The formation of a gut microbiome is complex, it is an interaction process of initial colonization, assembly and succession. The gut microbiome of an adult is a dynamic adaptive system, response to the changes in the surrounding environment. Microbe fitness in the gut community is driven by nutrient supply and stress limits. The microbe nutrient environment consists of 4 aspects, food supplied from the diet, animal ingestion, animal physiology and microbe-to-microbe competition. During the process of aging, animals' undergo a series of changes in physiology, appetite and metabolism. Aged people were found to have reduced appetite, food digestion and nutrient absorption (Zhu, Devine et al. 2010, Otsuka, Kato et al. 2016), which delayed and reduced the nutrient availability to the microbes. They are constantly competing for nutrients to survive. Limiting the nutrient source exaggerates such competition and eliminates populations from their shared habitat (Fredrickson and Stephanopoulos 1981, Ghoul and Mitri 2016). Changing in nutrient environment thus causes age-related microbial evaluation.

Under selective pressure, microbes that are not fit to the changes reduce their population dramatically and eventually went distinction. Alternatively, microbes can adjust and adapt to the new environment. They can derive into a new species that fits the new environment (Brucker and Bordenstein 2013), or change their forging habit to survive. Some microbes were able to forge carbon both from dietary protein and carbohydrate (Zeng, Xing et al. 2022). During the process of aging, the microbes were not aging with us. Instead, the microbes reproduce and replace by themselves.

Therefore, I hypothesise that microbe nutrient requirements stay the same over time, but that animal physiology changes in ways such that nutrient availability from a specific diet is altered. Concomitant changes in microbial community structure (or host immune functions) may act to further change the competition for nutrients or the stresses experienced by microbes. In this experiment, I manipulated the nutrient availability by diet formulation and assumed this is the main factor determining microbial nutrient availability in the gut while keeping other factors consistent. However, I did not test the effect of different components, as the study design used confined components to test the macronutrient ratios. The key observation was that the microbe-diet association changed over time.

In this experiment, all animals experience the same disturbance when transitioning from wholegrain to purified ingredients. The transition causes disturbance to the microbial community, result in assemble different community types according to the diet formula. Two microbial community types were identified using the PAM cluster algorithm after switching to purified diets. These two microbial types were recurrently observed in ToD6, ToD12 and ToD18. Microbial type I was dominated by *Akeermansia mucinphila* (ASV1) and microbial type II was dominated by *Facalibaculum* (ASV4). Although enterotyping was frequently used in microbial classification, there are some controversies about it due to its reproducibility (Knights, Ward et al. 2014, Costea, Hildebrand et al. 2018). Gut microbiome in laboratory mice were previously reported to have distinctive two enterotypes, one was dominated by *Bacteroides* and *Enterobacteriaceae* and the other was *Ruminococcus* and *Lachnospiraceae* (Hildebrand, Nguyen et al. 2013). These two enterotypes were different from both the baseline (SD) microbial types and the endpoint (ED) microbial types in this study. Multiple factors can result in such differences, such as different colonized microbes from the mother, different living environment (laboratory setting) and different food components from the lab diets. Therefore, enterotypes may be specific for different groups of individuals and the results may not be applied across different groups. However, enterotyping can be useful in understanding gut microbial activities and general health, if it is established for each group/population separately.

In my study, similar two microbial types were repeatedly observed in 3 groups of mice. For all 3 groups of mice, the two microbial types were consistently associated with 2 groups of diets, Type 1 with Diet 1, 16, 18 and Type 2 with Diet 2, 5, CR. Associations were found between the dietary macronutrient energy intake and the microbial community types. This indicates that there were common underlying biological mechanisms between the microbial type and the macronutrient energy intake. Moreover, microbial type switching was observed from Type 2 to Type 1 in 13 diets during aging. This suggests that either nutrient availability, stresses or a combination of both changed with time.

GAMs model was used to model the change in microbial relative abundance with macronutrients intake over time. Changing in nutrient response were found with microbes during aging. Opposite response towards carbohydrate and protein were found between the two selective ASVs, ASV1 and ASV4, for the two community types, respectively. Moreover, for ASV1, an increasing in response to fat was found during aging. Meanwhile, ASV4 was only

found animals that were having a low fat but high energy density food. At an old age, a close to linear correlation was observed between relative abundance of ASV4 and the fat intake. RDA analysis also showed that community type I linked to fat consumption, and type II to carbohydrate intake. This potentially suggests that the transition between community states 2 and 1 was primarily driven by fat intake. No significant model was generated with stand-alone protein intake for ASV4, indicating that protein had very little effect. This may be because animal adjust food intake to keep protein intake, when looking at actual food intake (Simpson and Raubenheimer 2005). The strength of this effect changed with age such that in very old animals, only these on extremely low fat were able to keep the community type with high energy density. Fat intake is associated with the secretion of bile acid, which can be further process by the gut microbiome into secondary bile acid. Aging leads to a decline in body function, which alters the composition of bile acid secretion and reduces the total amount of bile acids delivered to the intestine (Ferland, Tuchweber et al. 1989, Lee, Lee et al. 2016). Furthermore, age-related muscle loss slows gut transit time, allowing bile acids to remain in the gut for longer periods. These changes in bile acid hemostasis create conditions that favor bile acid-sensitive microbial populations, thereby altering the composition of the gut microbiome. To investigate this further, a detailed analysis of the bile acid profile in the cecal content is required. This examination will help to identify specific changes in bile acid composition and concentration within the cecum, providing deeper insights into how these alterations may influence microbial populations and overall gut health.

The age-related microbial community type change was likely due to the microbial compositional change (present/absent microbes). Difference in present and absent of microbes were observed in two microbial types and in conjunction with community types change (Figure 3-7). As the diets contain different macronutrient ratios and energy density, age-related metabolism changes cause different levels of nutrient competition among microbes. Some of the microbes were observed to persist through the physiological changes during aging via changing their response to nutrient intake (Supplementary Figure 7-17, Supplementary Figure 7-18, Supplementary Figure 7-19, Supplementary Figure 7-20). However, it is not possible with this method to distinguish between possible mechanisms for this such as mutational change and natural selection for variants. Moreover, although treated as the same, mice used in the 4 timepoints were different individuals. It is also possible, the difference in ASV response surfaces were simply individual variance among the ToD groups. To further test my hypothesis,

I should examine the microbial population in a longitudinal study, in which the same individuals were followed over time.

4 Characterising Longitudinal Microbial Temporal Stability over Lifetime

This chapter is under a project grant in collaboration with Prof. Steve Simpson at Charles Perkins Centre. The animal maintenance, other animal biological sampling and food/water intake recording were done by Dr. Amanda Brandon's team. Faecal sample collection, DNA extraction and microbial analysis were performed by me.

4.1 Introduction

Living organisms are dynamic systems that continuously change over time. Over a lifetime we can categorize these change processes as development, growth, adaptation/maintenance/repair and aging. Aging is distinct from the others in that it is 'unintentional' - it reflects loss in homeostatic control capacity owing to accumulation of 'damage' (Kirkwood 1977, Kirkwood and Holliday 1979). Development and growth are both 'capacity-building' processes that occur together with adaptive responses to maintain a stable body state (homeostatic control). All four are impacted by the external environment - both nutrient resources and stresses.

In the animal (or human) system, the somatic cells are clonally derived from the same origin after fertilization and gestational development of the embryo. It has a single genotype - but can adopt a range of different somatic states owing to epigenetic, regulatory factors interacting with environmental factors during development and growth. In contrast, the microbiome component of the holobiont is assembled from the external environment and thus additionally includes multiple genotypes. The concept of multi-stability has been proposed to explain its potential to adopt different stable states.

Healthy adult gut microbiome is in a constant equilibrium between different stable states in repones to short-term environment turbulence (Chang, VanInsberghe et al. 2020). However, long-term exposure to environmental stress causes microbiome state transition. (Blumberg and Powrie 2012) During aging, microbes experience long-time exposure to environmental cues like hormone and immune cytokine shift (McClanahan, Riches et al. 2015, Elyahu, Hekselman et al. 2019, Mogilenko, Shpynov et al. 2021, Pataky, Young et al. 2021, Wu, Muthyala et al. 2021). Different microbial compositions were observed for the aged individuals (Ke, Mitchell et al. 2021, Wilmanski, Diener et al. 2021, Wu, Muthyala et al. 2021). However, no data so far suggests when or how such state transition happens during aging. Longitudinal studies that follow individuals over period of time can track such process of microbial alteration during aging. By monitoring the microbial and host interaction over time, allows identify the relationship between age-related physiological change and microbiome change, thereby giving insights into potential host-microbiome interaction and the role of gut microbiome in aging.

In the previous chapter (Chapter 3), I showed that diet (both source components and nutrient compositions), assembly (primary colonization or starting microbiome) and time all have an impact on the microbial composition. However, I was not able to separate the relative

importance of chronic diet differences versus aging biology in both animal and microbiome compartments of the holobiont – this requires a longitudinal sampling design and the microbiome aspects are addressed here. In this study, the microbiome analysis focussed on an intensive sampling of a subset of individuals from a large cohort study of 1,008 mice. The aim is to understand the relative importance of different factors and how these factors interact with aging biology. I looked at the microbe evolution (evolutionary change in bacterial species), community recruitment (gain and loss of species over time), community resilience/stability (capacity to maintain a particular community structure), diet environment, nutrient intake and how these interact with aging biology (change in the animal behaviour and physiology over time).

In this part of the study, the number of diet formulations was reduced to 11 for reasons of feasibility. A subset of animals were intensively sampled to explore the effect on longitudinal gut microbiome dynamics over lifespan under different nutrient conditions. Controlled manipulation of nutrient intake was achieved through 9 diets with 6 different protein to carbohydrate ratios were selected from the 21 experimental diets used in Chapter 3. This includes 8 diets in *ad-lib* and a caloric restriction diet. These diets were having the same nutrient source but different energy densities. By keeping everything else the same, I am able to investigate how animals maintain their gut homeostasis under different macronutrient distributions during their lifetime. Additional 2 control diets, brown chow and AIN93G were also used as comparison.

As shown in Figure 4-1, to observe the process of how the microbiome adapts to the chronic physiological change over time, the mice were sampled at two temporal scales. Fecal samples were taken every 3 months for 15 months; then, the interval was shortened to every 2 months until natural death (or humane endpoint) to enable observation of correlations with physiological change associated with aging biology. It is known the gut microbiome varies on a daily basis (Johnson, Vangay et al. 2019). To account for such fluctuation, including gut microbial circadian rhythm, I also explored short-term temporal samples by collecting 4-5 independent fecal samples at each of the 2-3 monthly sampling windows.

The assessment of physiological aspects of aging biology was conducted on the whole cohort of animals throughout their lives. In previous chapter I showed that mice from the same cage shared a similar microbial structure. Therefore, microbial analysis was performed on a

randomly chosen focal mouse in each independent cage for 10 diets. Owing to the difference in lifespan, when the focal individual died, a cage mate was then followed until no animal survived in the cage. Thus, mouse of each gender was followed with overall 30-60 samples for the duration of adult life. In 1 diet, all 3 animals in the cage were followed to assess geographic effects. For these mice, one died early and giving a total of 5-60 samples per mouse.

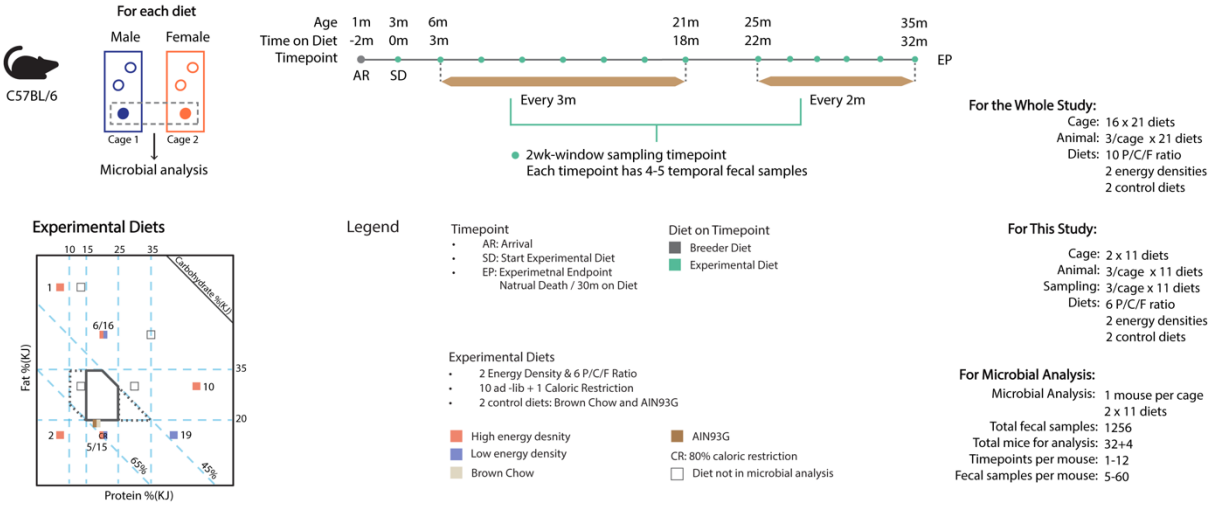

Figure 4-1. Experimental and diet design for the animal study reported in this chapter.
This experiment is a subset of a large longitudinal study, which took 11 out of 21 diet treatment groups for tracking microbial compositional change during aging. Each diet contains 1 cage of male mice and 1 cage of female mice. One focal mouse in each cage was followed every 3 months, then the sampling interval was shortened to every 2 months as the mice got older. At each time point, the mice were sampled 5 times (sampled every other day) in a 2 week-window period. Experimental diets used involving 9 diets from the previous chapter and 2 control diets, brown chow and AIN93G.

4.2 Methods

4.2.1 Animal

Male and female C57BL/6 mice (4 weeks old, n=66) were purchased from Animal Resources Centre (Perth, Australia). These mice arrived in 2 different cohorts with 20 days apart. They were randomly separated and housed three per cage in standard approved cages (Tecniplast GM500). They were fed standard chow for 8 weeks acclimation period before starting experiment diets (Specialty Feeds) At approximately 3 months of age, mice were provided with their experimental diets ad-lib, except for the caloric restriction mice. Each diet ended up having a cage of 3 male and a cage of 3 female mice. Mice feeding calorie restriction (CR) diet were having 20% restriction of food intake. For every 1g consumed by the diet H_21/64/15 (high energy density diet with a macronutrient composition C/P/F = 21/64/15) under ad-lib regime, 0.8g of the same food were provided to CR mice.

4.2.2 Diet composition

The experiment diets contain a total of 11 diets, involving 9 diets (8 ad-lib diets and 1 caloric restriction diet) from the age-related study in Chapter 3.2.2 plus two control diets, standard brown chow and AIN93G. The AIN93G used in this study is a modified diet with extra added vitamins. The diet compositions are given in Figure 4-1. Detailed source of nutrients composition was also provided in Supplementary Table 7-2. The 24h food and water intake were estimated as detailed in Chapter 2.2.2.

4.2.3 Sample collection

Fresh fecal pellets were collected every 3 months after having experimental diets for 3 months. Then, the collection interval was reduced to 2 months after having experimental diets for 18 months. At each collection window, 5 independent fecal samples were collected from each mouse between 10 am to 1 pm every other day during weekdays (over 10 days). The fecal samples were stored at -30^{o}C freezer until further processed.

4.2.4 Gut microbial analysis

For one mouse per cage, DNA extraction was performed as detailed in Chapter 2.2.3. Bacterial amplicon 16S rRNA gene sequencing was performed as detailed in Chapter 2.2.4. Microbial profiling was done with DADA2 as detailed in Chapter 2.2.5 with classification at the ASV level. Two filtering steps were applied, for abundance filtering an ASV must comprise of 0.01% of total reads, for ubiquity filtering an ASV must be present in at least 10% of samples. The number of sequence reads processed and filtered at each step is summarised in Supplementary Table 7-1. After filtering, the average reads per sample was 108,856.

4.2.4.1 MOFA+

To determine the feature-wise association of microbial ASVs and different time-on-diet groups or dietary groups, multi-omic factor analysis v2 (MOFA+) was performed using MOFA2 package v.1.6.0 (Argelaguet, Velten et al. 2018, Argelaguet, Arnol et al. 2020). Prior to performing MOFA+ analysis, centered log-ratio (CLR) transformation was done on the microbial abundance counts with the microbiome package v.1.18.0 (Lahti and Shetty 2018). A pseudo count of 0.5 was applied across the dataset to allow for the CLR transformation (Yamamura 1999)

For each analysis, the data input was arranged as 1 single view (1 single dataset) containing multiple groups, data grouped either as dietary groups (Figure 4-2A) or ToD groups (Figure 4-2B). Multi-group data arrangement was used so that I was able to get within group difference.

For example, when arranging data by dietary group, I can assess the age effect on the microbiome within a certain nutrient environment (the specific diet).

MOFA+ uses Bayesian inference and probabilistic models to estimate latent factors and associated the feature weight matrices to explain the variance across dataset (Argelaguet, Velten et al. 2018, Argelaguet, Arnol et al. 2020). For each analysis, 30 latent factors were used for model training. MOFA+ results were visualized using the built-in tools in the MOFA2 package. The analysis was followed on the R codes available https://biofam.github.io/MOFA2

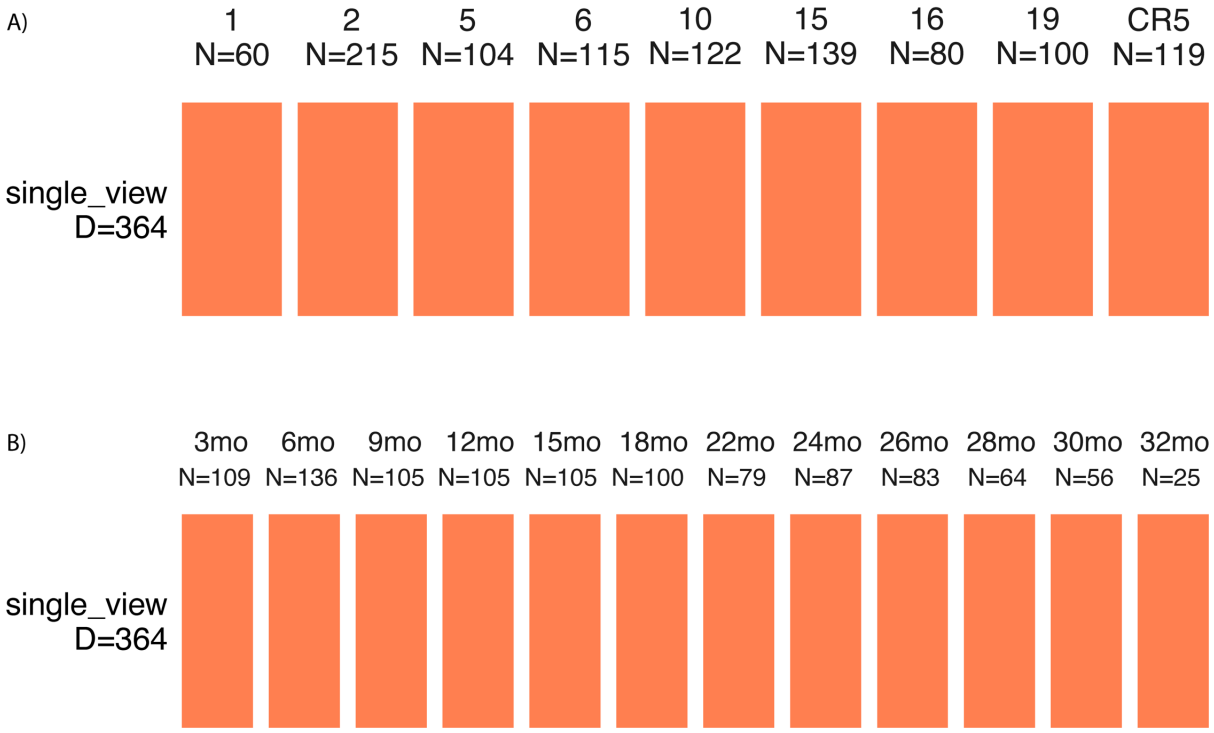

Figure 4-2. Data arrangement for MOFA+ analysis.
A) The data was arranged as a single view with multiple dietary groups. B) The data was arranged as a single view with multiple time-on-diet groups. D indicates 364 ASVs tested in this study.

4.2.4.2 Functional prediction

Bacterial metagenomes were predicted from bacterial 16S rRNA gene profiles with phylogenetic investigation of communities by reconstruction of unobserved states (PICRUSt) v1.1.4 by matching to the closest genome in the iMGMC database v1.3.0 (Lesker, Durairaj et al. 2020). Kyoto Encyclopedia of Genes and Genomes (KEGG) pathway were determined and annotated using ggpicrust2 package v. 1.7.2 (Yang, Mai et al. 2023). Differential abundance analysis was performed using ALDEx2 Wilcoxon rank test package v.2.28.1(Fernandes, Macklaim et al. 2013).

4.3 Results

Mice sourced from a common cage exhibit considerable variations in their lifespans. Considering these mice were from an identical genetic background, mice from the same cage were expected to have an similar microbial structure (Chapter 3). Therefore, in this study, a sequential replacement strategy was adopted to ensure of capturing the microbial landscape of these mice over their lifespans. Every mouse (all three mice in the same cage) in this study was samples. A random mouse (focal mouse) from each cage was used for microbial analysis. Occasionally, this focal mouse died much earlier than others in the same cage. There were five such cases. In these cases, a cage mate was randomly chosen as a replacement for microbial analysis (continued from the timepoint when the focal mouse was dead), until all mice in the same cage were died.

4.3.1 Dietary components have a strong effect on microbial composition

Diet component is known to have an impact on the gut microbial composition (Sonnenburg, Zheng et al. 2010, Holmes, Chew et al. 2017, Zeng, Xing et al. 2022). Different source of components affect the microbes via varying the accessibility to the microbes (Sonnenburg, Zheng et al. 2010). Additionally, when maintaining consistent source components, the distribution and intake of nutrients also play a role in shaping the microbial composition (Holmes, Chew et al. 2017). Microbes from different phyla were observed to exhibit preferences in dietary carbon or nitrogen from various macronutrients (Zeng, Xing et al. 2022). This study aims to look at the effect of nutrient distribution and intake on gut microbiome using 8 ad-lib diets and 1 caloric restriction diet. However, two control diets were also included, in which the source components were different (Supplementary Table 7-2).

To exam the effect of dietary components on microbial composition, the between-sample beta-diversity of all the samples (samples collected from all time points) was calculated using all three matrices, Bray-Curtis dissimilarity (Figure 4-3A), weighted UniFrac and unweighted UniFrac distance (Supplementary Figure 7-21). All three matrices showed that the microbiota of the mice were clustered together according to the food source. Overall, samples from mice on brown chow were clustered together and away from the samples that were having purified ingredients. In particular for 3 diets, the brown chow, AIN93G and Diet 5, which were matched in nutrient density. The main difference was that the brown chow contained more microbial accessible carbohydrate (MAC). This indicates that the 'chemical accessibility' of source macromolecule components to microbes has a bigger impact than their nutrients. When

nitrogen content (protein sources) was kept similar, then the nature of MAC is likely the strongest driver. Thus, the brown chow and AIN93G were excluded from further analysis of effects of macronutrient distribution so as to keep all the other variables consistent.

4.3.2 Diet and cage history have a larger impact on microbial composition than age

To better understand bacterial behaviour changes in response to environmental changes, multi-omics factor analysis v2 (MOFA+) was performed using CLR-transformed microbial ASV abundance. MOFA+ is an unsupervised statistical framework model that integrates multi-omics data into interpretable low-dimensional representations, helping identify sources of variation (Argelaguet, Arnol et al. 2020). The analysis was performed by testing for the diet groups or the age/ToD as the major source of variation either according to their dietary groups or according to time on diet.

MOFA+ latent factors from each analysis were then used to infer a non-linear manifold using MOFA+ built-in t-distributed stochastic neighbor embedding (t-SNE) tool. t-SNE is a technique to visualize high-dimensional data, as it is good at discriminating subpopulation (Platzer 2013, Li, Cerise et al. 2017). Both results show that the majority of the samples were clustered together by their dietary groups or/and cage gender/cage history (Figure 4-3B-a/d). Some exceptions were observed. With the analysis performed with samples grouped by time points, some samples from males on Diet 5 (dark green dots) are clustered with other samples (Figure 4-3B-a).

Although gut microbial composition was primarily effected by the diet, cage gender/ cage history also had a strong impact. Table 4-1 summarises the number of clusters assigned using MOFA+ analysis, with samples grouped by diet or ToD groups. The number of clusters were also associated with number of female/male mice used in the analysis. In Figure 4-3B-a/d, all samples on Diet 2 (light blue dots) were clustered close to each other and away from other diets. However, within the cluster, a clear separation was observed between the male and female cages (In Figure 4-3B-b/e). However, as only 1 cage of females and 1 cage of males was sampled in this study, I was not able to distinguish if such difference was due to gender difference or cage difference.

A unique 'geriatric microbiome' was not observed - age did not have a determinative 'global' effect when all the time points were considered, as the diet treatments still clustered

separately. However, aging biology (or senescence) did show some impact in that within each diet treatment group there was evidence for the time-based separation of response (Figure 4-3B-c/f). Within a dietary group, the samples were clustered together according to the time points, in particular, the younger time points were clustered together and away from the older time points. For Diet 6 (dark purple color), 3 clusters can be observed. 2 of the clusters belonged to the same male mice used in the study (Table 4-1, Figure 4-3B-c). These two clusters were separated far apart from each other (Figure 4-3B-c), with the left side cluster being samples from younger age (6 and 9 months on diet) (Figure 4-3B-d).

Both of the MOFA+ analysis results show that the microbial community structure is best explained by diet and cage/gender factors. Age also has an impact and can be seen within each individual. The difference in the microbial community over time could be caused by age-related animal physiological changes, or by microbial evolution in association with invasion of new taxa. However, such impact is minor compared to the diet and gender/cage history.

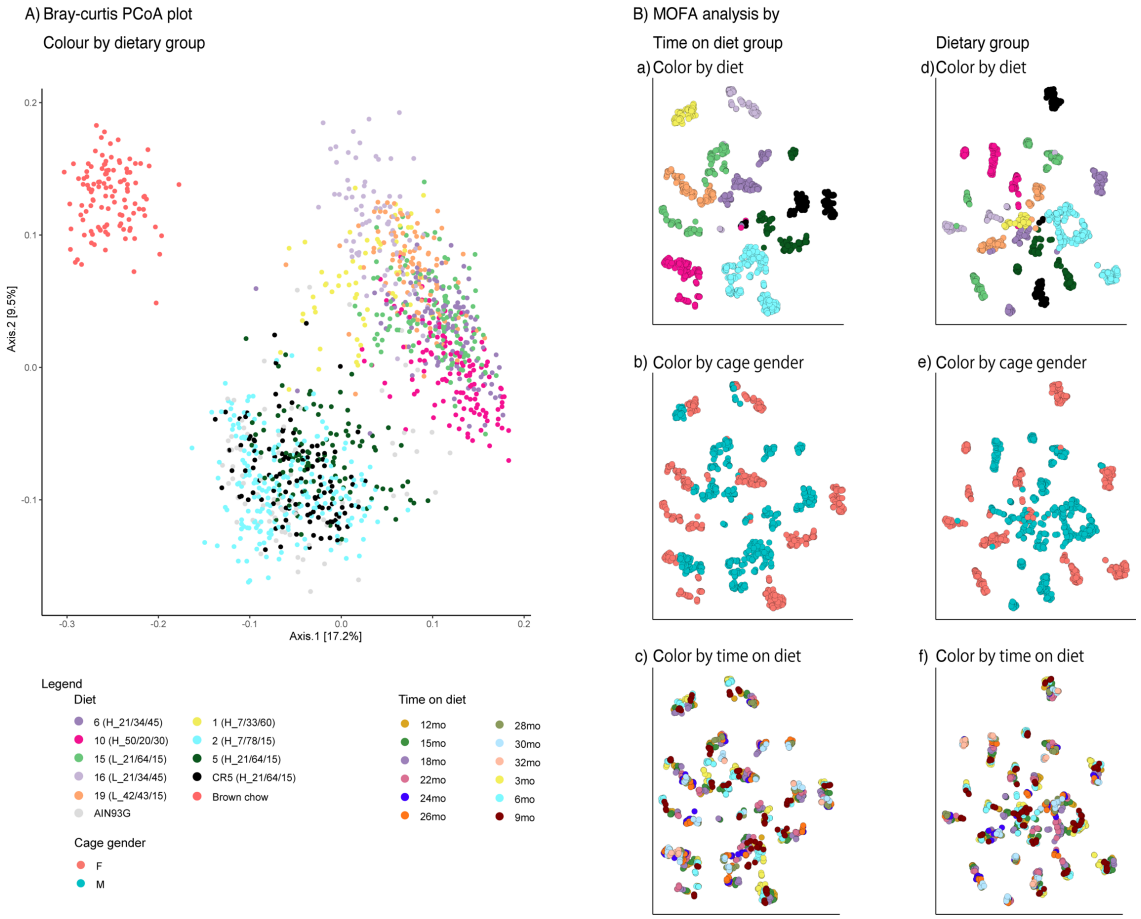

Figure 4-3. Diet and cage history are the primary effectors of microbial composition.
A) PCoA plot for Bray-Curtis dissimilarity of all samples, color by diet. (sample n = 1,526, mice n = 36). B) tsne-plot of MOFA+ result. Left panels (a-c), samples were analyzed by grouping by time on

diet; right panels(d-f), samples were analyzed by grouping by dietary groups. From top to bottom, the samples were colored by diet (a, d), cage gender (b, e) and time on diet (c, f), respectively.

Table 4-1. Number of clusters assigned by MOFA+ analysis

Diet	# of cluster (group by diet)	# of cluster (group by ToD)	# of mice	Comments
1	1	1	1M, 1F	-
2	2	2	1M, 1F	-
5	3	3	1M, 2F	2 clusters for male
CR5	2	2	1M, 1F	-
6	3	3	1M, 2F	2 clusters for male
10	3	2	1M, 2F	2 clusters for female
15	4	3	2M, 2F	2 for each in diet 2 for female in ToD
16	2	1	1M, 1F	-
19	2	2	1M, 1F	-

4.3.3 The effect of time is diet-dependent

First of all, the microbial response in each diet will be examined using MOFA+ analysis with data grouped by diet. MOFA+ analysis was performed using 30 different latent factors. Each latent factor contains a group of ASVs with different loadings. Among the factors examined, 29 meaningful factors were identified (Figure 4-4A), collectively explaining around 50% of the total microbial composition per diet (Figure 4-4B). The exception is Diet 1, for which only 18% of the total variance is explained. For each diet, 1 to 3 factors were enough to explain the majority of the variance.

Two different types of outcome were recognised. Diet 10 and 16, showed both strong gender/individual and age effect on microbes. With these diets, two groups of microbes were found associated with gender/individual and age effects, respectively. For example, Diet 16, factor 4 and 8 are the predominant ones that explain close to 50% of its variance (Figure 4-4A). Factor 14 (Figure 4-4C) and factor 4 (Figure 4-4D) are associated with the difference with respect to time on diet (aging) only. Samples from younger ages were cluster together and away from the samples from older ages. Meanwhile, factor 21(Figure 4-4C) and factor 8 (Figure 4-4D) was associated with primary the difference in gender/individual, where female samples were clustered together and away from the males. For factor 8 but not factor 21, age effects were also observed with the same gender mice from these factors.

Supplementary Figure 7-22 gives the top 20 weighted ASVs in 8 and 4. ASVs belongs *Baclli_RF39*, *Lachnospiraceae* and *Muribaculaceae* are associated with differences between gender/individual, while different sets of ASVs belonging to *Muribaculaceae* and *Lachnospiraceae* are associated with the time on diet/ chronological age. The negative sign in the plot means that ASV is heavily weighted on the samples located at the negative axis on the factor activity plot. *Akkermansia* was found to belong to both factors, which means that it is overrepresented in the young (3-9mo on diet) male mice.

Alternatively, one major group of microbes was responsible for both the gender and age difference like factor 11 for Diet 6 (Figure 4-4E). However, not all diets showed a strong impact of aging. For caloric restriction diet, for example, the predominant group of microbes, factor 10, can only explain the variance in gender/individual differences, not the age effect (Figure 4-4F).

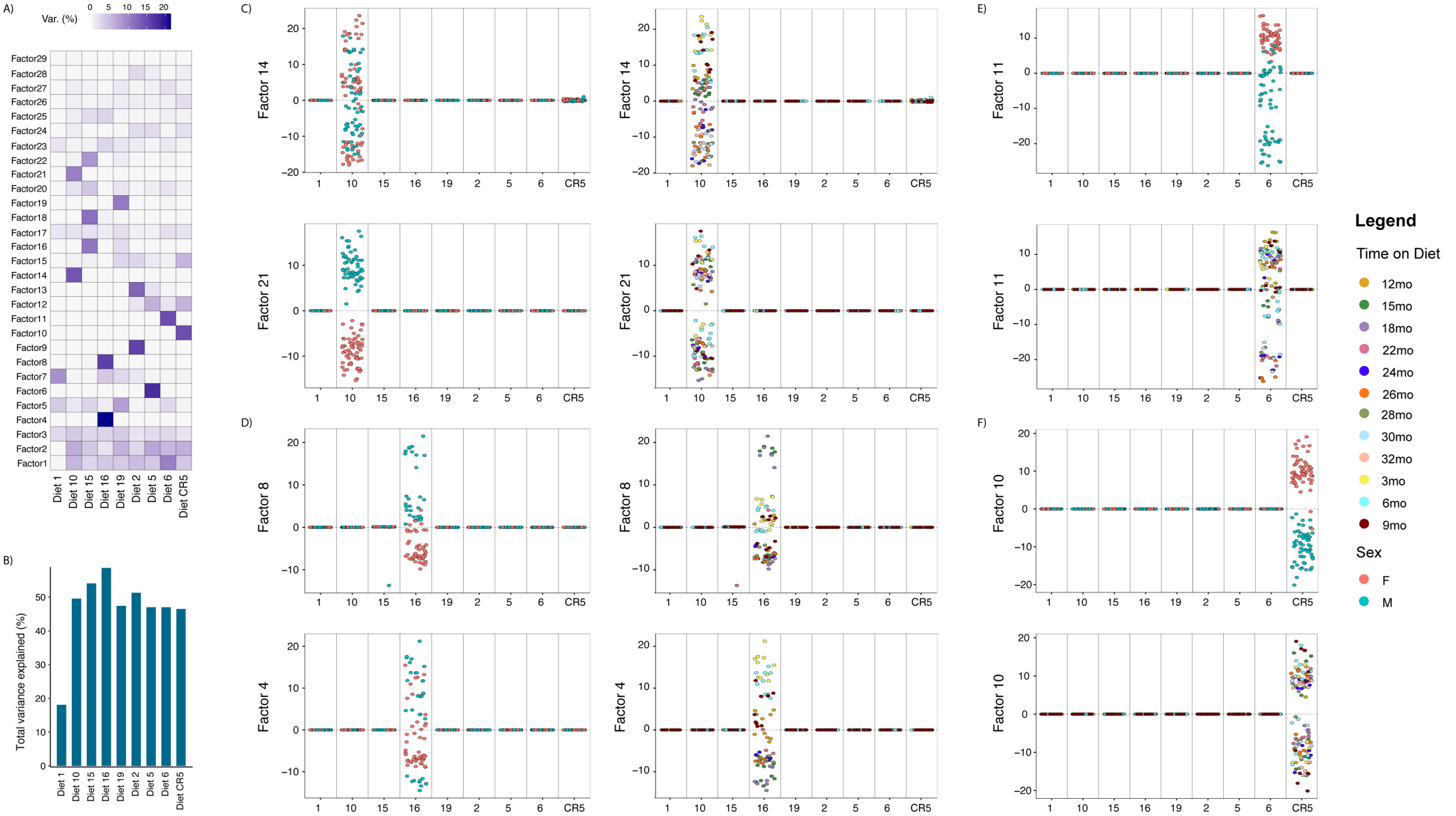

Figure 4-4. MOFA+ analysis with data grouped by diet.

A) MOFA+ identified 29 meaningful factors. B) The 29 factors explained 18-59% of total variance in each diet. C) The predominant factors in Diet 10 were associated with gender/individual and age differences, respectively. Top panels: Factor 14; bottom panels: Factor 21. D) The predominant factors in Diet 16 were associated with gender/individual and age differences, respectively. Top panels: Factor 8; bottom panels: Factor 4. F) The predominant factor in Diet 6 was associated with both gender/individual and age differences. F) The predominant factor in the caloric restriction diet was associated with gender/individual but not age difference.

4.3.4 Aging alters the microbial temporal stability

Given that microbial composition shows an age-related effect, the impact of aging on microbial temporal stability was examined first. In this study, 4-5 samples from each individual were collected over 10 days at each time point to follow the microbial temporal stability change over aging. Changes in stability were assessed by calculating the between-sample differences using Bray-Curtis dissimilarity at the ASV level among these 4-5 samples at each timepoint (Figure 4-5). Overall the gut microbiome was stable and the difference fluctuated between 0.1-0.3. The effect of aging on microbial stability was marginal, except for the high-fat diet (fat contained greater than 45), Diet 1, Diet 6 and Diet 16. Larger between-sample differences were observed at older age. With Diet 16, the difference was at maximum for the females at 22 months on diet and reduced at 24 months on diet. This suggests a potential microbial state transition for these mice during aging followed by the aged-related secondary succession.

4.3.5 Age is associated with gut microbial state transition

To quantitatively assess the change of microbial composition change over aging, I calculated the microbial difference in Bray-Curtis dissimilarity at ASV level between the baseline time points (6mon on diet) and other time points (Figure 4-6). 6 months on diet was picked because the previous chapter found that the microbiome consistently formed one of two microbial types after 6 months on these experimental diets. To ensure a fair comparison, the replaced cage mates were also compared with their own baseline samples. Increasing in differences were observed with aging for all samples. Peaks indicating larger changes in microbial structures were observed after 22mo on diet. For the female on Diet 16, a peak occurred at 26mo on diet, suggesting a possible microbial state transition at this point. However, this happens later than the loss of temporal stability found with this mouse. It is possible that loss of microbial temporal stability might be causing the microbial state transition.

To better capture microbial state transition, I looked at the taxa's relative abundance at family level for each diet across all time points (Supplementary Figure 7-23, Supplementary Figure 7-24 and Supplementary Figure 7-25) to look for absence/presence of microbes between time points. I also looked for dramatic changes in the relative abundance of the major taxa, during which the major taxa was overtaken by a different family. These signs were defined as a microbial state transition. The first state transition state often occurred around 6mo on diet (9mo old) was found in all cages. The second state transition varies among the diets, which is between 22mo to 24mo on diet (25mo to 27mo old). Furthermore, this state transition was not

seen in all cages. Two examples are given in Figure 4-7A. For the caloric retraction diet, both individuals have a stable microbial composition throughout followed lifespan starting from 6mo on diet. However, for the individuals on Diet 6, the second state transition was at 28mo for the female and 26mo for the male. In addition, for the female on Diet 16 (Supplementary Figure 7-23), an increase in *Clostridiacea* was observed at the cost *Akkermansiaceae* at 26mo on diet also indicating microbial state transition. This is consistent with the observation in Figure 4-6.

4.3.6 Aging is associated with 4 types of microbial behaviour

To access the microbial community in response to aging, MOFA+ analysis was performed with data grouped by time on diet. MOFA+ analysis identified 30 different factors collectively explain between 53% to 62% of the total microbial composition per time on diet. 4 different types of age-related microbial behaviors were recognized.

The first type of microbe response was 'resilience over aging'. For example, Factor 1 - 4, despite some oscillation, represent microbiome components that are stable throughout mice's lifetime. The second type was non-geriatric, which reduce/disappear at older age. Factors 7, 11, 20 and 22 capture significant effects at early time points but have no observable effect after 22mo, 15mo, 18mo and 24mo on diet, respectively. Factors 6 and 10 did not lose all effect but were found to consistently reduce during aging. The third type of microbe response was 'geriatric appearance'. Factors 9 and 19 were absent at early time points but appeared at 24mo and 22mo, respectively and Factors 8, 12, 13, 15, 16, 17 increased gradually over time. Finally, a potential fourth category of response is 'stochastic disturbance'. Here seen with factor 23 which was found to have a high loading on 15mo, which reduced a small amount on 18mo then back to the previous value. This may be associated with the temporary animal housing facility change at around 15mo on diet, when some cages were sent out to do behavior tests. It is possible that new environment caused microbial state transition, but was able to recover to the previous state after returning to the old environment.

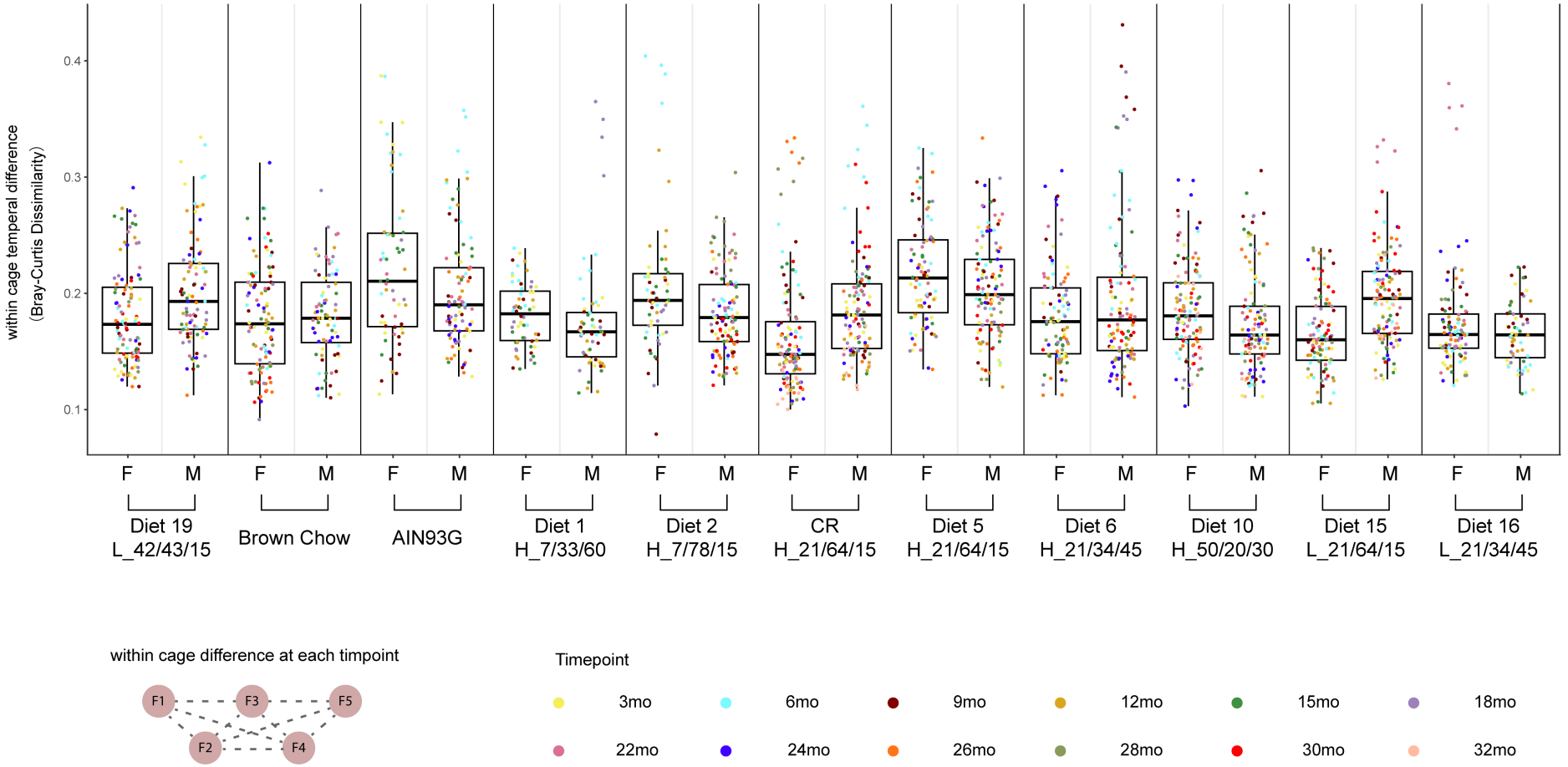

Figure 4-5. Microbial different among the 4-5 samples per mouse per timepoint.
The data includes both the focal mice and the replaced mice as well as their baseline samples at 6 month on diet. Diet 2 contains all animals from the same cage.

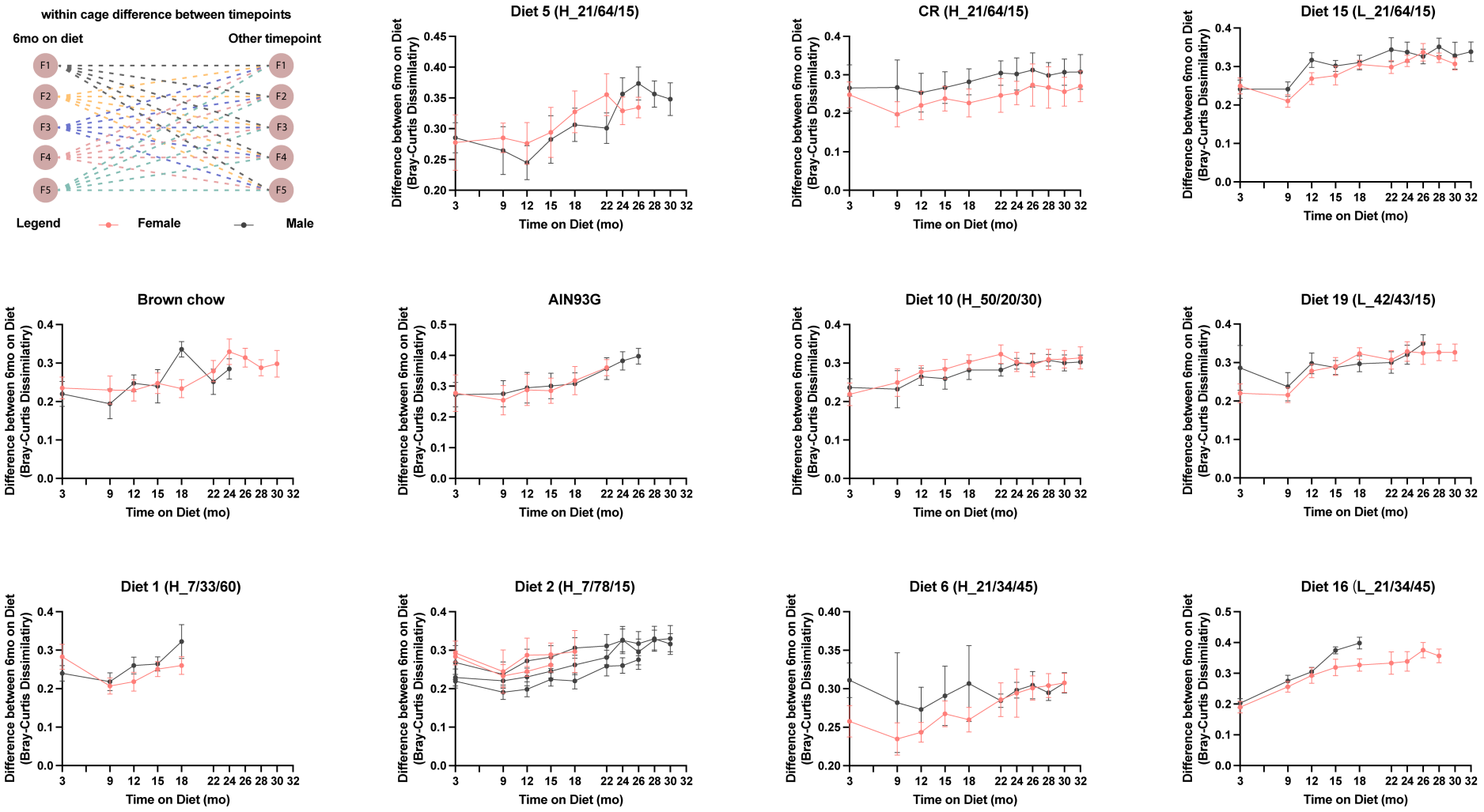

Figure 4-6. Microbial difference in Bray-Curtis dissimilarity between 6 months on diet and other time points.
Diet 2 includes all mice from the same cage. Each dot represents an average of 20-25 between two time points difference calculations. For the replaced cage mate, its own baseline samples (6mo on diet) were used for calculation.

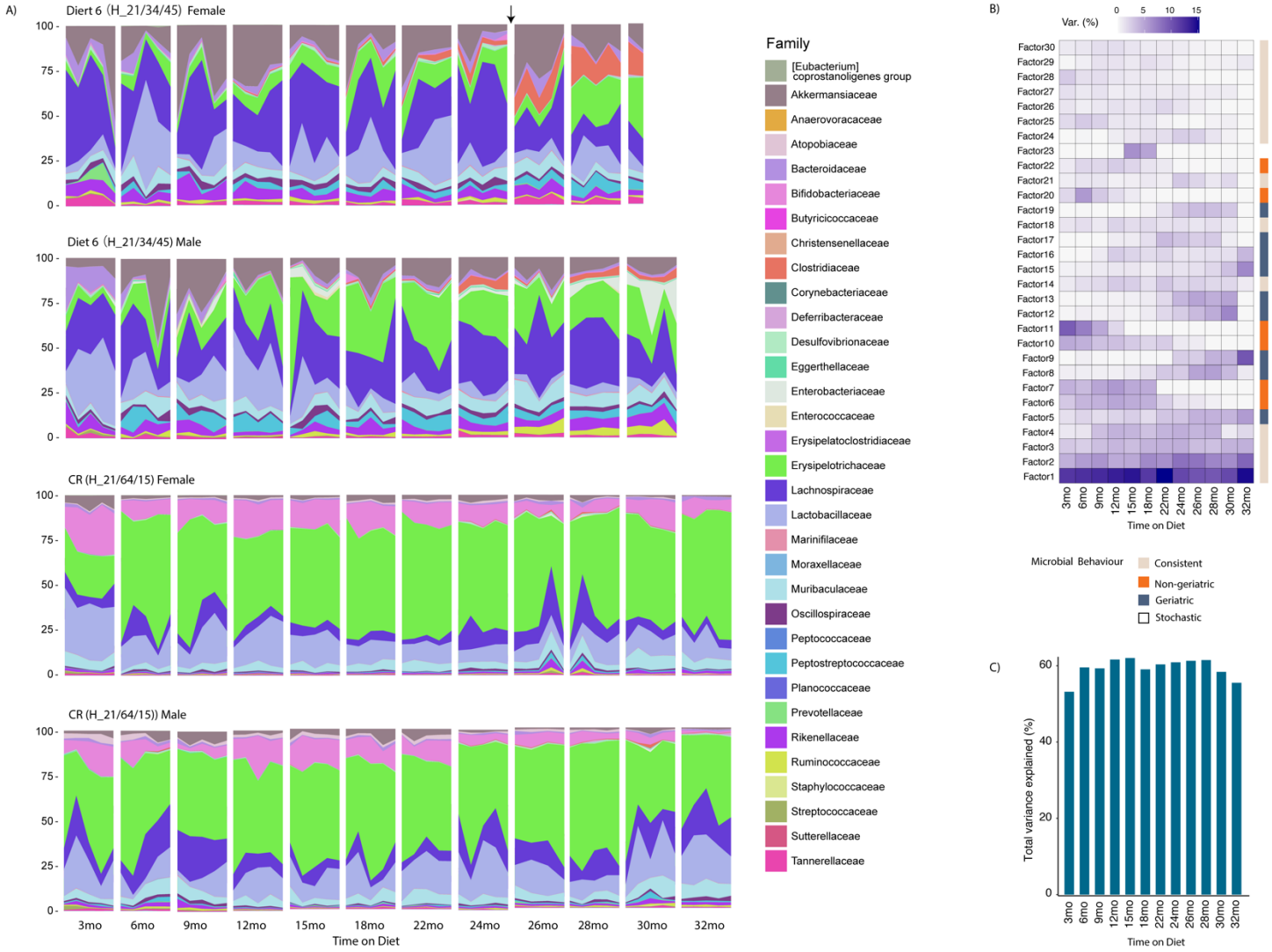

Figure 4-7. Age-related effect on microbial composition.

A) Taxa plot at family level for Diet 6 and the caloric restriction diet. Each small rectangle represents 2-5 pieces of faces collected at each time window. The arrow indicates switch of mouse. B) MOFA+ identified 30 factors. C) The 30 factors explained 53% to 62% of the total variance in each timepoint

4.3.7 The state transition was associated with microbial mutation

In the previous chapter, microbial evolution was observed at 4 timepoints, during which ASVs were derived into new ASVs. However, the animals in the previous chapter were not followed longitudinally. Different individuals were compared in 4 time-on-diet groups. Therefore, it is not possible to explicitly test for turnover due to evolution or invasion. In this longevity study, I could test the possibility that some observed changes with time may be due to evolutionary drift in the 16S rRNA marker gene (Ochman, Elwyn et al. 1999, Vera-Ponce de Leon, Schneider et al. 2022). Microbial evolutionary drift can result in appearing of new ASVs with the diminishing of the old ones. Here, *Lachnospireaea* is picked to test this hypothesis, as *Lachnospireaea* has the largest amount of different ASVs (159). It is most likely to look for evolutionary drift in this taxa. the mean relative abundance (average of 5 feces samples every other day) of *Lachnospireaea* at each timepoint was examined in two diets, Diet 2 and Diet 6.

Figure 4-8 shows a representative selection of ASVs in which pairs that were anti-correlated in one mouse are identified. (The full heatmap is given in Supplementary Figure 7-35.) Notably, in these pairs the emergent taxon is not unique to that animal. This means its appearance could be either via dispersal from another mouse, or by *de novo* mutation and selection (mutation sweep). I postulate that evolutionary distance may distinguish these possibilities - a shorter evolutionary distance (eg single nucleotide change) would favor a mutation sweep, whereas longer evolutionary distances in conjunciton with known presence in other animal sin the study favours dispersal as an explanation. For example, ASV156 disappeared at time on diet for 15mo in Female 1 on Diet 2 at which time ASV154 appeared. The emergent taxon ASV154 was not 1 nucleotide away from ASV156 (phylogenetic tree not shown), and was observed in many other mice. This likely supports that the appearance of ASV154 was due to taxon turnover. Meanwhile, for her cage mate, ASV299 and ASV312 appeared at 12mo on diet with the expense of ASV271 and ASV301. Although ASV301 was missing from other mice, it was not phylogenetically close to other ASVs in the same mouse. No pairs of the ASVs were found to the phylogenetically close-related. This indicates that mutational sweeps are unlikely to explain the observed patterns in my study. However, it was possible that such ASVs was too low to detect in this experiment.

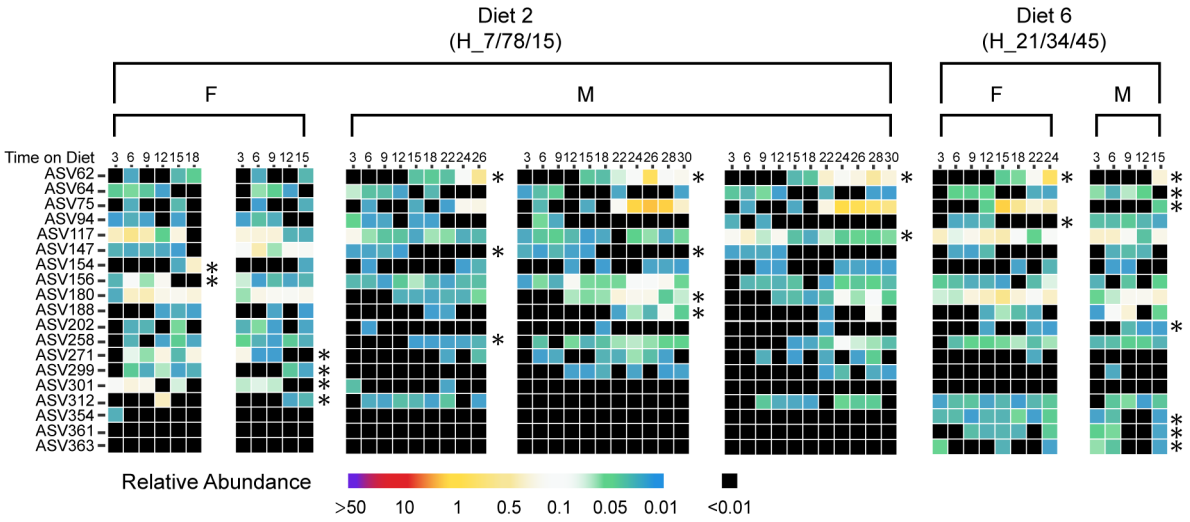

Figure 4-8. Heatmap of mean relative abundance of selected *Lachnospiraceae* ASVs as per timepoint per mouse for Diet 2 and Diet 6.
Each column presents one mouse and the pairs of presence and absence of ASVs were marked as * for each gender in each diet. The y-axis is each *Lachnospiraceae* ASVs and the x-axis is time on diet.

4.3.8 Mice gut microbiomes can be categorized into two enterotypes over long-term diet

The MOFA+ analysis with data grouped by diet identified two groups of microbial community outcomes across the tested diets. To better understand the compositional groups of microbiota, community typing was performed (n=1,054) using the Partition Around Medoids (PAM) clustering algorithm with both Bray-Curtis dissimilarity at ASV level (Figure 4-9A) and unweighted UniFrac distance (Supplementary Figure 7-26). The number of clusters, k, was determined based on the value of Calinski-Harabasz (CH) index (Supplementary Figure 7-26). The optimal cluster of k=2 was obtained when the CH index is at maximum.

PAM cluster analysis results in two distinctive community states (Figure 4-9A). Cluster 1 involves the majority of the mice on Diet 6, Diet 10, Diet 19 and all the population that were having Diet 15, Diet 16. Cluster 2 contains the majority of Diet 1 female population, the majority of the population on Diet 5, and all the population that were having Diet 2 and the caloric restriction diet. It is important to note that, diet 1 had a close to even split between two clusters, which was not observed in the previous chapter. Such difference seems to be gender/cage dependent, as 87% of males are in cluster 1 while 80% of females are in cluster 2 (Supplementary Table 7-10). This corresponds to the findings from the factor analysis. As the microbial structure of the female cage and male cage are very different, one factor cannot explain samples across both genders. Therefore, resulted in only 18% of samples can be

explained. However, as only 1 cage of females and 1 cage of males are examined, such distinctions may simply due to individual variance.

Core microbiome analysis for each cluster at ASV level reveals distinct microbial composition for each cluster (Figure 4-9B). Cluster 1's community members primarily share high relative abundance and high prevalence of *Akkermansia muciniphila* and *Erysipelotrichaceae Turicibacter*. *Erysipelotrichaceae Faecalibaculum rodentium* and *Erysipelotrichaceae Ileibacterium* are the most common taxa in the Cluster 2 community and presented in almost all samples.

To identify the signature ASVs in each cluster, I applied the ADLEx2 differential abundance analysis with assessed effect sizes to the dataset (Figure 4-9C). 364 ASVs after abundance and uniquity filtering were used as the input for ADLEx2. 295 out of 364 ASVs were found statistically significant different in abundance between the two clusters. Among them, 8 have an effect size greater than 1 in cluster 2, and 1 has effect size greater than 1 in cluster 1.

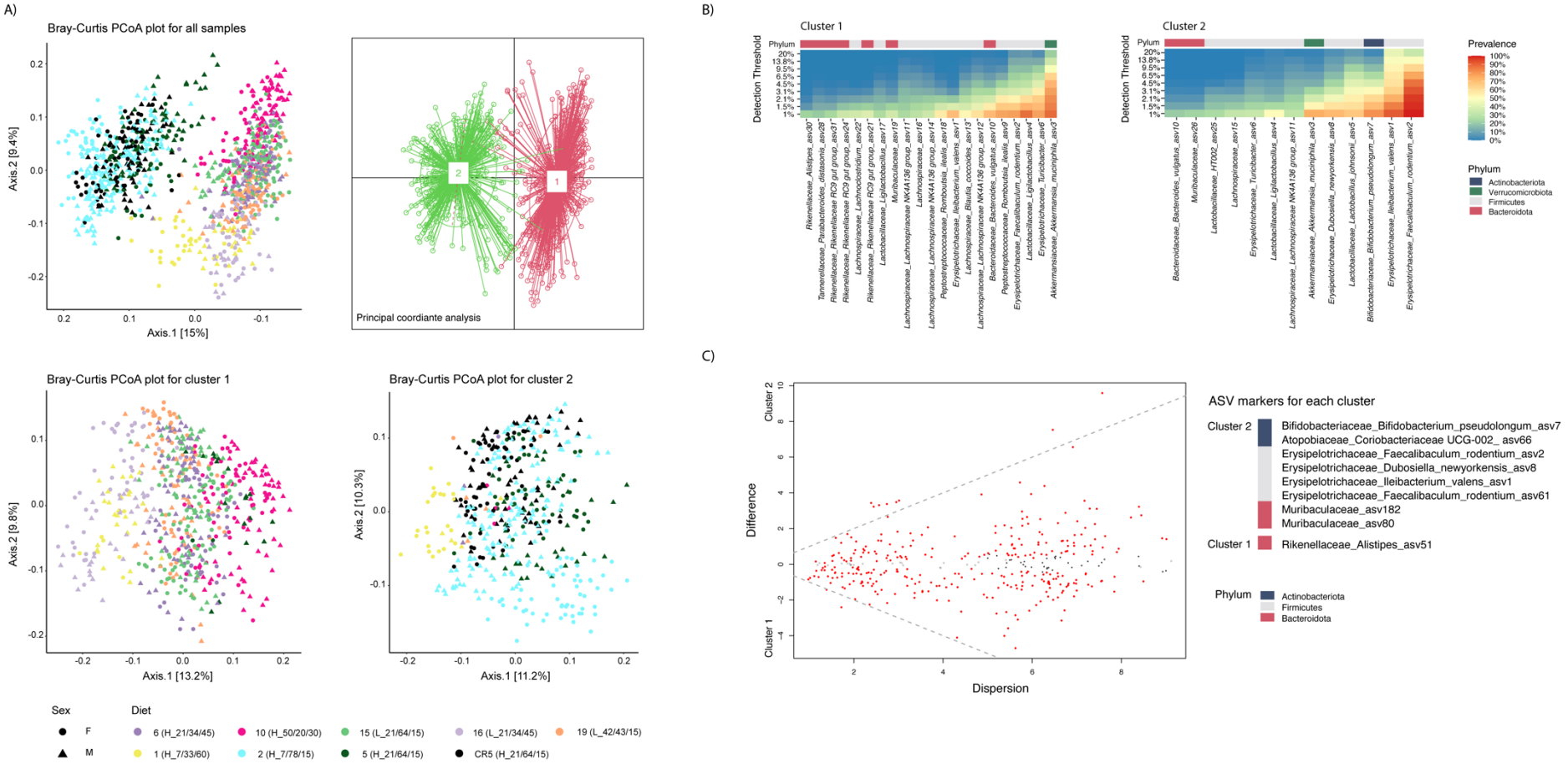

Figure 4-9. PAM cluster results in two distinctive enterotypes.

A) Top left: PCoA plot of Bray-Curtis dissimilarity at ASV level. Top right: PAM cluster of Bray-Curtis at ASV level shows 2 distinct clusters. Bottom left: PCoA plot of cluster 1. Bottom right: PCoA plot of cluster 2. (sample n = 1,054) B) Core microbiome for each cluster is shown as heat map of prevalence at different relative abundance detective thresholds. C) Significant ASVs in abundance between the two clusters given by ALDEx2. Red dots are significant ASVs and the grey dash lines present effect size larger than 1 in either cluster.

4.3.9 The two enterotypes are associated with different macronutrient energy intake

Considering the clusters are associated with diets, they might also be linked to macronutrient intake. Mice 24h food intake data were collected on a cage basis, and the intake for each mouse was calculated as a cage average. Except for the caloric restriction mice, which were kept consistent at 2.8g for males and 2.7g for females. PCA loading of the protein, carbohydrate and fat intake as kJ per mice per day were plotted together with the Bray Curtis dissimilarity (Figure 4-10A). The PCoA plot showed that the cluster was associated with macronutrient intake. Microbial type 2 (cluster 2) was related to carbohydrate energy intake while microbial type 1 (cluster 1) was related to fat energy intake. Meanwhile, both clusters are associated with protein-energy intake. This was agreed with the findings in the ToD18 group in the previous chapter.

Next, the actual macronutrient energy intake between the two clusters was directly compared (Figure 4-10B). Given only focal mice were followed in this subset, to avoid basis, the whole longevity study food intake was taken. All animals that were having Diet 2, Diet 5, caloric restriction diet and the females on diet 1 were manually assigned as cluster 2. Then the rest were assigned as cluster 1. Mann-Whitney test was used to compare the two groups. Mice subject to Cluster 2 were found significantly higher in carbohydrate energy intake, while lower in protein and fat energy intake compared to mice subject to Cluster 1. This suggests that dietary macronutrient intake is associated with the microbial community types in mice.

To test for a correlation between the metabolic traits (or physiological strategy) of the microbes and the diet conditions (or nutrient availability), I used PICRUSt to predict the metabolic potential of the microbiota using functional prediction (Figure 4-10D and E). Metagenomes were reconstructed from 16S rRNA gene dsequences using PICRUSt, which then was used to estimate the abundance of metabolic pathways listed in the Kyoto Encyclopedia of Genes and Genomes (KEGG) database (Kanehisa and Goto 2000). The predicted pathways show that carbohydrate digestion and absorption (ko04973) is enriched in cluster 2, while the fatty acid biosynthesis (ko00061) is enriched in cluster 1. These are consistent with findings from the nutrient intake. Interestingly, higher carbohydrate intake is associated with higher primary and secondary bile acid biosynthesis in cluster 2. For cluster 1, both the flagellar assembly (ko00061) and lipopolysaccharide (LPS) biosynthesis (ko00540) are enriched suggesting a more proinflammation status in the system.

4.3.10 The two enterotypes are associated with longevity in male

Previous study showed that mice with a high ratio of carbohydrates to protein diet exhibited an extended median lifespan (Solon-Biet, McMahon et al. 2014). Considering cluster 1 and cluster 2 are associated with differences in protein and carbohydrate intake respectively, I hypothesise that there is a difference in mice lifespan among the enterotypes. Therefore, I analysed the survival rate for both the subset in this study and the whole longevity mice population to see if there is a correlation between the enterotype and longevity. The survival rates were calculated separately for males, females, and also for both genders combined. The mice from the longevity study were assigned to each cluster as same as the food intake calculation.

Nonetheless, the absence of a substantial sample size likely contributed to the absence of any significant differences between the clusters within the subset (Supplementary Figure 7-29). Upon analysing the entire cohort, the clusters correlate the longevity in a gender-dependent manner (Figure 4-10C). Noteworthy distinctions were detected among males, while no such disparities were observed among females. These findings indicate the possibility of a more robust association between male longevity and both gut microbiome composition and dietary elements.

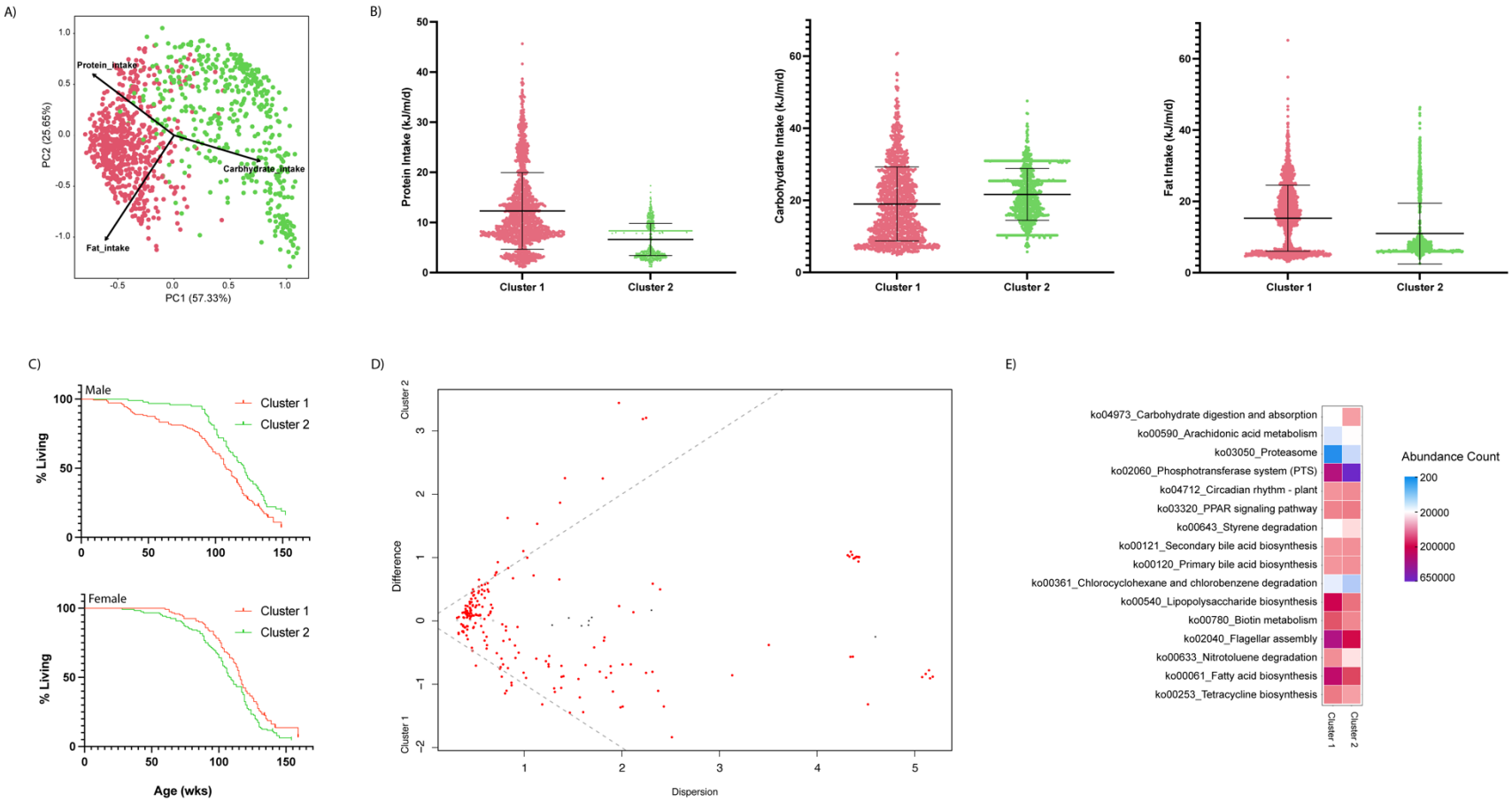

Figure 4-10. The two enterotypes are associated with different macronutrient intake and longevity in male mice.
A) PCA plot of macronutrient intake loading on top of Bray-Curtis dissimilarity. (samples n=1,054) B) Macronutrient energy intake for the whole longevity study. C) Survival ratio for the whole longevity study, separated as Male (top) and Female (bottom). D) ALDEx2 result MW plot of PICRUSt KEGG pathway abundance. Red dots are significant pathways and the gray dash lines present effective size larger than 1 in each cluster. (samples n=1,054). E) Heat plot of the abundance count of significant pathways from ALDEx2 results. * for B) and C) Cluster 1 and 2 were manually assigned. Cluster 1 includes Diet 2, Diet 5, Diet CR and Diet 1 females. And the rest was assigned to cluster 2.

4.3.11 These 2 enterotypes are universal and recurrent

For this study, only one focal mouse is followed for each cage, thus 2 mice for each diet. To ensure that this enterotype is applicable to other mice, enterotyping was also done with mice on the same diets in the timepoint study (the previous chapter), where a total of 24 mice were examined for each diet across 4 different timepoints. The endpoint caecal samples of selected 11 diets (Figure 4-11A) and of all 19 diets (Supplementary Figure 7-27) from all time points were pooled together to perform the PAM cluster. Two similar distinct clusters were also observed. Comparing to this study, a clearer separation was found with the caecal samples. All Diet 2, 5 and caloric restriction samples were assigned to cluster 2, and all the result diets were assigned to cluster 1. In particular for Diet 1, no gender difference was observed.

To confirm that the microbial structures in the clusters are similar to each other in both studies, I plotted the relative abundance of the phylum as per cluster for both study (Figure 4-11B) and core microbiota for each cluster in the timepoint study (Figure 4-11C). The phylum plot indicates that the clusters from both study shares a similar microbial composition. Cluster 1 all have a higher relative abundance of *Verrucomicrobiota*, *Desulfobacterota* and *Bacteroidota,* while clusters have a higher relative abundance of *Actinobacteriota* and *Firmicutes*. As different type of samples were used for analysis, the overall core microbiome composition in each cluster is difference for both studies. However, The clusters from both studies have the same most prevalent taxa, which is *Akkermansia* for cluster 1 and *Faecallibaculum* for cluster 2. Altogether, this indicates that the cluster from both studies are similar, which implies that the two enterotypes observed in this studies is also applicable for other mice that the same diets.

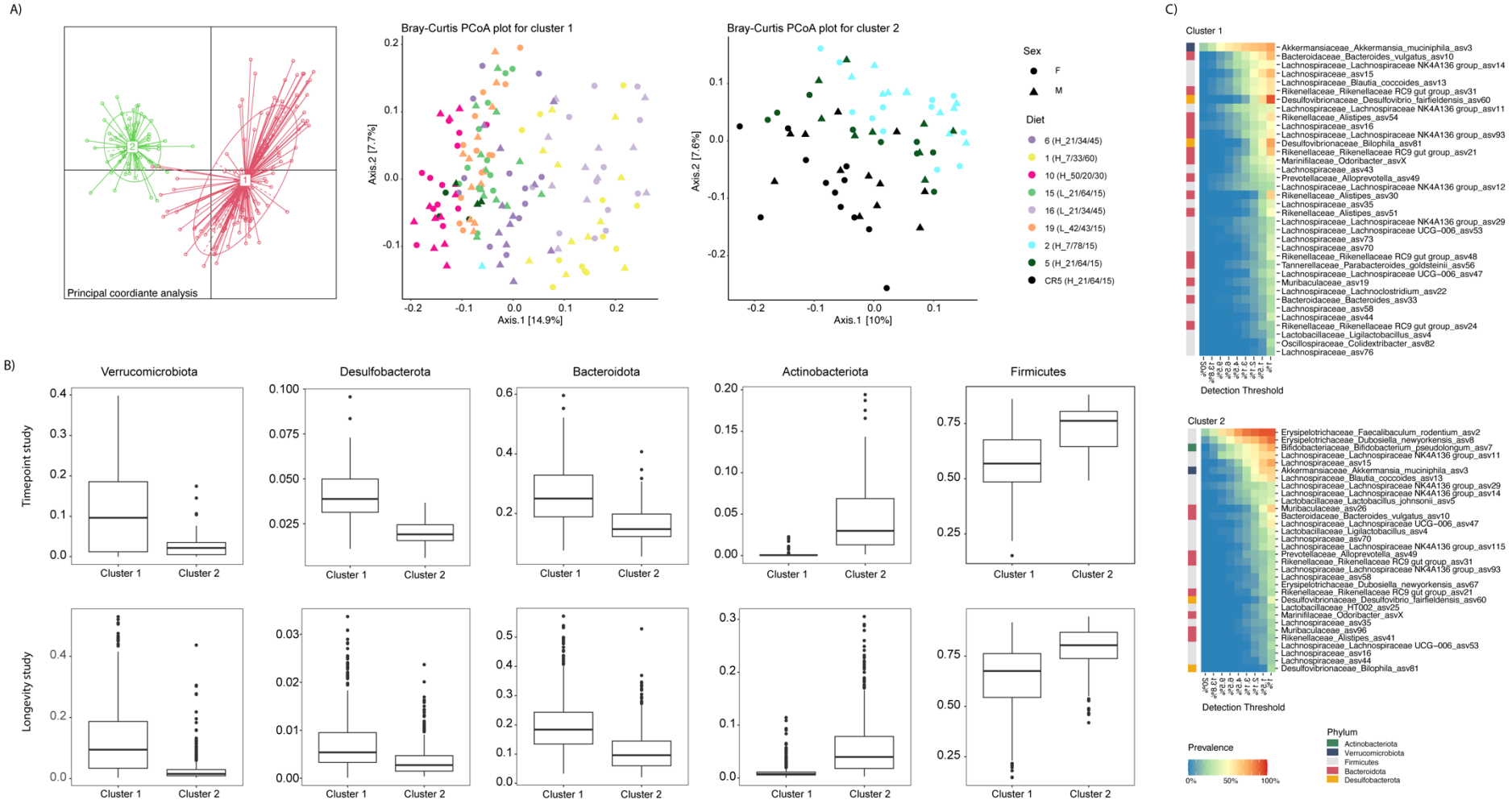

Figure 4-11. The enterotypes in mice's gut are recurrent.

A) Pam cluster of the Timepoints study (only includes diets used in longevity study, n = 214) also shows two distinctive clusters. From left to right. PAM cluster of Bray-Curtis at ASV level. PCoA plot of cluster 1. PCoA plot of cluster 2. B) Relative abundance of 5 different phylum in each cluster. Top panel: Timepoint study. Bottom panel: Longevity study microbiome subset analysis. C) Core microbiome for each cluster from the timepoint study is shown as heat map of prevalence at different relative abundance detective threshold.

4.4 Discussion

The process of biological aging is affected by multiple extrinsic factors, resulted in delay or early aging. The gut microbiome of an adult is stable but dynamic. It fluctuates in response to the physiological change due to aging. Distinctive microbial characteristics were found at different ages (Ke, Mitchell et al. 2021, Wilmanski, Diener et al. 2021, Wu, Muthyala et al. 2021). Thus, aging can be reflected in the microbiome as the transition of microbial community states. Two age-related transitions were captured. The first is between 3mo to 6mo on diet, and then between 22mo to 24mo on diet. The first transition stage is associated with mice full mature, after which age-related change can be observed (Flurkey, Currer et al. 2007).

Chronological aging of mice starts at 18 months old (equivalent to 15 months on diet in this study), where biomarkers of ageing are detected (Flurkey, Currer et al. 2007). However, the second age-related state transition observed was 7 months later than the chronological aging. The inconsistency of chronological and microbial age implies two possibilities. One of them is that microbial aging has two stages, with the first one around 18 months old and the other being 7 months later, at 25 months old. However, the early age-related state transition was not captured, as this change is not significant. Due to the resilience of the gut microbiome, it was able to recover back to its previous state. Also, in this study, such change was masked with environmental-related change due to an alteration in the housing facility. Therefore, it cannot be distinguished from environmental disturbance. The second stage starts at 25 months old, which is associated with a rapid decline in body function and animal death. Another possibility is that because of its stability, gut microbiome may have a delayed response to the biological aging, for at least 7 months.

The MOFA+ analysis result (grouping by time on diet) is likely to support the first hypothesis. Two groups of taxa, Factor 11 and Factor 20, were found to disappear at 15mo and 18mo on diets, respectively, corresponding to the first stage of microbial aging. Then, Factor 9 and 19 appeared at 22mo and 24mo on diet, respectively, at the cost of factor 7. This matches the second stage of microbial aging.

Furthermore, the two-stage microbial aging may actually be a prompt rather than delayed response to the biological aging. Human trial found 2 stages of biological aging at the age of 60 and 78 years old (Lehallier, Gate et al. 2019). Two peaks of aging associated proteins were detected in plasma over time, with the first wave being minimal and the second being

significantly larger (Lehallier, Gate et al. 2019). These two human ages happen to be equivalent to mice ages of 18-24 months old and 25 months old (Flurkey, Currer et al. 2007, Dutta and Sengupta 2016). Therefore, I hypothesize that the gut microbiome also has a similar two-stage aging process, which responds to the bio-molecular fluctuation during biological aging.

Although aging causes microbial state transition, ultimately the microbial composition is supported by exogenous resources obtained from the diet. In this study, I identified two microbial enterotypes in mice gut. These two enterotypes were also apparent in the timepoint study, thus suggesting these two enterotypes are universal for mice gut microbiota. Cluster 1 is high in both *Firmicutes* and *Bacteroidota*, while cluster 2 was dominated by *Firmicutes*. The two clusters were found to correlate with diet. Specially, cluster 1 is associated with higher protein and fat intake, while cluster 2 is associated with higher carbohydrate intake. This was consistent with findings in other papers, where Bacteroides were found to prefer dietary fiber, and Firmicutes prefer dietary protein (Holmes, Chew et al. 2017, Zeng, Xing et al. 2022). This indicates that dietary carbohydrate and protein intakes are the primary factors that shape the gut microbial composition.

Furthermore, microbial type 1 was found to associated with reduce longevity in male mice. This may associated with increasing in insulin sensitivity and systemic inflammation. Functional prediction revealed that microbial type 1 was enriched in pathways related to microbial flagellar assembly and LPS biosynthesis. Microbial-derived LPS can cross the intestinal barrier, triggering systematic inflammation, which contributes to the overall systematic inflammation due to aging (Rocha, Caldas et al. 2016). LPS can also activate toll-like receptor 4 (TLR4), leading to the upregulation of chronic inflammation and insulin resistance (Rocha, Caldas et al. 2016). Dietary saturated fat intake was found to increase LPS translocation and toll-like receptor 4 (TLR4) expression (Rocha, Caldas et al. 2016, Tomassen, Govers et al. 2023). This aligns with the findings in Chapter 3, which showed that microbial type 1 was associated with fat and protein intake, with lard being one of the fat sources used containing saturated fat.

Moreover, glucose tolerance test and blood insulin measurements were conducted on mice in Chapter 3 by others (Supplementary Figure 7-33 and Supplementary Figure 7-34). The results showed that male mice with microbial type 1 at ToD18 exhibited delayed blood glucose clearance and elevated blood insulin levels, but this pattern was not observed in other ToD

groups. This suggests increased insulin sensitivity in aged male mice with microbial type 1. Higher blood glucose and insulin level was previously found to be associated with the activation of hepatic mTOR and reduction of insulin-like growth factor 1 (IGF1) signalling, which all linked to longevity in mice (Solon-Biet, McMahon et al. 2014, Templeman, Flibotte et al. 2017). In addition, IGF1 circulating levels are positively correlated with dietary fat and dairy-sourced protein intake (Kaklamani, Linos et al. 1999). The protein in experimental diets was sourced primarily from casein and whey protein isolates. With microbial type 1 being linked to dietary fat and protein intake, may further influence IGF1 signalling and longevity in mice.

To find out the possible mechanism between the longevity in male mice and microbial type I, metabolomic and proteomic analysis result of liver, plasma and caecal content are required.

5 Diet Based Manipulation of metabolites for health

This chapter is under a project grant in collaboration with Prof. Stephen Simpson at Charles Perkins Centre. The animal maintenance, sample collection, sample process and data analysis were all done by me.

5.1 Introduction

Gnotobiotic model is commonly used to study the interaction between the host and the gut microbiome. Germ-free mice are a type of gnotobiotic model, which lacks all microorganisms. Therefore, it allows for transplant of the whole fecal microbiome, known as conventionalization. Comparing the germ-free mice with the conventionalized mice generates knowledge of physiology change and immune response due to microbial population (Östman, Rask et al. 2006, Fransen, Van Beek et al. 2017).

In previous chapters, two distinct microbial types were repeatedly observed within the mouse population. These microbial types were linked to the two groups of diets with different macronutrient ratios and energy densities. During aging, microbial type shifts were found from type 2 to type 1. Notably, microbial type 1 was associated with longevity in male mice. It is concluded that diet and microbiome change can modulate the rate of progression to immuno-senescence. To validate this hypothesis, a fecal matter transplant experiment was designed to examine if the aged-phenotype can be transferred by inoculating the microbiome from the aged mice to young germ-free mice. The aim of this study was to identify the role of microbes in diet strategies for healthy aging.

Aging is a whole-body process involving a decline in immune and physiological functions. Due to its complexity, it is not yet possible to directly measure aging. Instead, biomarkers, which are measurable indicators of biological processes, are often used to assess the rate of aging and suggest the biological age of an individual. Systematic inflammation was the primary biomarker used to indicate aging, which is referred to as chronic low-grade inflammation (Elyahu, Hekselman et al. 2019, Mogilenko, Shpynov et al. 2021). Inflammation can be measured through changes in immune response and cell senescence. A series of immune cells including T helper cells, cytotoxic T cells, exhausted T cells, and regulatory T cells, were found to increase with aging (McClanahan, Riches et al. 2015, Elyahu, Hekselman et al. 2019, Mogilenko, Shpynov et al. 2021). Additionally, cellular senescence and the rise of programmed cell death protein 1 (PD-1) and its receptor PD-L1, which are markers of cell apoptosis and T cell exhaustion, have also been observed (McClanahan, Riches et al. 2015, Onorati, Havas et al. 2022)

Inflammaging was also found to have a shared mechanism with obesity-related inflammation (Franceschi, Garagnani et al. 2018). With excess nutrient and energy intake, a combination of

both types of inflammations can occur in aged individuals (Franceschi, Garagnani et al. 2018). Meanwhile, changing in obesity-related metabolic parameters were observed during aging, like body weight gain, increasing in glucose tolerance and decreasing in insulin clearance (Leiter, Premdas et al. 1988, Oh, Seo et al. 2016, Binyamin, Werbner et al. 2020, Marmentini, Soares et al. 2021). Therefore, this study will use systemic inflammation and metabolic parameters as indicators of aging phenotypes.

In this study, one signature diet from each group was selected, Diet 6 (microbial type 1) and Diet 2 (microbial type 2). One cage of male mice (aged 106wk and 226wk, respectively) on each diet was picked from the longevity study (from the non-microbial analysis cohort) in Chapter 4, and served as microbial donors (Figure 5-1). After conventionalization, the young germ-free recipients were followed for 4 weeks by weekly sampling of faeces, monitoring of food intake and body weight change. Right before euthanasia, body composition and blood glucose tolerance data were collected. At the end of the experiment, spleen and mesenteric lymph nodes were harvested to examine the T cell population.

To validate that the difference in microbial composition is induced by diet, the conventionalized germ-free mice were fed with one of the following diets, Diet 6 (microbial type 1), Diet 2 (microbial type 2) or the control diet (AIN93G). Comparing different dietary treatment groups allows me to see if the diet is able to attenuate or worsen microbial effects on the immune response. Therefore, this study ends up having 7 different treatment groups. Each group consists of 12 -16 fecal samples and 3-4 cecal samples to examine the microbial compositional change. Additionally, 3-4 spleen and mesenteric lymph node samples are included to access aging phenotypical change.

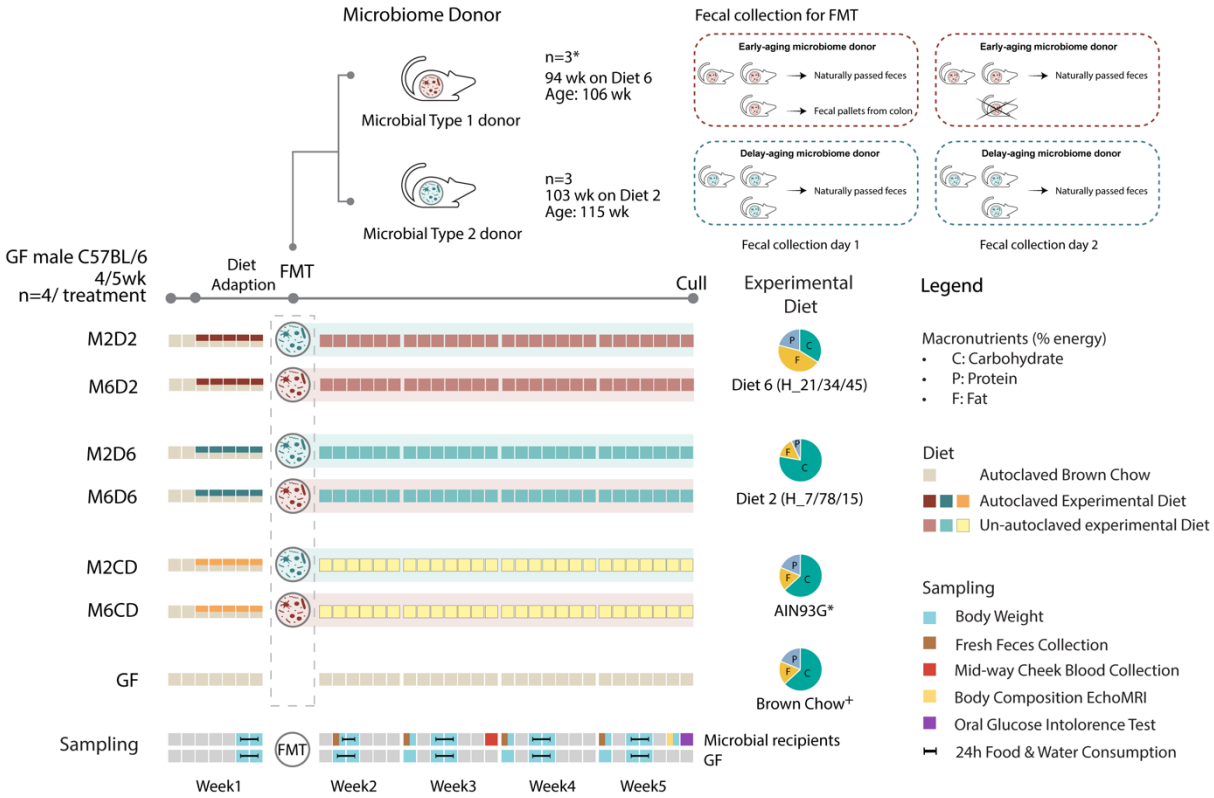

Figure 5-1. Experimental and diet design for the animal study reported in this chapter.
This experiment consists of 7 different groups, 6 microbial recipient groups and a germ-free control group. Each group contained 4 mice (2 cages of male mice and 2 mice per cage). The recipient mice received two types of microbiome, feces from donors on Diet 6 (microbial type I) and donors on Diet 2 (microbial type II). One cage of male mice on Diet 6 and one cage of male mice on Diet 2 were selected as microbiome donors. Fresh feces were collected from all members in the same cage for 2 consecutive days. One member of the microbial type II donors reached the human endpoint during the first of fecal collection day, therefore fecal pellets from its colon were collected instead. The recipient mice were fed with either the experimental diets (Diet 6, Diet 2) or the control diet (AIN93G) for 4 weeks after FMT. The GF mice remained germ free and fed with autoclaved brown chow throughout the experiment. 24h food/water intake and body weight were followed weekly for all groups. Fresh feces were collected 2 days after FMT, and then every week for the recipient mice.
(*AIN93G uses different protein and oil sources than the experimental diets. + Brown chow uses different macronutrient source than the experimental diets)

5.2 Methods

5.2.1 Animal

Germ-free male C57BL/6 mice (5wk old, n=25; 4wk, n=3) were purchased from Walter and Eliza Hall Institute of Medical Research (Melbourn, Vic, Australia). They were randomly separated into 7 groups and housed 2 per cage in standard approved cages (Technoplast) in the Germ-free facility (Charles Perkins Centre, The University of Sydney, NSW, Australia). They underwent acclimation and diet adaption for 1 week after arrival. During this period, they were fed autoclaved standard chow (Specialty Feed) *ad libitum* on day 1 and 2. As a diet adaption process, starting from day 3, all germ-free recipient mice (excluding the germ-free control group) were fed with a 50:50 combination of autoclaved standard chow and experimental diets.

After the acclimation and FMT, all microbial recipient mice switched to the unautoclaved experimental diets.

5.2.2 Microbiota transplant

2 cages (3 per cage) of specific pathogen-free male C57BL/6 mice (from the large longevity cohort in Chapter 5) were used as donors for gut microbiota transplants, refer as microbial type I donors and microbial type II donors. Microbial type I donors were on Diet 6(P/C/F = 21/34/45, energy density 14.7MJ/kg) for 94wk/23.4mo (aged 106wk), while the Microbial type II donors were on Diet 2 (P/C/F = 7/78/15, energy density 14.7 MJ/kg) for 103wk/25.7mo (aged 115wk). All groups of germ-free recipient mice were conventionalized using one shot of oral gavage fecal transplantation and living in cages containing the donor mice's old bedding to receive a complete microbiome from the donor mice.

To make the fecal slurry for transplantation, fresh fecal pellets from all 3 mice in the same cage were collected (around 2 pm) over 2 consecutive days. However, one member of the microbial type II donors reached the human endpoint during the first of fecal collection day, therefore fecal pellets from its colon were collected instead. Thus, the microbial type II donors ended up to have 3 members on collection day 1 and 2 members on collection day 2. On the day of collection, fresh feces were pooled together and suspended in sterile PBS (1g/10mL) and suspended by vortexing. Large particles were removed by centrifugation (100g, 2 min). The supernatant was carefully pipetted out and mixed with 10% glycerol. The fecal slurry was stored at -80^{o}C until further use. The fecal slurry were prepared under normal aerobic condition. On the day of the fecal transplant, the fecal slurry of the same donor from both collection days was mixed for oral gavage. Each recipient mouse was administrated 200uL fecal slurry. The conventionalized mice were transferred to the PC1 holding room in the animal facility (Charles Perkins Centre, The University of Sydney, NSW, Australia).

5.2.3 Diet composition and food/water intake monitoring

The experiment diets contain an early-aging diet (Diet 6), a delay-aging diet (Diet 2), AIN93G and a standard chow diet, all from Specialty Feeds. The early-aging and delay-aging diets were picked as one each from the two microbial clusters in Chapter 5 and based on the overall survival rate and health condition of the whole longevity cohorts.

Delay-aging diet contained 7% calories from protein, 78% calories from carbohydrate, and 15% calories from fat, 14.7MJ/kg; early-aging diet contained 21% calories from protein, 34% calories from carbohydrate, and 45% calories from fat, 14.7MJ/kg. Detailed diet compositions are given in Supplementary Table 7-2.

Food and water consumption were assessed in each week. The 24h food and water intake were estimated as detailed in Chapter 2.2.2.

5.2.4 Gut microbial analysis

Fresh fecal samples were collected 2 days after the fecal transplant, then every week in the morning between 10 am to 12 pm. The feces were stored at -80^{o}C until further processing. At the end of the experiment, mice were culled, caecal content was collected and stored in Eppendorf tubes at -80^{o}C until further processing.

DNA extraction was performed for each sample as detailed in Chapter 2.2.3. Bacterial amplicon 16S rRNA gene sequencing was performed as detailed in Chapter 2.2.4. Microbial profiling was done with DADA2 as detailed in Chapter 2.2.5 with classification at the ASV level. Two filtering steps were applied, for abundance filtering an ASV must comprise of 0.01% of total reads, for ubiquity filtering an ASV must be present in at least 10% of samples. The number of sequence reads processed and filtered at each step is summarised in Supplementary Table 7-1. After filtering, the average reads per sample was 101,085.

5.2.5 Body composition

Body composition (fat and lean mass) was assessed for all germ-free recipients the day before the oral glucose tolerance test by EchoMRI-900 (EchoMRI). Prior to each session, the machine was calibrated using a canola oil standard.

5.2.6 Oral glucose tolerance test and plasma insulin analysis

Oral glucose tolerance test were performed on all germ-free recipients (n=22) the day before cull. Animals were fasted 6 hrs prior to testing starting at 7 am by removing their food from the cage and only leaving them with water. Basal glucose levels were determined using a glucose test strip (Accu-Chek Performa) and glucometer (Accu-check Performa II). 25% (w/v) Glucose solution (2g/kg lean mass) was then administered via oral gavage. Tail tip blood was sampled at 15, 30, 45, 60 and 90min post-gavage.

10uL of blood at basal level and 15min after administering glucose were also collected for plasma insulin level measurement. Plasma insulin levels were measured with the Mouse Ultrasensitive Insulin Elisa Kit (Crystal Chem) using whole blood samples.

5.2.7 Spleen and MLN cells analysis by flow cytometry

Spleen and MLN were harvested and incubated with 500U/mL collagenase IV (StemCell Technologies) in RPMI1640 (Gibco) and Piece Universal nuclease for cell lysis (Thermo Fisher Scientific) at 37^{o}C for 45 min. The tissue was forced through a 70μm MACS smart strainer (Miltenyi Biotech), and red blood cells were depleted with ACK lysis buffer (Gibco). Subsequently, the cells were re-suspended in RPMI1640 medium with 10% FBS (MLN cells) or RPMI1640 medium (Spleen cells). An aliquot of each sample that contains 2×10^6 cells was transferred into 96-well polypropylene V-shape plates. To minimize background noise, Fc receptors were blocked using anti-CD16/CD32 monoclonal antibody (Clone 93, 1:12.5 dilution; Biolegend) for 15 min on ice.

Cell surface expression was assessed by staining with the following monoclonal antibodies: CD3-Brilliant Violet 510 (Clone 17A2, Biolegend), CD4-APC-Fire 750 (Clone GK1.5, Biolegend), CD8a-Brilliant Violet 650 (Clone 53-6.7, Biolegend), CD27-Brilliant Violet 785 (Clone LG.3A10, Biolegend), CD62L-Brilliant Violet 711(Clone MEL-14, Biolegend), CD45-FITC (Clone 30-F11, Biolegend), CD44-PE-Cy7 (Clone IM7, Biolegend), PD-1-Pacific Blue (Clone 29F.1A12, Biolegend), and PD-L1-Brilliant Violet 605 (Clone 10F.9G2, Biolegend). For detection of intracellular expression of FOXP3, cells were permeabilized and fixed with the FOXP3 Fix/Perm Buffer (eBioscience). Then, they were incubated with the anti-FOXP3-Alexa Fluor 647 monoclonal antibody (Clone 150D, Biolegend).

For all antibodies used, UltraComp eBeads composition beads (Invitrogen) were used for creating fluorochrome reference controls in Cytek SpectroFlo software (Cytek Biosciences). Cell Viability was determined using LIVE/DEAD fixable blue dead cell stain kit (Invitrogen). Cell analysis was performed with a 5-laser Cytek Aurora spectral flow cytometer (Cytek Biosciences).

5.2.8 Gating strategy for spectral flow cytometry data

FlowJo (version 10.9.0) was used to process the data from spectral flow cytometry. Figure 5-2 gives the gating strategy for identifying CD4+ and CD8a+ T cell populations from mice MLN and spleen single cell suspensions. FOXP3+ cells were identified from CD4+ T helper cells.

PD-1 expression was identified from both CD4+ AND CD8a+ T cells by using the negative gate from each respective fluorescence-minus-one (FMO) control as shown in Figure 5-3.

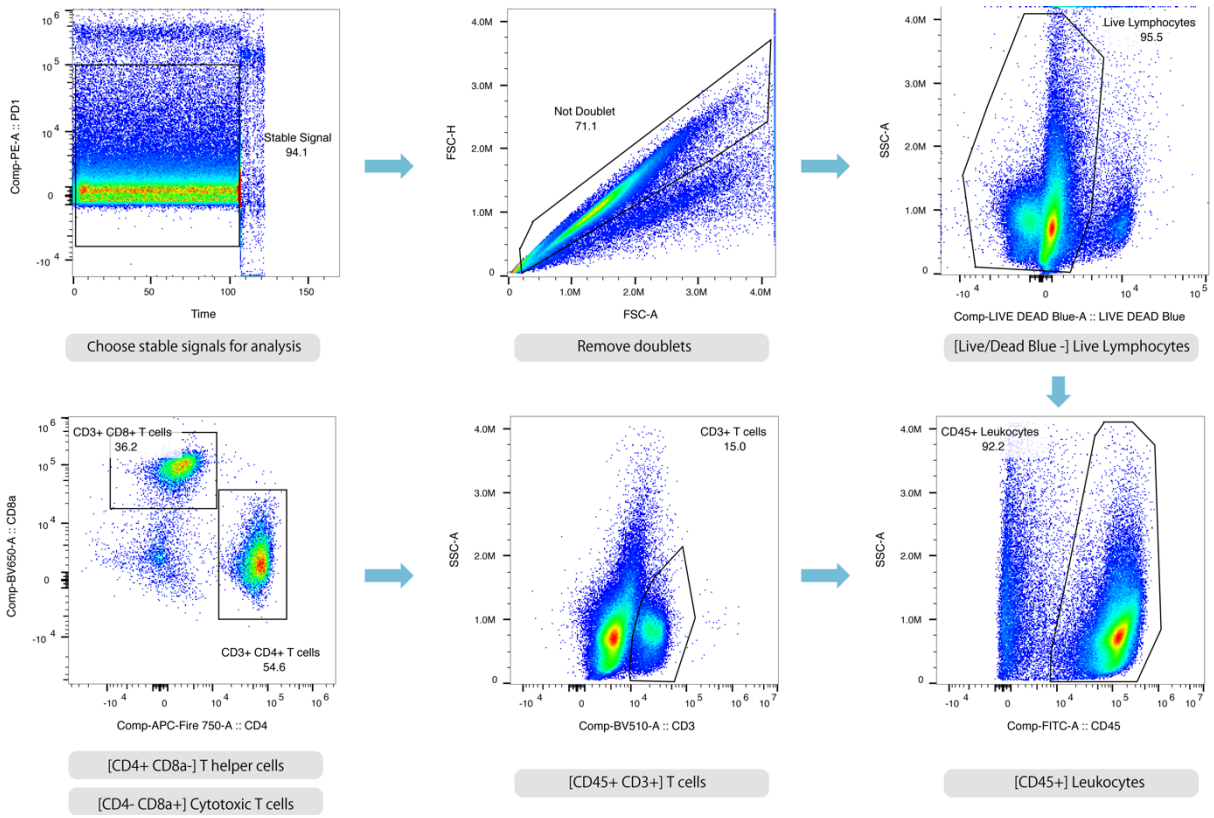

Figure 5-2. Identification of T cell subsets from MLN and spleen single cell suspension using FlowJo.

Mouse MLN and spleen single cell suspension were analysed using spectral flow cytometry. Stable signals were used for further analysis. Doublets were identified and eliminated on a forward scatter height vs forward scatter area plot for all cells. Live lymphocytes were then identified from the side scatter area plot as Live/Dead Blue-. Sequentially, leukocytes were identified from live lymphocytes as CD45+, and T cells were identified from leukocytes as CD3+. T cell subsets were then further divided into CD3+ CD4+ T helper cells and CD3+ CD8a+ cytotoxic T cells.

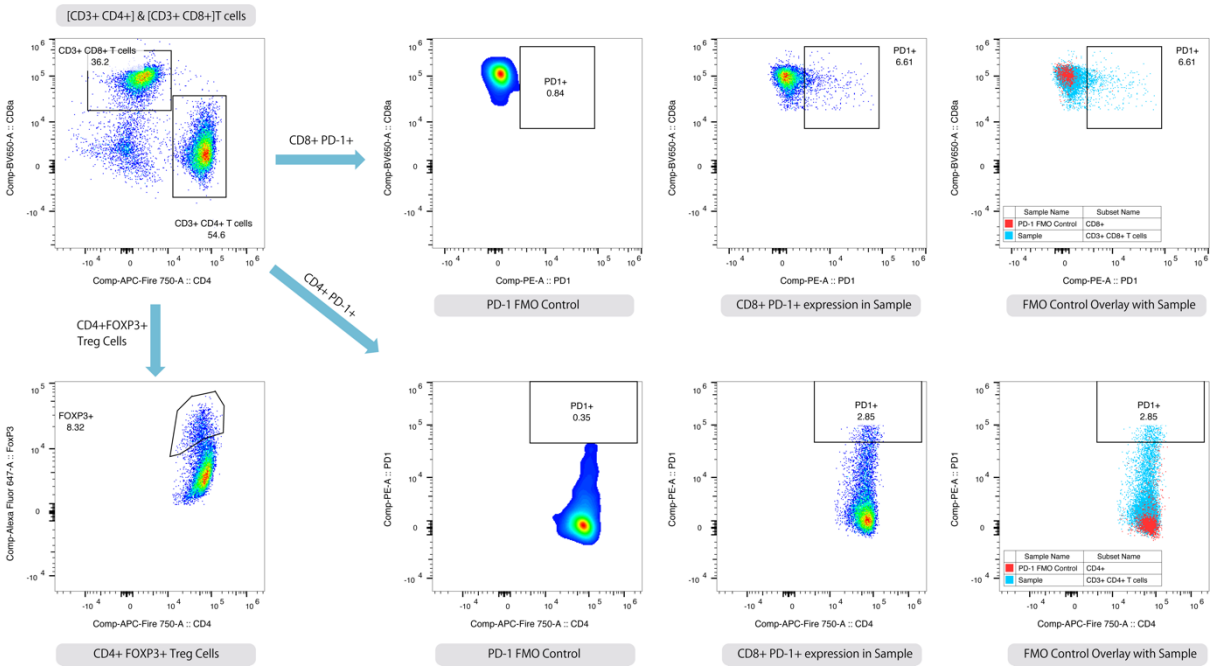

Figure 5-3. Identification of regulatory T cell and programmed cell death protein 1 expression using FlowJo.
From the CD3+CD4+ T helper cells and CD3+CD8+ cytotoxic T cells determined in Figure 5-2, FOXP3+ TReg cells and PD-1 expression were further identified. FOXP3+ TReg cells were identified from T Helper cells as CD4+ FOXP3+. PD-1 was identified from both T helper cells and cytotoxic T cells using the gate from PD1 fluorescence-minus-one control.

5.3 Results

To examine if the old phenotype is transferable via the gut microbiome, a series of aged phenotypes were assessed in the mice colonized with microbes from different donors. To test if the phenotype is also affected by diet or a combination of diet and microbiome, recipient mice that had different diets were compared.

5.3.1 Gut microbiome might be associated with differences in fat mass gain

Aging is associated with body weight gain and obesity (Binyamin, Werbner et al. 2020). To examine if such age-related weight gain is associated with microbiome and diet, the body weight of recipient mice was monitored 3 times a week throughout the experiment. The weight change was calculated as a percentage of body weight gain to ensure fair comparison. The body weight gain since FMT is given in Figure 5-4A. For all treatment groups, increasing in mice body weight was observed as the mice were fully maturing. On average, when having Diet 6 (H_21/34/45) and AIN93G, the microbial type 1 recipients (donor on Diet 6) gained more weight than the microbial type 2 recipient (donor on Diet 2). However, for the mice on Diet 2, an opposite effect was seen.

The weighted gain in microbial type 2 recipients was contributed by fat mass, regardless if they had the same diet as the donor or not (Figure 5-4B-C). For the reciprocal mice that received type 1 microbiome, more lean mass contributed to the weight gain (Figure 5-4B-C). However, no significant differences were found in food intake among different treatment groups (Figure 5-4E). Instead, type I microbiome recipient mice that were on Diet 2 were drinking significantly more water compared to other mice (Figure 5-4D).

Interestingly, for microbial type 2 recipients, Diet 6 group were heavier than Diet 2 group. However, the latter were having more fat mass and less lean mass than the former. It implies that type 2 microbiome recipients were more active when on Diet 6, than on the same diet as the donor. Receiving microbiome from donner with a low fat diet history, facilitates energy expenditure when having a high fat diet (Bäckhed, Ding et al. 2004, Ridaura, Faith et al. 2013). The higher protein ratio in Diet 6 also helps with muscle formation.

5.3.2 Insulin and blood glucose

Aging was also associated with increasing in glucose tolerance and decreasing in insulin clearance (Leiter, Premdas et al. 1988, Oh, Seo et al. 2016, Binyamin, Werbner et al. 2020, Marmentini, Soares et al. 2021). This is confirmed by the mice from the timepoint study where the TOD18 (time on diet for 18mo, i.e. 21mo old) group has a lower blood glucose iAUC value than TOD1 group, regardless of diet (Figure 5-4D). In this study, for the mice on Diet 2, the type 2 microbiome recipients (donor on Diet 2) were having a lower average blood glucose iAUC value than the type 1 microbiome recipients (donor on Diet 6). Not much difference were observed in other treatment groups. Overall, one way ANOVA does not show significant difference at $p<0.05$ among all treatment groups. This is also likely due to the scale of the experiment to give enough statistical power.

For the blood insulin level, the timepoint study shows that only the mice had the bad diet (Diet 6) for 18mo (Figure 5-4E) show high of blood insulin iAUC values. This indicates that 15min after gavage with glucose, high level of insulin was still in these mice's blood. However, the same thing is not observed with mice on Diet 2 or young adult mice (TOD1 groups). This suggests that having Diet 2 tenuate age-related decreasing in insulin clearance. In this study, all recipient mice had similar blood insulin AUC values as the young adult mice (TOD1 groups) from the Timepoint study. One way ANOVA also does not show significant difference at $p<0.05$ among all treatment groups. This implied that age-related decreasing in insulin

clearance were not transferable via the gut microbiome. However, it is also possible that this experiment does not have enough samples to give meaningful statistical significance.

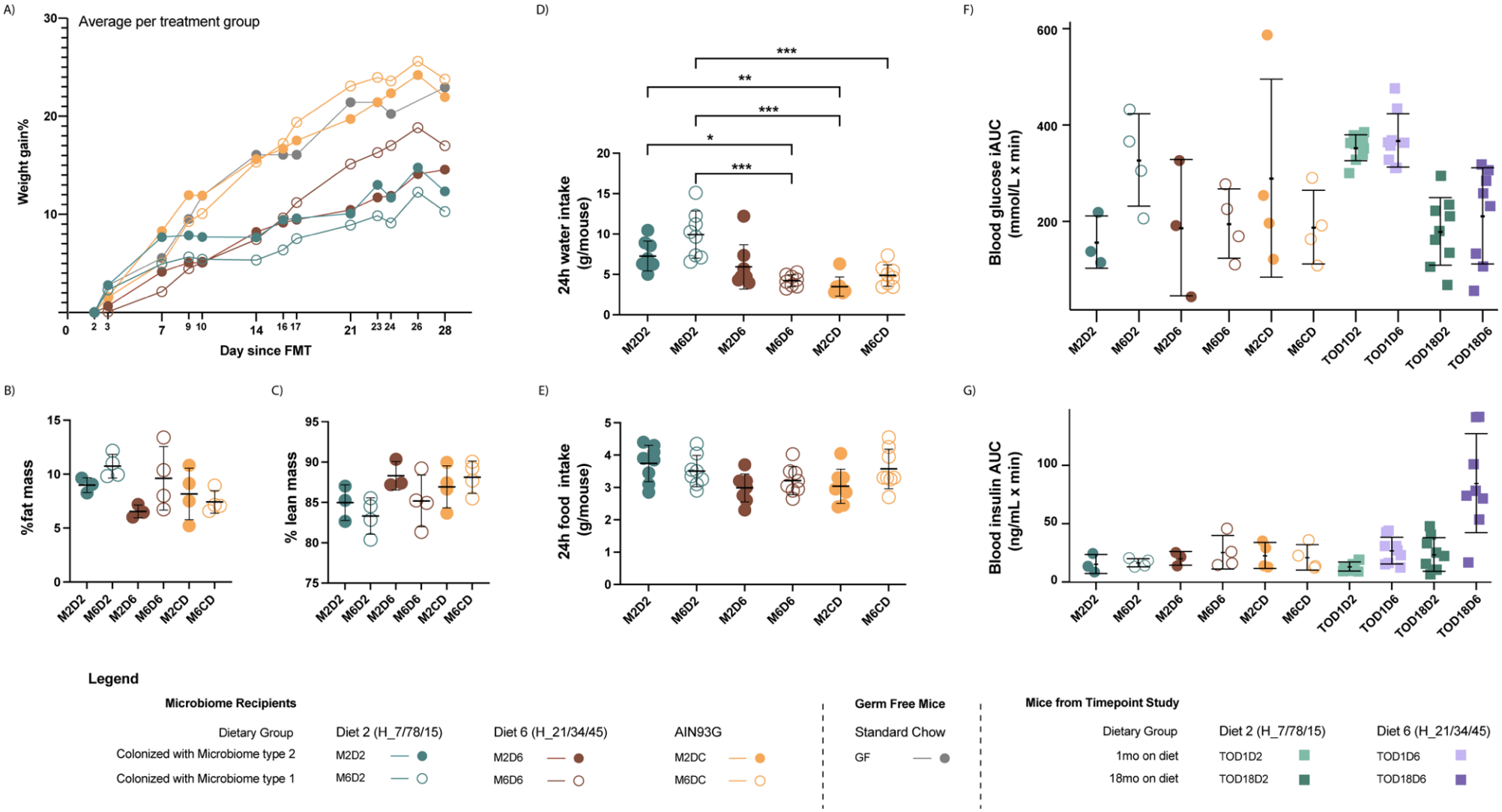

Figure 5-4. Microbial composition is associated with difference metabolic outcomes in gnotobiotic mice.
A) Percentage body weight gain after fecal matter transplant as an average of 3-4 mice in each treatment group. B) Percentage fat mass of body weight for each conventionalized treatment group. C) Percentage lean mass of body weight for each conventionalized treatment group. D) 24h water intake as cage average of 3-4 mice (*: $p<0.05$, **: $0.001<p<0.05$, ***: $p<0.001$). E) 24h food intake as cage average of 3-4 mice. F) Glucose tolerance (incremental area under curve, iAUC) for microbial recipient mice and male mice on Diet 2 and Diet 6 from the timepoint in Chapter 4. G) Change of blood insulin concentration (Area under curve: AUC) for microbial recipient mice and male mice on Diet 2 and Diet 6 from the timepoint in Chapter 4.

5.3.3 Aged microbiome and diet may alter the MLN and spleen immune cell population

Next, the systematic inflammation was examined in both the recipient and germ-free control mice. Aiming to see if the age-related inflammation can be transferable with the gut microbiome. Then, to investigate if the inflammation status is affected by diet or a combination of diet and microbiome. Therefore, the immune cell population was examined using fresh harvest mouse mesenteric lymphocytes and spleen, then analysed using spectral flow cytometry.

Live lymphocytes, and T cells (CD3+ T cells) were measured in both MLN and spleen cell suspensions as percentages in total cells Figure 5-5. T cell subsets, cytotoxic T lymphocytes (CD8+ T cells), T helper cells (CD4+ T cells), and regulatory T cells (FOXP3+ TReg cells) were further analysed (Figure 5-6). Cell senescence marker PD-1 was also analysed (Figure 5-7). The Kruskal-Wallis test was used to determine whether there were significant differences among the experimental groups. Due to the small scale of the gnotobiotic experiment and the high variability between individuals, no statistical significance was found for any of the markers at a *p-value* less than 0.05. This suggests that there were no statistically significant differences in systemic inflammation or cell senescence across the experimental groups.

However, a trend was observed among the treatment groups, with a noticeable difference in averages between the recipients and GF mice for MLN CD3+ T cells (Figure 5-5), CD4+ T helper cells and FoxP3+ regulatory T cells (Figure 5-6). This indicates the establishment of the immune system with gut microbial colonization, where more T cells were activated. The difference observed in MLN, not in the spleen suggests that the immune system development is localized not systematic.

Type II microbiome recipient mice tend to have a higher total T cell (Figure 5-5), and helper T cell (Figure 5-6) in mesenteric lymphocytes compared to Type I microbiome recipients when having either Diet 2 or Diet 6 but not AIN93G. Meanwhile, type II microbiome recipient mice's Foxp3+ regulatory T cells were higher in both mesenteric lymphocyte and spleen cells. This suggests self-regulatory mechanism in the mice's immune system to balance between pro- and anti- inflammation.

Less CD4 cell exhaustion was observed in mesenteric lymph nodes with mice on Diet 2 regardless of which type of microbiome they received (Figure 5-7). This potentially suggests

that Diet 2 was able to attenuate age-related cell senescence regardless of the microbial composition of the mice.

However, it is important to note that right after FMT, two mice received microbiome from the donor on Diet 2 were lost. One of them was found dead in the cage the next morning after FMT, the other one reached humane endpoint about 5 hours after FMT. Post-mortem check did not find any issue with the organ or obvious wounds/tear on the esophagus. It is not sure what caused the death of these two mice. Considering that both mice received the same microbiome, the death event may be related to the microbiome or the process of colonization.

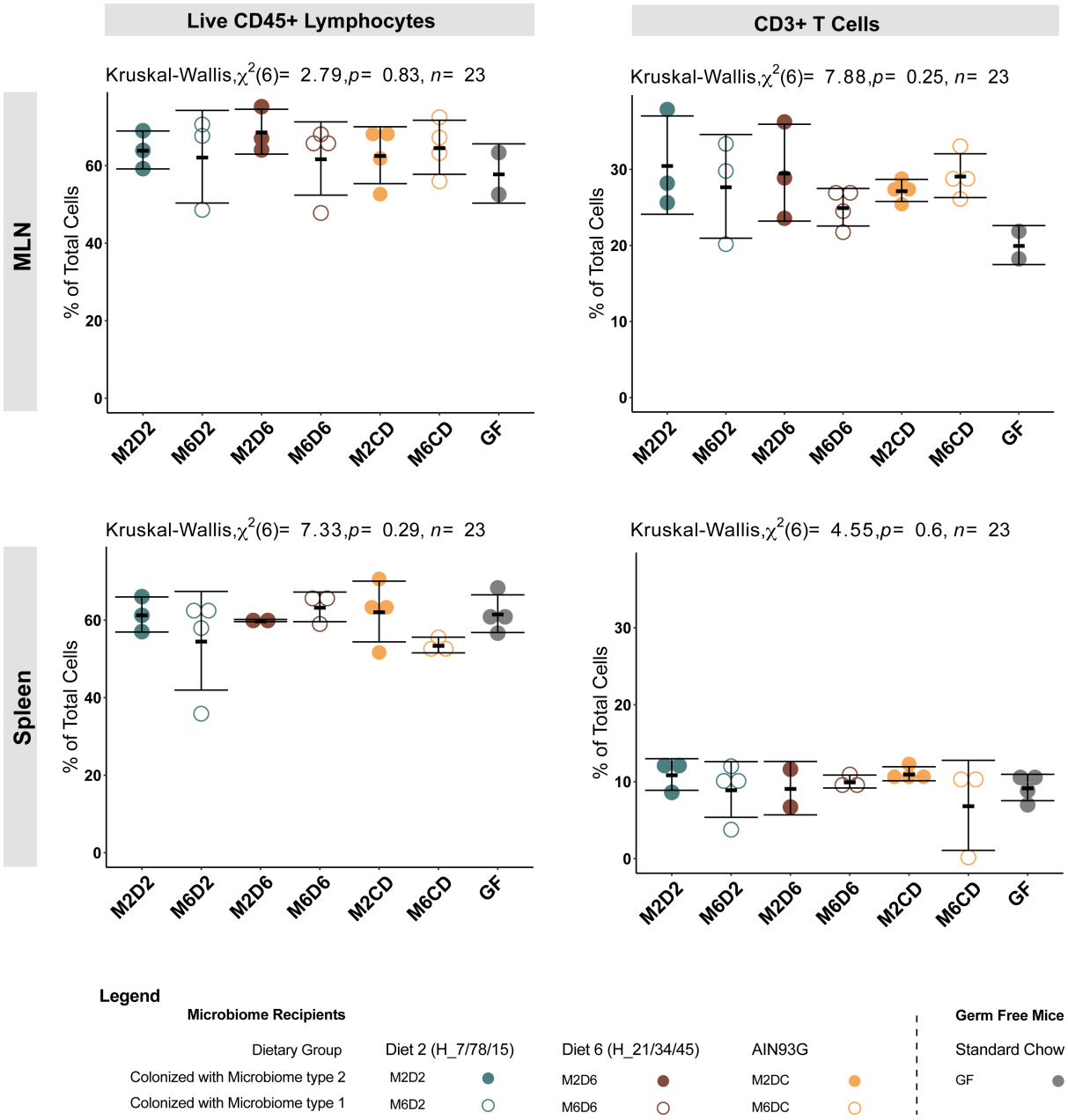

Figure 5-5. Mesenteric and splenic lymphocyte population in germ-free and microbial recipient mice.
Data are presented as individual data points and mean ± SD. Statistical significance was determined by the Kruskal-Wallis test.

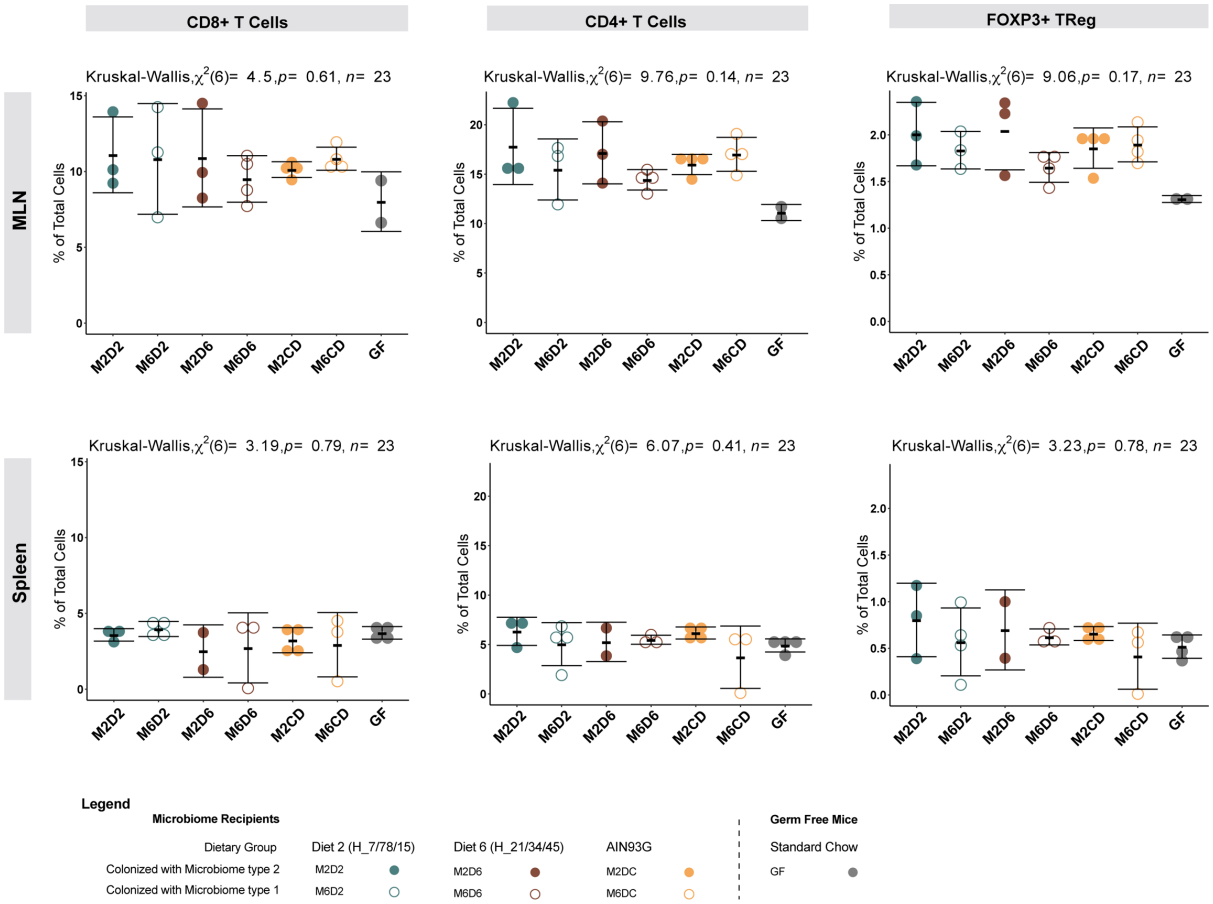

Figure 5-6. Mesenteric and splenic T cell population in germ-free and microbial recipient mice.
Data are present as individual data points and mean ± SD. Statistical significance was determined by the Kruskal-Wallis test.

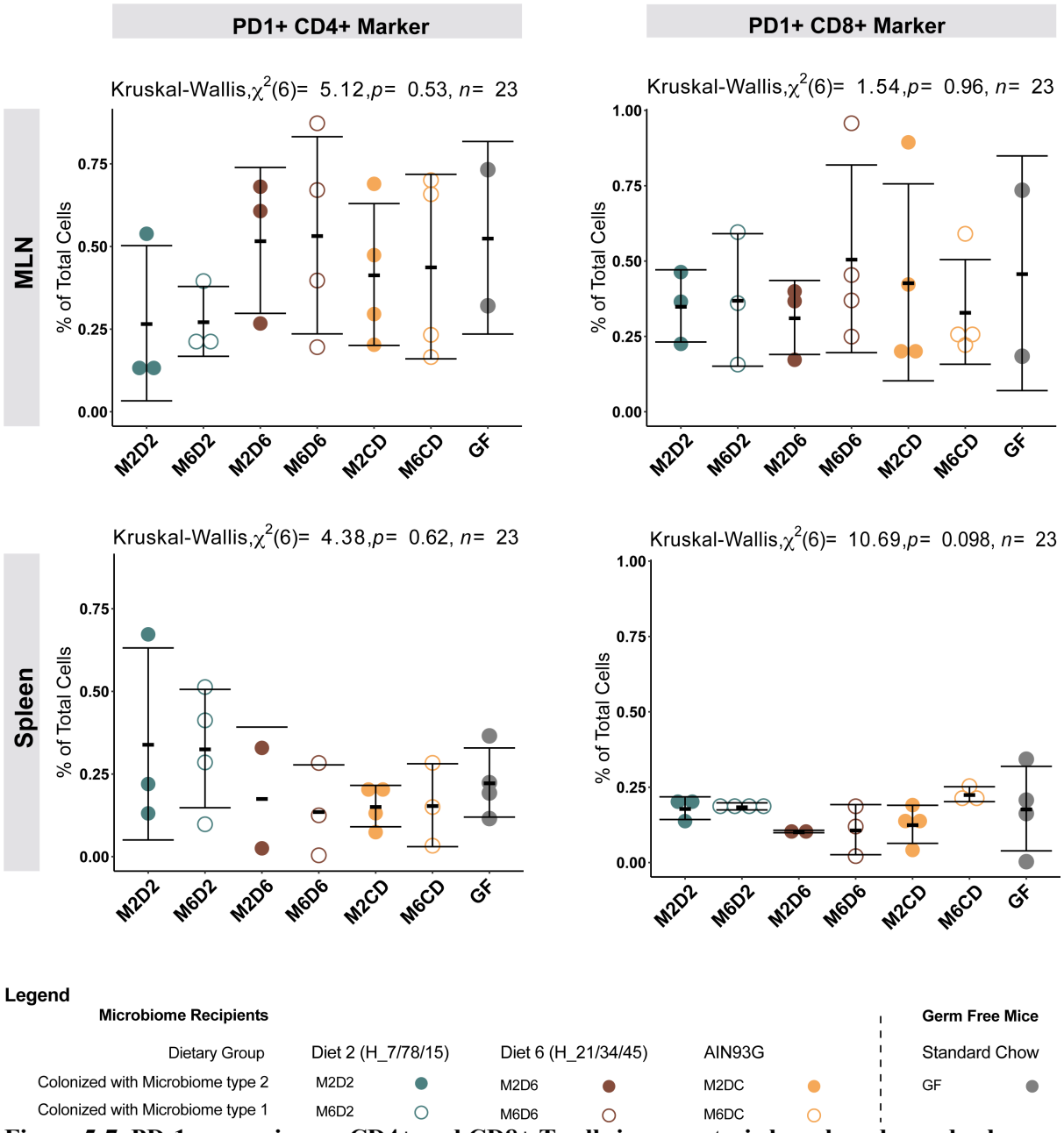

Figure 5-7. PD-1 expression on CD4+ and CD8+ T cells in mesenteric lymph nodes and spleen. Data are present as individual data points and mean ± SD. Statistical significance was determined by the Kruskal-Wallis test.

5.3.4 Time on colonization had a major effect

Next, the microbial composition in the recipient mice was examined. To track the process of microbial colonization and assembly, fresh faces were collected weekly starting from 2 days after FMT. Species richness curves showed initial colonized microbes (T1) had a simpler microbial composition in all mice, regardless of the donor (Figure 5-8A). Between-sample beta-diversity analysis at ASV level was performed on all samples using all three matrices confirmed the T1 communities were distinct with greater differences observed between the start points and later time points as shown in Figure 5-8C. The later samples (T2, T3, T4 and

EP) were more dispersed, with a pattern of samples from different times being distributed in axis 1 (25.5%) and differences in donors distributed in Axis 2 (19.9%) indicating that the duration of colonization had a major effect, while the type of donor microbiome had the secondary effect. During the process of colonization, more unique ASVs were observed in the samples collected at later time points (Figure 5-8A). This indicates that different types of microbes were entering the community, which can be from the food, the environment and the evolution from the colonized microbes.

Within-sample diversity, Inverse Simpson Index, shows the mice on Diet 2 had less individual variance compared to the mice that were on Diet 6 and AIN93G (Figure 5-8B and Supplementary Figure 7-37). Moreover, regardless of which microbiome they received, mice on Diet 2 were less diversified compared with mice on Diet 6. A higher overall InvSimpson index was observed with mice on Diet 6. Although more unique ASVs were observed, the diversity of the microbes was decreasing over time with mice on Diet 2. This indicates that after the initial colonization, these mice's gut was dominated by several abundant taxa. During the following colonization and microbial assembly, some of these taxa no longer proliferating and reduced their population, thus becoming rare species. In contrast, mice on diet 6, increased the diversity for the first 2 weeks after FMT. This suggests that some of the rare species increased its abundance, and become one of the major species.

The taxa plot with the top 20 genera (Figure 5-9) shows the same story. More genera were observed in the mice on Diet 6 than on Diet 2. Meanwhile, for the mice on Diet 6, compared to the first sampling point (2 days after FMT), the relative abundance of some of the rare genus increased at the second sampling point (1 week after FMT), like *Alistipes, Lachnospiraceae NK4A136 group* and *Ligilactobacillus*. Mice on Diet 2, however, were initially dominated by several major genus. Then, as the population decreased over time, they became less abundant. The microbial type 2 recipients on Diet 2 initially had a high relative abundance of *Ileibacterium* and *Akkermansia* at Timepoint 1. The population of *Ileibacterium* dropped at Timepoint 2 (7 days post-FMT), and that of Akkermansia dropped at Timepoint 3. Both of them became less abundant since then. This trend corresponds with the observation in the alpha diversity. Although having the same diet, different donors contribute to different microbial compositions. Overall, mice that received the microbes from the same donor tend to have a similar microbial composition, regardless of what diet they have.

5.3.5 Donor had a secondary effect

To better understand the compositional groups of microbiota, community typing was performed at global level using the Partition Around Medoids (PAM) clustering algorithm with both Bray-Curtis dissimilarity at ASV level (Figure 5-8D), weighted UniFrac distance (Supplementary Figure 7-26C). The number of clusters, k, was determined based on the value of the Calinski-Harabasz (CH) index (Supplementary Figure 7-26A/B). The optimal cluster of k=2 was obtained when the CH index was at maximum.

PAM cluster analysis resulted in two distinctive clusters correspond mainly by the donor, note that this set is a continues changing microbiome (Figure 5-8D). The two clusters are separated mainly by the donor microbiome. Cluster 1 involves all mice that received microbiome from donor on Diet 6, while Cluster 2 have mice with donor on Diet 2 (microbial type 2). However, there are 5 samples in exception (Table 5-1). All of them received microbiome from mice on Diet 2, but clustered together with mice that received microbiome from donor on Diet 6. For mice G1_5.2 and G2_3.1, only samples collected 2 days after FMT were in cluster 1. This maybe because the microbes just resided in the colon and still in the process of stabilization. For mouse G1_3.1, samples collected between 1week to 3 weeks after FMT were in cluster 1. This suggests a possible influence of diet on microbiome composition.

Table 5-1. Exceptional samples in Cluster 1

Mouse ID	On diet	Collection timepoint
G1_5.2	AIN93G	2 days after FMT
G2_3.1	Diet 6	2 days after FMT
G1_3.1	Diet 6	1 week after FMT
G1_3.1	Diet 6	2 weeks after FMT
G1_3.1	Diet 6	3 weeks after FMT

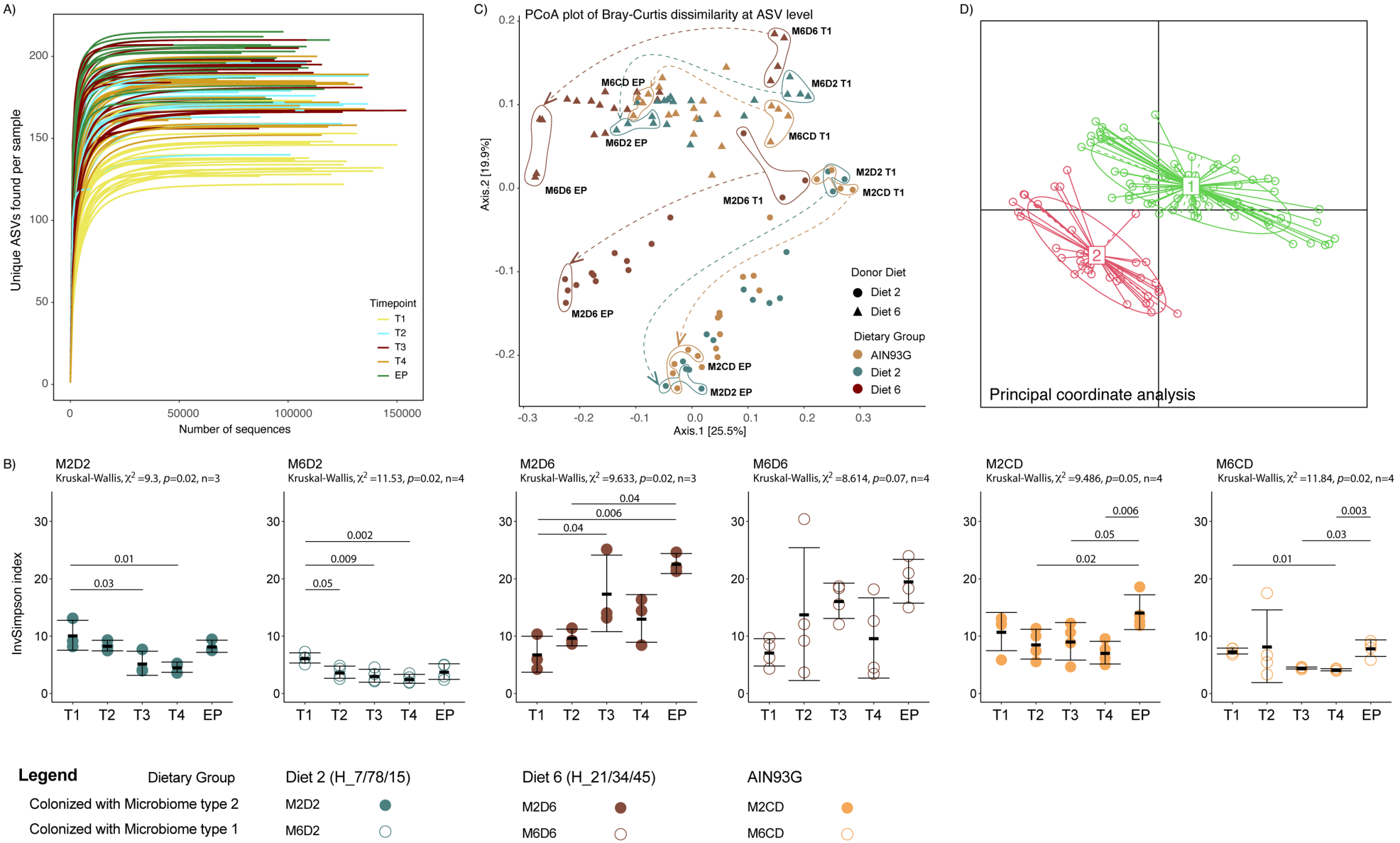

Figure 5-8. The gut microbial composition in recipient mice diversify over time but overall clustered according to donor.
A) Unique ASVs in each sample, colored by collecting timepoints. (EP was the endpoint cecal samples while T1-T4 were fecal samples collected weekly. B) With-in samples inverse Simpson index for each treatment group over time. The significance was determined using the Kruskal-Wallis test, followed by pairwise comparisons with the Wilcoxon test and correction for multiple comparisons using the Benjamini-Hochberg procedure.C) PCoA plot of Bray-Curtis dissimilarity for all samples, colored by collecting timepoints. D) PAM cluster of Bray-Curtis dissimilarity at ASV level gives two clusters, and is associated with 2 different microbial donors.

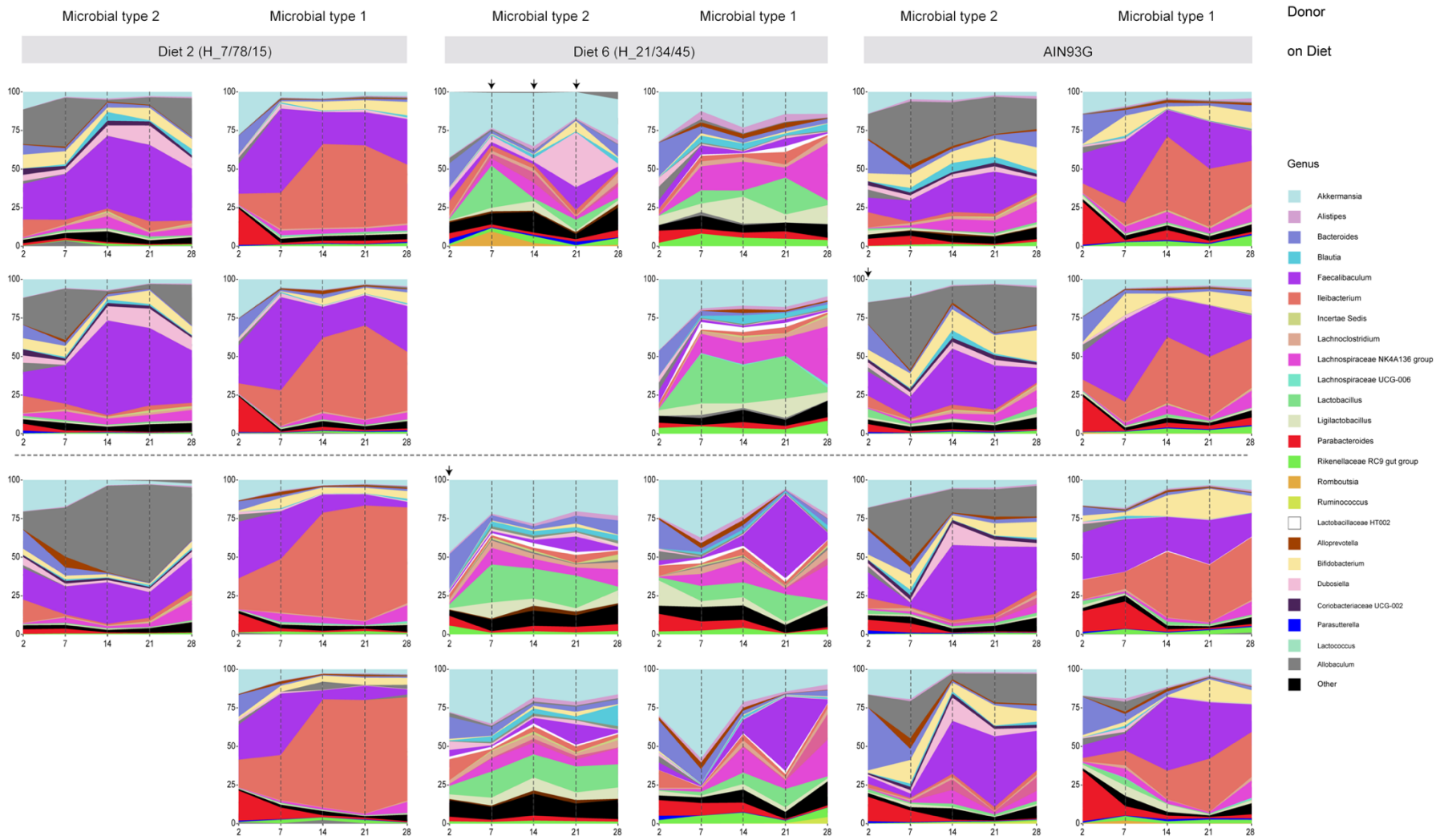

Figure 5-9. Stagger plot of the top 20 taxa at the genus level for each mouse.
Each stagger plot represents one individual, and the black dashed line was the collection point (X-axis as the days since FMT). The first 4 samples were fecal samples and the last one is cecal sample. Each column indicates each treatment group. The first two plots in each column were mice from the same cage, separated by the grey dashed line. The arrow indicates the samples as outliers from the PAM cluster at ASV level.

5.3.6 The effect of diet was observed on stable microbial community

Considering the global analysis involving a set of dynamic samples, further analysis was performed with samples that were more stable. Therefore, fecal samples at Timepoint 3 and Timepoint 4 was picked. Between-sample Bray-Curtis dissimilarity at ASV level showed 4 distinct clusters (Figure 5-10A). Community typing was then performed using the Partition Around Medoids (PAM) clustering algorithm with Bray-Curtis dissimilarity at ASV level. The value of the Calinski-Harabasz (CH) index were found to be at max when k=2 (2 clusters) (Figure 5-10B). However, the value was only a slightly lower when k=4. This indicates that, forming 4 groups of community may also be an option. Therefore, analysis on both partition options were performed. Comparing the samples assigned to 2 clusters (k2) with those assigned to 4 clusters (k4), it appears that one cluster in k2 is split into two distinct clusters in k4 (Figure 5-10C/D/E). Therefore, the clusters in k4 was referred based on the clusters in k2, as 1A, 1B and 2A, 2B. 1A and 1B were from cluster 1 in k2, while 2A and 2B were from cluster 2 in k2.

When partitioned into 2 clusters, the samples were solely clustered based on the donor microbial community. However, when clustered into 4 groups, the samples were splited based on the dietary groups. Diet 2 and AIN93G were clustered together (1A/2A), while Diet 6 were clustered together (1B/2B). As the AIN93G (P/C/F= 18.8/63.4/17.8) and Diet 2 (P/C/F = 7/78/15) were having close macronutrient ratio, mice on these diets had a similar microbial composition compared to the ones on Diet 6. This showed that diet also had an effect on the microbial community. With stabled microbial community, a stronger effect was observed with diet, which was close to the effect of the donor microbial types.

When the microbial composition of each cluster was analyzed using core microbiome analysis, a stronger dietary effect was observed (Figure 5-12). Specifically, the core microbiome analysis showed that clusters 1A and 2A shared a similar microbial composition, with *Akkermensia* (ASV1) being the most abundant taxa in both clusters followed by *Lactobacillus johnsonii* (ASV5). Meanwhile, clusters 1B and 2B exhibited a similar composition, with *Faecalibaculum rodentium* (asv2) and *Bifidobacterium pseudolongum* (asv7) being the top taxa. This finding highlights the dietary influence on the stabilized microbiome, as clusters 1A and 2A followed the same diet, while clusters 1B and 2B were also on the same diet.

Interestingly, unlike at the genus level, the dietary effect was also observed at the family level. Taxa plot at the family level (Figure 5-11) shows that samples from mice on the same diet were

having a similar microbial composition. This suggest a potential functional succession on nutrient utilization at family level.

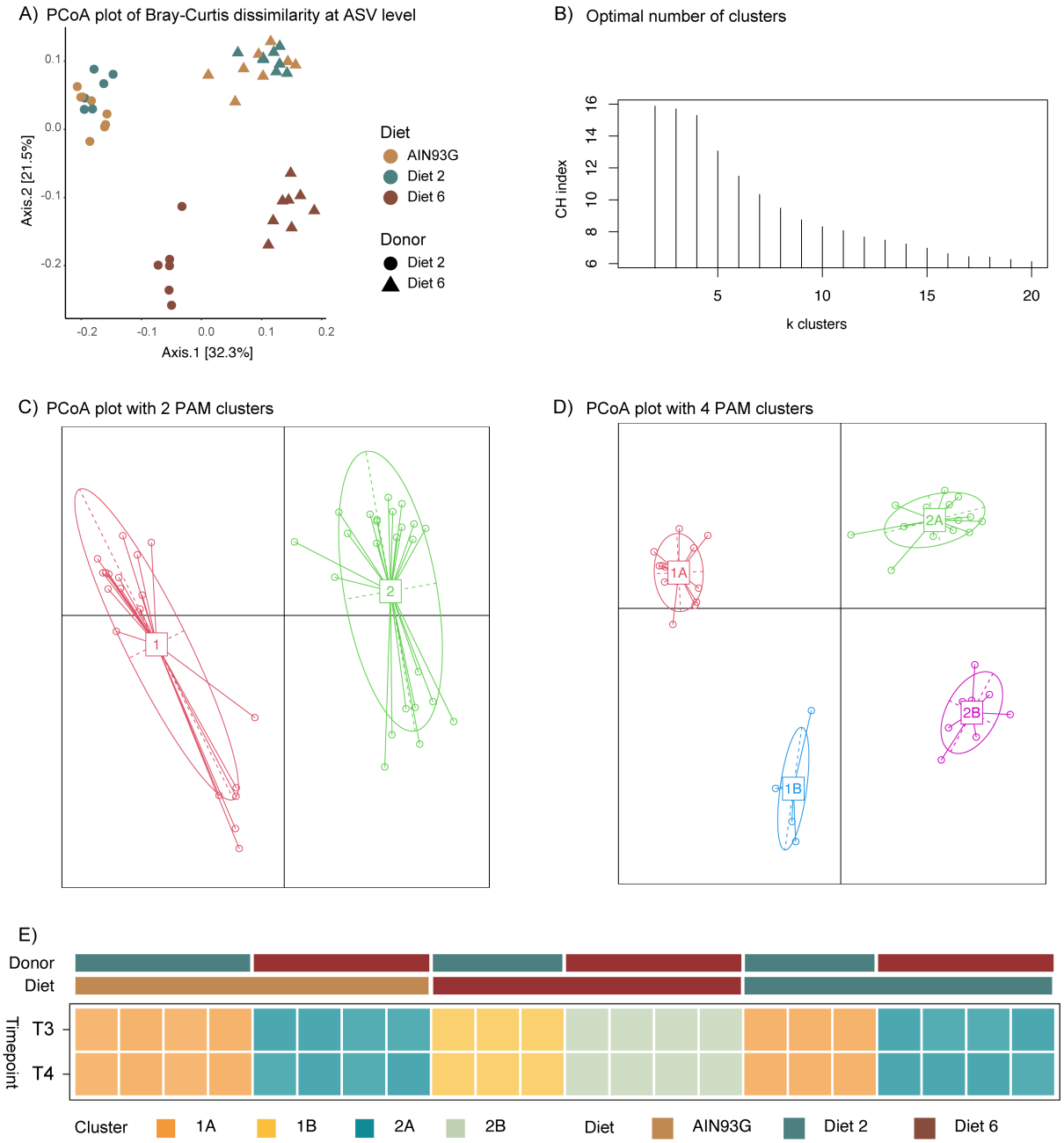

Figure 5-10. Both donor and diet has a determined effect on microbial composition.
A) PCoA plot of Bray-Curtis dissimilarity at ASV level for T3 and T4 fecal samples. B) Optimal number of clusters was determined by the CH index. C) Highest CH index gives 2 clusters for Bray-Curtis dissimilarity at ASV level. D) CH index also showed that 4 clusters may also be a Pam cluster of Bray-Curtis dissimilarity at ASV level gives 2 clusters. E) The clusters are associated with the diet intake. Each column indicates each mouse. Each small square represent one samples, and arrange from top to bottom as collection order.

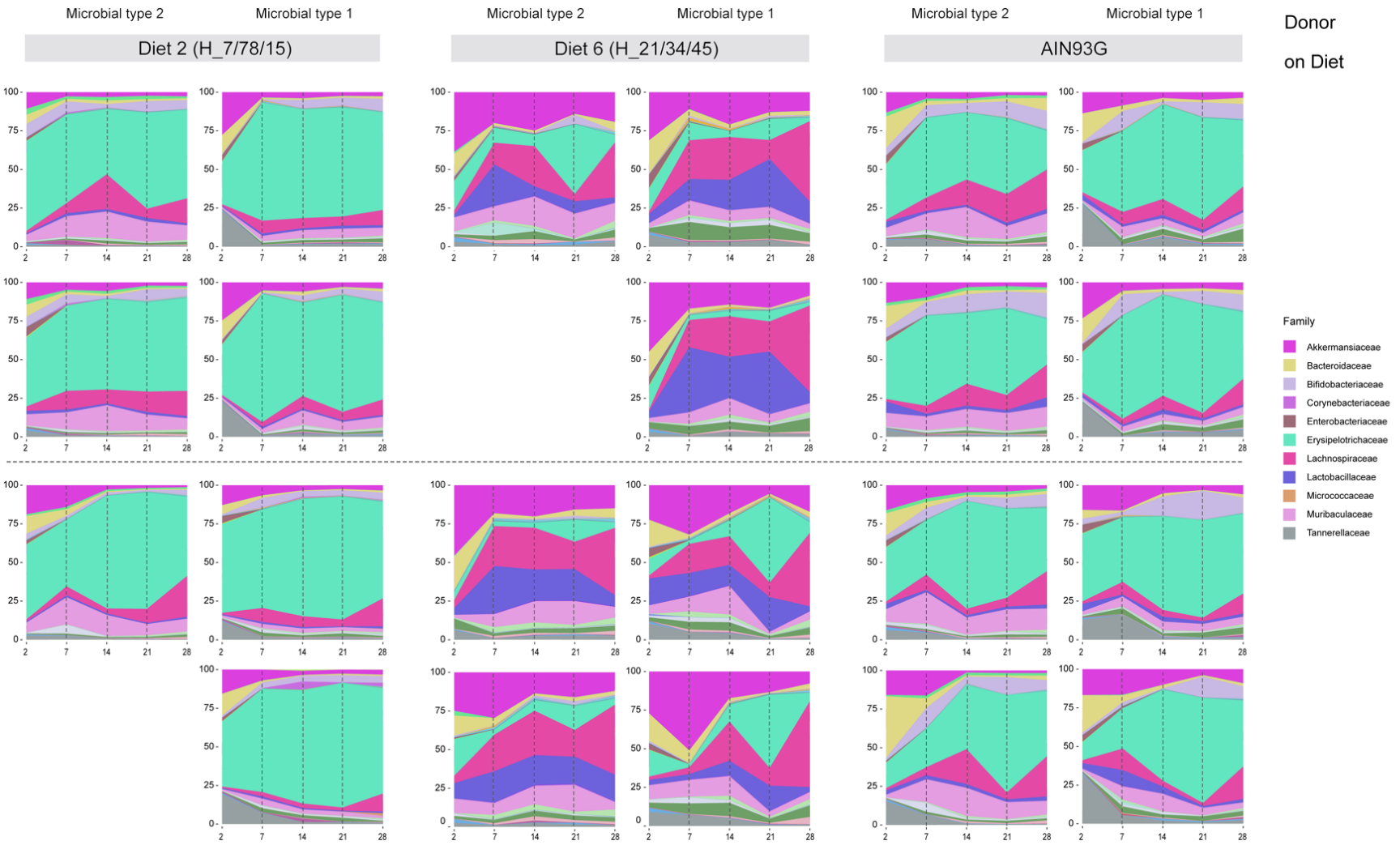

Figure 5-11. Stagger plot at the family level for each mouse.
Each stagger plot represents one individual, and the black dashed line was the collection point (X-axis as the days since FMT). The first 4 samples were fecal samples and the last one is cecal sample. Each column indicates each treatment group. The first two plots in each column were mice from the same cage, separated by the grey dashed line. Dead mice were listed as blank.

5.3.7 Dietary shapes the microbial community in a way similar to the longevity study

The two microbial donors used in this study were on diets that belong to two different microbial clusters in the longevity study, were diet 6 belongs to microbial cluster 1 and diet 2 belonges to microbial cluster 2. In this study, it was found that, for the stabilized microbiome, animals on the same diets were found to have a similar microbial community. Therefore, it is aiming to determine whether the diet-derived microbial community in this study is the same as the one observed in the longevity study. To do so, a comparison was made between the core microbiome and the relative abundance of the phylum in the clusters from both studies. (Figure 5-12). Both analysis found that the diet derived microbial composition between two studies were not exactly the same. However, they share the same signature taxa.

The core microbiome (Figure 5-12A) indicates that dietary drived clusters in both studies have the same most prevalent ASV, which is *Akkermansia* for Diet 6 (cluster 1B and 2B) and *Faecalibaclum* for Diet 2 (cluster 1A and 2A). However, cluster 1 in this study also has a high prevalence of *Faecalibaclum* and *Ileibacterium*, while for cluster 2 in this study, *Ileibacterium* was having a high prevalence. This indicates that the diety drived clusters in this study are more similar comparing to that in the longevity study.

Next, the relative abundance of all seven phyla was compared in all PAM clusters from the two studies. (Figure 5-12B). Out of the 7 phyla, 5 of them shared the same trend in both studies, which consists over 97% of the microbes. However, difference were found in the relative abundance of two minority phylum *Proteobacteria* and *Deferribacterota*. The dietary clusters in the longevity studies had a similar amount of *Proteobacteria* and *Deferribacterota*. However, in this study, PAM cluster 1B had the highest amount of *Proteobacteria*. The samples in cluster 1B were from mice on Diet 6 while received initial microbiome from Diet 2 donors. For *Deferribacterota*, Pam cluster 2B in study had the highest relative abundance. The samples om cluster 2B were also from mice on Diet 6. However, these mice received initial microbiome from a different donors. This suggests a donor effects persisted on the stabilized microbial community, and such effects were on the minority groups. However, as the microbial community become stable, the merging effect of diet overrides the donor effects.

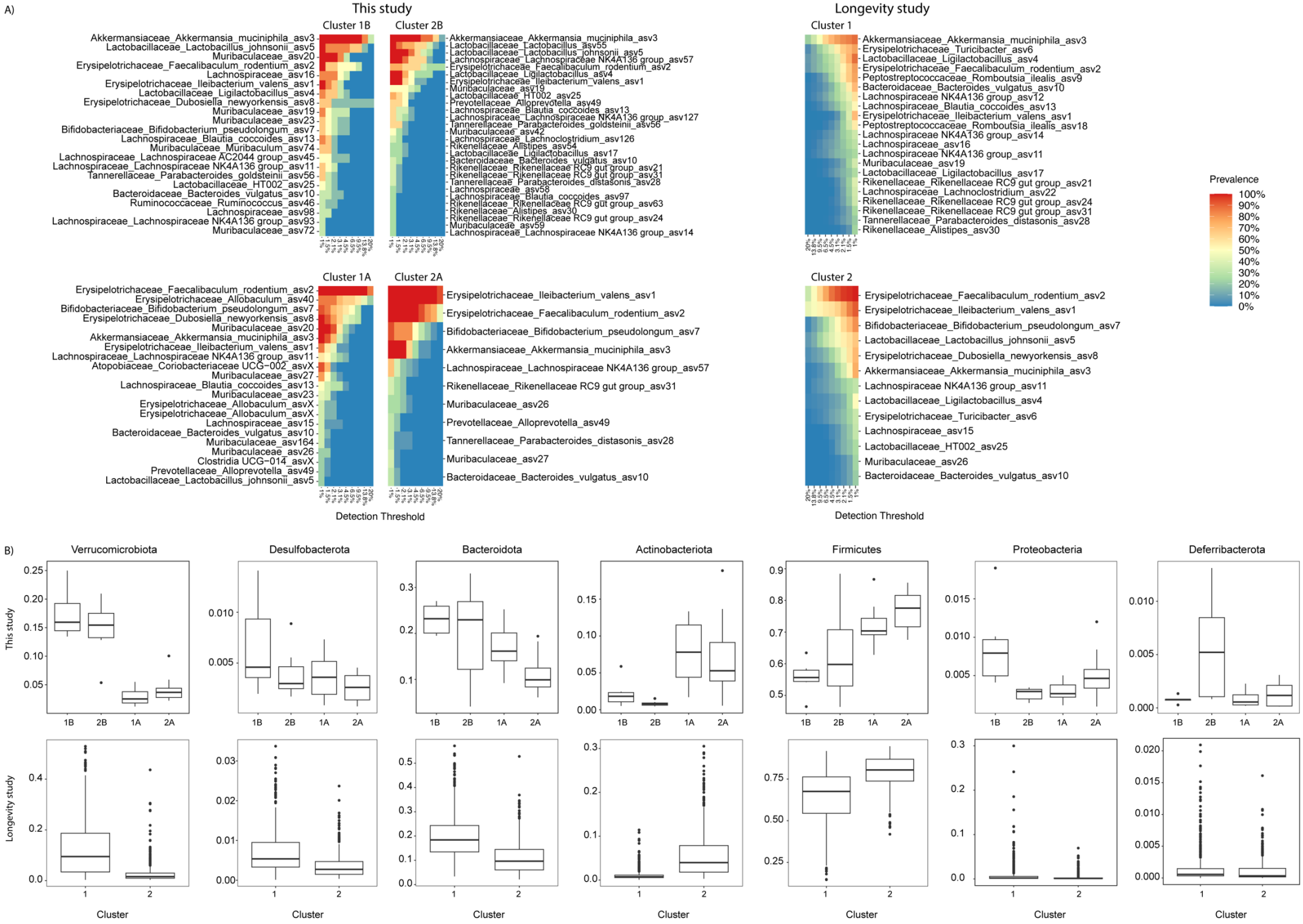
A)
This study
Cluster 1B
Akkermansiaceae_Akkermansia_muciniphila_asv3
Lactobacillaceae_Lactobacillus_johnsonii_asv5
Muribaculaceae_asv20
Erysipelotrichaceae_Faecalibaculum_rodentium_asv2
Lachnospiraceae_asv16
Erysipelotrichaceae_Ileibacterium_valens_asv1
Lactobacillaceae_Ligilactobacillus_asv4
Erysipelotrichaceae_Dubosiella_newyorkensis_asv8
Muribaculaceae_asv19
Muribaculaceae_asv23
Bifidobacteriaceae_Bifidobacterium_pseudolongum_asv7
Lachnospiraceae_Blautia_coccoides_asv13
Muribaculaceae_Muribaculum_asv74
Lachnospiraceae_Lachnospiraceae AC2044 group_asv45
Lachnospiraceae_Lachnospiraceae NK4A136 group_asv11
Tannerellaceae_Parabacteroides_goldsteinii_asv56
Lactobacillaceae_HT002_asv25
Bacteroidaceae_Bacteroides_vulgatus_asv10
Ruminococcaceae_Ruminococcus_asv46
Lachnospiraceae_asv98
Lachnospiraceae_Lachnospiraceae NK4A136 group_asv93
Muribaculaceae_asv72
Cluster 2B
Akkermansiaceae_Akkermansia_muciniphila_asv3
Lactobacillaceae_Lactobacillus_asv55
Lactobacillaceae_Lactobacillus_johnsonii_asv5
Lachnospiraceae_Lachnospiraceae NK4A136 group_asv57
Erysipelotrichaceae_Faecalibaculum_rodentium_asv2
Lactobacillaceae_Ligilactobacillus_asv4
Erysipelotrichaceae_Ileibacterium_valens_asv1
Muribaculaceae_asv19
Lactobacillaceae_HT002_asv25
Prevotellaceae_Alloprevotella_asv49
Lachnospiraceae_Blautia_coccoides_asv13
Lachnospiraceae_Lachnospiraceae NK4A136 group_asv127
Tannerellaceae_Parabacteroides_goldsteinii_asv56
Muribaculaceae_asv42
Lachnospiraceae_Lachnoclostridium_asv126
Rikenellaceae_Alistipes_asv54
Lactobacillaceae_Ligilactobacillus_asv17
Bacteroidaceae_Bacteroides_vulgatus_asv10
Rikenellaceae_Rikenellaceae RC9 gut group_asv21
Rikenellaceae_Rikenellaceae RC9 gut group_asv31
Tannerellaceae_Parabacteroides_distasonis_asv28
Lachnospiraceae_asv58
Lachnospiraceae_Blautia_coccoides_asv97
Rikenellaceae_Rikenellaceae RC9 gut group_asv63
Rikenellaceae_Alistipes_asv30
Rikenellaceae_Rikenellaceae RC9 gut group_asv24
Muribaculaceae_asv59
Lachnospiraceae_Lachnospiraceae NK4A136 group_asv14
Cluster 1A
Erysipelotrichaceae_Faecalibaculum_rodentium_asv2
Erysipelotrichaceae_Allobaculum_asv40
Bifidobacteriaceae_Bifidobacterium_pseudolongum_asv7
Erysipelotrichaceae_Dubosiella_newyorkensis_asv8
Muribaculaceae_asv20
Akkermansiaceae_Akkermansia_muciniphila_asv3
Erysipelotrichaceae_Ileibacterium_valens_asv1
Lachnospiraceae_Lachnospiraceae NK4A136 group_asv11
Atopobiaceae_Coriobacteriaceae UCG−002_asvX
Muribaculaceae_asv27
Lachnospiraceae_Blautia_coccoides_asv13
Muribaculaceae_asv23
Erysipelotrichaceae_Allobaculum_asvX
Erysipelotrichaceae_Allobaculum_asvX
Lachnospiraceae_asv15
Bacteroidaceae_Bacteroides_vulgatus_asv10
Muribaculaceae_asv164
Muribaculaceae_asv26
Clostridia UCG−014_asvX
Prevotellaceae_Alloprevotella_asv49
Lactobacillaceae_Lactobacillus_johnsonii_asv5
Cluster 2A
Erysipelotrichaceae_Ileibacterium_valens_asv1
Erysipelotrichaceae_Faecalibaculum_rodentium_asv2
Bifidobacteriaceae_Bifidobacterium_pseudolongum_asv7
Akkermansiaceae_Akkermansia_muciniphila_asv3
Lachnospiraceae_Lachnospiraceae NK4A136 group_asv57
Rikenellaceae_Rikenellaceae RC9 gut group_asv31
Muribaculaceae_asv26
Prevotellaceae_Alloprevotella_asv49
Tannerellaceae_Parabacteroides_distasonis_asv28
Muribaculaceae_asv27
Bacteroidaceae_Bacteroides_vulgatus_asv10
Detection Threshold
Longevity study
Cluster 1
Akkermansiaceae_Akkermansia_muciniphila_asv3
Erysipelotrichaceae_Turicibacter_asv6
Lactobacillaceae_Ligilactobacillus_asv4
Erysipelotrichaceae_Faecalibaculum_rodentium_asv2
Peptostreptococcaceae_Romboutsia_ilealis_asv9
Bacteroidaceae_Bacteroides_vulgatus_asv10
Lachnospiraceae NK4A136 group_asv12
Lachnospiraceae_Blautia_coccoides_asv13
Erysipelotrichaceae_Ileibacterium_valens_asv1
Peptostreptococcaceae_Romboutsia_ilealis_asv18
Lachnospiraceae NK4A136 group_asv14
Lachnospiraceae_asv16
Lachnospiraceae NK4A136 group_asv11
Muribaculaceae_asv19
Lactobacillaceae_Ligilactobacillus_asv17
Rikenellaceae_Rikenellaceae RC9 gut group_asv21
Lachnospiraceae_Lachnoclostridium_asv22
Rikenellaceae_Rikenellaceae RC9 gut group_asv24
Rikenellaceae_Rikenellaceae RC9 gut group_asv31
Tannerellaceae_Parabacteroides_distasonis_asv28
Rikenellaceae_Alistipes_asv30
Cluster 2
Erysipelotrichaceae_Faecalibaculum_rodentium_asv2
Erysipelotrichaceae_Ileibacterium_valens_asv1
Bifidobacteriaceae_Bifidobacterium_pseudolongum_asv7
Lactobacillaceae_Lactobacillus_johnsonii_asv5
Erysipelotrichaceae_Dubosiella_newyorkensis_asv8
Akkermansiaceae_Akkermansia_muciniphila_asv3
Lachnospiraceae NK4A136 group_asv11
Lactobacillaceae_Ligilactobacillus_asv4
Erysipelotrichaceae_Turicibacter_asv6
Lachnospiraceae_asv15
Lactobacillaceae_HT002_asv25
Muribaculaceae_asv26
Bacteroidaceae_Bacteroides_vulgatus_asv10
Detection Threshold
Prevalence
100%
90%
80%
70%
60%
50%
40%
30%
20%
10%
0%
B)
Verrucomicrobiota
Desulfobacterota
Bacteroidota
Actinobacteriota
Firmicutes
Proteobacteria
Deferribacterota
This study
Longevity study
1B
2B
1A
2A
Cluster

Figure 5-12. Comparison of the microbial composition of Pam clusters in this study with that of the longevity study.
A) Comparing core microbiome of clusters in this study the longevity study (ASV numbers in this study were matched with the ASV numbers in the longevity study. Unmatched ASVs are noted as X) B) The relative abundance of the phylum in all 4 clusters. The top panel is this study. The bottom is the longevity study, involving 9 diets and 1,054 fecal samples.

5.4 Discussion

The adult microbiome is dynamic. It changes in response to the environmental changes during aging. My previous study in Chapter 4 found two microbial clusters in the males mice population. These two clusters were associated with dietary intake and longevity. I then hypothesised that such variance in longevity is associated with the difference in gut microbiome and diet. In this study, I examined if the aging phenotype is transferable via the gut microbiome. I then addressed the question of how diet-induced changes in the gut microbiome impacted the aging phenotype.

My study found that no aging phenotypes were transferred with the gut microbiome, as no significant differences were found among treatment groups both at localized area and systematically. It is possible that the localized inflammation was not transferrable via the gut microbiome. A similar result was observed with a study from Qiao, Zhou et al. (2023), in which no differences were found in colon inflammation cytokines between the young and old microbiome recipients. However, for this study, a trend was still observed among the treatment groups, shown as 1 standard deviation different in group average. Thus, the lack of significance was likely due to the limited sample size of this study and high individual variance. In particular, the sample size was determined, initially during study design, based on the power analysis using a sample microbiome data.

The type II microbiome recipient mice showed a possible higher level of CD4+ and Foxp3+ compared to the type I microbiome recipient. Higher level of CD4+ T-cells and regulatory T cells were often observed in aged mice (Elyahu, Hekselman et al. 2019, Mogilenko, Shpynov et al. 2021). However, high level of Foxp3+ on Treg cells was associated with the secretion of IL-10, an anti-inflammation cytokine (Schmitt, Rink et al. 2013, Saito, Nishikawa et al. 2016). Thus, high level of Foxp3+ in the type II microbiome suggests type II microbiome, as part of animals' self-regulatory mechanism, was able to suppress the age-related inflammation. To confirm this, future studies should test both the pro-inflammation cytokines, like IL-6 and NF-κB, as well as anti-inflammation cytokines, like IL-10, in the colon tissue or in the blood.

Meanwhile, more CD3+, FoxP3+ and CD4+ cell populations were found in the recipients than the germ-free mice. This was expected to be seen between the germ-free and conventional mice (Östman, Rask et al. 2006, Niess, Leithäuser et al. 2008). However, it was not able to tell if such differences were due to microbial colonization only or because of a combination of the

microbial colonization and aging. Therefore, to answer this question, future study should include a control group of mice that received microbiome from the same donor at a younger age as a comparison. In such way, it can be certain that the difference was due to aged microbiome not the colonization of gut microbiome.

The microbial analysis, meanwhile, observed 'geographic' or donor effects at fine taxonomic resolution. Diet (or resource) effects are seen at deeper phylogenetic groups perhaps reflecting evolutionarily conserved life history strategies. The different was likely due to the trait-base assembly and succession (Guittar, Shade et al. 2019). The germ-free mice initially received gut microbiome from a single shot of fecal slurry via oral gavage. Because the microbiome came from different donors, distinct microbial species were introduced into the gastrointestinal tract. Along with the microbiomes, the recipient mice were also provided a specific diet, which selectively influenced microbial colonization and initial assembly. For mice on the same diet but having different microbiome origins, although specific microbial species differed, their gut microbiomes shared a similar ability to utilize nutrients.

Microbes need both carbon and nitrogen for growth (Holmes, Chew et al. 2017). They can get these nutrients either from exogenous sources like diet or endogenous source like mucus layer and urea (Holmes, Chew et al. 2017, Zeng, Xing et al. 2022). When the dietary sourced nutrients become limited, the microbes will turn to endogenous sources for survival (Holmes, Chew et al. 2017). The two experimental diets used in this study contained different protein-to-carbohydrate ratios, for Diet 2 the ratio is 7/78/15 (P/C/F) and for Diet 6 is 21/34/45 (P/C/F). For Diet 2, high amount of carbohydrate is associated with a limited amount of protein intake. Therefore, protein is likely to be the limiting resource, and nitrogen forging microbes were likely to thrive. However, it is important to note that all diets used purified ingredients, which has limited amount of dietary fibre. The main source of dietary fibre is from the wheat starch, which contains about 0.085% of resistant starch (Tharanathan and Tharanathan 2001). This is equivalent to 0.43g/kg in Diet 2 and 0.18g/kg in Diet 6. Therefore, it is also possible that microbes were also need to forging carbon source from the gut environment like the mucin glucan.

This is particularly *Erysipelotrichaceae* is the most abundant family in mice that were having Diet 2 (Figure 5-11). For the mice received microbiome from donors on Diet 2, *Allobaculum* and *Faecalibaculum* were the main genus in *Erysipelotrichaceae* (Figure 5-9). For the mice

received microbiome from donors on Diet 6, *Faecalibaculum* and *Ileibacterium* were the main genus in *Erysipelotrichaceae* (Figure 5-9). *Allobaculum*, *Faecalibaculum* and *Ileibacterium* were all known to utilize both the dietary carbon the endogenous nitrogen source (Holmes, Chew et al. 2017, van Muijlwijk, van Mierlo et al. 2021, Zeng, Xing et al. 2022, Chu, Li et al. 2023). Moreover, mice on AIN93G (18.8/63.4/17.8) and Diet 2 (7/78/15) were having a similar microbial composition, especially at the family level. This may also be because of the trait-based succession, as these two diets have a similar carbohydrate-to-protein ratio.

Furthermore, mice on Diet 2 showed a lower level of CD4 cell exhaustion in MLN irrelevant of which type of initial microbiome the mice received. This potentially suggests that Diet 2 was able to attenuate age-related cell senescence. Such effects may be via microbiome-dependent manner. Both groups of mice on Diet 2 were found to have large relative abundant of *Faecalibaculum rodentium* in their gut, suggesting the potential functional role of this microbes. Previous study showed that *Faecalibaculum rodentium* has anti-tumorigenesis property via the production of short-chain fatty acid (SCFA), butyrate (Zagato, Pozzi et al. 2020). However, no immune response was observed during this process (Zagato, Pozzi et al. 2020). In addition, SCFA is primarily produced via microbial fermentation of indigestible polysaccharide, which is limited in this study (Rowland, Gibson et al. 2018). Therefore, the anti-inflammatory/anti-aging effect was not likely due to the produce of SCFA. Duodenum microbial analysis, meanwhile, identified the role of *Faecalibaculum rodentium* in maintaining epithelial cell turnover and major histocompatibility complex class II (MHCII) expression via retinoic acid signaling (Cao, Bae et al. 2022). MHCII can modulate CD4+ cells and regulate immune response (Cao, Bae et al. 2022). To verify this, MCHII expression and retinoic acid concentration in the colon need to be tested.

It is also worth mentioning a prior study that employed a geometric framework and purified ingredients to examine the effects of diet on aging found that a high carbohydrate-to-protein ratio was associated with increased lifespan in mice. (Solon-Biet, McMahon et al. 2014). This effect was associated with the activation of hepatic mammalian target of rapamycin (mTOR) and elevated levels of circulating branched-chain amino acids (BCAAs) and glucose (Solon-Biet, McMahon et al. 2014). However, Diet 2 did not show a significant increase or even a trend toward higher blood glucose levels, suggesting that its effect on prolonging aging may operate through a different pathway.

This experiment lacks metabolomic and proteomic analyses of plasma and cecal content. Therefore, it is hard to associate the aging phenotype with the microbiome difference directly. Future studies or analysis should include both of them to make firm conclusion.

6 Final Discussion and Conclusions

Differences in gut microbial compositions were observed between elder individuals and young adults (Ke, Mitchell et al. 2021, Wilmanski, Diener et al. 2021, Wu, Muthyala et al. 2021). Such difference in microbial structure was associated with multiple age-related diseases, including neuro-degenerating disease and cardiovascular disease (Brunt, Gioscia-Ryan et al. 2019, Kundu, Lee et al. 2019, Brunt, Casso et al. 2021). The discovery of the similarity between age-associated low-grade inflammation and obesity-induced inflammation points to the role gut microbiome plays in energy harvesting and nutrient metabolism during aging (Franceschi, Garagnani et al. 2018). The overarching aim of this thesis is to investigate how the diet (macronutrient composition and intake pattern) impacts the gut microbiome and host physiology during aging. In this thesis, diet was simplified into 3 different macronutrients, carbohydrate, protein and fat. Diets were varied in macronutrient ratios, energy densities and eating habits (CR vs *ad-lib*). To address this aim, I conducted a cross-section study to look at the aged-related changes at community level (Chapter 3), a longevity study to track the age-related changes in the individuals (Chapter 4) and a FMT experiment to understand the mechanistic link behind it (Chapter 5). The common finding across these studies was that aging did have an impact on gut microbial composition. However, such impact was diet dependent and was marginal compared to the dietary effect.

6.1 The microbial types are universal

At the community level, recurrent two microbial types were found in both Chapter 3 and Chapter 4. Microbial type I was high in *Bacterodiota, Desulfobacterota* and *Verrucomicrobiota (Akkermansia)*, while microbial type II was high in *Firmicutes* and *Actinobacteriota*. Enterotypes was also observed in other laboratory mice (Hildebrand, Nguyen et al. 2013). Due to the different in diets and mice housing history, the enterotypes were different between this thesis and other studies. Moreover, , this thesis revealed a less distinct disparity in phylum level relative abundance between the enterotypes. This is likely because mice were fed purified ingredients, thus the microbes were less influenced by diet. Thus, the two enterotypes had similar microbial compositions.

These two microbial types were associated with the diet, especially the dietary macronutrient energy intakes. Type I was derived by fat intake and type II by carbohydrate. This aligned with the nutrient preferred by the phylum (Holmes, Chew et al. 2017, Zeng, Xing et al. 2022). During aging, a one-directional microbial type shift was found from type II to type I, primarily

before the mice reached the old age, 21 months old (Chapter 3). These microbial types were then associated with the longevity in male mice, with microbial type II being delay aging and microbial I being early aging (Chapter 4).

In humans, such aging associated microbes were also observed. However, instead of microbiome as a whole unity, groups of microbes was found to associated with early/delay aging. Ghosh, Shanahan et al. (2022) summarized 3 groups of microbes in human gut which were associated with aging. Decreasing of Group 1 microbes (*Faecalibacterium*, *Roseburia* and ect) and increasing of group 3 microbes (*Eggerthella*, *Bilophila* and ect) were associated with healthy aging while increasing group 2 microbes (*Akkermansia*, *Christensenellaceae* and ect) correlates to diseases and functional decline. However, humans had a more diverse and uncontrolled diet. Their gut microbiome also received more host inaccessible carbohydrates compared to the diets used in thesis. Therefore, it was not possible to directly compare the results from this thesis to results from human trials. For example, *Akkermansia* from Group 3 in human studies, was increased with aging and correlates to health aging. In this thesis, in contrast, *Akkermansia* was found high in Microbial Type I and was associated with early aging, particularly with male mice. However, results from this thesis and the human studies all suggest that microbiome was able to reflect the animal's health status during aging. It would be possible to the "predict" aging/longevity via monitoring the gut microbial compositional change.

6.2 The age-related microbial behavior

The emergent microbial behavior during aging can be categorized into 2 stages as mapped in Figure 6-1. At normal conditions, the gut microbiome was metastable. It fluctuates between different states (Chapter 4 and Chapter 5). Overall, the differences between states stay similar over time (Chapter 4). However, changing in diet or physiological status resulted in microbiota to jump to a new states (Chapter 5). At the community level, this was shown as the microbial type shift from type II to type I (Chapter 3). Although microbial type shift was associated with microbial compositional change, no obvious microbial state transition was observed in individuals (Chapter 4). Thus, I hypothesise that the 1st stage of aging involves microbial type transition with a minor microbial state transition at individual level. As the diets contained different macronutrient ratios, the rate of such shift was found diet-specific (Chapter 3 and Chapter 4). The 2nd stage of aging was opposite from the 1st stage of aging, where no further microbial shift was observed at community level but a dramatic state transition was found in

individuals. Depending on the diet, the onset of this state transition also varies, ranging from 25-27 months of age (Chapter 4).

Given the age-related microbial behavior, I further hypothesis that such microbial type shift and microbial state transition can be used to predict the longevity in mice, particularly in male mice. When comparing the lifespan data from Chapter 4 with the microbial type shift data in Chapter 3, mice had early microbial shift exhibiting a higher mortality rate by 18 months on diet. This correlation was especially pronounced with the male population, where half of the populations were dead for Diet 1, 16 and 18 (Supplementary Figure 7-32). Populations with these diets were had microbial type I at 6 months on diet. Varied death rates were observed with the microbial type I mice. A higher mortality rate was found in Diet 6 than Diet 8 at 12 months on diet, even though all mice were had microbial type I microbiome. The early death in male mice was likely more closely linked to the second stage of aging rather than the first stage of aging, i.e. the microbial type shift. The type II microbial composition potentially triggering the anti-inflammatory mechanism in males (Chapter 5). Therefore, delaying the microbial type shift or/and microbial state transition might keep the healthy state of the microbiome, reduce immune senescence and prolong the lifespan. However, such association was less apparent with the females. in particular with Diet 2 (Supplementary Figure 7-30, Supplementary Figure 7-31). Early death was found in Diet 2, even though the microbial type was kept as type II through and through.

It is important to note that there was some inconsistency in lifespan between the timepoint study (Chapter 3) and longevity study (Chapter 4). In Chapter 3, all mice, except one (from ToD18), survived through the whole experimental period. However, in Chapter 4, mice reached endpoints before 18 months on diet. In particular, for Diet 1, 16 and 18, about half of the male population and a quarter of the female population died by the 18 months on diet. This was likely due to the human intervention during Chapter 3's study. From and 3R's perspective during the animal study, in order to reduce the total number, some mice switched cohorts during the experiment. For example, some mice originally in ToD18 were switched to ToD1, due to fighting or health issue. Therefore, mice in ToD18 and ToD12, in a certain way, were manually filtered out the short-lived ones. In contrast, mice in Chapter 4 remained within the same cohorts and lived out their full natural lifespans. No manual selection happened with them. Thus, difference in lifespan was observed between the two studies. Considering mice in Chapter 4 experience little interference, their lifespan data was more reliable.

This microbiome aging behavior theory can also offer insight into the impact of caloric restriction on aging. The caloric restriction diet was known to prolong longevity in individuals and reverse the aging process (Anstey, Stankov et al. 1993). In this thesis, the gut microbiome from mice on caloric restriction diet were identified as microbial type II throughout their lifespan (Chapter 3 and Chapter 4). No microbial type drift was observed. Furthermore, the microbial composition of individuals remains stable at the duration of this experiment (the mice were still alive at the 32mo on diet cut-line), with no dramatic compositional changes/state transitions observed (Chapter 4). All of these indications suggest a healthy state of the microbiome, which contributes to prolonging lifespan.

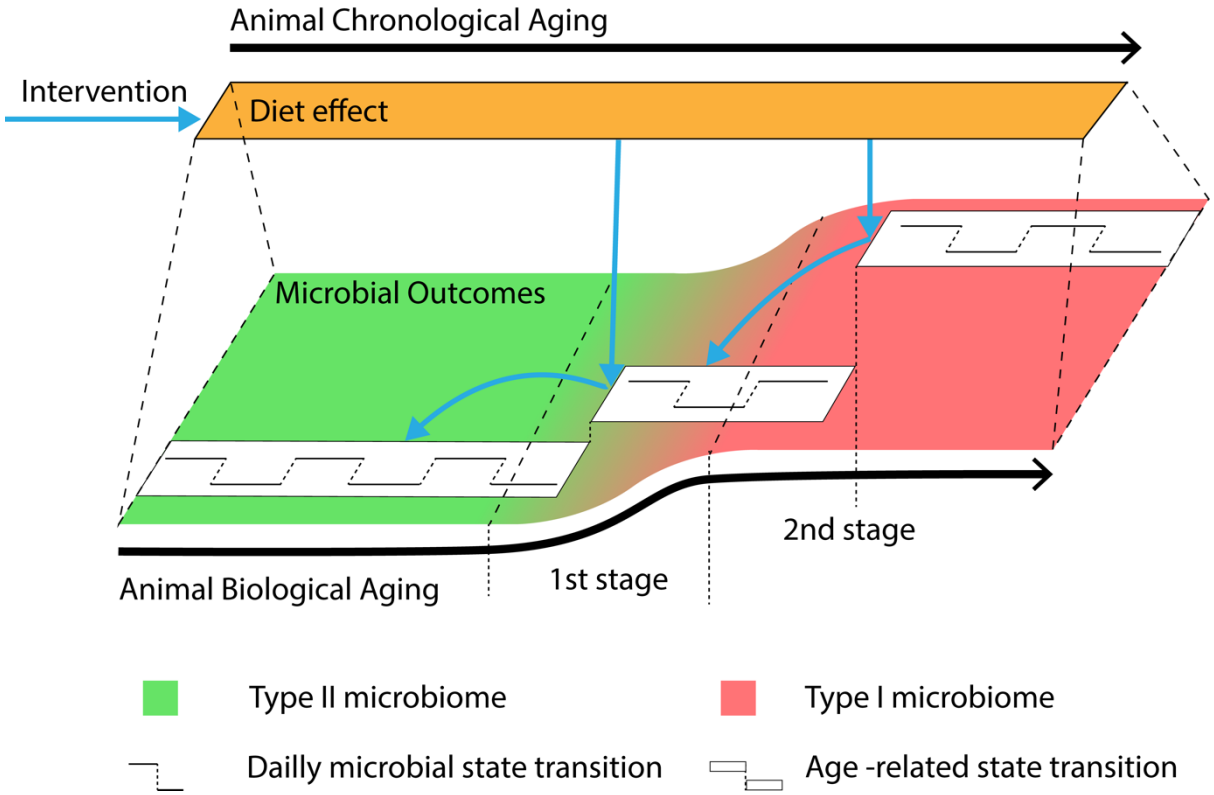

Figure 6-1. Age-related microbial change was diet dependent and can be reversed by dietary intervention.

6.3 Gender difference

The gender differences in longevity might be associated with the variations in the microbiome. Biological differences between genders can select for gender-specific microbiota and diet-microbiota interaction, resulting in variant dietary outcomes (Fransen, van Beek et al. 2017, Maric, Krieger et al. 2022) In this thesis, I found no significant gender difference in microbial response at earlier time points (before 18 months on diet) when switching diets from whole grain to purified diet (Chapter 3). This was likely because the purified diets lacked microbial-

accessible carbohydrates. Thus, the microbial response to diet between females and males was similar. However, as the animals got older, larger gender differences were observed (Chapter 3 and Chapter 4). Increasing in the gender variance may be associated with the physiological difference between aged female and male mice (Jin, Yang et al. 2023). Meanwhile, the microbiome can also add to the gender difference in the immune system in return (Fransen, van Beek et al. 2017). Collectively, these were reflected in the varying rates of immune aging and lifespan between females and males.

One of the purpose for these studies was to understand the aging biology to improve health in humans. However, there is a difference between the human and mice physiologies. In humans, a diminishing of gender difference in microbiome were observed over aging (de la Cuesta-Zuluaga, Kelley et al. 2019, Zhang, Zhong et al. 2021). Such opposite phenomenon might be associated with the changes in sex hormone levels. Estradiol and bioavailable testosterone levels were reduced by over two-thirds in older human beings, but remained unchanged in older male mice, and only slightly decreased in older female mice (Dubal, Broestl et al. 2012). Therefore, it may not be able to directly apply the results to humans. To better mimic human conditions, future studies can include actions like gonadal hormone depletion to eliminate the effects of sex hormones in the aged microbiome (Dubal, Broestl et al. 2012).

6.4 The dietary effect

As mentioned before, the aging effects on the gut microbiome were diet-dependent. It was actually an outcome of dietary selection, or to be more precise, nutrient selection. The host have limited access to metabolic resources, which were distributed among growth, maintaining functionality and repairing the damage (Kirkwood 1977, Kirkwood and Holliday 1979). Thus, aging alters nutrient metabolism and nutrient environment for the microbes. Microbes that didn't fit the new nutrient environment become extinct. In both Chapter 3 and Chapter 4, multiple *Muribaculaceae* ASVs were found missing after microbial drift and microbial state transition. Some microbes adjust to fit the environment by mutating to a different ASVs, in particular with *Lachnospiraceae*. Other ASVs changes their nutrient forging strategies to fit the new environment. This was achieved by either switching the energy source to a different macronutrient or obtain from other recourse like endogenous nitrogen or mucin layer (Holmes, Chew et al. 2017, Zeng, Xing et al. 2022). For these microbes, their relative abundance did not very much during aging (Chapter 3).

The diet influences nutrient selection in the gut microbiome over time, with its impact often surpassing that of aging biology on the gut microbiome. This was observed in Chapter 4, where the gut microbiome was clustered according to the diet rather than the chorological age of the mice. Also, in Chapter 5, I found that regardless which type of microbiome they received, Diet 2 could potentially attenuate immunosenescent. Meanwhile, the microbial Type I recipients on Diet 2 was able to show a microbial structure that was similar to the animals on Diet 2. This also suggests that diet can override the impact of aging biology on the gut. Therefore, dietary intervention can be implant to help delay/reverse age-related microbial type shift and state transition. Thus, reducing the aged-related inflammation and function decline.

Moreover, *Faecalibacterium* was found to be an signature microbe for microbial community type II in both Chapter 3 and Chapter 4. This taxa was selective by a few diets, including Diet 2, 3, 5, 9 and the caloric restriction diet. The GAM model in Chapter 3 also showed that *Faecalibacterium* was inversely proportionally to the dietary fat intake. However, when following individual mice in Chapter 4, this taxa was also found to be present in other diets at older age (Supplementary Figure 7-38 , indicated by reddish purple color). In particularly with the male mice on Diet 6, large amount of *Faecalibacterium* (about 20%) was found in the gut after 22 month on diet. Such observation, however, was not found in the female in Diet 6. With mice on other high fat diets like Diet 10 (containing 50% fat), a spike of *Faecalibacterium* population was also found in the males after 30 month on diet. This may potentially supports the three-stage aging theory for microbiome in Chapter 4. Chapter 3 only captures the microbial activity and nutrient response till 18 month on diet, which was within the first stage of microbial aging. By 22 month on diet or later, a new microbial state was reached, a different microbial behaviour was observed. To confirm this, the microbial analysis should include all mice in all 21 diets after 18 month on diet to perform GAM modelling.

6.5 Other

Although microbiome was predominantly associated with diet, not all variance can be explained by the diet. In both Chapter 3 and Chapter 4, diet were only explained up 59% of the variance. Such percentage reduces with aging, which can be seen in with-in samples ASVs evenness and richness (Chapter 3). Meanwhile, increasing in gender difference was observed with aging (Chapter 3). For the same diet, gender differences were observed with microbial composition or in conjunction with aging (Chapter 4). Chapter 5 also found that the initial microbial colonization and functional assembly also effects the microbial composition at ASV

level. Interestingly, at family level, the dietary effect can be observed. Such influence can last at least 1 month. However, Chapter 3 showed that, after switching diets for 6mo, the microbiome can be restabilized.

6.6 Conclusion

Overall, my thesis identified different levels of impact on gut microbiome between diet and aging biology. It provides evidence for potential dietary intervention in slowing/reducing age-related decline and promoting healthy aging. My research also categorized the microbial types and correlated them with diet and health outcomes. This can be applied to simplify the individual intervention and serve as markers to identify health deterioration, contributing towards the future of targeted microbial intervention.

7 Supplementary

Supplementary Table 7-1. Summary of 16S rRNA gene sequencing reads before and after abundance and ubiquity filtering.

			# of samples	Min reads per sample	Max reads per sample	Median reads	Total ASV	Average unique ASV per sample
Chapter 3*	All sample	Before filtering	827	10,345	111,333	36,774	13,703	185
		After filtering	827	10,146	109,848	35,455	386	146
	EP only	Before filtering	454	12,359	109,149	36,824	13,702	182
		After filtering	454	12,101	106,678	36,070	372[#]	150
	batch1 (2 runs)	Before filtering	270	-	-	-	-	228
		After filtering	270	-	-	-	-	165
	batch2 (1 run)	Before filtering	224	-	-	-	-	144
		After filtering	224	-	-	-	-	125
	batch3 (2 runs)	Before filtering	333	-	-	-	-	178
		After filtering	333	-	-	-	-	146
Chapter 4°		Before filtering	1,255	8,909	218,240	109,270	14,583	299
		After filtering	1,255	8,839	218,026	107,444	364	243
Chapter 5°		Before filtering	110	9,095	155,683	105,714	1,382	219
		After filtering	110	8,970	154,311	104,845	252	173

*Chapter 3 samples were separated into 3 different sequencing batches using MiSeq with about 5-7 month apart. Depends on the samples size, samples were separated into different sequencing runs. All samples were sequenced using Illumina MiSeq.

°Chapter 4 and Chapter 5 samples were sequenced together in 4 runs. All samples were sequenced using Illumina NextSeq 1000.

only uniquity filtering was applied.

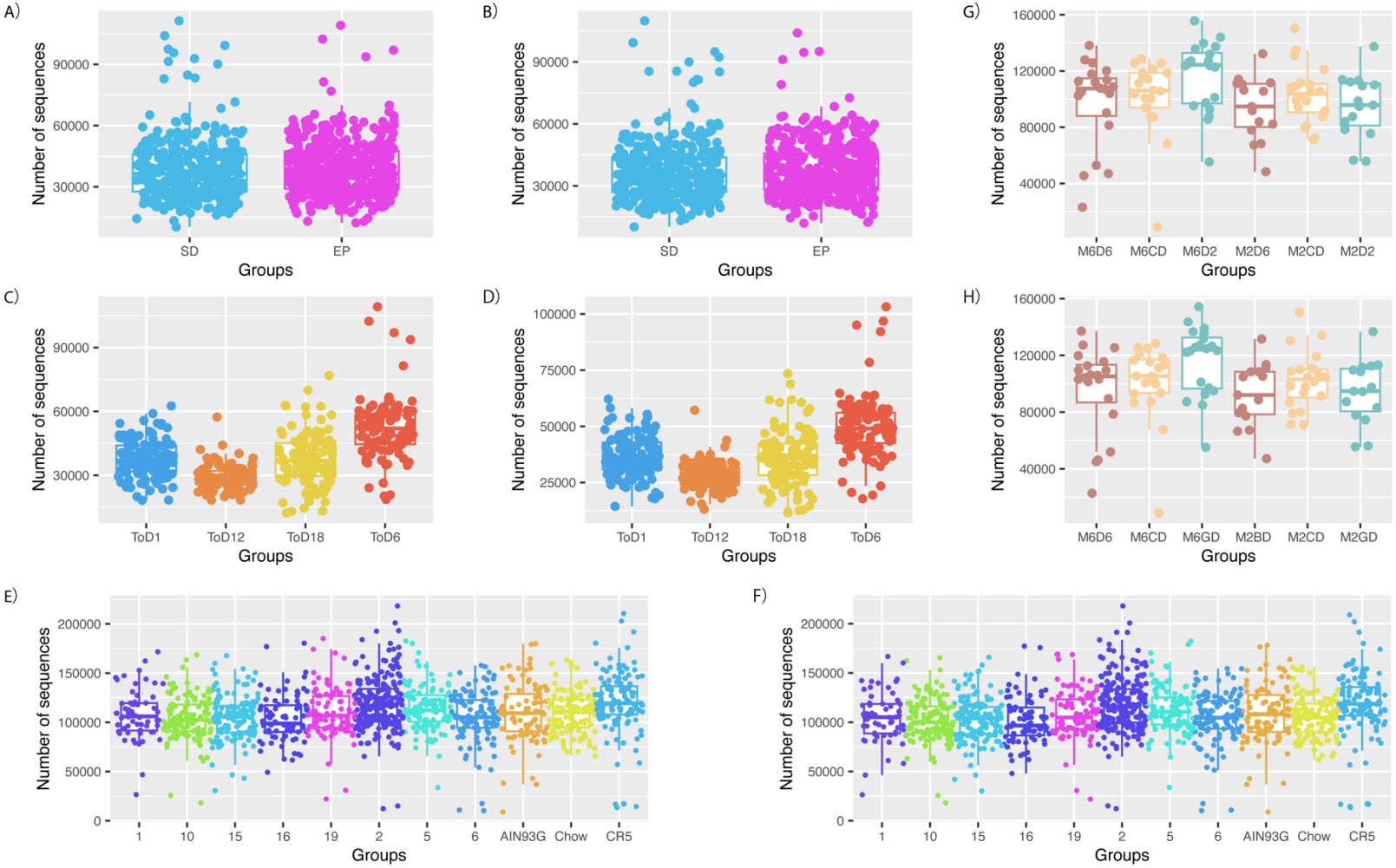

Supplementary Figure 7-1. 16S rRNA gene sequencing read depth before and after abundance and ubiquity filtering.
A)-D) Sequence read depth for each sample in Chapter 3 before (A and C) and after (B and D) filtering. A)-B) SD and EP samples were filtered together. Samples were grouped by status, i.e. SD or EP. C)-D) All EP samples were subset and filtered separately. Samples were grouped by ToD groups. E)-F) Sequence read depth for each sample in Chapter 4 before (E) and after (F) filtering. Samples were grouped by Diet. G)-H) Sequence read depth for each sample in Chapter 5 before (G) and after (H) filtering. Samples were grouped by treatment group.

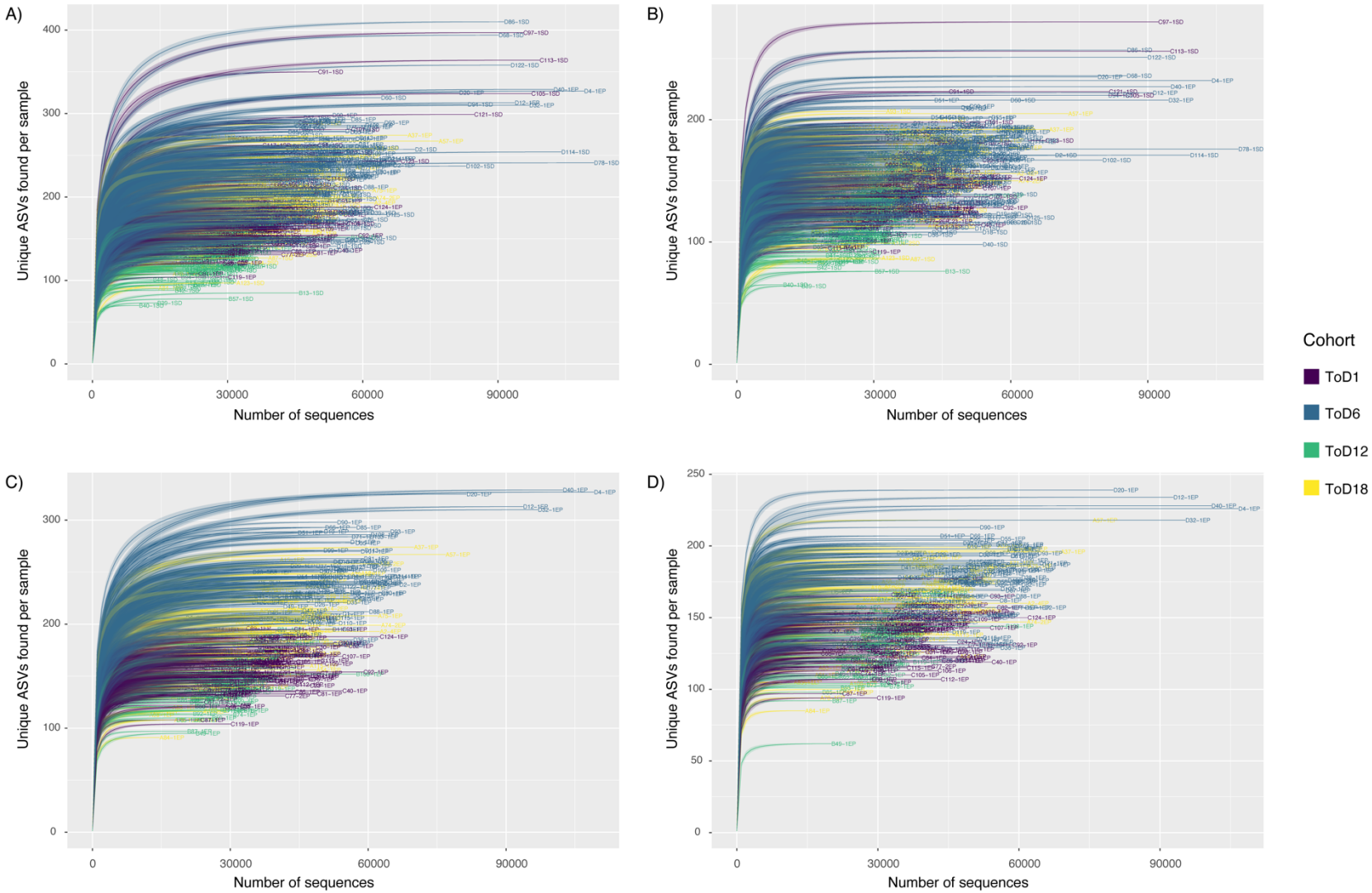

Supplementary Figure 7-2. Rarefaction curve for samples before and after abundance and ubiquity filtering in Chapter 3.
A) and B) SD and EP samples were filtered together. A)Before filtering and B) after filtering. Samples were coloured by experimental cohorts. C)-D) All EP samples were subset and filtered separately. C) Before filtering and D) after filtering. Samples were coloured by experimental cohorts.

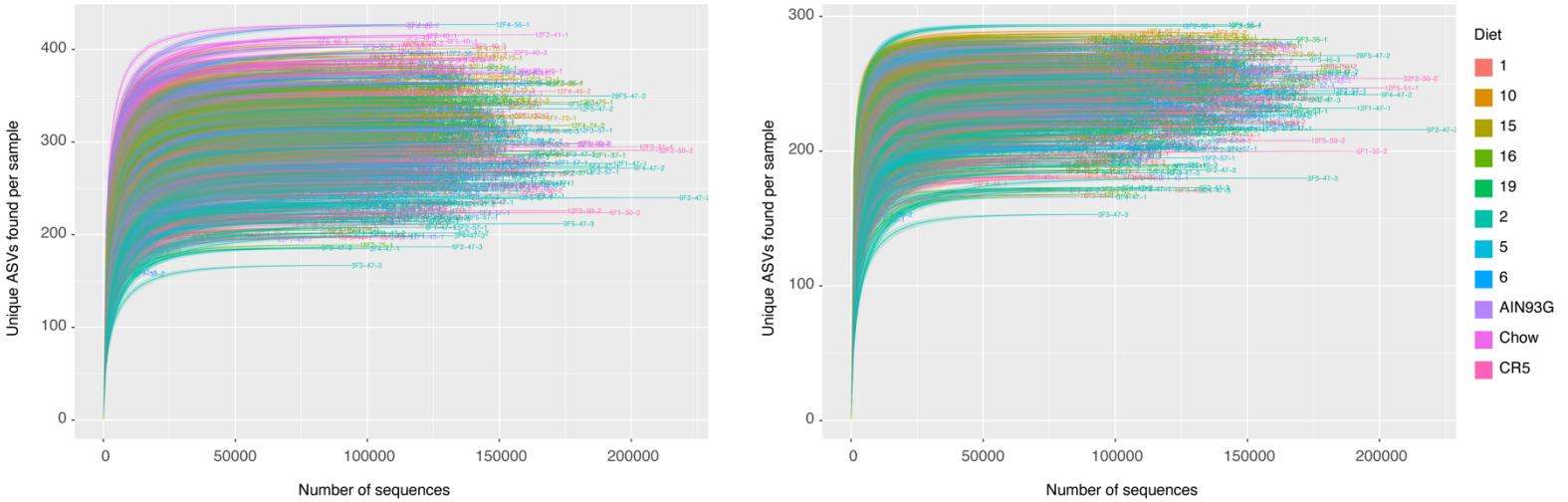

Supplementary Figure 7-3. Rarefaction curve for samples before and after abundance and ubiquity filtering in Chapter 4.
Left: before filtering and right: after filtering. Samples were coloured by experimental diets.

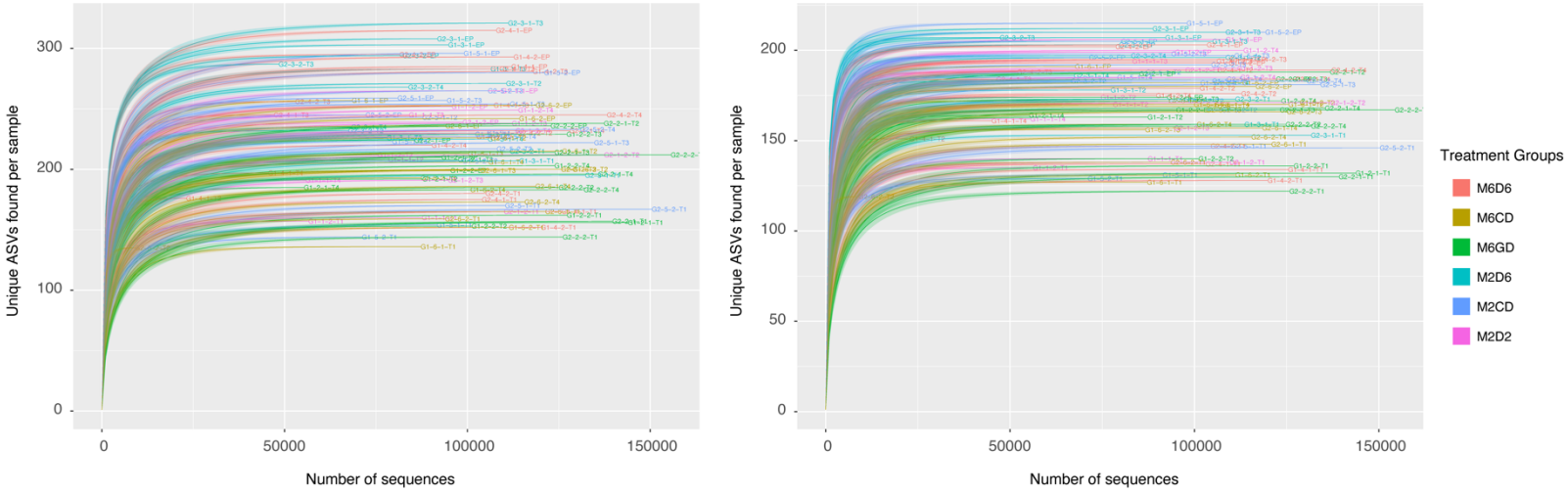

Supplementary Figure 7-4. Rarefaction curve for samples before and after abundance and ubiquity filtering in Chapter 5.
Left: before filtering and right: after filtering. Samples were coloured by experimental diets.

Supplementary Table 7-2. Summary of diet composition used in Chapter 3, Chapter 4 and Chapter 5.

Diet	Energy Density (MJ/Kg)	Macronutrients Distribution (% Energy) (P/C/F)	Protein (g/kg)		Carbohydrate (g/kg)			Fat (g/kg)				Other	Study in Chapter		
			Protein Mix[#]	Casein	Sucrose	Wheat Starch	Dextrinized Starch	Soybean Oil	Lard	Linseed Oil	Canola Oil	Cellulose	4	5	6
1	14.7	7/33/60	71	-	51	208	68	150	70	22	-	320	●	●	
2	14.7	7/78/15	71	-	124	501	163	37	17.5	5.4	-	40	●	●	●
3	14.7	14/56/30	142	-	88	358	117	75	35	11	-	134	●		
4	14.7	14/26/60	142	-	40	163	53	150	70	21.5	-	320	●		
5	14.7	21/64/15	213	-	101	410	134	37	17.5	5.4	-	41	●	●	
6	14.7	21/34/45	213	-	53	215	70	112	52	16	-	227	●	●	●
7	14.7	30/40/30	305	-	63	254	83	75	35	11	-	135	●		
8	14.7	35/20/45	356	-	31	124	83	112	53	16	-	229	●		
9	14.7	42/43/15	427	-	68	274	89	37	17.5	5.4	-	42	●		
10	14.7	50/20/30	508	-	31	124	40	75	35	11	-	136	●	●	
12	10.5	7/78/15	50.8	-	88	356	116	29.6	9.2	4.2	-	305	●		
13	10.5	14/56/30	102	-	63	254	83	59	18.5	8.4	-	372	●		
15	10.5	21/64/15	152	-	72	291	95	29.6	9.2	4.2	-	306	●	●	
16	10.5	21/34/45	152	-	37	152	49	89	28	13	-	440	●	●	
17	10.5	30/40/30	218	-	44	180	58	59	18.5	8.4	-	373	●		
18	10.5	35/20/45	254	-	21.3	86	28	89	28	13	-	440	●		
19	10.5	42/43/15	305	-	47	195	62	29.6	9.2	4.2	-	307	●	●	
20	10.5	50/20/30	363	-	21	86	28	59	18.5	8.4	-	375	●		
CR5*	14.7	21/64/15	213	-	101	410	134	37	17.5	5.4	-	41	●	●	
AIN93 G	14.6	18.8/63.4/17.8	-	200	100	404	132	-	-	-	70	50		●	●
Chow[+]	14.2	23/65/12	lupin, soya meal, fish meal		wheat barley			Mixed vegetable oil, Canola oil						●	●

***Caloric restriction diet has is the same as diet 5 but with 20% less food intake.

+Standard chow diet uses different dietary source for protein, carbohydrate and fat.

#Protein mix is made from Casein, Whey Protein Isolate and supplemented Leucine, Threonine, Methionine, Tyrosine, Phenylalanine, Tryptophan, Alanine, Aspartic Acid, Arginine, Glycine, Histidine and Serine.

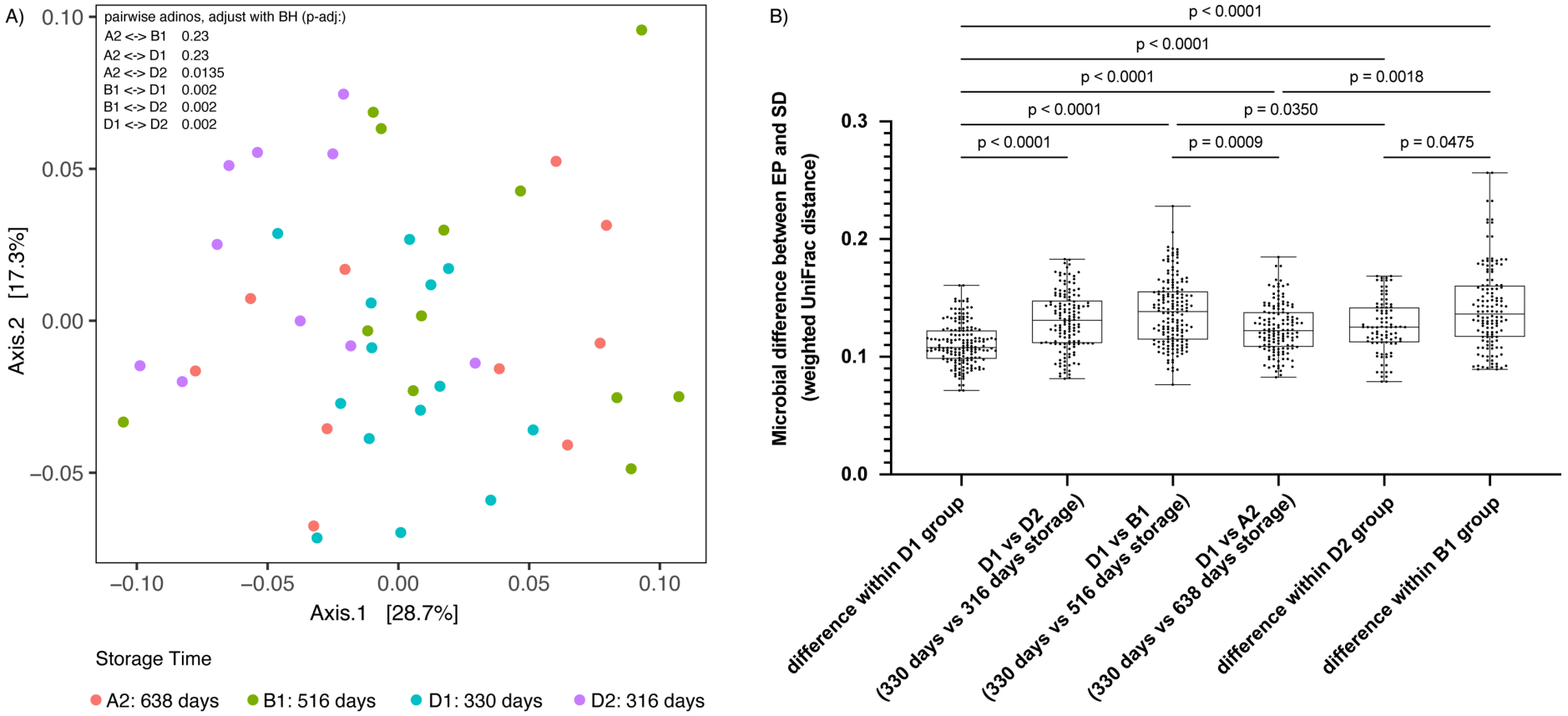

Supplementary Figure 7-5. Beta diversity analyses do not indicate any effect of storage time.
A)PCoA plot of weighted Unifrac distance of a subset SD samples in Chapter 3Statistical significance was determined by the pairwise adonis test and post-hoc Benjamini-Hochberg procedure. B) Weighted Unifrac distance difference within and between group. Statistical significance was determined by one-way ANOVA followed by Dunn's test.

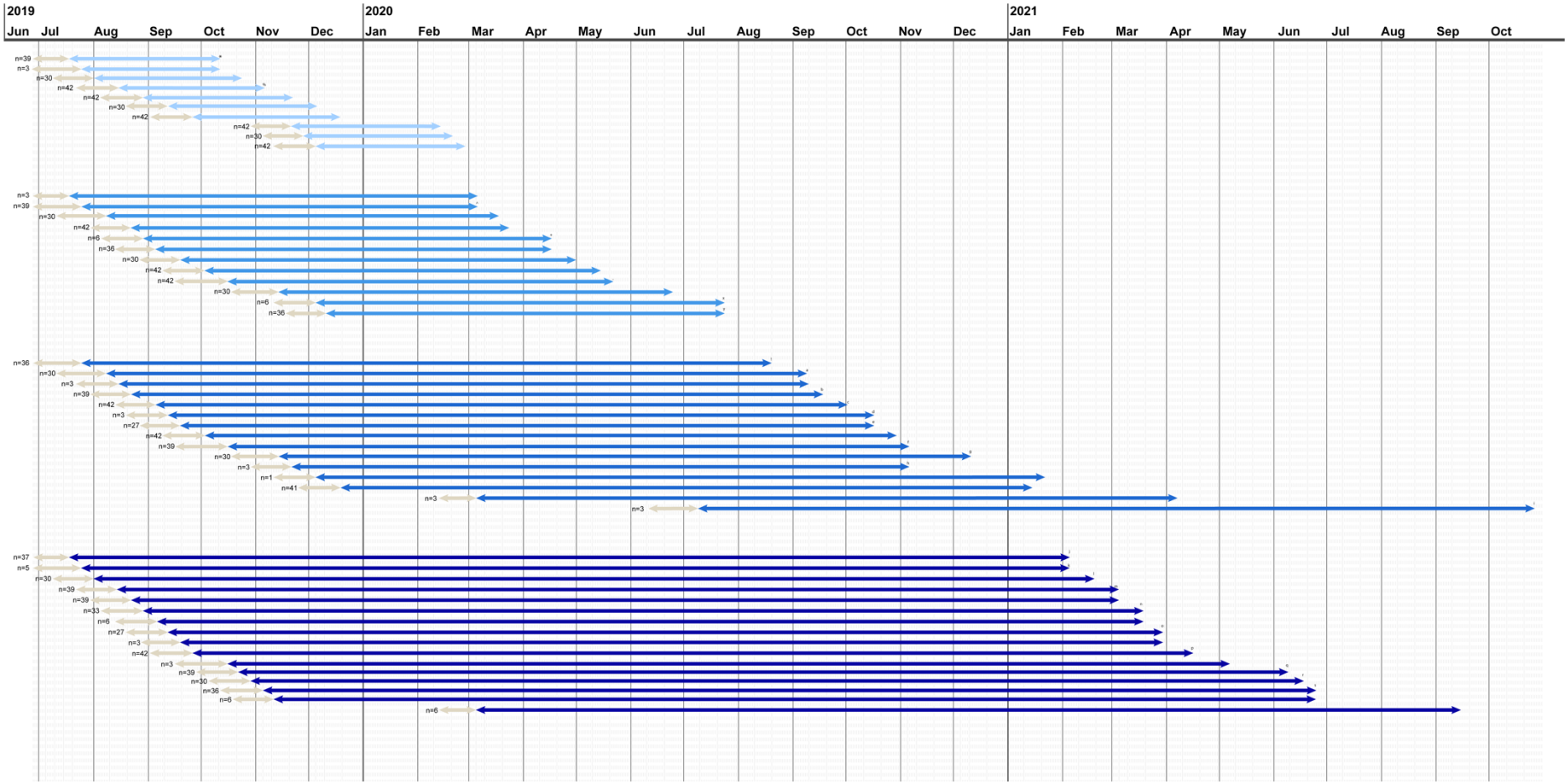

Supplementary Figure 7-6. Mice involved in Chapter 3 spread over 19 different birth cohorts.
To Each group contains at least 9 different birth cohorts, and majority were born and arrived within 5month in 2019 to avoid systematic error.

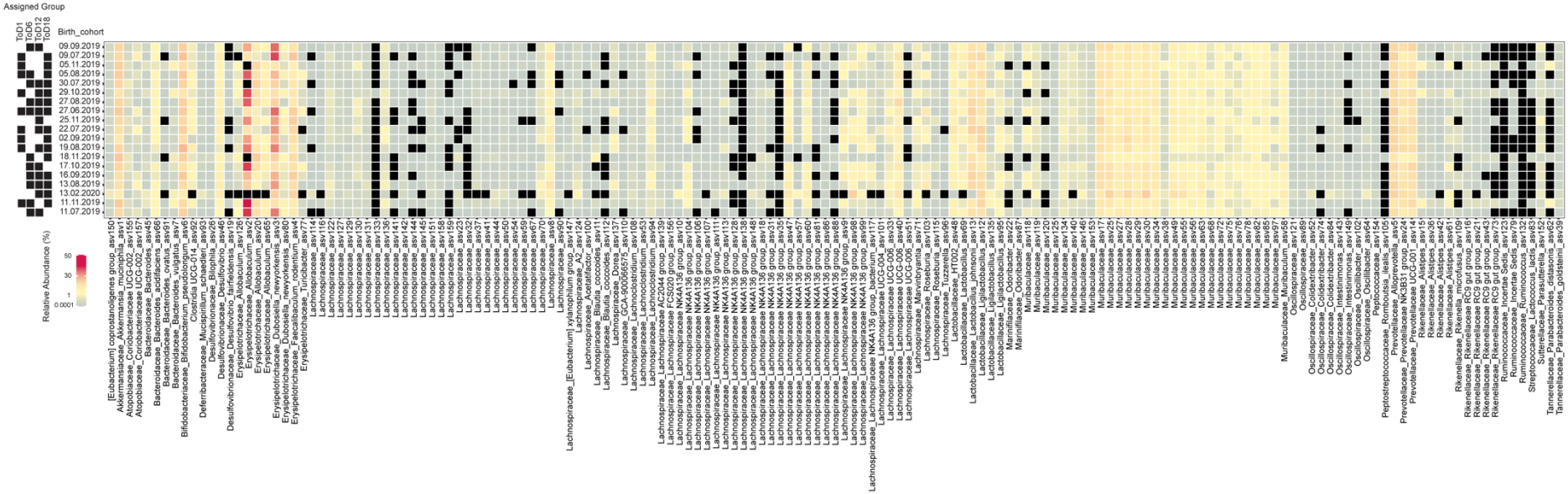

Supplementary Figure 7-7. The heatmap of average of relative abundance of top 159 ASVs for each birth cohort.
Each square is an average of multiple samples' relative abundance. The left panel is the assigned cohort for each birth cohort.

Supplementary Table 7-3. Statistical analysis show no difference between dietary groups using beta-diversity at baseline in Chapter 3.*

Diet pair	Bray-Curtis	Unifrac	Weighted Unifrac	Diet pair	Bray-Curtis	Unifrac	Weighted Unifrac	Diet pair	Bray-Curtis	Unifrac	Weighted Unifrac	Diet pair	Bray-Curtis	Unifrac	Weighted Unifrac
1 vs 10	0.32	0.24	0.31	**10 vs 7**	0.40	0.82	0.64	**12 vs 7**	0.49	0.60	0.42	**15 vs 16**	0.99	1.00	0.90
1 vs 11	0.42	0.38	0.38	**10 vs 8**	0.99	1.00	0.94	**12 vs 8**	0.88	0.82	0.71	**15 vs 17**	0.63	0.62	0.56
1 vs 12	0.55	0.62	0.47	**10 vs 9**	0.89	0.80	0.90	**12 vs 9**	1.00	1.00	1.00	**15 vs 18**	0.84	1.00	0.90
1 vs 13	0.49	0.54	0.34	**10 vs CR_5**	0.98	1.00	0.77	**12 vs CR_5**	0.50	0.38	0.31	**15 vs 19**	0.89	0.96	0.94
1 vs 14	0.32	0.21	0.27	**11 vs 12**	0.84	0.81	0.58	**13 vs 14**	0.61	0.38	0.35	**15 vs 2**	0.49	0.30	0.52
1 vs 15	0.42	0.30	0.33	**11 vs 13**	0.50	0.45	0.39	**13 vs 15**	0.88	1.00	0.64	**15 vs 20**	0.41	0.38	0.38
1 vs 16	0.56	0.54	0.49	**11 vs 14**	0.56	0.56	0.56	**13 vs 16**	1.00	1.00	0.96	**15 vs 3**	0.46	0.42	0.34
1 vs 17	0.62	0.38	0.70	**11 vs 15**	0.55	0.62	0.47	**13 vs 17**	0.45	0.38	0.44	**15 vs 4**	0.47	0.27	0.58
1 vs 18	0.44	0.38	0.38	**11 vs 16**	0.58	0.78	0.59	**13 vs 18**	1.00	1.00	1.00	**15 vs 5**	0.40	0.24	0.31
1 vs 19	0.32	0.38	0.38	**11 vs 17**	0.33	0.38	0.38	**13 vs 19**	0.98	1.00	0.96	**15 vs 6**	0.46	0.32	0.31
1 vs 2	0.96	0.30	0.53	**11 vs 18**	0.47	0.44	0.45	**13 vs 2**	0.73	0.84	0.66	**15 vs 7**	0.91	0.73	0.66
1 vs 20	0.22	0.13	0.27	**11 vs 19**	0.58	0.49	0.54	**13 vs 20**	0.83	0.83	0.71	**15 vs 8**	0.63	0.91	0.61
1 vs 3	0.96	1.00	0.90	**11 vs 2**	0.42	0.32	0.38	**13 vs 3**	0.32	0.44	0.31	**15 vs 9**	0.96	0.96	1.00
1 vs 4	0.49	0.38	0.47	**11 vs 20**	0.55	0.43	0.47	**13 vs 4**	0.28	0.35	0.40	**15 vs CR_5**	0.55	0.71	0.44
1 vs 5	1.00	1.00	1.00	**11 vs 3**	0.38	0.49	0.31	**13 vs 5**	0.38	0.36	0.28	**16 vs 17**	0.46	0.44	0.60
1 vs 6	0.96	0.78	0.75	**11 vs 4**	0.40	0.45	0.38	**13 vs 6**	0.55	0.49	0.35	**16 vs 18**	1.00	1.00	1.00
1 vs 7	0.52	0.71	0.33	**11 vs 5**	0.40	0.38	0.38	**13 vs 7**	0.50	0.96	0.60	**16 vs 19**	0.97	1.00	1.00
1 vs 8	0.50	0.44	0.44	**11 vs 6**	0.38	0.38	0.32	**13 vs 8**	1.00	1.00	1.00	**16 vs 2**	0.71	0.59	0.69
1 vs 9	0.61	0.81	0.54	**11 vs 7**	0.38	0.43	0.38	**13 vs 9**	0.99	1.00	0.90	**16 vs 20**	0.56	0.60	0.58
1 vs CR_5	0.22	0.11	0.11	**11 vs 8**	0.58	0.50	0.46	**13 vs CR_5**	0.96	0.96	0.69	**16 vs 3**	0.49	0.96	0.44
10 vs 11	0.50	0.45	0.47	**11 vs 9**	0.50	0.71	0.40	**14 vs 15**	0.54	0.38	0.31	**16 vs 4**	0.40	0.39	0.60
10 vs 12	0.60	0.63	0.61	**11 vs CR_5**	0.45	0.30	0.31	**14 vs 16**	0.55	0.38	0.31	**16 vs 5**	0.49	0.43	0.39
10 vs 13	0.96	1.00	1.00	**12 vs 13**	0.89	0.88	0.60	**14 vs 17**	0.31	0.11	0.30	**16 vs 6**	0.50	0.56	0.38
10 vs 14	0.73	0.38	0.38	**12 vs 14**	0.50	0.24	0.31	**14 vs 18**	0.61	0.32	0.36	**16 vs 7**	0.55	0.89	0.47
10 vs 15	0.49	0.75	0.61	**12 vs 15**	1.00	0.89	0.99	**14 vs 19**	0.74	0.45	0.44	**16 vs 8**	1.00	1.00	1.00
10 vs 16	0.97	1.00	0.90	**12 vs 16**	1.00	1.00	1.00	**14 vs 2**	0.50	0.32	0.31	**16 vs 9**	1.00	1.00	1.00
10 vs 17	0.22	0.28	0.38	**12 vs 17**	0.96	0.62	0.96	**14 vs 20**	0.77	0.56	0.44	**16 vs CR_5**	0.96	0.88	0.47
10 vs 18	1.00	1.00	1.00	**12 vs 18**	0.93	1.00	0.87	**14 vs 3**	0.32	0.24	0.26	**17 vs 18**	0.33	0.24	0.47
10 vs 19	0.89	0.82	1.00	**12 vs 19**	0.74	0.80	0.78	**14 vs 4**	0.42	0.24	0.31	**17 vs 19**	0.33	0.38	0.66
10 vs 2	0.46	0.62	0.60	**12 vs 2**	0.33	0.24	0.45	**14 vs 5**	0.27	0.11	0.26	**17 vs 2**	0.40	0.14	0.47
10 vs 20	0.96	0.98	0.87	**12 vs 20**	0.49	0.30	0.38	**14 vs 6**	0.32	0.21	0.25	**17 vs 20**	0.22	0.24	0.31
10 vs 3	0.22	0.30	0.28	**12 vs 3**	0.50	0.82	0.47	**14 vs 7**	0.49	0.38	0.34	**17 vs 3**	0.44	0.38	0.46
10 vs 4	0.22	0.21	0.38	**12 vs 4**	0.40	0.38	0.58	**14 vs 8**	0.67	0.38	0.32	**17 vs 4**	0.49	0.49	0.59
10 vs 5	0.22	0.20	0.27	**12 vs 5**	0.49	0.50	0.47	**14 vs 9**	0.49	0.24	0.31	**17 vs 5**	0.56	0.38	0.60
10 vs 6	0.32	0.25	0.30	**12 vs 6**	0.38	0.25	0.32	**14 vs CR_5**	0.74	0.42	0.32	**17 vs 6**	0.44	0.38	0.38
								17 vs 7	0.36	0.43	0.39	**17 vs 8**	0.32	0.24	0.43

* pair-wise adonis followed by Benjamini-Hochberg procedure

Supplementary Table 7-4. Statistical analysis between ToD groups using beta-diversity at baseline in Chapter 3*

	Bray-Curtis	Unifrac	Weighted Unifrac
ToD1 vs ToD6	0.001	0.001	0.0012
ToD1 vs ToD12	0.001	0.001	0.0012
ToD1 vs ToD18	0.001	0.001	0.002
ToD6 vs ToD12	0.001	0.001	0.009
ToD6 vs ToD18	0.001	0.001	0.0516
ToD12 vs ToD18	0.001	0.001	0.054

* pair-wise adonis followed by Benjamini-Hochberg procedure

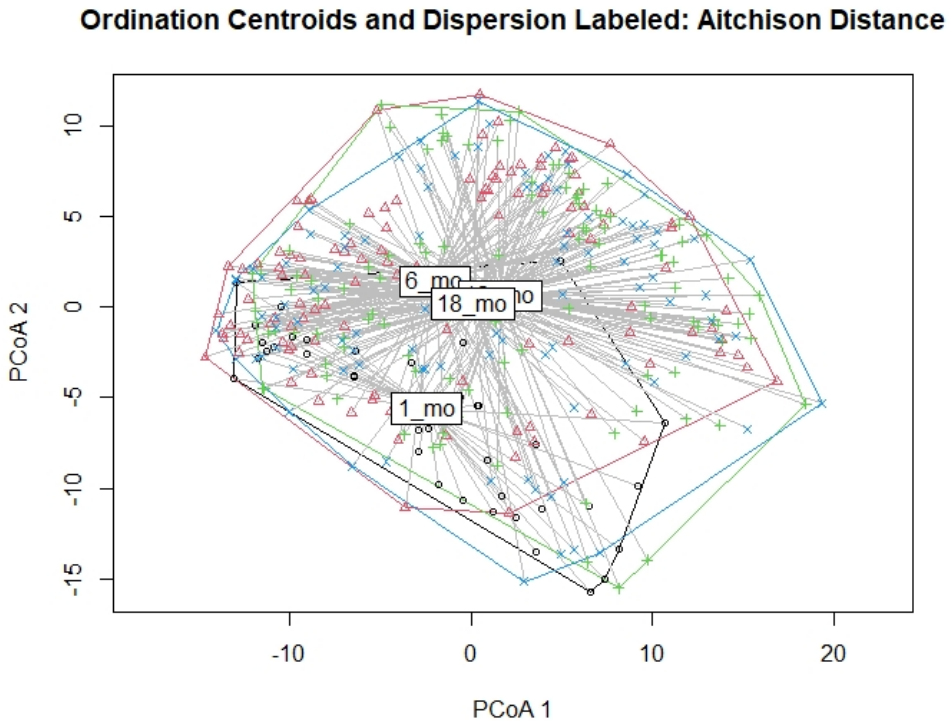

Supplementary Figure 7-8. Dispersion analysis showed that the samples from ToD1 group is within the dispersion of other groups.

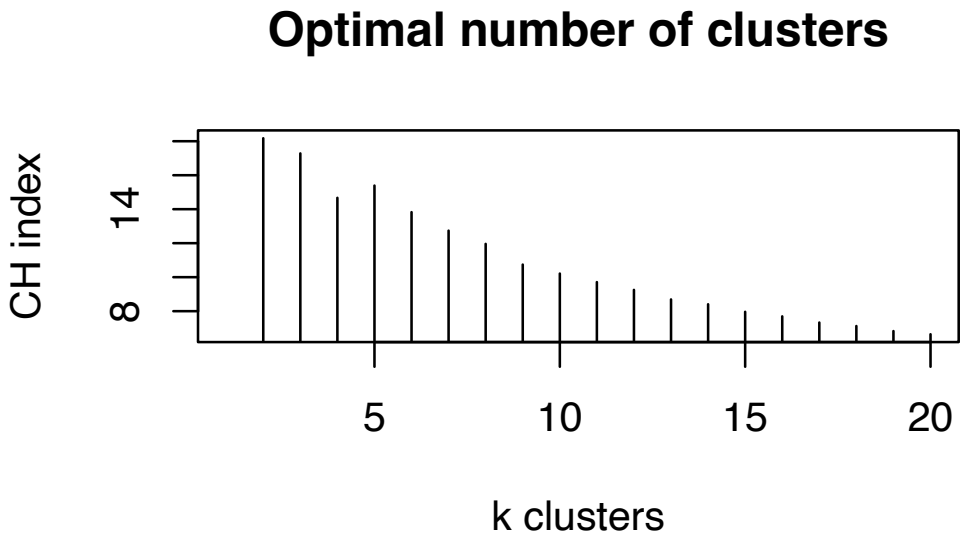

Supplementary Figure 7-9. The optimal number baseline cluster was determined by the maximum CH index.

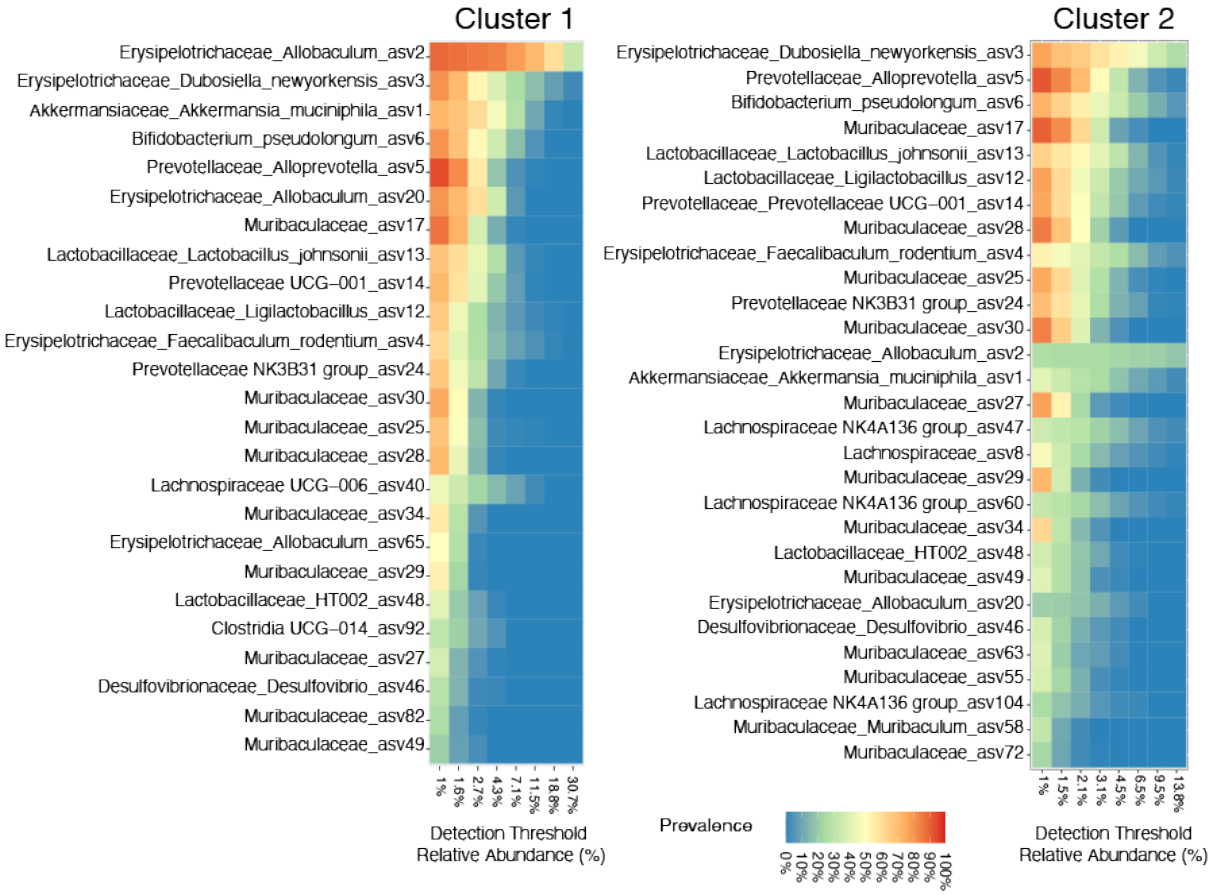

Supplementary Figure 7-10. Heatmap of core microbiome in each baseline clusters.

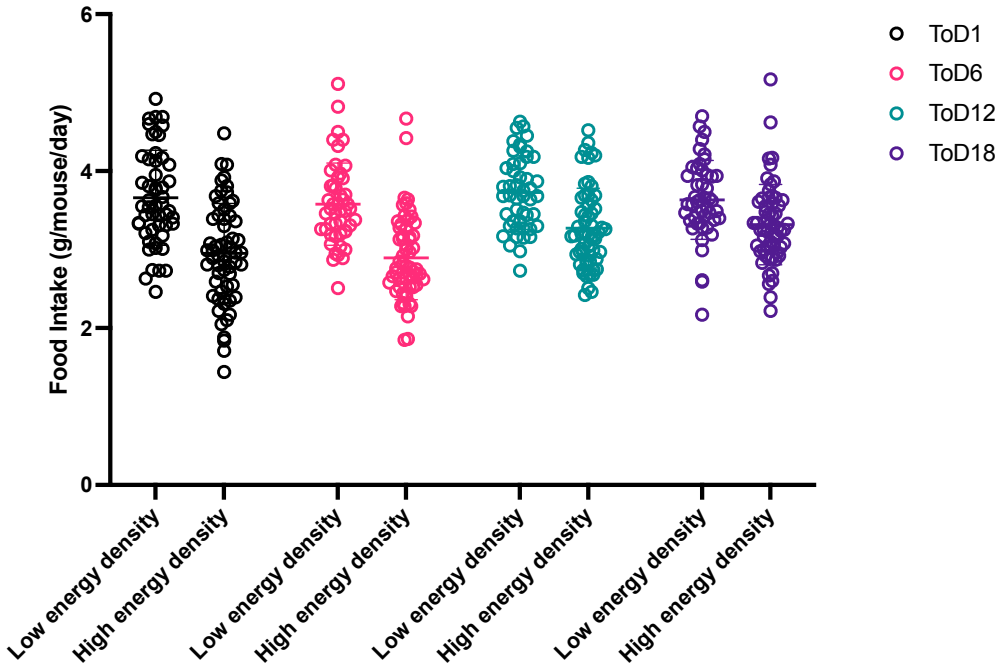

Supplementary Figure 7-11. The food dry matter intake grouped by energy density.
The total dry food intake was token as a 24h cage average.

Supplementary Table 7-5. ALDEx2 effective size result for the ASVs in Figure 3-7.

	ToD6	ToD12	ToD18
Erysipelotrichaceae_Dubosiella_newyorkensis_asv3	0.53714661	0.96981001	1.17852366
Erysipelotrichaceae_Faecalibaculum_rodentium_asv4	0.58606561	1.09107676	2.48094702
Bifidobacteriaceae_Bifidobacterium_pseudolongum_asv6	-	1.01713479	1.33512895
Rikenellaceae_Alistipes_asv15	-1.8685501	-0.6307835	-0.6660356
Rikenellaceae_Rikenellaceae RC9 gut group_asv20	-0.8311686	-0.5987628	-0.8143876
Rikenellaceae_Alistipes_asv40	-0.7624801	-0.87371	-1.2941604

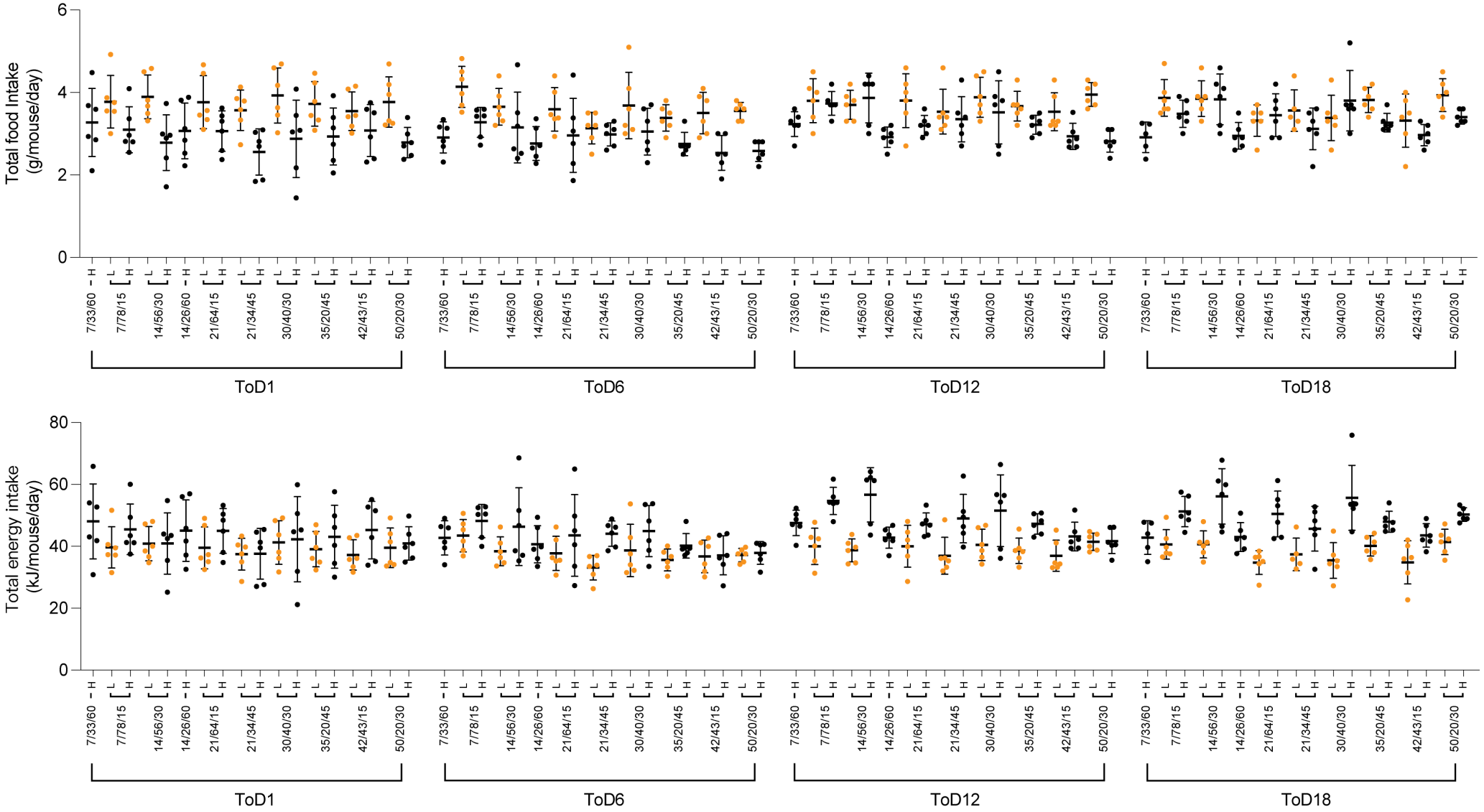

Supplementary Figure 7-12. The lower energy density diets were associated with higher food intake but lower overall energy intake.
The top panel is 24h total dry food intake as a cage average, and the bottom panel is 24h total energy intake as a cage average. For each panel, L represents the diet energy density as 10.5kJ/g and H represent the diet energy density as 15.7kJ/g.

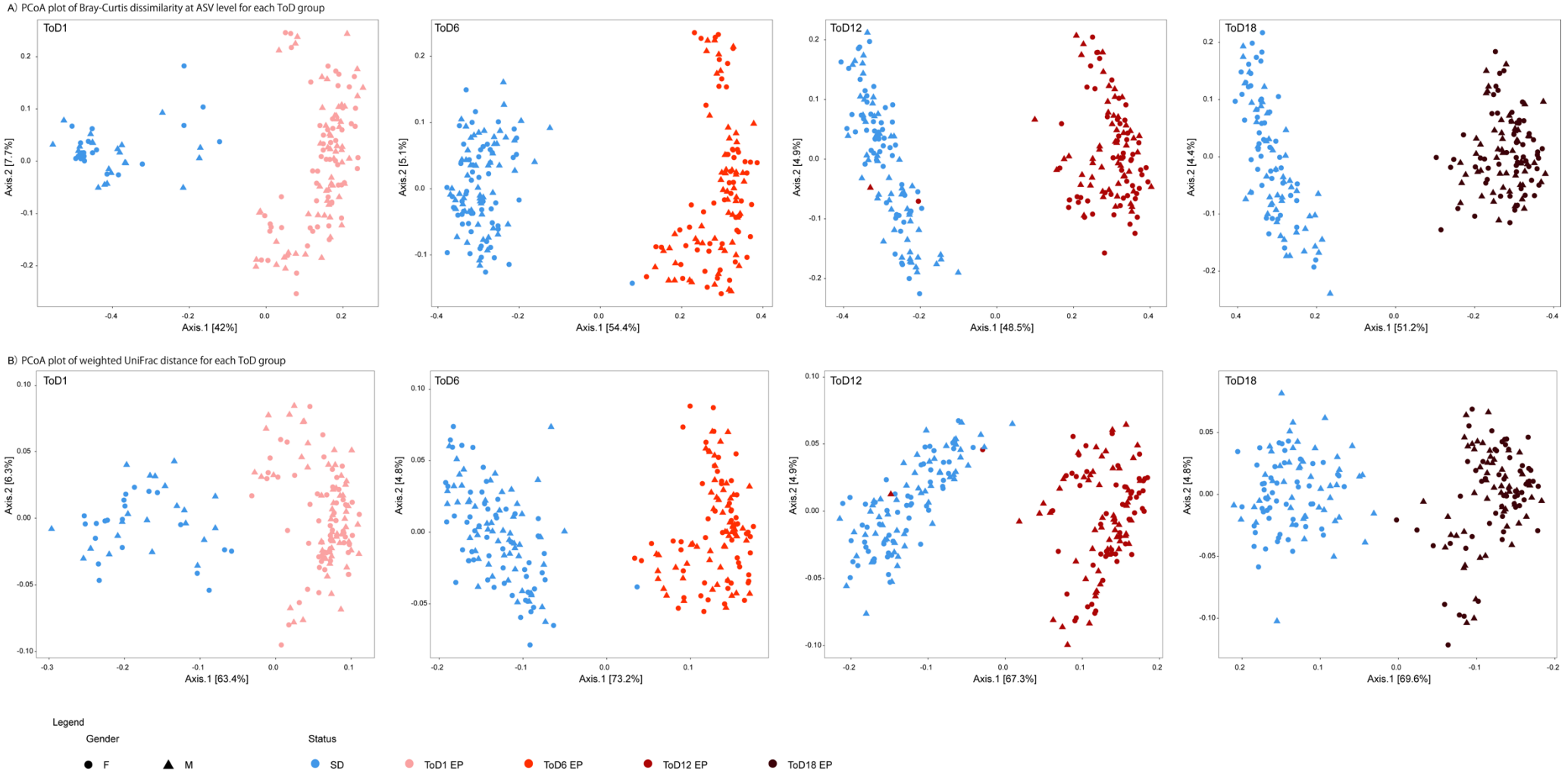

Supplementary Figure 7-13. PCoA plot of SD fecal samples and EP cecal samples for each ToD group using different beta diversity metrices.
A) Bray-Curtis Dissimilarity at ASV level. B)Weighted UniFrac distance. SD samples are labelled as blue and EP samples are labelled as red.

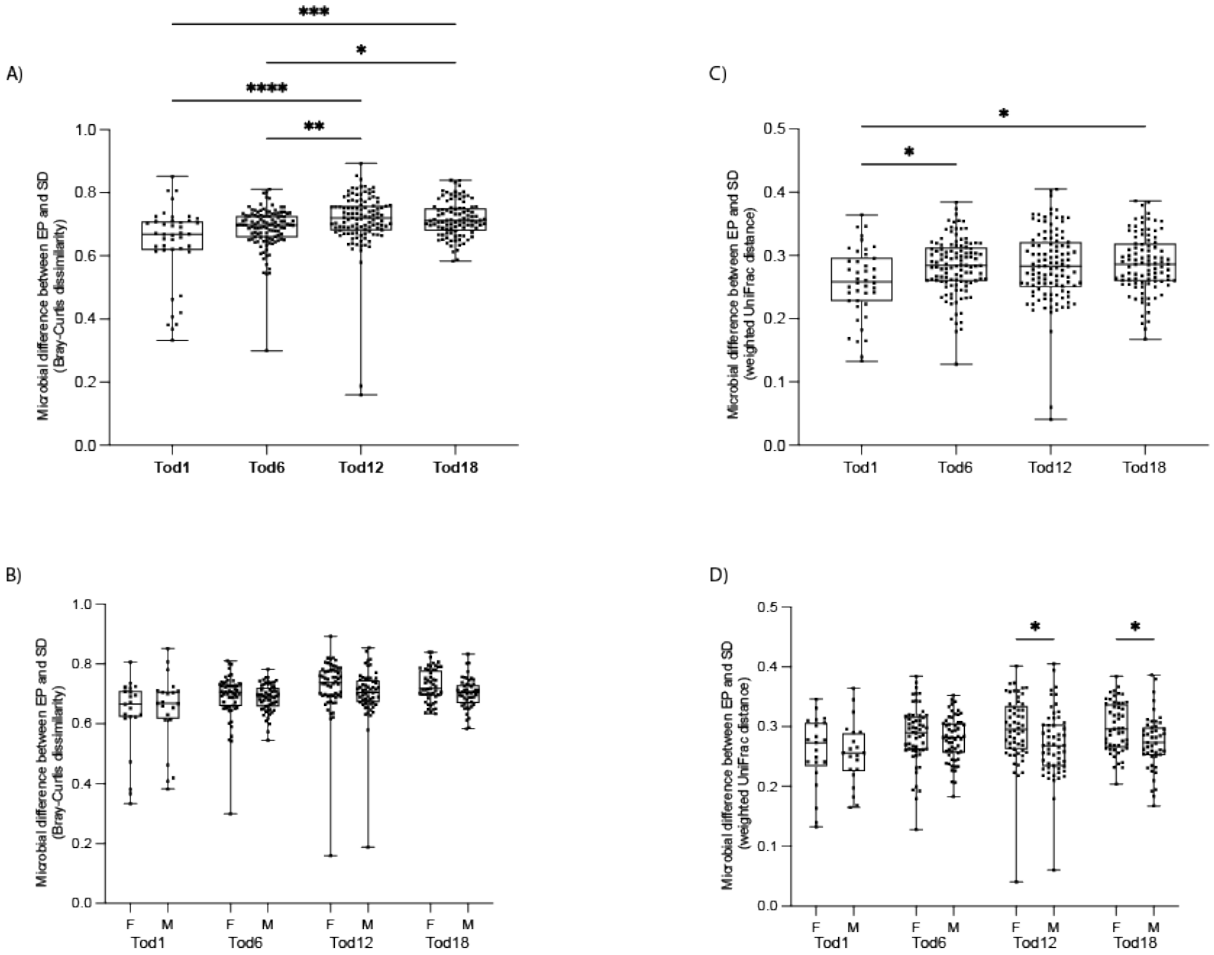

Supplementary Figure 7-14. Comparison of microbial difference between EP and SD.
A) and B) Bray-Curtis dissimilarity at ASV level. A) Comparison among ToD groups. B) Comparison between genders within each ToD group. C) and D) Weighted UniFrac distance. C) Comparison among ToD groups. D) Compatision between grnders within each ToD group. (Only the groups with significant difference were marked; ***: p<0.001k, **:0.001< p<0.01, *: p<0.05)

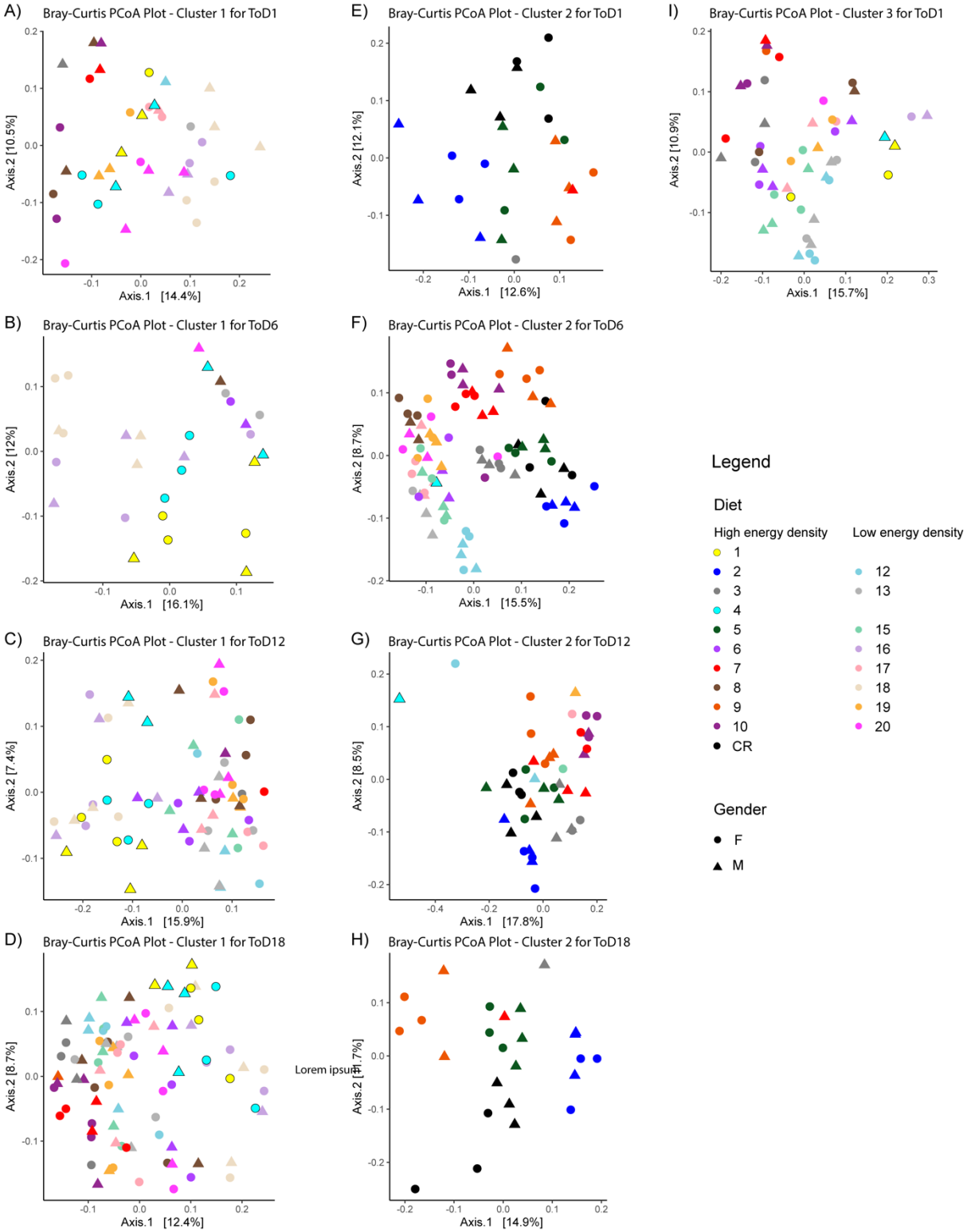

Supplementary Figure 7-15. PCoA plot of Bray-Curtis dissimilarity at ASV level for each PAM cluster colored by diet.

Left panel is cluster 1, middle panel is cluster 2 and right panel is cluster 3. From Top to bottom are ToD6, ToD12 and ToD18, respectively.

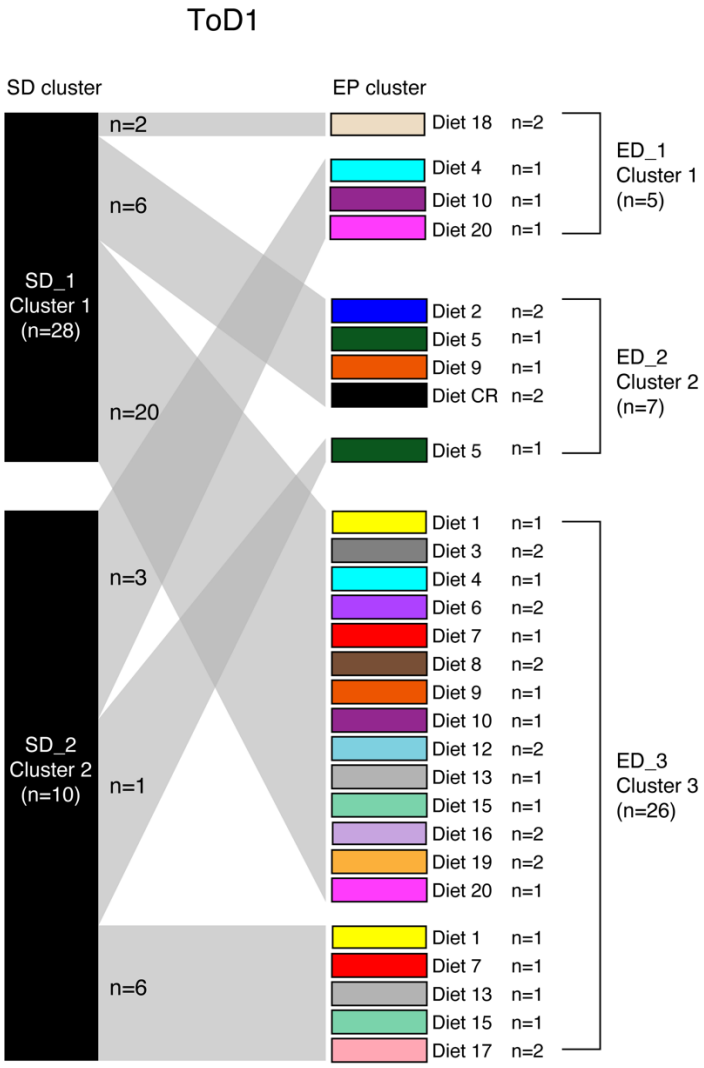

Supplementary Figure 7-16. Sankey diagram of samples changes from SD cluster to EP cluster in ToD1 group in Chapter 3.

Supplementary Table 7-6. GAM statistics for Figure 3-11 ToD1.
Dev = deviance explained, n.s. = p value >0.05

ToD1		Prot	Carb	Fat	P x C	P x F	C x F	P x C X F	N data points
InvSimpson	*p*	n.s.	n.s.	n.s.	n.s.	n.s.	n.s.	n.s.	**114**
	AIC	837	838	838	838	839	838	842	
	Dev (%)	1.0	1.1	0.7	4.1	1.6	7.9	10.8	
Observed	*p*	n.s.	n.s.	n.s.	n.s.	n.s.	0.034	0.038	**114**
	AIC	949	942	948	943	950	938	946	
	Dev (%)	0.2	9.6	1.2	13.2	1.4	19.9	17.1	
Shannon	*p*	n.s.	n.s.	n.s.	n.s.	n.s.	n.s.	n.s.	**114**
	AIC	43	42	44	41	45	44	44	

ToD1		Prot	Carb	Fat	P x C	P x F	C x F	P x C X F	N data points
	Dev (%)	1.5	3.7	0.3	9.8	1.8	7.9	13.9	
Verrucomicrobiota	*p*	n.s.	0.016	0.035	n.s.	n.s.	n.s.	0.032	**114**
	AIC	499	489	496	493	497	495	497	
	Dev (%)	2.3	18.6	3.9	11.4	5.9	7.7	15.7	
Actinobacteriota	*p*	n.s.	0.000	0.000	0.000	0.000	0.000	0.000	**114**
	AIC	674	632	649	635	653	622	623	
	Dev (%)	4.5	34.9	30.1	34.8	24.4	44.0	46.6	
Bacteroidota	*p*	0.006	n.s.	n.s.	0.014	0.021	n.s.	n.s.	**114**
	AIC	944	951	952	945	946	953	954	
	Dev (%)	6.7	1.9	0.0	7.5	6.7	3.3	11.5	
Firmicutes	*p*	0.001	n.s.	n.s.	0.013	0.005	n.s.	0.002	**114**
	AIC	1,087	1,093	1,097	1,085	1,089	1,089	1,085	
	Dev (%)	8.7	7.3	0.6	17.2	9.1	17.4	23.7	
Desulfobacterota	*p*	n.s.	0.035	0.038	n.s.	n.s.	n.s.	0.026	**114**
	AIC	491	484	482	486	488	486	487	
	Dev (%)	0.0	6.7	17.0	7.0	10.3	8.5	16.2	
Deferribacterota	*p*	n.s.	n.s.	n.s.	n.s.	n.s.	n.s.	n.s.	**114**
	AIC	447	446	447	447	448	448	455	
	Dev (%)	0.0	1.1	0.4	1.7	0.4	0.9	7.0	
Cyanobacteria	*p*	n.s.	n.s.	n.s.	n.s.	n.s.	n.s.	n.s.	**114**
	AIC	514	512	512	513	514	513	522	
	Dev (%)	0.1	2.1	1.7	3.0	1.7	2.7	7.1	
Proteobacteria	*p*	n.s.	0.003	0.000	0.005	0.000	0.001	0.001	**114**
	AIC	562	547	546	546	547	541	548	
	Dev (%)	0.5	17.9	13.4	21.8	13.6	27.3	24.2	
Akkermansiaceae_asv1	*p*	n.s.	0.016	0.035	n.s.	n.s.	n.s.	0.032	**111**
	AIC	499	489	496	493	497	495	497	
	Dev (%)	2.3	18.6	3.9	11.4	5.9	7.7	15.7	
Prevotellaceae_asv5	*p*	n.s.	n.s.	n.s.	n.s.	n.s.	n.s.	n.s.	**71**
	AIC	529	528	530	528	526	532	538	
	Dev (%)	7.1	12.2	2.2	14.1	14.9	2.3	9.4	
Bacteroidaceae_asv7	*p*	0.000	0.000	0.006	0.000	0.001	0.000	0.000	**114**
	AIC	374	366	382	364	374	367	368	
	Dev (%)	18.7	22.6	21.5	28.1	22.1	23.4	31.2	
Lachnospiraceae_asv8	*p*	n.s.	n.s.	n.s.	n.s.	n.s.	n.s.	n.s.	**113**
	AIC	348	345	346	344	348	347	348	
	Dev (%)	2.3	8.0	4.5	14.3	5.4	9.3	13.9	

ToD1		Prot	Carb	Fat	P x C	P x F	C x F	P x C X F	N data points
Lachnospiraceae_asv9	*p*	n.s.	0.001	0.044	0.005	0.030	0.004	0.040	**71**
	AIC	563	555	559	557	560	556	563	
	Dev (%)	7.5	8.8	6.9	9.0	7.3	9.5	15.1	
Lachnospiraceae_asv10	*p*	n.s.	n.s.	n.s.	n.s.	n.s.	n.s.	n.s.	**70**
	AIC	554	557	556	553	555	558	562	
	Dev (%)	3.0	2.3	1.2	7.4	4.0	1.4	10.7	
Lachnospiraceae_asv11	*p*	n.s.	n.s.	n.s.	n.s.	n.s.	n.s.	n.s.	**106**
	AIC	442	443	444	443	442	445	453	
	Dev (%)	3.0	1.7	0.9	3.4	4.1	2.0	6.8	
Lactobacillaceae_asv12	*p*	n.s.	n.s.	0.003	n.s.	0.001	0.007	0.000	**111**
	AIC	384	389	382	384	369	378	370	
	Dev (%)	7.4	3.3	7.5	11.4	24.7	14.1	27.4	
Rikenellaceae_asv15	*p*	n.s.	0.000	0.001	0.000	0.000	0.000	0.000	**114**
	AIC	322	313	311	293	306	308	299	
	Dev (%)	4.9	11.5	14.6	26.9	20.7	16.6	31.9	
Rikenellaceae_asv16	*p*	0.001	n.s.	n.s.	0.001	0.009	n.s.	0.023	**113**
	AIC	385	392	390	384	385	392	391	
	Dev (%)	8.7	10.3	10.2	11.6	11.5	13.3	17.1	
Lachnospiraceae_asv17	*p*	n.s.	n.s.	0.001	0.041	0.008	0.002	0.042	**106**
	AIC	457	457	448	450	447	450	457	
	Dev (%)	6.5	5.0	10.2	17.5	20.8	10.4	16.7	
Desulfovibrionaceae_asv18	*p*	n.s.	0.041	0.013	0.045	0.038	0.023	0.004	**114**
	AIC	221	217	215	217	211	215	212	
	Dev (%)	0.1	3.7	5.4	5.4	16.2	6.6	20.2	
Rikenellaceae_asv20	*p*	n.s.	0.000	0.002	0.001	0.005	0.000	0.000	**113**
	AIC	329	312	316	312	314	310	310	
	Dev (%)	4.1	15.3	13.1	19.2	20.1	18.0	28.4	
Marinifilaceae_asv21	*p*	n.s.	n.s.	n.s.	n.s.	n.s.	n.s.	n.s.	**64**
	AIC	542	542	539	544	542	542	551	
	Dev (%)	0.3	0.6	5.6	0.3	4.4	5.6	6.2	
Lachnospiraceae_asv22	*p*	n.s.	n.s.	n.s.	n.s.	n.s.	n.s.	n.s.	**57**
	AIC	548	548	548	548	549	550	559	
	Dev (%)	0.9	0.6	0.4	2.0	1.0	0.6	4.5	
Desulfovibrionaceae_asv25	*p*	0.018	0.000	0.000	0.000	0.001	0.000	0.000	**114**
	AIC	248	232	232	227	238	232	220	
	Dev (%)	17.0	24.4	31.3	29.6	24.4	25.6	39.2	
Muribaculaceae_asv26	*p*	n.s.	0.000	0.000	0.000	0.000	0.000	0.000	**112**

ToD1		Prot	Carb	Fat	P x C	P x F	C x F	P x C X F	N data points
	AIC	358	346	331	342	330	331	334	
	Dev (%)	2.5	10.9	23.8	15.9	26.7	23.7	30.3	
Muribaculaceae_asv28	*p*	n.s.	n.s.	n.s.	n.s.	n.s.	n.s.	n.s.	
	AIC	463	459	463	465	462	463	468	**91**
	Dev (%)	1.2	15.9	1.2	1.3	7.9	3.0	10.8	
Lachnospiraceae_asv29	*p*	0.019	n.s.	n.s.	n.s.	0.025	n.s.	n.s.	
	AIC	535	540	539	537	535	541	547	**63**
	Dev (%)	4.8	9.8	1.4	4.9	6.4	1.5	7.9	
Lachnospiraceae_asv30	*p*	0.002	0.000	0.000	0.000	0.000	0.000	0.000	
	AIC	505	481	503	479	495	482	484	**47**
	Dev (%)	24.1	32.0	17.3	37.4	26.9	35.9	37.5	
Lachnospiraceae_asv31	*p*	0.000	0.002	n.s.	0.000	0.001	0.028	0.009	
	AIC	451	456	466	450	452	456	458	**97**
	Dev (%)	12.2	8.3	0.3	14.5	12.8	13.8	19.5	
Rikenellaceae_asv34	*p*	n.s.	0.000	0.000	0.001	0.000	0.000	0.000	
	AIC	324	306	298	305	300	297	302	**112**
	Dev (%)	0.1	16.2	22.4	20.2	24.9	25.4	28.6	
Lachnospiraceae_asv35	*p*	n.s.	n.s.	n.s.	n.s.	n.s.	n.s.	n.s.	
	AIC	380	374	379	377	381	378	387	**109**
	Dev (%)	0.0	13.7	1.9	12.6	1.1	6.8	8.1	
Muribaculaceae_asv36	*p*	n.s.	n.s.	n.s.	0.000	n.s.	n.s.	0.001	
	AIC	446	445	443	424	440	446	433	**108**
	Dev (%)	3.6	15.2	15.8	29.7	13.4	3.9	24.2	
Tannerellaceae_asv37	*p*	n.s.	0.009	0.038	0.001	n.s.	0.017	n.s.	
	AIC	469	463	466	459	467	464	468	**106**
	Dev (%)	0.9	6.0	3.8	11.1	4.5	7.1	14.5	
Lachnospiraceae_asv39	*p*	n.s.	n.s.	n.s.	n.s.	n.s.	n.s.	n.s.	
	AIC	482	482	482	484	480	484	488	**99**
	Dev (%)	4.1	0.8	1.8	1.8	11.1	0.9	9.1	
Rikenellaceae_asv40	*p*	n.s.	0.000	0.031	0.000	0.037	0.000	0.000	
	AIC	393	370	392	372	387	371	379	**109**
	Dev (%)	5.0	27.8	5.3	21.6	14.6	21.8	25.9	
Rikenellaceae_asv41	*p*	n.s.	0.012	0.012	0.024	n.s.	0.021	0.043	
	AIC	401	394	391	395	394	393	398	**106**
	Dev (%)	0.0	5.5	10.5	6.5	9.9	8.6	15.0	
Lachnospiraceae_asv42	*p*	n.s.	n.s.	n.s.	n.s.	n.s.	n.s.	n.s.	**107**
	AIC	457	457	456	459	458	458	468	

ToD1		Prot	Carb	Fat	P x C	P x F	C x F	P x C X F	N data points
	Dev (%)	0.1	0.0	0.7	0.1	0.8	0.8	4.4	
Bacteroidaceae_asv43	*p*	n.s.	0.038	0.007	0.002	0.012	0.008	0.035	**105**
	AIC	448	446	440	440	440	442	446	
	Dev (%)	2.1	3.8	9.6	10.4	12.2	8.4	16.3	
Muribaculaceae_asv47	*p*	n.s.	0.000	0.006	0.000	0.033	0.000	0.000	**69**
	AIC	467	443	457	443	458	444	449	
	Dev (%)	0.4	20.8	9.4	23.5	12.2	23.1	26.3	
Lachnospiraceae_asv48	*p*	0.015	0.004	n.s.	0.011	0.004	0.003	0.009	**114**
	AIC	326	319	328	319	323	323	325	
	Dev (%)	6.0	15.0	4.8	17.3	9.5	10.0	19.5	
Lachnospiraceae_asv49	*p*	0.001	n.s.	n.s.	0.004	0.013	n.s.	n.s.	**69**
	AIC	518	526	526	520	519	528	528	
	Dev (%)	9.3	2.8	6.1	9.4	12.6	6.8	14.3	
Oscillospiraceae_asv50	*p*	n.s.	0.017	0.001	0.032	0.007	0.001	0.044	**112**
	AIC	272	266	258	267	261	260	270	
	Dev (%)	0.0	5.0	12.4	6.0	12.1	11.5	14.9	
Lachnospiraceae_asv51	*p*	n.s.	n.s.	0.018	n.s.	0.008	n.s.	n.s.	**96**
	AIC	448	451	446	450	444	448	453	
	Dev (%)	3.1	0.6	4.9	3.1	8.3	4.9	12.2	
Lachnospiraceae_asv52	*p*	n.s.	n.s.	n.s.	n.s.	n.s.	n.s.	n.s.	**112**
	AIC	309	310	310	311	311	308	313	
	Dev (%)	5.8	2.6	0.0	1.7	4.6	8.9	11.5	
Muribaculaceae_asv53	*p*	n.s.	0.000	0.019	0.000	0.041	0.001	0.001	**53**
	AIC	473	451	467	449	469	454	458	
	Dev (%)	0.0	20.6	5.9	24.5	5.6	20.5	24.3	
Muribaculaceae_asv54	*p*	0.001	n.s.	0.005	0.001	0.000	0.011	0.013	**108**
	AIC	373	385	377	372	367	378	379	
	Dev (%)	9.8	0.0	6.8	12.6	16.0	7.7	17.8	
Muribaculaceae_asv56	*p*	0.000	n.s.	0.003	0.000	0.000	0.012	0.000	**90**
	AIC	409	422	415	400	401	417	402	
	Dev (%)	11.7	1.3	7.6	20.3	20.8	7.6	28.1	
Lachnospiraceae_asv57	*p*	n.s.	n.s.	n.s.	n.s.	n.s.	n.s.	0.021	**91**
	AIC	504	504	503	505	497	496	501	
	Dev (%)	1.7	1.8	4.9	2.0	15.3	14.7	17.2	
Rikenellaceae_asv59	*p*	0.001	n.s.	0.001	0.001	0.000	0.005	0.000	**71**
	AIC	396	408	392	392	388	393	393	
	Dev (%)	12.9	4.8	20.9	21.0	18.6	22.9	25.9	

ToD1		Prot	Carb	Fat	P x C	P x F	C x F	P x C X F	N data points
Oscillospiraceae_asv61	*p*	0.030	n.s.	n.s.	n.s.	n.s.	n.s.	n.s.	**114**
	AIC	170	175	177	173	172	175	176	
	Dev (%)	7.6	2.3	0.5	6.8	9.8	4.4	14.1	
Bacteroidaceae_asv63	*p*	n.s.	n.s.	n.s.	n.s.	n.s.	n.s.	n.s.	**100**
	AIC	399	404	402	404	402	399	407	
	Dev (%)	10.2	0.3	6.4	2.2	10.8	14.6	11.2	
Lachnospiraceae_asv64	*p*	n.s.	n.s.	n.s.	n.s.	n.s.	n.s.	n.s.	**92**
	AIC	438	441	440	440	440	442	448	
	Dev (%)	4.1	0.0	0.9	2.6	2.2	0.4	7.5	
Muribaculaceae_asv65	*p*	n.s.	n.s.	n.s.	n.s.	n.s.	n.s.	n.s.	**48**
	AIC	454	454	454	456	453	455	462	
	Dev (%)	0.3	0.3	2.1	6.5	7.4	1.0	7.3	
Lachnospiraceae_asv67	*p*	0.000	0.000	n.s.	0.000	0.000	0.000	0.000	**89**
	AIC	365	368	389	358	353	371	360	
	Dev (%)	24.1	21.3	5.3	33.0	38.3	20.3	36.2	
Lachnospiraceae_asv68	*p*	n.s.	0.000	0.000	0.000	0.000	0.000	0.000	**70**
	AIC	487	470	459	469	462	455	464	
	Dev (%)	0.0	13.3	22.5	15.7	22.0	28.7	28.7	
Rikenellaceae_asv70	*p*	n.s.	n.s.	n.s.	n.s.	n.s.	n.s.	n.s.	**42**
	AIC	517	518	511	519	515	516	522	
	Dev (%)	0.8	0.1	7.9	0.8	6.8	7.1	9.8	
Oscillospiraceae_asv71	*p*	n.s.	0.001	0.015	0.002	0.033	0.001	0.017	**82**
	AIC	467	456	461	458	461	456	464	
	Dev (%)	2.0	12.0	8.0	11.0	10.1	13.0	17.1	
Muribaculaceae_asv72	*p*	n.s.	0.000	0.003	0.000	0.023	0.000	0.003	**109**
	AIC	323	307	310	304	314	306	312	
	Dev (%)	8.2	13.6	12.3	16.9	10.9	15.8	20.9	
Muribaculaceae_asv73	*p*	n.s.	0.000	0.018	0.000	n.s.	0.001	0.004	**86**
	AIC	468	452	458	452	464	454	460	
	Dev (%)	2.5	13.9	18.2	15.4	9.6	14.9	20.0	
Muribaculaceae_asv75	*p*	0.034	0.000	0.021	0.001	0.001	0.013	0.030	**74**
	AIC	396	392	400	392	392	392	401	
	Dev (%)	14.7	10.5	4.6	12.3	12.0	20.0	15.8	
Ruminococcaceae_asv76	*p*	n.s.	0.021	n.s.	0.026	n.s.	n.s.	n.s.	**83**
	AIC	464	459	463	459	461	461	463	
	Dev (%)	0.0	4.7	0.8	6.3	8.8	4.7	14.4	
Streptococcaceae_asv79	*p*	0.000	0.001	n.s.	0.000	0.000	0.000	0.000	**108**

ToD1		Prot	Carb	Fat	P x C	P x F	C x F	P x C X F	N data points
	AIC	345	388	399	340	338	373	327	
	Dev (%)	42.5	19.4	8.4	47.9	48.7	30.4	57.2	
Oscillospiraceae_asv80	*p*	n.s.	0.001	0.000	0.014	0.001	0.000	0.000	**106**
	AIC	338	324	321	329	322	302	309	
	Dev (%)	2.9	22.6	18.1	17.2	19.4	37.1	35.5	
Lachnospiraceae_asv82	*p*	0.006	0.012	n.s.	0.008	0.016	n.s.	0.006	**43**
	AIC	485	486	486	485	481	487	483	
	Dev (%)	6.5	5.6	7.5	8.4	16.0	8.0	21.3	
Marinifilaceae_asv83	*p*	n.s.	0.011	0.040	0.036	n.s.	0.025	0.024	**112**
	AIC	290	280	282	278	284	280	286	
	Dev (%)	0.6	10.1	12.7	17.1	10.2	13.0	16.4	
Lachnospiraceae_asv84	*p*	n.s.	n.s.	n.s.	n.s.	n.s.	n.s.	n.s.	**76**
	AIC	504	505	506	505	508	505	511	
	Dev (%)	7.6	5.8	3.7	11.6	1.2	10.1	11.8	
Oscillospiraceae_asv85	*p*	n.s.	0.018	0.012	n.s.	0.015	0.023	0.023	**82**
	AIC	449	441	442	443	443	439	444	
	Dev (%)	0.7	10.6	6.8	10.9	7.3	17.2	18.4	
Lachnospiraceae_asv86	*p*	0.024	0.019	n.s.	0.025	n.s.	n.s.	n.s.	**85**
	AIC	470	470	474	470	472	471	479	
	Dev (%)	4.5	4.8	6.4	6.4	4.8	5.0	9.8	
Bacteroidaceae_asv87	*p*	0.000	0.000	0.040	0.000	0.000	0.000	0.000	**51**
	AIC	419	426	457	408	425	419	410	
	Dev (%)	34.6	28.6	9.0	42.6	34.1	36.9	46.8	
Deferribacteraceae_asv88	*p*	n.s.	n.s.	n.s.	n.s.	n.s.	n.s.	n.s.	**82**
	AIC	447	446	447	447	448	448	455	
	Dev (%)	0.0	1.1	0.4	1.7	0.4	0.9	7.0	
Lachnospiraceae_asv90	*p*	0.032	0.000	0.001	0.000	0.002	0.000	0.000	**113**
	AIC	250	236	239	238	238	237	239	
	Dev (%)	7.0	17.0	23.2	16.9	22.3	19.7	26.2	
Lachnospiraceae_asv94	*p*	n.s.	n.s.	n.s.	n.s.	n.s.	n.s.	n.s.	**56**
	AIC	435	437	438	438	438	439	443	
	Dev (%)	7.2	1.1	0.6	2.3	2.1	1.2	9.2	
Lachnospiraceae_asv95	*p*	n.s.	0.042	n.s.	n.s.	n.s.	n.s.	n.s.	**57**
	AIC	491	489	492	491	493	491	499	
	Dev (%)	1.4	3.6	1.9	3.8	2.0	3.6	9.1	
Oscillospiraceae_asv96	*p*	n.s.	n.s.	n.s.	n.s.	n.s.	n.s.	n.s.	**71**
	AIC	436	440	441	441	443	441	441	

ToD1		Prot	Carb	Fat	P x C	P x F	C x F	P x C X F	N data points
	Dev (%)	12.4	4.1	8.2	5.9	2.1	5.3	15.0	
Lachnospiraceae_asv100	*p*	n.s.	n.s.	n.s.	0.011	n.s.	0.038	n.s.	**71**
	AIC	490	483	487	483	489	485	491	
	Dev (%)	0.2	15.9	2.3	7.8	2.4	5.7	12.2	
Lachnospiraceae_asv101	*p*	n.s.	n.s.	n.s.	n.s.	n.s.	n.s.	n.s.	**99**
	AIC	391	393	387	391	388	388	393	
	Dev (%)	1.7	0.4	9.5	3.4	9.1	11.5	13.1	
Rikenellaceae_asv102	*p*	n.s.	n.s.	n.s.	n.s.	n.s.	n.s.	n.s.	**66**
	AIC	431	431	428	433	430	428	434	
	Dev (%)	0.2	0.4	3.3	0.4	3.1	5.7	10.9	
Lachnospiraceae_asv103	*p*	n.s.	0.001	0.000	0.001	0.000	0.000	0.000	**54**
	AIC	420	408	400	408	402	398	403	
	Dev (%)	0.0	9.8	16.4	11.7	16.5	19.2	25.0	
Lachnospiraceae_asv104	*p*	n.s.	n.s.	n.s.	n.s.	n.s.	n.s.	n.s.	**81**
	AIC	462	464	462	464	462	463	473	
	Dev (%)	1.4	0.1	1.8	1.4	3.7	2.6	5.5	
Lachnospiraceae_asv105	*p*	n.s.	n.s.	n.s.	n.s.	n.s.	n.s.	n.s.	**51**
	AIC	520	522	522	524	522	523	530	
	Dev (%)	3.1	1.4	0.4	1.5	5.6	0.9	7.3	
Lachnospiraceae_asv108	*p*	n.s.	0.001	0.019	0.001	0.004	0.004	0.003	**82**
	AIC	436	421	431	426	430	423	428	
	Dev (%)	3.0	20.0	8.0	12.8	9.5	21.1	21.1	
Lachnospiraceae_asv109	*p*	n.s.	n.s.	0.000	n.s.	0.000	0.001	0.002	**104**
	AIC	409	406	392	410	393	391	397	
	Dev (%)	0.3	14.0	14.8	1.2	15.0	18.8	22.7	
Muribaculaceae_asv111	*p*	n.s.	0.000	0.004	0.002	0.020	0.006	0.012	**94**
	AIC	330	318	319	320	322	315	325	
	Dev (%)	8.1	10.8	12.2	11.0	11.7	23.0	18.0	
Muribaculaceae_asv112	*p*	n.s.	n.s.	n.s.	n.s.	n.s.	n.s.	n.s.	**70**
	AIC	422	424	422	424	423	426	429	
	Dev (%)	1.5	0.0	3.5	1.6	3.8	0.9	8.9	
Oscillospiraceae_asv113	*p*	n.s.	n.s.	n.s.	n.s.	0.035	n.s.	n.s.	**110**
	AIC	308	308	308	308	306	307	310	
	Dev (%)	3.0	3.5	6.0	4.5	5.9	8.6	14.0	
Lachnospiraceae_asv114	*p*	n.s.	0.001	0.009	0.002	0.030	0.001	0.001	**98**
	AIC	363	351	354	346	356	350	348	
	Dev (%)	0.1	10.2	8.7	18.5	8.2	12.5	23.5	

ToD1		Prot	Carb	Fat	P x C	P x F	C x F	P x C X F	N data points
Lachnospiraceae_asv116	*p*	0.000	0.001	0.011	0.000	0.000	0.000	0.000	**58**
	AIC	362	427	434	368	363	414	366	
	Dev (%)	52.5	19.9	10.8	52.8	54.4	25.2	56.7	
Muribaculaceae_asv117	*p*	n.s.	n.s.	n.s.	n.s.	n.s.	n.s.	n.s.	**114**
	AIC	178	180	182	181	183	182	189	
	Dev (%)	6.0	1.3	0.0	4.3	4.4	1.5	7.3	
Lachnospiraceae_asv118	*p*	0.016	n.s.	n.s.	n.s.	0.019	n.s.	n.s.	**96**
	AIC	408	412	412	410	408	409	414	
	Dev (%)	5.1	3.4	3.0	5.9	6.9	7.4	13.2	
Lachnospiraceae_asv120	*p*	n.s.	n.s.	0.001	n.s.	0.003	0.019	0.013	**77**
	AIC	452	450	441	450	442	443	446	
	Dev (%)	2.2	2.3	9.6	9.1	10.2	11.9	17.8	
Lachnospiraceae_asv121	*p*	n.s.	n.s.	n.s.	n.s.	n.s.	n.s.	0.047	**63**
	AIC	401	397	402	397	399	400	400	
	Dev (%)	1.7	5.4	0.0	8.7	9.8	5.6	14.7	
Lachnospiraceae_asv122	*p*	n.s.	0.000	0.024	0.000	n.s.	0.000	0.000	**80**
	AIC	429	399	419	395	423	401	406	
	Dev (%)	0.1	23.9	16.1	27.5	7.9	24.2	29.2	
Lachnospiraceae_asv130	*p*	0.010	n.s.	0.048	0.032	0.004	0.019	n.s.	**51**
	AIC	440	446	441	441	437	440	448	
	Dev (%)	5.9	0.5	4.6	6.0	9.7	6.9	12.1	
Lachnospiraceae_asv131	*p*	0.000	0.000	0.003	0.000	0.000	0.000	0.000	**44**
	AIC	391	412	439	382	383	411	393	
	Dev (%)	45.3	36.9	15.5	52.8	52.8	37.1	49.1	
Lachnospiraceae_asv133	*p*	n.s.	n.s.	n.s.	n.s.	0.035	n.s.	n.s.	**49**
	AIC	438	441	438	440	436	438	448	
	Dev (%)	2.9	0.1	3.2	3.1	5.9	4.6	7.6	
Lachnospiraceae_asv135	*p*	0.000	0.000	0.049	0.000	0.003	0.000	0.000	**75**
	AIC	428	420	442	415	430	421	427	
	Dev (%)	20.2	26.4	6.0	33.8	24.2	30.3	27.4	
Lachnospiraceae_asv138	*p*	n.s.	n.s.	n.s.	n.s.	n.s.	n.s.	n.s.	**62**
	AIC	432	432	430	434	433	431	439	
	Dev (%)	0.0	0.2	3.4	0.3	2.3	7.1	7.9	
Staphylococcaceae_asv139	*p*	n.s.	n.s.	0.027	n.s.	0.041	0.046	n.s.	**58**
	AIC	417	419	414	419	414	414	423	
	Dev (%)	1.5	0.0	4.3	1.7	5.6	5.4	10.8	
Oscillospiraceae_asv140	*p*	0.005	0.017	0.035	0.001	0.001	0.002	0.005	**78**

ToD1		Prot	Carb	Fat	P x C	P x F	C x F	P x C X F	N data points
	AIC	419	419	423	417	415	419	420	
	Dev (%)	10.3	15.6	6.4	12.3	14.6	10.4	19.8	
Eubacterium_asv141	*p*	n.s.	n.s.	n.s.	n.s.	n.s.	n.s.	n.s.	**92**
	AIC	419	421	421	421	421	423	430	
	Dev (%)	1.6	0.4	0.0	1.6	1.6	0.5	6.3	
Lachnospiraceae_asv142	*p*	n.s.	n.s.	0.002	n.s.	0.009	0.008	n.s.	**78**
	AIC	364	362	355	363	357	357	367	
	Dev (%)	0.1	2.8	8.1	3.4	8.2	8.3	11.6	
Muribaculaceae_asv144	*p*	n.s.	n.s.	n.s.	n.s.	n.s.	n.s.	n.s.	**66**
	AIC	384	384	381	386	384	384	391	
	Dev (%)	0.3	0.2	4.0	0.2	3.9	4.3	7.6	
Lachnospiraceae_asv145	*p*	n.s.	n.s.	n.s.	n.s.	n.s.	n.s.	n.s.	**48**
	AIC	468	468	465	470	467	468	474	
	Dev (%)	4.6	2.9	8.9	2.9	9.6	8.3	11.7	
Peptococcaceae_asv146	*p*	n.s.	0.008	n.s.	0.026	n.s.	0.029	n.s.	**85**
	AIC	410	403	409	405	410	405	415	
	Dev (%)	0.6	6.2	2.5	6.3	5.2	6.2	9.3	
Oscillospiraceae_asv147	*p*	0.000	0.017	n.s.	0.000	0.000	n.s.	0.001	**56**
	AIC	426	437	441	425	428	438	431	
	Dev (%)	16.4	9.6	9.7	21.2	16.6	13.0	25.2	
Staphylococcaceae_asv149	*p*	n.s.	n.s.	n.s.	n.s.	n.s.	n.s.	n.s.	**65**
	AIC	425	424	425	423	427	426	434	
	Dev (%)	1.1	1.8	0.8	4.5	1.6	1.9	7.1	
Lachnospiraceae_asv152	*p*	n.s.	0.000	0.002	0.001	0.006	0.000	0.000	**97**
	AIC	352	330	339	333	337	332	335	
	Dev (%)	0.5	24.6	12.9	20.9	19.8	19.5	25.5	
Lachnospiraceae_asv154	*p*	n.s.	0.047	0.018	n.s.	n.s.	0.032	n.s.	**86**
	AIC	404	400	399	400	399	399	405	
	Dev (%)	0.1	3.5	4.9	5.1	10.5	6.0	12.5	
Ruminococcaceae_asv155	*p*	n.s.	n.s.	n.s.	n.s.	n.s.	n.s.	n.s.	**62**
	AIC	466	465	460	467	463	466	467	
	Dev (%)	0.0	2.1	11.4	2.9	11.9	5.0	12.9	
Lachnospiraceae_asv157	*p*	n.s.	n.s.	n.s.	n.s.	n.s.	n.s.	0.028	**47**
	AIC	418	419	422	418	416	420	421	
	Dev (%)	7.8	11.7	3.4	12.4	13.7	7.3	16.0	
Lachnospiraceae_asv158	*p*	n.s.	n.s.	n.s.	n.s.	n.s.	n.s.	n.s.	**88**
	AIC	347	349	353	351	354	353	357	

ToD1		Prot	Carb	Fat	P x C	P x F	C x F	P x C X F	N data points
	Dev (%)	14.6	5.7	0.5	6.8	1.9	5.0	10.9	
Lachnospiraceae_asv159	*p*	n.s.	0.019	0.002	n.s.	0.002	0.004	0.044	**49**
	AIC	447	443	439	445	438	439	447	
	Dev (%)	1.8	4.8	8.2	5.0	10.3	9.5	14.9	
Oscillospiraceae_asv163	*p*	n.s.	0.000	0.008	0.000	n.s.	0.000	0.011	**65**
	AIC	443	427	433	429	444	428	439	
	Dev (%)	2.3	15.1	20.4	15.2	5.7	15.8	18.0	
Lachnospiraceae_asv165	*p*	n.s.	0.002	0.000	0.012	0.000	0.000	0.003	**88**
	AIC	333	319	321	322	319	307	325	
	Dev (%)	2.1	18.5	12.1	20.1	14.6	31.3	20.8	
Lachnospiraceae_asv169	*p*	0.000	0.000	n.s.	0.000	0.000	0.000	0.000	**98**
	AIC	286	300	317	282	288	299	288	
	Dev (%)	26.9	17.8	3.9	32.2	28.6	21.2	35.2	
Lachnospiraceae_asv171	*p*	n.s.	n.s.	n.s.	n.s.	n.s.	n.s.	n.s.	**38**
	AIC	333	333	333	335	335	334	343	
	Dev (%)	0.0	0.3	0.3	0.3	0.3	1.0	6.5	
Lachnospiraceae_asv172	*p*	n.s.	n.s.	0.006	n.s.	0.018	0.021	n.s.	**47**
	AIC	456	456	449	458	450	450	460	
	Dev (%)	0.2	0.5	6.6	0.6	7.0	6.7	10.6	
Ruminococcaceae_asv174	*p*	0.003	n.s.	n.s.	0.010	0.003	n.s.	0.017	**66**
	AIC	415	423	421	417	414	420	418	
	Dev (%)	7.7	0.6	2.7	7.9	10.0	5.1	18.9	
Lachnospiraceae_asv176	*p*	0.046	0.050	0.029	n.s.	0.019	n.s.	0.019	**81**
	AIC	433	432	434	431	429	431	434	
	Dev (%)	6.0	9.4	4.2	12.0	13.4	15.4	16.9	
Lachnospiraceae_asv177	*p*	n.s.	n.s.	n.s.	n.s.	n.s.	n.s.	n.s.	**40**
	AIC	457	461	460	463	462	460	468	
	Dev (%)	7.4	0.2	1.4	0.2	1.4	2.3	7.3	
Lachnospiraceae_asv179	*p*	n.s.	n.s.	0.009	n.s.	0.013	n.s.	n.s.	**50**
	AIC	453	452	444	452	446	446	455	
	Dev (%)	0.4	1.1	8.2	2.7	8.0	10.6	12.1	
Desulfovibrionaceae_ asv180	*p*	n.s.	0.000	0.011	0.001	0.037	0.000	0.000	**107**
	AIC	301	282	292	285	296	280	286	
	Dev (%)	3.8	19.8	19.8	19.4	11.0	24.5	25.5	
Oscillospiraceae_asv186	*p*	n.s.	0.009	0.001	0.001	0.006	0.002	0.006	**74**
	AIC	431	420	416	420	419	414	424	
	Dev (%)	0.8	18.4	15.2	12.1	15.2	19.3	19.4	

ToD1		Prot	Carb	Fat	P x C	P x F	C x F	P x C X F	N data points
Bacteroidaceae_asv187	*p*	n.s.	0.036	n.s.	n.s.	n.s.	n.s.	n.s.	**87**
	AIC	423	417	421	415	421	418	423	
	Dev (%)	1.0	8.8	4.9	13.8	7.0	12.6	14.9	
Rikenellaceae_asv188	*p*	0.008	0.029	n.s.	0.032	0.018	0.006	0.004	**102**
	AIC	262	260	266	259	259	254	259	
	Dev (%)	6.2	14.4	4.3	14.7	13.8	21.5	21.2	
Lachnospiraceae_asv190	*p*	n.s.	n.s.	n.s.	n.s.	n.s.	n.s.	n.s.	**47**
	AIC	457	456	457	458	459	458	468	
	Dev (%)	0.0	1.5	0.0	0.5	0.0	2.3	4.3	
Lachnospiraceae_asv191	*p*	0.016	n.s.	n.s.	n.s.	n.s.	n.s.	n.s.	**98**
	AIC	379	384	384	381	379	384	384	
	Dev (%)	5.1	0.4	0.9	5.2	9.5	2.1	13.7	
Lachnospiraceae_asv193	*p*	n.s.	n.s.	n.s.	n.s.	n.s.	n.s.	n.s.	**52**
	AIC	460	461	461	462	462	463	473	
	Dev (%)	0.5	0.1	0.0	0.6	0.5	0.1	3.4	
Rikenellaceae_asv194	*p*	n.s.	0.005	n.s.	0.024	n.s.	0.019	n.s.	**86**
	AIC	370	359	368	361	369	362	370	
	Dev (%)	0.5	10.6	2.4	11.4	2.7	9.5	13.5	
Ruminococcaceae_asv196	*p*	n.s.	n.s.	0.046	n.s.	n.s.	n.s.	n.s.	**45**
	AIC	454	456	448	456	454	458	457	
	Dev (%)	2.0	0.7	16.1	4.5	8.4	1.7	13.3	
Oscillospiraceae_asv201	*p*	0.001	n.s.	n.s.	0.019	0.009	n.s.	0.017	**49**
	AIC	419	432	433	423	422	434	430	
	Dev (%)	15.3	2.6	3.5	17.1	15.7	2.6	17.1	
Lachnospiraceae_asv202	*p*	n.s.	0.000	0.001	0.000	0.006	0.000	0.000	**60**
	AIC	438	422	430	419	430	420	421	
	Dev (%)	6.2	16.4	10.3	26.2	14.3	19.5	28.6	
Eggerthellaceae_asv203	*p*	n.s.	n.s.	0.048	n.s.	n.s.	n.s.	0.008	**49**
	AIC	348	348	345	340	346	346	341	
	Dev (%)	0.6	0.8	3.4	15.4	3.9	4.6	18.8	
Lachnospiraceae_asv204	*p*	n.s.	n.s.	n.s.	n.s.	n.s.	n.s.	n.s.	**59**
	AIC	396	393	397	396	398	393	398	
	Dev (%)	1.3	5.8	2.1	5.4	3.5	9.7	12.9	
Lachnospiraceae_asv205	*p*	0.017	0.000	0.005	0.000	0.000	0.000	0.002	**47**
	AIC	403	388	394	390	392	387	397	
	Dev (%)	5.0	16.5	20.0	16.7	15.0	19.0	22.1	
Oscillospiraceae_asv206	*p*	n.s.	n.s.	n.s.	n.s.	n.s.	n.s.	n.s.	**77**

ToD1		Prot	Carb	Fat	P x C	P x F	C x F	P x C X F	N data points
	AIC	383	383	384	385	384	385	391	
	Dev (%)	5.5	1.9	1.5	2.5	3.3	2.5	8.9	
Lachnospiraceae_asv208	*p*	n.s.	n.s.	n.s.	n.s.	n.s.	n.s.	n.s.	
	AIC	391	387	392	390	394	392	400	**41**
	Dev (%)	10.0	12.4	1.6	9.1	0.6	3.0	8.5	
Lachnospiraceae_asv211	*p*	n.s.	n.s.	0.022	n.s.	0.026	n.s.	0.024	
	AIC	330	331	326	331	326	328	327	**81**
	Dev (%)	1.5	1.4	4.6	5.6	6.4	5.6	16.3	
Oscillospiraceae_asv212	*p*	0.018	n.s.	n.s.	n.s.	n.s.	n.s.	n.s.	
	AIC	366	371	371	368	368	373	381	**53**
	Dev (%)	4.9	0.6	0.0	4.9	4.9	0.7	5.8	
Lachnospiraceae_asv214	*p*	0.002	n.s.	0.004	0.009	0.000	0.014	0.000	
	AIC	394	408	396	395	388	398	391	**57**
	Dev (%)	12.5	0.0	12.3	17.7	19.3	11.8	25.1	
Lachnospiraceae_asv215	*p*	n.s.	0.000	0.000	0.000	0.000	0.000	0.000	
	AIC	396	371	372	374	373	370	375	**39**
	Dev (%)	0.0	30.5	20.5	21.9	23.8	24.3	27.7	
Peptococcaceae_asv218	*p*	n.s.	0.033	0.000	n.s.	0.000	0.000	0.003	
	AIC	345	337	323	343	325	325	336	**91**
	Dev (%)	7.4	17.2	18.4	4.9	18.4	18.5	20.6	
Lachnospiraceae_asv223	*p*	0.008	n.s.	n.s.	n.s.	0.048	n.s.	0.011	
	AIC	361	370	371	367	366	367	366	**48**
	Dev (%)	14.8	2.6	1.5	10.0	8.5	8.2	18.2	
Sutterellaceae_asv225	*p*	n.s.	0.002	0.001	0.008	0.000	0.000	0.006	
	AIC	338	323	320	324	324	322	330	**56**
	Dev (%)	0.6	18.2	24.5	19.2	13.7	15.5	20.7	
Ruminococcaceae_asv228	*p*	n.s.	n.s.	n.s.	n.s.	n.s.	n.s.	n.s.	
	AIC	462	458	459	459	460	459	465	**48**
	Dev (%)	0.5	8.9	3.3	10.5	3.9	4.4	12.8	
Eggerthellaceae_asv230	*p*	n.s.	n.s.	n.s.	n.s.	n.s.	n.s.	n.s.	
	AIC	337	337	341	337	341	340	344	**48**
	Dev (%)	6.6	9.9	1.1	12.4	7.0	11.4	12.0	
Oscillospiraceae_asv231	*p*	0.002	0.000	0.012	0.000	0.001	0.000	0.000	
	AIC	334	324	335	323	325	324	318	**42**
	Dev (%)	11.3	21.0	11.8	24.2	24.6	23.5	33.2	
Muribaculaceae_asv232	*p*	n.s.	0.000	0.000	0.000	0.000	0.000	0.000	**74**
	AIC	360	331	337	308	336	324	315	

ToD1		Prot	Carb	Fat	P x C	P x F	C x F	P x C X F	N data points
	Dev (%)	1.7	23.8	20.9	38.7	24.6	29.7	42.4	
Gastranaerophilales_ asv236	*p*	n.s.	n.s.	n.s.	0.024	n.s.	n.s.	n.s.	**61**
	AIC	393	399	399	394	397	401	402	
	Dev (%)	15.1	0.6	0.4	6.5	3.7	0.7	10.7	
Lachnospiraceae_asv238	*p*	0.000	0.002	n.s.	0.000	0.000	0.004	0.000	**40**
	AIC	336	369	376	338	338	369	349	
	Dev (%)	32.1	8.1	4.3	31.6	31.5	9.5	33.0	
Lachnospiraceae_asv243	*p*	n.s.	n.s.	n.s.	n.s.	n.s.	n.s.	n.s.	**47**
	AIC	373	373	370	372	371	372	378	
	Dev (%)	0.9	1.1	3.3	3.6	6.8	5.8	9.7	
Oscillospiraceae_asv246	*p*	n.s.	n.s.	n.s.	n.s.	n.s.	n.s.	n.s.	**77**
	AIC	308	307	308	307	309	310	315	
	Dev (%)	1.0	3.8	0.5	3.6	1.4	2.3	9.4	
Lachnospiraceae_asv248	*p*	0.004	n.s.	n.s.	0.019	0.004	n.s.	0.010	**58**
	AIC	409	417	414	408	407	410	410	
	Dev (%)	7.0	0.2	3.0	10.1	9.7	12.7	18.2	
Lachnospiraceae_asv250	*p*	n.s.	0.041	0.000	0.038	0.001	0.000	0.000	**58**
	AIC	390	383	368	380	369	363	370	
	Dev (%)	1.1	8.4	26.4	15.6	23.4	29.6	27.3	
Lachnospiraceae_asv254	*p*	n.s.	0.018	n.s.	0.044	n.s.	0.042	0.015	**66**
	AIC	327	318	321	317	323	318	321	
	Dev (%)	0.8	8.8	8.2	14.0	9.8	12.1	17.3	
Ruminococcaceae_asv257	*p*	n.s.	n.s.	n.s.	n.s.	n.s.	n.s.	n.s.	**78**
	AIC	296	298	300	298	299	302	304	
	Dev (%)	4.9	5.0	0.0	8.2	2.2	0.0	11.2	
Erysipelatoclostridiaceae_ asv266	*p*	n.s.	0.001	n.s.	0.003	n.s.	0.005	0.005	**43**
	AIC	436	426	438	428	438	427	431	
	Dev (%)	4.2	12.0	1.6	11.9	3.8	14.1	19.6	
Oscillospiraceae_asv267	*p*	0.023	n.s.	n.s.	n.s.	n.s.	n.s.	n.s.	**49**
	AIC	290	295	294	292	292	294	298	
	Dev (%)	4.5	0.6	2.6	4.7	4.6	7.6	11.7	
Gastranaerophilales_ asv268	*p*	n.s.	0.022	n.s.	n.s.	n.s.	0.046	n.s.	**43**
	AIC	375	371	373	373	374	372	383	
	Dev (%)	0.9	4.6	2.8	4.6	3.8	5.4	7.5	
Oscillospirales_asv269	*p*	n.s.	n.s.	n.s.	n.s.	n.s.	n.s.	0.034	**74**
	AIC	315	320	319	318	312	322	317	
	Dev (%)	5.8	0.1	1.5	8.3	15.9	0.2	15.5	

ToD1		Prot	Carb	Fat	P x C	P x F	C x F	P x C X F	N data points
Rhodospirillales_asv270	*p*	n.s.	n.s.	0.000	0.019	0.000	0.000	0.009	**66**
	AIC	385	378	368	379	370	369	378	
	Dev (%)	0.2	10.0	13.8	6.9	13.9	14.8	18.4	
Ruminococcaceae_asv276	*p*	0.012	0.043	0.034	0.011	0.024	n.s.	n.s.	**50**
	AIC	320	326	322	322	320	324	328	
	Dev (%)	9.2	3.6	8.9	7.9	12.2	10.4	15.4	
Gastranaerophilales_ asv279	*p*	n.s.	n.s.	n.s.	n.s.	n.s.	n.s.	n.s.	**39**
	AIC	264	265	265	263	266	267	269	
	Dev (%)	1.3	0.3	0.0	7.7	1.3	0.4	10.2	
Oscillospiraceae_asv283	*p*	0.000	0.002	n.s.	0.001	0.001	0.005	0.001	**54**
	AIC	324	324	336	321	319	325	323	
	Dev (%)	11.5	15.3	3.6	16.7	25.1	15.1	24.6	
Muribaculaceae_asv286	*p*	n.s.	n.s.	n.s.	n.s.	n.s.	n.s.	n.s.	**40**
	AIC	215	213	209	214	212	207	221	
	Dev (%)	0.2	1.9	8.5	3.2	4.5	17.4	8.7	
Anaerovoracaceae_ Eubacterium_asv289	*p*	n.s.	n.s.	n.s.	n.s.	n.s.	n.s.	n.s.	**54**
	AIC	270	269	270	270	271	271	274	
	Dev (%)	0.2	0.6	0.3	1.4	2.7	0.7	10.0	
Lachnospiraceae_asv292	*p*	0.035	n.s.	0.028	0.049	n.s.	0.000	0.001	**40**
	AIC	339	341	339	344	339	317	332	
	Dev (%)	14.0	11.2	12.4	5.3	16.1	33.4	25.6	
Ruminococcaceae_asv300	*p*	0.000	n.s.	n.s.	0.002	0.001	n.s.	0.036	**43**
	AIC	332	343	345	334	334	345	342	
	Dev (%)	11.0	1.7	0.2	11.0	11.3	1.7	15.3	
Ruminococcaceae_asv301	*p*	0.007	n.s.	0.036	0.013	0.025	n.s.	n.s.	**52**
	AIC	320	322	320	320	318	322	326	
	Dev (%)	6.3	5.3	8.3	7.6	11.3	9.5	14.5	
Clostridia_asv303	*p*	n.s.	0.001	0.000	0.001	0.001	0.000	0.000	**45**
	AIC	285	272	269	268	270	266	266	
	Dev (%)	12.7	17.7	16.5	23.5	19.9	22.4	28.9	
Lachnospiraceae_asv312	*p*	n.s.	n.s.	n.s.	n.s.	n.s.	n.s.	0.013	**42**
	AIC	297	295	294	297	293	288	290	
	Dev (%)	0.0	2.0	5.5	1.8	10.2	14.7	17.7	
Rhodospirillales_asv315	*p*	n.s.	n.s.	n.s.	n.s.	n.s.	n.s.	n.s.	**47**
	AIC	360	358	355	359	358	358	364	
	Dev (%)	0.1	4.2	16.9	3.0	3.7	4.1	11.6	
Butyricicoccaceae_asv318	*p*	0.016	0.000	0.000	0.000	0.000	0.000	0.000	**55**

ToD1		Prot	Carb	Fat	P x C	P x F	C x F	P x C X F	N data points
	AIC	299	284	273	286	268	270	267	
	Dev (%)	8.1	20.1	28.0	20.8	34.1	33.9	38.8	
Anaerovoracaceae_asv320	*p*	0.018	0.000	0.000	0.000	0.000	0.000	0.000	**69**
	AIC	262	233	230	236	227	220	229	
	Dev (%)	7.6	28.8	33.2	28.7	36.1	40.5	39.2	
Tannerellaceae_ Paraasv331	*p*	0.031	0.003	n.s.	n.s.	n.s.	0.007	0.021	**46**
	AIC	385	384	391	384	389	385	388	
	Dev (%)	8.9	7.5	2.8	13.3	9.2	8.5	16.7	

Supplementary Table 7-7. GAM statistics for Figure 3-11 ToD6.
Dev = deviance explained, n.s. = p value >0.05

Tod6	GAM	Prot	Carb	Fat	P x C	P x F	C x F	P x C X F	N data points
InvSimpson	*p*	0.020	n.s.	n.s.	n.s.	n.s.	n.s.	n.s.	**114**
	AIC	855	864	863	865	864	863	870	
	Dev (%)	20.2%	1.3%	3.6%	3.4%	6.2%	8.0%	8.9%	
Observed	*p*	n.s.	n.s.	0.004	0.002	n.s.	0.024	0.007	**114**
	AIC	1,021	1,020	1,010	1,006	1,015	1,016	1,016	
	Dev (%)	2.9%	5.4%	21.6 %	23.0%	18.7 %	10.7%	19.9%	
Shannon	*p*	0.004	n.s.	n.s.	0.036	n.s.	n.s.	0.029	**114**
	AIC	69	79	82	73	79	76	80	
	Dev (%)	23.7%	6.6%	8.2%	16.9%	15.3 %	14.3%	17.3%	
Verrucomicrobiota	*p*	n.s.	n.s.	n.s.	n.s.	n.s.	n.s.	n.s.	**114**
	AIC	540	539	542	541	542	540	551	
	Dev (%)	1.4%	2.5%	0.0%	2.7%	1.4%	3.2%	5.8%	
Actinobacteriota	*p*	n.s.	0.000	0.000	0.000	0.002	0.000	0.000	**114**
	AIC	645	628	630	628	631	620	625	
	Dev (%)	3.8%	16.1%	16.2 %	17.6%	17.5 %	28.0%	28.4%	
Firmicutes	*p*	0.003	n.s.	n.s.	0.003	0.003	n.s.	0.004	**114**
	AIC	1,105	1,114	1,114	1,100	1,106	1,111	1,106	
	Dev (%)	9.3%	2.8%	1.6%	17.2%	9.8%	10.4%	20.0%	
Desulfobacterota	*p*	0.003	0.001	n.s.	0.001	0.004	0.008	0.046	**114**
	AIC	478	476	485	475	479	477	485	

Tod6	GAM	Prot	Carb	Fat	P x C	P x F	C x F	P x C X F	N data points
	Dev (%)	8.6%	10.2%	3.9%	12.5%	9.6%	12.0%	15.3%	
Bacteroidota	*p*	0.012	n.s.	0.045	0.002	0.049	n.s.	0.002	**114**
	AIC	968	972	971	957	966	972	962	
	Dev (%)	5.6%	7.8%	3.5%	19.2%	12.7 %	6.7%	22.9%	
Deferribacterota	*p*	0.005	n.s.	n.s.	n.s.	0.026	n.s.	n.s.	**114**
	AIC	444	452	449	444	442	450	451	
	Dev (%)	6.9%	0.2%	2.6%	13.3%	20.2 %	4.1%	14.8%	
Cyanobacteria	*p*	n.s.	0.000	0.000	0.000	0.000	0.000	0.000	**114**
	AIC	517	495	480	473	476	474	469	
	Dev (%)	2.4%	25.1%	37.5 %	38.9%	40.7 %	38.1%	44.7%	
Proteobacteria	*p*	0.008	0.002	0.000	0.000	0.000	0.000	0.000	**114**
	AIC	593	585	570	552	559	568	551	
	Dev (%)	6.0%	14.1%	31.1 %	41.5%	39.0 %	29.1%	43.4%	
Akkermansiaceae_asv1	*p*	n.s.	n.s.	n.s.	n.s.	n.s.	n.s.	n.s.	**111**
	AIC	540	539	542	541	542	540	551	
	Dev (%)	1.4%	2.5%	0.0%	2.7%	1.4%	3.2%	5.8%	
Erysipelotrichaceae_asv3	*p*	n.s.	0.000	0.000	0.000	0.000	0.000	0.000	**43**
	AIC	552	531	524	527	526	517	522	
	Dev (%)	1.8%	17.5%	23.5 %	22.1%	24.4 %	30.5%	33.8%	
Erysipelotrichaceae_asv4	*p*	n.s.	0.000	0.000	0.000	0.000	0.000	0.000	**52**
	AIC	559	524	541	524	539	520	527	
	Dev (%)	5.6%	29.8%	24.0 %	30.8%	23.1 %	34.6%	37.3%	
Prevotellaceae_asv5	*p*	n.s.	n.s.	n.s.	n.s.	n.s.	n.s.	0.007	**89**
	AIC	526	521	524	519	525	520	520	
	Dev (%)	0.9%	7.5%	4.0%	12.1%	5.0%	12.1%	19.0%	
Bacteroidaceae_asv7	*p*	0.001	0.000	0.001	0.000	0.000	0.000	0.000	**113**
	AIC	381	363	380	356	367	365	362	
	Dev (%)	14.8%	25.7%	18.1 %	36.9%	29.8 %	25.8%	35.6%	
Lachnospiraceae_asv8	*p*	0.043	n.s.	0.011	n.s.	0.014	n.s.	0.000	**114**
	AIC	293	293	290	292	284	289	280	
	Dev (%)	3.6%	7.8%	5.7%	9.3%	17.5 %	11.5%	25.1%	
Lachnospiraceae_asv9	*p*	n.s.	0.025	n.s.	0.001	n.s.	0.019	0.003	**60**
	AIC	561	555	560	545	559	550	552	
	Dev (%)	2.2%	11.1%	2.7%	19.8%	12.0 %	19.1%	22.8%	
Lachnospiraceae_asv10	*p*	n.s.	n.s.	n.s.	n.s.	n.s.	n.s.	n.s.	**92**
	AIC	529	528	530	530	530	526	534	

Tod6	GAM	Prot	Carb	Fat	P x C	P x F	C x F	P x C X F	N data points
	Dev (%)	1.7%	3.4%	1.6%	3.0%	2.4%	7.3%	11.0%	
Lachnospiraceae_asv11	*p*	n.s.	n.s.	n.s.	n.s.	n.s.	0.026	n.s.	**95**
	AIC	518	518	514	514	516	513	519	
	Dev (%)	0.9%	0.7%	11.3 %	13.3%	3.9%	6.3%	13.3%	
Lactobacillaceae_asv12	*p*	0.000	n.s.	0.001	0.001	0.002	0.047	0.000	**112**
	AIC	353	366	353	352	355	363	357	
	Dev (%)	19.0%	10.8%	24.4 %	25.9%	22.7 %	14.3%	24.6%	
Lactobacillaceae_asv13	*p*	0.001	0.001	0.003	0.001	0.006	0.013	0.000	**49**
	AIC	447	445	441	444	443	445	437	
	Dev (%)	8.9%	10.3%	19.5 %	12.9%	16.7 %	15.1%	27.2%	
Rikenellaceae_asv15	*p*	0.002	0.001	0.000	0.000	0.000	0.000	0.000	**114**
	AIC	345	338	300	286	290	296	279	
	Dev (%)	9.4%	19.9%	43.0 %	51.2%	50.7 %	46.4%	56.0%	
Rikenellaceae_asv16	*p*	0.000	n.s.	0.000	0.000	0.000	0.000	0.000	**114**
	AIC	437	451	433	424	415	431	419	
	Dev (%)	16.0%	11.2%	18.7 %	31.8%	34.0 %	21.6%	37.4%	
Lachnospiraceae_asv17	*p*	0.001	0.000	n.s.	0.004	0.043	0.001	0.002	**110**
	AIC	380	383	393	382	388	385	386	
	Dev (%)	21.3%	12.0%	12.4 %	20.9%	13.9 %	12.1%	22.0%	
Desulfovibrionaceae_asv 18	*p*	n.s.	0.000	0.000	0.000	0.000	0.000	0.000	**114**
	AIC	218	195	196	193	197	190	198	
	Dev (%)	0.6%	21.0%	19.2 %	25.0%	22.0 %	27.5%	28.4%	
Rikenellaceae_asv20	*p*	0.037	0.000	0.000	0.000	0.000	0.000	0.000	**114**
	AIC	289	272	256	265	271	269	264	
	Dev (%)	14.6%	21.2%	40.2 %	27.2%	31.6 %	26.6%	35.8%	
Marinifilaceae_asv21	*p*	n.s.	0.005	n.s.	0.032	n.s.	0.044	n.s.	**84**
	AIC	526	519	525	516	526	520	525	
	Dev (%)	4.0%	6.9%	6.6%	19.5%	2.4%	9.3%	14.4%	
Lachnospiraceae_asv22	*p*	n.s.	n.s.	n.s.	n.s.	n.s.	n.s.	n.s.	**96**
	AIC	476	473	474	475	475	474	486	
	Dev (%)	0.3%	3.0%	2.2%	3.1%	2.7%	3.7%	5.6%	
Desulfovibrionaceae_asv 25	*p*	0.011	0.000	0.001	0.000	0.000	0.000	0.000	**114**
	AIC	339	330	334	321	325	326	325	
	Dev (%)	10.3%	18.2%	14.1 %	28.6%	24.9 %	19.3%	29.5%	
Muribaculaceae_asv26	*p*	n.s.	0.006	0.000	0.000	0.000	0.000	0.001	**113**

Tod6	GAM	Prot	Carb	Fat	P x C	P x F	C x F	P x C X F	N data points
	AIC	330	319	311	317	314	310	316	
	Dev (%)	13.7%	16.1%	20.8 %	14.2%	17.2 %	18.9%	24.7%	
Muribaculaceae_asv28	*p*	n.s.	n.s.	n.s.	n.s.	n.s.	n.s.	n.s.	**110**
	AIC	377	374	372	375	376	374	383	
	Dev (%)	0.9%	7.3%	11.6 %	8.0%	2.4%	6.4%	8.8%	
Lachnospiraceae_asv29	*p*	n.s.	n.s.	n.s.	n.s.	n.s.	n.s.	n.s.	**94**
	AIC	486	486	486	488	486	483	491	
	Dev (%)	2.0%	3.4%	2.7%	3.8%	3.7%	8.0%	11.6%	
Lachnospiraceae_asv30	*p*	0.000	0.000	0.004	0.000	0.000	0.000	0.000	**81**
	AIC	507	486	511	486	496	487	495	
	Dev (%)	10.6%	25.7%	7.2%	26.5%	20.1 %	26.1%	30.3%	
Lachnospiraceae_asv31	*p*	0.000	n.s.	0.019	0.000	0.000	0.001	0.000	**111**
	AIC	327	354	346	330	326	344	330	
	Dev (%)	24.1%	7.1%	16.6 %	22.4%	27.9 %	12.8%	32.1%	
Muribaculaceae_asv32	*p*	n.s.	n.s.	0.000	n.s.	0.002	0.001	0.001	**109**
	AIC	328	325	307	327	312	310	313	
	Dev (%)	0.0%	6.6%	24.5 %	10.4%	17.4 %	19.4%	24.2%	
Rikenellaceae_asv34	*p*	n.s.	0.000	0.000	0.000	0.000	0.000	0.000	**114**
	AIC	215	192	169	185	168	163	174	
	Dev (%)	12.4%	22.8%	38.7 %	32.0%	41.2 %	46.4%	42.2%	
Lachnospiraceae_asv35	*p*	n.s.	n.s.	0.021	0.039	0.045	n.s.	n.s.	**113**
	AIC	310	310	306	307	307	308	315	
	Dev (%)	1.2%	4.1%	4.7%	5.7%	5.4%	4.9%	11.7%	
Muribaculaceae_asv36	*p*	0.023	n.s.	0.046	0.015	0.005	n.s.	0.012	**113**
	AIC	357	366	362	358	357	363	359	
	Dev (%)	12.6%	0.0%	3.5%	9.7%	9.0%	4.1%	17.9%	
Tannerellaceae_asv37	*p*	n.s.	0.000	0.000	0.000	0.001	0.000	0.000	**109**
	AIC	465	440	452	436	453	438	446	
	Dev (%)	0.1%	19.6%	11.0 %	24.7%	11.5 %	22.1%	27.0%	
Lachnospiraceae_asv39	*p*	0.000	0.000	n.s.	0.000	0.000	0.000	0.000	**100**
	AIC	384	392	423	372	387	395	381	
	Dev (%)	33.5%	32.4%	4.2%	44.6%	30.1 %	29.4%	41.6%	
Rikenellaceae_asv40	*p*	0.045	0.000	0.000	0.000	0.000	0.000	0.000	**109**
	AIC	411	377	377	378	367	366	361	
	Dev (%)	5.7%	29.7%	31.6 %	33.4%	41.8 %	40.9%	46.8%	
Rikenellaceae_asv41	*p*	n.s.	0.008	0.004	0.035	n.s.	0.005	0.000	**107**

Tod6	GAM	Prot	Carb	Fat	P x C	P x F	C x F	P x C X F	N data points
	AIC	399	390	386	391	392	385	383	
	Dev (%)	4.9%	12.0%	18.8 %	15.3%	15.5 %	19.9%	25.9%	
Lachnospiraceae_asv42	*p*	n.s.	0.021	n.s.	n.s.	n.s.	n.s.	0.046	**108**
	AIC	418	408	414	413	413	413	414	
	Dev (%)	0.1%	12.4%	3.2%	8.9%	10.1 %	10.1%	16.4%	
Bacteroidaceae_asv43	*p*	n.s.	0.011	0.000	0.001	0.001	0.000	0.001	**111**
	AIC	420	410	403	403	403	402	408	
	Dev (%)	1.8%	15.2%	15.2 %	19.4%	18.8 %	17.4%	22.8%	
Desulfovibrionaceae_asv 44	*p*	n.s.	n.s.	0.001	n.s.	0.004	0.016	n.s.	**41**
	AIC	390	386	379	386	381	380	389	
	Dev (%)	0.1%	5.4%	9.4%	7.4%	9.4%	11.9%	13.8%	
Lactobacillaceae_asv46	*p*	0.015	0.004	0.001	0.032	0.018	0.002	0.000	**38**
	AIC	367	364	355	363	360	353	345	
	Dev (%)	5.2%	7.3%	20.2 %	15.5%	18.2 %	23.3%	32.7%	
Muribaculaceae_asv47	*p*	n.s.	0.000	0.000	0.000	0.000	0.000	0.000	**60**
	AIC	440	413	410	412	411	403	410	
	Dev (%)	1.3%	23.8%	25.6 %	27.6%	26.5 %	31.4%	34.3%	
Lachnospiraceae_asv48	*p*	n.s.	0.030	n.s.	0.044	n.s.	n.s.	n.s.	**113**
	AIC	363	358	361	359	363	360	366	
	Dev (%)	0.0%	4.1%	8.3%	5.5%	1.8%	4.4%	10.8%	
Lachnospiraceae_asv49	*p*	n.s.	n.s.	n.s.	n.s.	n.s.	n.s.	n.s.	**84**
	AIC	470	468	472	469	472	468	475	
	Dev (%)	2.4%	6.7%	0.4%	7.7%	2.6%	8.1%	11.2%	
Oscillospiraceae_asv50	*p*	0.007	0.000	0.000	0.000	0.000	0.000	0.000	**114**
	AIC	154	129	134	131	128	120	127	
	Dev (%)	8.8%	27.2%	31.0 %	27.5%	29.3 %	39.2%	37.2%	
Lachnospiraceae_asv51	*p*	n.s.	n.s.	n.s.	n.s.	n.s.	n.s.	n.s.	**109**
	AIC	390	390	388	392	390	391	398	
	Dev (%)	0.3%	0.4%	7.0%	0.5%	4.5%	2.8%	7.0%	
Lachnospiraceae_asv52	*p*	0.026	n.s.	n.s.	0.039	n.s.	n.s.	n.s.	**114**
	AIC	256	263	266	262	262	265	265	
	Dev (%)	17.7%	2.7%	0.5%	5.7%	11.4 %	2.7%	15.3%	
Muribaculaceae_asv53	*p*	n.s.	0.000	0.000	0.000	0.000	0.000	0.000	**61**
	AIC	435	407	398	404	400	392	399	
	Dev (%)	0.9%	22.9%	29.6 %	27.6%	30.6 %	33.2%	37.1%	
Muribaculaceae_asv54	*p*	0.005	0.021	0.000	0.000	0.000	0.000	0.000	**114**

Tod6	GAM	Prot	Carb	Fat	P x C	P x F	C x F	P x C X F	N data points
	AIC	324	323	288	296	283	288	286	
	Dev (%)	6.7%	12.6%	32.3 %	30.3%	36.1 %	35.7%	42.1%	
Lachnospiraceae_asv55	*p*	n.s.	n.s.	n.s.	n.s.	n.s.	0.047	0.023	**40**
	AIC	488	485	487	485	484	480	486	
	Dev (%)	4.2%	5.5%	3.7%	8.1%	13.4 %	14.5%	16.4%	
Muribaculaceae_asv56	*p*	0.000	0.044	0.002	0.000	0.000	0.000	0.000	**94**
	AIC	392	401	391	365	379	377	362	
	Dev (%)	14.9%	8.4%	22.1 %	37.4%	29.2 %	31.3%	42.1%	
Lachnospiraceae_asv57	*p*	0.007	n.s.	n.s.	0.002	0.041	n.s.	0.001	**102**
	AIC	416	420	423	408	415	417	411	
	Dev (%)	9.2%	6.6%	5.8%	18.3%	17.6 %	16.1%	23.3%	
Rikenellaceae_asv59	*p*	0.029	0.000	0.000	0.000	0.000	0.000	0.000	**92**
	AIC	446	435	417	398	413	404	391	
	Dev (%)	6.3%	15.5%	29.1 %	41.7%	32.6 %	40.8%	49.6%	
Tannerellaceae_asv60	*p*	0.025	0.002	0.000	0.000	0.000	0.000	0.000	**70**
	AIC	539	530	529	507	522	524	515	
	Dev (%)	9.0%	20.4%	14.8 %	31.0%	25.6 %	22.3%	34.5%	
Oscillospiraceae_asv61	*p*	n.s.	n.s.	n.s.	n.s.	n.s.	n.s.	n.s.	**114**
	AIC	159	160	159	160	158	162	163	
	Dev (%)	2.7%	5.9%	5.0%	2.9%	8.6%	1.7%	12.7%	
Bacteroidaceae_asv63	*p*	0.023	n.s.	n.s.	n.s.	0.028	n.s.	n.s.	**104**
	AIC	352	357	355	352	352	355	360	
	Dev (%)	4.6%	1.5%	3.0%	9.2%	6.2%	7.9%	12.8%	
Lachnospiraceae_asv64	*p*	0.007	0.008	n.s.	0.049	0.049	0.021	0.020	**112**
	AIC	319	319	325	318	320	320	321	
	Dev (%)	6.3%	6.1%	2.6%	11.6%	7.6%	6.8%	16.8%	
Muribaculaceae_asv65	*p*	n.s.	n.s.	n.s.	n.s.	n.s.	n.s.	0.014	**112**
	AIC	303	304	303	303	300	305	298	
	Dev (%)	0.9%	0.7%	0.5%	5.4%	12.2 %	0.7%	17.5%	
Lachnospiraceae_asv67	*p*	0.000	0.000	0.000	0.000	0.000	0.000	0.000	**104**
	AIC	354	342	360	338	342	339	334	
	Dev (%)	35.9%	33.3%	28.6 %	36.7%	36.2 %	39.1%	46.7%	
Lachnospiraceae_asv68	*p*	0.047	0.005	0.000	0.000	0.000	0.000	0.000	**73**
	AIC	470	461	449	439	445	447	437	
	Dev (%)	6.7%	19.3%	22.5 %	34.0%	28.1 %	28.3%	38.4%	
Muribaculaceae_asv69	*p*	0.040	0.001	0.000	0.000	0.000	0.000	0.000	**66**

Tod6	GAM	Prot	Carb	Fat	P x C	P x F	C x F	P x C X F	N data points
	AIC	351	344	329	323	325	326	321	
	Dev (%)	9.8%	16.5%	23.3 %	35.7%	32.5 %	29.8%	38.0%	
Rikenellaceae_asv70	*p*	n.s.	0.027	n.s.	n.s.	n.s.	0.046	n.s.	**56**
	AIC	502	500	502	502	505	501	510	
	Dev (%)	7.9%	4.3%	6.7%	4.4%	5.3%	5.4%	9.4%	
Oscillospiraceae_asv71	*p*	n.s.	0.000	0.000	0.000	0.000	0.000	0.000	**109**
	AIC	359	333	345	319	336	328	318	
	Dev (%)	13.4%	24.6%	19.9 %	39.9%	30.2 %	34.4%	42.9%	
Muribaculaceae_asv72	*p*	0.030	n.s.	0.000	n.s.	0.004	0.032	0.000	**113**
	AIC	247	253	234	250	238	245	232	
	Dev (%)	11.1%	2.5%	27.7 %	15.3%	21.5 %	15.9%	30.4%	
Muribaculaceae_asv73	*p*	0.003	0.000	0.013	0.000	0.006	0.001	0.001	**83**
	AIC	415	406	414	406	410	403	409	
	Dev (%)	8.6%	14.9%	11.7 %	16.3%	17.7 %	23.8%	24.1%	
Erysipelotrichaceae_asv74	*p*	n.s.	n.s.	n.s.	n.s.	n.s.	n.s.	n.s.	**72**
	AIC	441	440	439	441	442	441	447	
	Dev (%)	0.0%	1.9%	7.4%	4.5%	0.5%	2.9%	8.3%	
Muribaculaceae_asv75	*p*	0.002	n.s.	n.s.	0.022	0.007	n.s.	0.016	**95**
	AIC	350	360	359	349	352	361	353	
	Dev (%)	8.3%	0.1%	4.4%	15.7%	8.5%	2.8%	18.9%	
Ruminococcaceae_asv76	*p*	n.s.	0.002	0.000	0.001	0.004	0.001	0.000	**112**
	AIC	318	303	306	296	304	297	299	
	Dev (%)	8.9%	17.5%	11.1 %	25.7%	18.6 %	25.3%	28.5%	
Streptococcaceae_asv79	*p*	0.000	0.018	n.s.	0.000	0.000	0.001	0.000	**114**
	AIC	319	355	364	322	319	344	327	
	Dev (%)	36.1%	14.8%	2.0%	33.4%	37.9 %	26.0%	38.5%	
Oscillospiraceae_asv80	*p*	n.s.	0.000	0.000	0.000	0.000	0.000	0.000	**114**
	AIC	221	207	196	198	194	191	195	
	Dev (%)	8.0%	19.6%	26.3 %	28.1%	31.7 %	33.2%	34.6%	
Muribaculaceae_asv81	*p*	n.s.	0.000	0.000	0.000	0.000	0.000	0.000	**52**
	AIC	351	330	323	324	322	313	318	
	Dev (%)	3.3%	19.5%	26.7 %	29.0%	31.2 %	34.0%	36.2%	
Lachnospiraceae_asv82	*p*	n.s.	0.005	0.000	0.002	0.002	0.002	0.003	**65**
	AIC	473	462	461	457	463	458	463	
	Dev (%)	0.3%	10.8%	10.6 %	17.9%	10.7 %	17.0%	20.6%	

Tod6	GAM	Prot	Carb	Fat	P x C	P x F	C x F	P x C X F	N data points
Marinifilaceae_asv83	*p*	n.s.	0.001	0.000	0.000	0.000	0.000	0.000	**114**
	AIC	285	269	250	260	250	250	255	
	Dev (%)	0.0%	14.6%	27.7 %	25.6%	31.6 %	27.8%	33.2%	
Lachnospiraceae_asv84	*p*	0.002	n.s.	n.s.	0.010	0.008	n.s.	0.002	**79**
	AIC	454	465	464	455	454	468	457	
	Dev (%)	14.0%	12.5%	12.8 %	21.1%	20.2 %	2.5%	22.1%	
Oscillospiraceae_asv85	*p*	n.s.	0.019	0.023	0.001	n.s.	n.s.	0.002	**104**
	AIC	361	354	358	344	358	356	351	
	Dev (%)	2.3%	13.2%	4.5%	20.5%	9.0%	11.0%	23.1%	
Lachnospiraceae_asv86	*p*	0.009	n.s.	0.004	0.032	0.034	n.s.	0.030	**97**
	AIC	404	409	395	406	401	404	407	
	Dev (%)	5.9%	1.9%	23.5 %	6.0%	13.9 %	13.6%	15.8%	
Bacteroidaceae_asv87	*p*	0.000	0.002	0.005	0.000	0.000	0.001	0.000	**64**
	AIC	422	437	439	426	424	429	431	
	Dev (%)	30.4%	16.7%	17.4 %	22.2%	25.7 %	26.2%	27.7%	
Deferribacteraceae_asv88	*p*	0.005	n.s.	n.s.	n.s.	0.026	n.s.	n.s.	**86**
	AIC	444	452	449	444	442	450	451	
	Dev (%)	6.9%	0.2%	2.6%	13.3%	20.2 %	4.1%	14.8%	
Lachnospiraceae_asv90	*p*	0.000	0.000	0.016	0.000	0.000	0.000	0.000	**114**
	AIC	206	212	235	202	203	213	208	
	Dev (%)	35.5%	30.4%	16.0 %	34.2%	32.9 %	32.2%	37.8%	
Muribaculaceae_asv91	*p*	n.s.	0.000	0.000	0.000	0.001	0.000	0.000	**61**
	AIC	425	406	402	404	405	399	405	
	Dev (%)	0.0%	17.5%	24.0 %	18.3%	22.5 %	24.3%	26.6%	
Lachnospiraceae_asv94	*p*	n.s.	n.s.	n.s.	n.s.	n.s.	n.s.	n.s.	**96**
	AIC	414	414	416	414	418	416	419	
	Dev (%)	12.4%	3.2%	2.1%	11.1%	1.4%	3.2%	13.1%	
Lachnospiraceae_asv95	*p*	n.s.	n.s.	n.s.	n.s.	n.s.	0.011	0.022	**65**
	AIC	471	466	472	468	473	465	468	
	Dev (%)	2.6%	9.6%	0.5%	10.0%	1.7%	8.8%	16.5%	
Oscillospiraceae_asv96	*p*	0.039	0.000	0.000	0.000	0.000	0.000	0.000	**112**
	AIC	335	316	313	315	313	312	316	
	Dev (%)	14.6%	22.9%	28.7 %	28.4%	32.6 %	27.1%	31.9%	
Peptostreptococcaceae_asv98	*p*	n.s.	n.s.	n.s.	n.s.	n.s.	n.s.	n.s.	**86**
	AIC	455	456	453	456	456	456	464	

Tod6	GAM	Prot	Carb	Fat	P x C	P x F	C x F	P x C X F	N data points
	Dev (%)	2.1%	2.6%	11.4 %	4.8%	8.2%	4.2%	7.9%	
Lachnospiraceae_asv99	*p*	n.s.	0.002	0.002	0.003	0.016	0.001	0.013	**53**
	AIC	468	459	453	452	455	455	463	
	Dev (%)	1.7%	8.1%	17.7 %	24.0%	20.1 %	14.1%	17.6%	
Lachnospiraceae_asv100	*p*	n.s.	0.000	0.001	0.000	0.002	0.000	0.000	**78**
	AIC	428	404	423	402	423	399	397	
	Dev (%)	15.4%	24.9%	9.2%	29.8%	10.9 %	32.1%	37.8%	
Lachnospiraceae_asv101	*p*	0.018	0.004	0.000	0.000	0.000	0.000	0.000	**91**
	AIC	392	384	373	355	367	357	353	
	Dev (%)	4.9%	15.7%	21.2 %	37.4%	32.4 %	37.6%	42.2%	
Rikenellaceae_asv102	*p*	n.s.	0.001	0.002	0.000	0.010	0.000	0.001	**75**
	AIC	437	422	428	414	430	416	420	
	Dev (%)	0.4%	12.9%	7.9%	22.2%	8.0%	22.7%	25.7%	
Lachnospiraceae_asv103	*p*	0.030	n.s.	0.000	0.000	0.000	0.000	0.000	**87**
	AIC	452	450	431	434	430	432	435	
	Dev (%)	4.1%	11.0%	20.3 %	19.9%	22.7 %	20.8%	28.3%	
Lachnospiraceae_asv104	*p*	0.000	0.031	n.s.	0.000	0.000	0.001	0.000	**92**
	AIC	384	404	409	383	385	391	387	
	Dev (%)	21.5%	9.5%	8.2%	26.0%	22.3 %	23.3%	31.1%	
Lachnospiraceae_asv107	*p*	n.s.	n.s.	n.s.	n.s.	n.s.	n.s.	n.s.	**56**
	AIC	439	434	438	436	440	439	445	
	Dev (%)	0.1%	9.1%	0.3%	8.9%	0.3%	1.5%	9.5%	
Lachnospiraceae_asv108	*p*	n.s.	0.000	0.000	0.000	0.000	0.000	0.000	**95**
	AIC	392	365	374	359	368	360	357	
	Dev (%)	0.4%	22.3%	16.7 %	30.0%	27.4 %	31.0%	36.1%	
Lachnospiraceae_asv109	*p*	n.s.	n.s.	0.007	0.010	0.045	0.037	n.s.	**102**
	AIC	400	395	394	394	395	394	401	
	Dev (%)	0.5%	9.3%	6.3%	7.9%	7.1%	9.1%	13.5%	
Muribaculaceae_asv111	*p*	0.015	n.s.	n.s.	0.030	n.s.	n.s.	0.013	**101**
	AIC	297	307	305	296	301	305	301	
	Dev (%)	10.8%	0.0%	7.0%	19.9%	13.2 %	3.3%	17.8%	
Muribaculaceae_asv112	*p*	0.000	0.000	n.s.	0.000	0.013	0.000	0.000	**94**
	AIC	391	384	401	384	392	377	384	
	Dev (%)	11.1%	18.9%	4.6%	18.1%	15.9 %	22.4%	28.2%	
Oscillospiraceae_asv113	*p*	0.002	n.s.	n.s.	0.005	0.006	n.s.	n.s.	**114**
	AIC	194	203	203	195	195	204	207	

Tod6	GAM	Prot	Carb	Fat	P x C	P x F	C x F	P x C X F	N data points
	Dev (%)	8.6%	0.8%	0.6%	9.2%	8.8%	1.9%	10.3%	
Lachnospiraceae_asv114	*p*	n.s.	0.001	0.001	0.003	0.000	0.001	0.001	**82**
	AIC	361	347	349	347	348	343	348	
	Dev (%)	2.2%	14.8%	12.5 %	19.9%	14.4 %	21.8%	24.5%	
Ruminococcaceae_asv115	*p*	0.024	n.s.	n.s.	n.s.	0.030	n.s.	0.026	**42**
	AIC	469	474	468	470	465	466	470	
	Dev (%)	4.5%	0.2%	6.1%	4.9%	11.6 %	13.0%	16.1%	
Lachnospiraceae_asv116	*p*	0.000	0.000	0.035	0.000	0.000	0.000	0.000	**75**
	AIC	272	346	386	275	273	342	302	
	Dev (%)	68.1%	40.2%	16.7 %	69.5%	70.1 %	43.2%	61.6%	
Muribaculaceae_asv117	*p*	n.s.	n.s.	n.s.	n.s.	n.s.	n.s.	n.s.	**113**
	AIC	177	180	180	181	180	181	187	
	Dev (%)	6.1%	0.1%	1.4%	1.1%	9.3%	1.1%	7.8%	
Lachnospiraceae_asv118	*p*	0.003	n.s.	0.013	0.008	0.000	0.002	0.016	**97**
	AIC	347	358	354	347	344	350	355	
	Dev (%)	14.6%	7.3%	5.4%	16.7%	15.2 %	10.8%	17.2%	
Lachnospiraceae_asv119	*p*	n.s.	0.016	n.s.	0.017	n.s.	0.040	0.023	**46**
	AIC	453	445	451	445	453	444	449	
	Dev (%)	0.0%	7.8%	2.4%	10.0%	2.2%	13.1%	16.4%	
Lachnospiraceae_asv120	*p*	0.008	n.s.	0.000	0.000	0.000	0.000	0.000	**69**
	AIC	417	420	409	401	405	396	392	
	Dev (%)	6.2%	4.9%	12.8 %	21.3%	17.2 %	29.8%	35.2%	
Lachnospiraceae_asv121	*p*	0.018	n.s.	0.031	n.s.	n.s.	n.s.	0.036	**52**
	AIC	394	402	394	402	398	402	400	
	Dev (%)	14.5%	3.0%	13.9 %	7.1%	11.9 %	4.4%	16.6%	
Lachnospiraceae_asv122	*p*	n.s.	0.007	0.002	0.017	0.022	0.014	0.004	**95**
	AIC	353	346	342	348	343	344	346	
	Dev (%)	2.8%	9.2%	13.9 %	8.9%	18.3 %	15.7%	20.3%	
Lachnospiraceae_asv124	*p*	n.s.	n.s.	0.014	0.010	n.s.	0.014	0.002	**62**
	AIC	452	450	444	445	445	440	442	
	Dev (%)	1.3%	8.4%	11.9 %	9.0%	13.4 %	19.4%	21.8%	
Muribaculaceae_asv129	*p*	0.049	n.s.	n.s.	n.s.	0.012	0.015	n.s.	**45**
	AIC	326	331	325	329	325	325	332	
	Dev (%)	5.9%	3.5%	10.8 %	4.9%	7.6%	7.3%	12.9%	
Lachnospiraceae_asv130	*p*	0.005	n.s.	0.025	0.003	0.003	0.024	0.002	**77**

Tod6	GAM	Prot	Carb	Fat	P x C	P x F	C x F	P x C X F	N data points
	AIC	429	431	427	420	422	426	425	
	Dev (%)	7.0%	13.4%	16.4 %	19.0%	16.8 %	16.0%	21.8%	
Lachnospiraceae_asv131	*p*	0.004	0.000	0.000	0.000	0.000	0.000	0.000	**62**
	AIC	384	359	372	360	366	356	355	
	Dev (%)	12.1%	29.0%	21.8 %	31.9%	28.2 %	34.4%	39.4%	
Oscillospiraceae_asv132	*p*	n.s.	n.s.	n.s.	n.s.	n.s.	n.s.	n.s.	**71**
	AIC	425	423	425	425	425	425	433	
	Dev (%)	1.2%	3.2%	1.7%	3.3%	3.3%	3.7%	8.3%	
Lachnospiraceae_asv133	*p*	0.018	n.s.	0.016	0.010	0.004	0.044	0.007	**80**
	AIC	417	421	412	409	409	414	415	
	Dev (%)	4.9%	1.8%	15.4 %	17.5%	15.3 %	13.3%	18.9%	
Muribaculaceae_asv134	*p*	n.s.	0.002	0.000	0.001	0.000	0.000	0.000	**114**
	AIC	220	207	200	200	202	196	203	
	Dev (%)	0.4%	13.5%	16.7 %	22.1%	16.7 %	23.8%	25.7%	
Lachnospiraceae_asv135	*p*	n.s.	0.000	0.013	0.000	0.002	0.000	0.001	**81**
	AIC	400	377	391	378	385	379	387	
	Dev (%)	3.8%	20.5%	17.5 %	21.3%	26.0 %	22.3%	25.6%	
Muribaculaceae_asv136	*p*	0.005	n.s.	0.004	0.000	0.000	0.041	0.000	**38**
	AIC	348	358	343	329	333	349	330	
	Dev (%)	9.9%	0.8%	21.6 %	31.3%	29.5 %	14.2%	33.2%	
Lachnospiraceae_ Eubacterium_asv137	*p*	0.001	n.s.	0.003	0.000	0.000	0.001	0.000	**59**
	AIC	404	413	402	392	393	393	394	
	Dev (%)	10.4%	4.3%	14.6 %	23.2%	24.9 %	26.1%	28.4%	
Lachnospiraceae_asv138	*p*	0.001	n.s.	n.s.	0.035	0.008	n.s.	0.001	**71**
	AIC	400	416	412	407	403	409	405	
	Dev (%)	19.1%	1.8%	14.6 %	15.7%	19.3 %	14.4%	22.4%	
Oscillospiraceae_asv140	*p*	0.000	0.000	n.s.	0.000	0.000	0.002	0.003	**100**
	AIC	316	320	330	315	315	322	322	
	Dev (%)	15.0%	11.1%	3.8%	16.3%	15.7 %	11.1%	20.8%	
Eubacterium_asv141	*p*	n.s.	n.s.	n.s.	n.s.	n.s.	n.s.	n.s.	**69**
	AIC	389	389	389	391	390	389	399	
	Dev (%)	1.3%	0.5%	1.1%	0.5%	1.1%	2.6%	5.5%	
Lachnospiraceae_asv142	*p*	n.s.	n.s.	n.s.	n.s.	0.027	n.s.	n.s.	**96**
	AIC	334	336	334	336	332	336	336	
	Dev (%)	3.1%	1.4%	3.8%	3.2%	6.3%	2.9%	14.3%	

Tod6	GAM	Prot	Carb	Fat	P x C	P x F	C x F	P x C X F	N data points
Sutterellaceae_asv143	*p*	0.000	0.000	0.016	0.000	0.000	0.000	0.000	**42**
	AIC	328	351	365	336	349	345	330	
	Dev (%)	41.1%	20.9%	20.4 %	36.5%	28.2 %	30.1%	42.0%	
Muribaculaceae_asv144	*p*	n.s.	0.014	0.006	0.001	0.009	0.007	0.017	**112**
	AIC	243	237	233	223	232	231	239	
	Dev (%)	5.8%	7.7%	13.6 %	28.0%	21.5 %	18.3%	18.2%	
Lachnospiraceae_asv145	*p*	0.000	0.000	n.s.	0.000	0.000	0.000	0.000	**65**
	AIC	420	415	438	404	418	413	407	
	Dev (%)	18.4%	23.3%	10.6 %	33.8%	22.1 %	29.4%	36.3%	
Peptococcaceae_asv146	*p*	0.023	0.000	0.001	0.002	0.000	0.000	0.001	**103**
	AIC	304	296	300	297	298	295	301	
	Dev (%)	17.8%	16.1%	13.6 %	21.9%	16.5 %	18.7%	22.8%	
Oscillospiraceae_asv147	*p*	0.000	0.001	0.003	0.000	0.000	0.001	0.000	**89**
	AIC	370	379	380	367	367	376	372	
	Dev (%)	22.8%	17.9%	22.6 %	25.5%	31.4 %	20.7%	29.4%	
Staphylococcaceae_asv149	*p*	n.s.	n.s.	n.s.	n.s.	n.s.	n.s.	n.s.	**55**
	AIC	391	396	396	395	396	398	399	
	Dev (%)	8.4%	0.5%	0.3%	3.6%	3.8%	0.9%	10.9%	
Lachnospiraceae_asv152	*p*	n.s.	0.000	0.001	0.000	0.001	0.000	0.000	**103**
	AIC	312	294	303	289	299	294	287	
	Dev (%)	2.9%	18.3%	10.1 %	28.2%	17.9 %	20.3%	32.5%	
Lachnospiraceae_asv154	*p*	0.009	0.009	0.003	0.000	0.002	0.009	0.000	**70**
	AIC	378	377	380	365	370	381	366	
	Dev (%)	10.5%	21.8%	7.5%	25.0%	21.3 %	8.2%	29.7%	
Ruminococcaceae_asv155	*p*	n.s.	n.s.	n.s.	n.s.	n.s.	n.s.	n.s.	**69**
	AIC	411	410	412	413	413	411	418	
	Dev (%)	1.5%	3.1%	0.0%	2.6%	0.3%	4.8%	7.9%	
Lachnospiraceae_asv157	*p*	n.s.	0.000	0.033	0.001	0.009	0.006	0.008	**80**
	AIC	381	369	374	370	374	368	374	
	Dev (%)	0.4%	10.5%	11.2 %	11.7%	8.1%	17.1%	18.7%	
Lachnospiraceae_asv158	*p*	n.s.	n.s.	n.s.	n.s.	n.s.	n.s.	n.s.	**110**
	AIC	243	243	243	245	245	245	251	
	Dev (%)	0.0%	0.0%	0.4%	0.0%	0.8%	0.1%	6.9%	
Lachnospiraceae_asv159	*p*	0.012	n.s.	n.s.	n.s.	n.s.	n.s.	0.010	**67**
	AIC	411	416	411	413	408	415	410	

Tod6	GAM	Prot	Carb	Fat	P x C	P x F	C x F	P x C X F	N data points
	Dev (%)	5.5%	1.3%	10.5 %	6.4%	18.7 %	8.0%	19.0%	
Tannerellaceae_asv160	*p*	n.s.	0.025	n.s.	n.s.	n.s.	n.s.	n.s.	**52**
	AIC	429	424	428	426	428	426	432	
	Dev (%)	0.3%	4.4%	1.6%	4.7%	9.7%	4.6%	11.2%	
Oscillospiraceae_asv161	*p*	0.000	n.s.	n.s.	0.000	0.000	n.s.	0.000	**86**
	AIC	368	386	385	360	363	380	361	
	Dev (%)	15.6%	3.0%	2.3%	25.7%	25.8 %	14.6%	31.7%	
Lachnospiraceae_asv162	*p*	n.s.	n.s.	n.s.	n.s.	0.041	n.s.	n.s.	**56**
	AIC	427	428	426	424	425	426	429	
	Dev (%)	2.8%	3.7%	8.5%	10.5%	6.6%	7.7%	14.1%	
Oscillospiraceae_asv163	*p*	0.048	0.000	0.018	0.000	0.003	0.000	0.000	**78**
	AIC	394	375	391	378	386	377	382	
	Dev (%)	5.7%	20.4%	8.3%	21.4%	13.7 %	20.6%	25.6%	
Lachnospiraceae_asv165	*p*	0.000	0.000	n.s.	0.000	0.002	0.000	0.000	**88**
	AIC	242	226	250	226	238	222	229	
	Dev (%)	13.3%	26.1%	12.9 %	27.7%	25.8 %	34.0%	33.3%	
Muribaculaceae_asv168	*p*	n.s.	n.s.	n.s.	n.s.	n.s.	n.s.	n.s.	**83**
	AIC	389	390	389	390	391	391	392	
	Dev (%)	3.3%	1.8%	8.7%	8.1%	3.4%	2.8%	12.6%	
Lachnospiraceae_asv169	*p*	0.000	0.000	0.006	0.000	0.000	0.000	0.000	**105**
	AIC	260	261	271	255	259	262	261	
	Dev (%)	27.0%	18.9%	21.5 %	24.4%	21.9 %	23.7%	29.8%	
Lachnospiraceae_asv172	*p*	n.s.	n.s.	n.s.	n.s.	n.s.	n.s.	n.s.	**40**
	AIC	405	408	406	407	404	408	413	
	Dev (%)	2.5%	0.0%	3.9%	3.0%	10.3 %	4.5%	9.3%	
Ruminococcaceae_asv174	*p*	n.s.	n.s.	n.s.	n.s.	n.s.	n.s.	n.s.	**91**
	AIC	368	367	368	369	369	368	375	
	Dev (%)	1.1%	3.6%	1.1%	3.5%	1.5%	5.4%	8.1%	
Lachnospiraceae_asv176	*p*	n.s.	n.s.	n.s.	0.033	n.s.	n.s.	n.s.	**80**
	AIC	370	376	373	370	371	376	379	
	Dev (%)	9.7%	4.2%	9.1%	5.9%	13.0 %	7.7%	10.0%	
Lachnospiraceae_asv177	*p*	n.s.	n.s.	n.s.	n.s.	n.s.	n.s.	n.s.	**52**
	AIC	416	416	419	416	417	415	420	
	Dev (%)	3.0%	4.6%	1.6%	9.0%	6.6%	11.4%	13.6%	
Lachnospiraceae_asv179	*p*	n.s.	0.006	0.000	0.000	0.000	0.001	0.001	**56**
	AIC	396	386	384	377	383	378	386	

Tod6	GAM	Prot	Carb	Fat	P x C	P x F	C x F	P x C X F	N data points
	Dev (%)	3.5%	17.1%	13.2 %	25.4%	15.1 %	26.4%	23.2%	
Desulfovibrionaceae_ asv180	*p*	0.000	0.010	n.s.	0.000	0.002	0.035	0.010	**111**
	AIC	253	263	266	254	254	260	262	
	Dev (%)	13.5%	5.8%	12.9 %	14.0%	15.4 %	13.6%	18.3%	
Lachnospiraceae_asv184	*p*	n.s.	0.032	n.s.	n.s.	n.s.	n.s.	n.s.	**39**
	AIC	307	304	306	306	307	306	316	
	Dev (%)	2.0%	4.1%	10.4 %	4.2%	3.1%	4.1%	7.9%	
Lachnospiraceae_asv185	*p*	n.s.	0.044	n.s.	0.018	n.s.	n.s.	0.004	**59**
	AIC	410	407	416	403	414	412	405	
	Dev (%)	7.5%	12.4%	0.0%	19.0%	10.7 %	11.6%	22.0%	
Oscillospiraceae_asv186	*p*	n.s.	0.004	n.s.	0.017	0.038	0.013	n.s.	**79**
	AIC	376	371	376	373	374	372	385	
	Dev (%)	2.2%	7.1%	2.8%	7.1%	5.7%	7.5%	8.6%	
Bacteroidaceae_asv187	*p*	n.s.	n.s.	0.045	n.s.	n.s.	n.s.	0.011	**93**
	AIC	344	346	339	346	340	343	340	
	Dev (%)	3.0%	0.4%	10.0 %	6.3%	12.1 %	10.1%	18.0%	
Rikenellaceae_asv188	*p*	0.001	n.s.	0.015	0.004	0.001	0.037	0.002	**109**
	AIC	199	215	207	200	198	206	203	
	Dev (%)	14.8%	0.0%	8.0%	18.0%	17.7 %	11.3%	22.3%	
Lachnospiraceae_asv190	*p*	n.s.	n.s.	n.s.	n.s.	n.s.	n.s.	n.s.	**46**
	AIC	411	412	412	413	413	413	414	
	Dev (%)	0.3%	0.3%	0.1%	3.6%	0.4%	0.2%	10.9%	
Lachnospiraceae_asv191	*p*	0.046	0.000	0.019	0.003	0.003	0.002	0.001	**92**
	AIC	348	332	346	334	335	333	335	
	Dev (%)	3.5%	20.9%	4.8%	24.2%	20.5 %	24.4%	26.1%	
Lachnospiraceae_asv193	*p*	n.s.	n.s.	n.s.	n.s.	n.s.	n.s.	n.s.	**62**
	AIC	401	404	404	401	403	404	407	
	Dev (%)	7.5%	1.1%	4.0%	6.4%	5.4%	6.1%	11.0%	
Rikenellaceae_asv194	*p*	n.s.	n.s.	0.025	n.s.	n.s.	n.s.	0.021	**100**
	AIC	296	293	290	294	292	289	291	
	Dev (%)	4.8%	4.2%	5.9%	5.1%	6.7%	11.0%	18.4%	
Bacteroidaceae_asv198	*p*	0.003	n.s.	0.003	0.000	0.001	0.026	0.001	**52**
	AIC	354	361	348	340	343	352	348	
	Dev (%)	7.5%	7.7%	23.1 %	25.3%	26.8 %	16.0%	24.5%	
Oscillospiraceae_asv201	*p*	0.004	0.004	n.s.	0.002	0.003	0.012	0.001	**67**
	AIC	393	392	400	391	390	395	390	

Tod6	GAM	Prot	Carb	Fat	P x C	P x F	C x F	P x C X F	N data points
	Dev (%)	9.8%	12.8%	5.5%	12.8%	14.9 %	10.6%	23.2%	
Lachnospiraceae_asv202	*p*	n.s.	0.023	0.001	0.032	0.008	0.002	0.046	**73**
	AIC	344	338	329	339	333	333	341	
	Dev (%)	0.0%	4.5%	14.0 %	6.0%	11.8 %	10.8%	14.8%	
Eggerthellaceae_asv203	*p*	n.s.	0.005	0.000	0.007	0.000	0.000	0.001	**68**
	AIC	300	292	274	290	273	274	286	
	Dev (%)	0.0%	7.2%	21.1 %	11.0%	29.1 %	21.9%	23.4%	
Lachnospiraceae_asv204	*p*	0.000	0.032	0.028	0.000	0.000	0.000	0.000	**81**
	AIC	366	382	380	352	363	366	359	
	Dev (%)	22.0%	8.8%	14.9 %	34.7%	22.2 %	24.7%	34.0%	
Lachnospiraceae_asv205	*p*	n.s.	0.001	n.s.	0.003	0.014	0.006	0.030	**72**
	AIC	371	363	371	365	368	365	371	
	Dev (%)	3.3%	9.9%	4.5%	10.0%	7.4%	11.1%	15.8%	
Oscillospiraceae_asv206	*p*	0.000	0.001	0.015	0.000	0.000	0.004	0.002	**99**
	AIC	279	293	297	289	280	291	294	
	Dev (%)	31.8%	12.0%	11.5 %	16.2%	31.3 %	23.3%	23.6%	
Lachnospiraceae_asv208	*p*	n.s.	0.050	n.s.	n.s.	n.s.	n.s.	0.003	**71**
	AIC	363	361	364	360	360	362	357	
	Dev (%)	5.7%	9.9%	3.1%	16.3%	11.7 %	9.9%	21.1%	
Lachnospiraceae_asv211	*p*	0.024	0.008	0.000	0.000	0.000	0.000	0.000	**109**
	AIC	266	258	244	238	241	242	240	
	Dev (%)	4.5%	18.0%	21.0 %	31.5%	25.7 %	29.4%	34.5%	
Oscillospiraceae_asv212	*p*	0.000	n.s.	n.s.	0.000	0.000	0.010	0.000	**83**
	AIC	329	345	348	325	329	341	330	
	Dev (%)	17.5%	6.9%	2.4%	24.7%	18.7 %	11.5%	27.6%	
Lachnospiraceae_asv214	*p*	0.001	n.s.	n.s.	0.001	0.002	0.022	0.002	**63**
	AIC	352	366	362	351	350	355	354	
	Dev (%)	13.4%	6.0%	6.3%	16.8%	18.7 %	17.3%	23.4%	
Lachnospiraceae_asv215	*p*	n.s.	0.000	0.000	0.000	0.000	0.000	0.000	**54**
	AIC	387	372	367	353	366	364	355	
	Dev (%)	5.1%	15.6%	23.2 %	35.6%	25.5 %	26.2%	37.0%	
Rikenellaceae_asv216	*p*	n.s.	0.002	0.004	0.001	0.008	0.002	0.026	**57**
	AIC	434	430	424	428	425	427	436	
	Dev (%)	10.4%	8.5%	19.4 %	11.4%	22.4 %	12.2%	16.1%	
Peptococcaceae_asv218	*p*	n.s.	0.005	0.000	0.018	0.000	0.000	0.000	**112**

Tod6	GAM	Prot	Carb	Fat	P x C	P x F	C x F	P x C X F	N data points
	AIC	279	271	255	270	250	254	251	
	Dev (%)	4.9%	12.3%	21.7 %	17.3%	28.4 %	23.5%	35.1%	
Peptostreptococcaceae_ asv219	*p*	n.s.	n.s.	n.s.	n.s.	n.s.	n.s.	n.s.	**44**
	AIC	401	403.2 61925 27154 2+O5 02:O5 22	404	403	402	403	412	
	Dev (%)	2.7%	0.7%	5.7%	2.7%	3.2%	2.5%	6.5%	
Lachnospiraceae_asv223	*p*	0.000	n.s.	0.001	0.000	0.000	0.003	0.001	**66**
	AIC	364	376	361	356	355	360	365	
	Dev (%)	12.0%	13.4%	22.6 %	26.6%	20.5 %	23.8%	23.1%	
Ruminococcaceae_asv22 4	*p*	n.s.	n.s.	n.s.	n.s.	n.s.	n.s.	n.s.	**43**
	AIC	387	390	387	389	388	387	396	
	Dev (%)	8.1%	3.9%	1.9%	1.4%	3.0%	3.2%	7.9%	
Sutterellaceae_asv225	*p*	n.s.	0.000	0.005	0.000	0.023	0.001	0.000	**47**
	AIC	342	324	329	314	330	322	319	
	Dev (%)	1.6%	16.6%	17.1 %	29.1%	19.4 %	22.4%	29.8%	
Eggerthellaceae_asv230	*p*	n.s.	0.036	0.006	0.003	0.015	0.025	0.025	**53**
	AIC	296	294	293	289	294	292	296	
	Dev (%)	9.1%	6.7%	6.5%	11.6%	7.3%	10.2%	16.3%	
Oscillospiraceae_asv231	*p*	0.000	0.001	0.021	0.000	0.000	0.002	0.000	**93**
	AIC	266	302	310	264	265	300	270	
	Dev (%)	38.8%	19.9%	10.6 %	44.9%	42.1 %	25.2%	44.5%	
Muribaculaceae_asv232	*p*	n.s.	0.002	0.000	0.007	0.000	0.000	0.001	**92**
	AIC	329	317	311	317	312	308	315	
	Dev (%)	1.5%	11.5%	15.8 %	15.3%	16.1 %	22.4%	24.0%	
Muribaculaceae_asv235	*p*	n.s.	n.s.	n.s.	n.s.	n.s.	n.s.	n.s.	**76**
	AIC	282	282	279	283	280	279	284	
	Dev (%)	5.1%	3.4%	8.0%	4.0%	11.0 %	11.4%	15.3%	
Gastranaerophilales_ asv236	*p*	0.047	0.035	0.000	0.000	0.002	0.000	0.000	**66**
	AIC	364	360	349	343	348	346	348	
	Dev (%)	3.5%	12.8%	18.6 %	25.2%	25.2 %	23.3%	28.5%	
Lachnospiraceae_asv237	*p*	n.s.	0.001	0.000	0.000	0.003	0.000	0.000	**49**
	AIC	388	377	372	369	373	369	370	

Tod6	GAM	Prot	Carb	Fat	P x C	P x F	C x F	P x C X F	N data points
	Dev (%)	0.8%	9.9%	15.5 %	18.6%	18.3 %	20.9%	26.8%	
Lachnospiraceae_asv238	*p*	0.002	n.s.	n.s.	0.011	0.007	n.s.	0.029	**71**
	AIC	331	344	340	335	335	341	342	
	Dev (%)	14.0%	1.7%	13.7 %	12.1%	11.0 %	11.1%	15.9%	
Bacilli_asv240	*p*	0.045	n.s.	0.007	0.019	0.006	n.s.	0.039	**47**
	AIC	334	336	331	329	330	330	335	
	Dev (%)	3.5%	2.7%	6.2%	11.4%	8.8%	11.7%	15.2%	
Lachnospiraceae_asv241	*p*	0.001	0.000	0.009	0.000	0.002	0.000	0.000	**62**
	AIC	358	349	359	346	353	348	344	
	Dev (%)	12.1%	17.9%	21.9 %	25.2%	24.8 %	20.3%	32.4%	
Lachnospiraceae_asv243	*p*	n.s.	n.s.	n.s.	n.s.	n.s.	n.s.	n.s.	**86**
	AIC	306	300	305	302	307	302	312	
	Dev (%)	1.1%	8.1%	10.2 %	8.8%	5.5%	8.9%	9.2%	
Oscillospiraceae_asv246	*p*	n.s.	0.002	n.s.	0.009	n.s.	0.003	0.002	**98**
	AIC	243	231	244	234	244	230	232	
	Dev (%)	1.9%	12.6%	1.2%	12.1%	6.4%	15.2%	21.9%	
Lachnospiraceae_asv248	*p*	n.s.	n.s.	0.003	0.027	0.000	0.000	0.001	**47**
	AIC	333	333	322	326	321	316	322	
	Dev (%)	3.4%	5.8%	18.4 %	15.8%	15.0 %	20.7%	24.2%	
Ruminococcaceae_asv249	*p*	n.s.	0.034	n.s.	n.s.	n.s.	n.s.	n.s.	**39**
	AIC	395	391	398	393	397	393	405	
	Dev (%)	5.0%	6.7%	0.2%	6.5%	2.5%	6.3%	7.3%	
Lachnospiraceae_asv250	*p*	0.011	n.s.	n.s.	0.048	0.038	n.s.	0.009	**68**
	AIC	309	318	319	310	309	319	310	
	Dev (%)	10.6%	1.9%	0.3%	12.9%	14.2 %	4.8%	20.4%	
Lachnospiraceae_asv252	*p*	0.000	0.047	n.s.	0.000	0.000	n.s.	0.000	**45**
	AIC	315	343	347	317	317	344	328	
	Dev (%)	25.4%	4.9%	2.2%	25.1%	25.3 %	6.8%	27.5%	
Lachnospiraceae_asv254	*p*	n.s.	0.001	0.000	0.000	0.000	0.000	0.000	**88**
	AIC	303	287	279	269	279	275	273	
	Dev (%)	2.5%	18.8%	23.6 %	28.8%	25.6 %	29.1%	34.7%	
Ruminococcaceae_asv257	*p*	n.s.	n.s.	0.047	n.s.	n.s.	n.s.	n.s.	**101**
	AIC	258	259	251	260	250	259	259	
	Dev (%)	1.1%	0.0%	14.7 %	1.4%	16.7 %	1.7%	13.2%	

Tod6	GAM	Prot	Carb	Fat	P x C	P x F	C x F	P x C X F	N data points
Muribaculaceae_asv258	*p*	0.001	0.000	n.s.	0.000	0.000	0.000	0.000	**47**
	AIC	226	210	236	206	215	212	205	
	Dev (%)	13.5%	25.9%	9.1%	31.9%	26.8 %	25.5%	37.0%	
Oscillospiraceae_asv261	*p*	n.s.	n.s.	0.033	n.s.	n.s.	0.044	n.s.	**50**
	AIC	352	353	348	354	349	348	354	
	Dev (%)	0.8%	0.1%	4.0%	0.8%	6.4%	5.5%	12.1%	
Lachnospiraceae_asv262	*p*	n.s.	n.s.	0.013	n.s.	n.s.	n.s.	n.s.	**41**
	AIC	256	258	247	257	253	252	260	
	Dev (%)	3.3%	1.6%	17.1 %	4.7%	10.0 %	12.1%	12.0%	
Ruminococcaceae_asv263	*p*	n.s.	n.s.	n.s.	n.s.	n.s.	n.s.	n.s.	**40**
	AIC	370	366	370	368	370	367	376	
	Dev (%)	0.3%	6.9%	5.9%	6.3%	7.0%	7.5%	10.1%	
Oscillospiraceae_asv267	*p*	n.s.	n.s.	0.005	n.s.	0.015	0.018	0.017	**56**
	AIC	208	207	201	204	203	203	203	
	Dev (%)	0.9%	3.6%	6.8%	8.1%	7.3%	7.0%	18.3%	
Gastranaerophilales_asv268	*p*	n.s.	0.000	0.000	0.000	0.000	0.000	0.000	**54**
	AIC	370	348	343	325	330	338	325	
	Dev (%)	1.5%	23.2%	29.5 %	39.2%	39.6 %	28.1%	42.2%	
Oscillospirales_asv269	*p*	n.s.	n.s.	0.005	n.s.	0.009	0.017	n.s.	**67**
	AIC	258	261	252	257	253	254	264	
	Dev (%)	2.1%	4.3%	6.9%	4.3%	8.2%	7.1%	10.1%	
Rhodospirillales_asv270	*p*	n.s.	0.000	0.001	0.000	0.007	0.000	0.001	**59**
	AIC	338	326	319	317	323	321	324	
	Dev (%)	0.7%	10.5%	26.4 %	19.5%	22.9 %	15.4%	23.6%	
Lachnospiraceae_asv272	*p*	n.s.	0.000	0.000	0.000	0.000	0.000	0.000	**63**
	AIC	273	249	251	243	254	240	245	
	Dev (%)	8.1%	24.3%	21.4 %	33.4%	22.4 %	34.4%	34.7%	
Oscillospiraceae_asv274	*p*	0.009	0.004	0.015	0.005	0.001	0.006	0.015	**61**
	AIC	359	355	357	355	353	355	360	
	Dev (%)	5.9%	10.4%	9.2%	10.8%	12.7 %	11.5%	17.4%	
Ruminococcaceae_asv276	*p*	0.000	0.000	n.s.	0.000	0.001	0.000	0.000	**81**
	AIC	306	302	323	300	312	303	303	
	Dev (%)	24.3%	24.0%	7.5%	27.8%	18.2 %	24.9%	32.4%	
Gastranaerophilales_asv279	*p*	n.s.	n.s.	n.s.	n.s.	n.s.	n.s.	n.s.	**66**

Tod6	GAM	Prot	Carb	Fat	P x C	P x F	C x F	P x C X F	N data points
	AIC	263	260	258	262	260	260	262	
	Dev (%)	0.0%	2.6%	5.9%	3.1%	5.3%	5.8%	13.9%	
Oscillospiraceae_asv283	*p*	0.024	0.008	n.s.	0.015	n.s.	0.024	0.005	**70**
	AIC	275	273	278	272	278	273	275	
	Dev (%)	11.4%	11.9%	8.4%	19.2%	11.9 %	15.0%	19.9%	
Muribaculaceae_asv286	*p*	n.s.	0.001	0.000	0.000	0.010	0.002	0.000	**48**
	AIC	173	163	162	152	162	158	143	
	Dev (%)	5.9%	10.1%	10.9 %	29.1%	16.3 %	20.1%	35.3%	
Anaerovoracaceae_ Eubacterium_asv289	*p*	n.s.	n.s.	n.s.	n.s.	n.s.	n.s.	n.s.	**54**
	AIC	198	200	197	199	197	198	208	
	Dev (%)	1.9%	0.0%	2.9%	2.4%	4.2%	3.4%	6.6%	
Ruminococcaceae_asv290	*p*	n.s.	0.037	n.s.	n.s.	n.s.	n.s.	n.s.	**42**
	AIC	207	199	207	207	209	208	207	
	Dev (%)	0.0%	18.7%	0.7%	7.5%	0.7%	2.2%	14.0%	
Lachnospiraceae_asv292	*p*	0.009	n.s.	n.s.	0.001	0.022	n.s.	0.013	**49**
	AIC	283	288	288	274	284	285	283	
	Dev (%)	6.0%	1.8%	1.3%	15.9%	6.7%	10.2%	18.1%	
Lachnospiraceae_asv296	*p*	n.s.	0.001	0.000	0.000	0.002	0.001	0.000	**40**
	AIC	223	212	208	204	209	209	208	
	Dev (%)	7.2%	15.6%	21.2 %	28.2%	25.0 %	22.4%	27.3%	
Lachnospiraceae_asv299	*p*	n.s.	n.s.	n.s.	n.s.	n.s.	n.s.	n.s.	**56**
	AIC	195	194	195	196	192	195	201	
	Dev (%)	4.3%	3.2%	7.5%	3.4%	11.3 %	3.7%	10.7%	
Ruminococcaceae_asv300	*p*	0.021	n.s.	n.s.	0.019	0.038	n.s.	n.s.	**51**
	AIC	298	303	302	297	299	303	302	
	Dev (%)	4.7%	0.1%	1.6%	6.9%	5.7%	1.7%	15.0%	
Ruminococcaceae_asv301	*p*	0.000	0.003	n.s.	0.000	0.000	0.009	0.003	**66**
	AIC	275	286	289	275	275	288	284	
	Dev (%)	16.6%	7.8%	11.4 %	17.4%	17.6 %	8.2%	21.0%	
Clostridia_asv303	*p*	n.s.	n.s.	0.045	n.s.	n.s.	n.s.	n.s.	**62**
	AIC	269	265	265	264	266	266	274	
	Dev (%)	0.7%	4.0%	3.6%	12.6%	4.7%	5.2%	9.7%	
Oscillospiraceae_asv305	*p*	n.s.	n.s.	n.s.	n.s.	n.s.	n.s.	n.s.	**71**
	AIC	219	222	222	221	220	224	226	
	Dev (%)	2.8%	0.2%	0.4%	3.0%	3.5%	0.4%	10.5%	

Tod6	GAM	Prot	Carb	Fat	P x C	P x F	C x F	P x C X F	N data points
Clostridia.vadinBB60. group_asv311	*p*	n.s.	0.002	0.000	0.003	0.000	0.000	0.000	**57**
	AIC	345	335	317	330	319	317	325	
	Dev (%)	0.3%	8.5%	21.9 %	17.9%	21.9 %	23.1%	27.3%	
Lachnospiraceae_asv312	*p*	n.s.	n.s.	0.009	n.s.	0.033	0.039	n.s.	**79**
	AIC	255	250	248	248	250	249	258	
	Dev (%)	0.1%	6.2%	5.9%	10.5%	5.9%	8.6%	11.5%	
Rhodospirillales_asv315	*p*	n.s.	0.000	0.000	0.000	0.000	0.000	0.000	**52**
	AIC	332	308	312	287	300	303	290	
	Dev (%)	2.2%	20.5%	20.9 %	39.4%	34.8 %	26.3%	40.4%	
Butyricicoccaceae_asv31 8	*p*	0.000	0.000	0.000	0.000	0.000	0.000	0.000	**72**
	AIC	272	229	245	232	231	220	220	
	Dev (%)	11.1%	40.1%	36.8 %	40.2%	39.1 %	46.4%	51.0%	
Rikenellaceae_asv319	*p*	0.000	n.s.	0.000	0.000	0.000	0.002	0.000	**61**
	AIC	264	283	262	251	251	267	255	
	Dev (%)	20.7%	7.2%	21.5 %	37.2%	34.0 %	22.5%	34.4%	
Anaerovoracaceae_asv32 0	*p*	n.s.	0.000	0.000	0.000	0.000	0.000	0.000	**81**
	AIC	271	224	226	220	228	205	216	
	Dev (%)	8.2%	35.8%	39.5 %	40.0%	40.3 %	46.2%	47.8%	
Lachnospiraceae_asv323	*p*	0.025	n.s.	0.008	0.020	0.005	0.023	0.024	**38**
	AIC	277	282	276	275	273	278	278	
	Dev (%)	6.1%	10.3%	6.1%	10.8%	11.8 %	6.6%	17.9%	
Ruminococcaceae_asv32 4	*p*	0.000	0.049	0.049	0.000	0.002	0.010	0.006	**49**
	AIC	276	286	286	277	277	279	284	
	Dev (%)	14.5%	12.5%	9.3%	14.9%	17.7 %	20.1%	21.1%	
Lachnospiraceae_asv325	*p*	0.000	n.s.	0.026	0.002	0.001	n.s.	0.000	**49**
	AIC	263	274	269	257	255	268	255	
	Dev (%)	10.9%	6.0%	7.5%	24.9%	22.7 %	10.8%	27.9%	
Anaerovoracaceae_ Eubacterium_asv332	*p*	n.s.	0.001	0.000	0.000	0.000	0.000	0.000	**43**
	AIC	271	257	251	247	253	247	249	
	Dev (%)	0.4%	12.8%	16.8 %	23.7%	16.9 %	23.0%	28.5%	
Bacilli_asv336	*p*	n.s.	0.005	n.s.	n.s.	n.s.	n.s.	n.s.	**43**
	AIC	233	221	235	232	235	235	239	
	Dev (%)	4.1%	22.3%	5.9%	10.3%	5.8%	6.0%	12.2%	

Tod6	GAM	Prot	Carb	Fat	P x C	P x F	C x F	P x C X F	N data points
Ruminococcaceae_asv339	*p*	n.s.	n.s.	0.001	0.036	0.004	0.000	0.012	**38**
	AIC	355	357	340	350	343	345	353	
	Dev (%)	7.9%	2.4%	21.7%	19.7%	18.6%	13.5%	17.9%	
Lachnospiraceae_asv347	*p*	0.012	n.s.	n.s.	0.037	0.023	n.s.	n.s.	**38**
	AIC	262	266	268	264	263	268	273	
	Dev (%)	5.5%	2.5%	0.6%	5.8%	6.6%	2.5%	9.6%	
Lachnospiraceae_asv350	*p*	n.s.	n.s.	n.s.	n.s.	n.s.	n.s.	n.s.	**40**
	AIC	217	217	216	217	217	218	224	
	Dev (%)	3.3%	0.7%	1.6%	7.1%	6.4%	1.2%	8.6%	
Ruminococcaceae_asv362	*p*	0.018	0.001	n.s.	0.002	0.016	0.003	n.s.	**45**
	AIC	255	248	254	250	254	250	261	
	Dev (%)	4.9%	9.9%	14.2%	10.5%	7.1%	9.9%	12.6%	
Lachnospiraceae_asv372	*p*	n.s.	n.s.	0.029	n.s.	n.s.	n.s.	n.s.	**39**
	AIC	176	170	172	173	173	170	177	
	Dev (%)	0.3%	10.1%	4.2%	9.4%	4.8%	10.2%	13.0%	

Supplementary Table 7-8. GAM statistics for Figure 3-11 ToD12.
Dev = deviance explained, n.s. = p value >0.05

ToD12	GAM	Prot	Carb	Fat	P x C	P x F	C x F	P x C X F	N data points
InvSimpson	*p*	0.004	n.s.	n.s.	n.s.	0.009	n.s.	0.033	**114**
	AIC	832	845	842	837	838	847	841	
	Dev (%)	14.2%	0.5%	13.2%	11.1%	8.1%	0.6%	17.0%	
Observed	*p*	0.010	n.s.	0.009	0.024	0.010	n.s.	0.011	**114**
	AIC	956	961	949	951	955	955	956	
	Dev (%)	5.7%	2.8%	20.2%	16.6%	8.0%	11.7%	18.0%	
Shannon	*p*	0.004	n.s.	n.s.	0.013	0.004	n.s.	0.020	**114**
	AIC	75	86	80	77	78	87	82	
	Dev (%)	10.8%	0.7%	16.1%	12.0%	9.4%	4.8%	16.8%	
Verrucomicrobiota	*p*	n.s.	n.s.	n.s.	n.s.	n.s.	0.025	0.023	**114**
	AIC	523	524	523	522	524	520	522	
	Dev (%)	11.6%	2.2%	7.4%	10.3%	8.5%	6.4%	16.4%	
Actinobacteriota	*p*	n.s.	0.000	0.001	0.001	0.034	0.000	0.000	**114**
	AIC	643	625	628	623	636	618	619	

ToD12	GAM	Prot	Carb	Fat	P x C	P x F	C x F	P x C X F	N data points
	Dev (%)	3.2%	20.3%	21.8 %	27.2%	12.4 %	29.1%	31.1%	
Bacteroidota	*p*	n.s.	n.s.	0.022	0.000	n.s.	n.s.	0.002	**114**
	AIC	986	987	981	973	988	983	979	
	Dev (%)	5.1%	9.9%	20.0 %	16.1%	4.2%	14.7%	21.6%	
Firmicutes	*p*	0.001	n.s.	0.002	0.001	0.005	0.033	0.000	**114**
	AIC	1,172	1,183	1,165	1,164	1,173	1,172	1,164	
	Dev (%)	10.0%	0.2%	23.7 %	24.3%	11.1 %	17.5%	27.1%	
Desulfobacterota	*p*	0.000	0.041	0.000	0.003	0.001	0.000	0.000	**114**
	AIC	515	525	508	514	512	494	508	
	Dev (%)	12.9%	5.6%	25.8 %	19.2%	20.8 %	36.9%	29.1%	
Deferribacterota	*p*	n.s.	n.s.	n.s.	n.s.	n.s.	n.s.	n.s.	**114**
	AIC	447	446	447	446	448	448	450	
	Dev (%)	0.4%	0.6%	0.5%	7.1%	0.8%	0.8%	10.6%	
Proteobacteria	*p*	0.007	0.011	0.000	0.000	0.000	0.001	0.000	**114**
	AIC	535	542	519	517	510	530	524	
	Dev (%)	20.4%	5.6%	32.4 %	30.0%	38.4 %	20.5%	30.4%	
Cyanobacteria	*p*	n.s.	0.000	0.000	0.000	0.003	0.000	0.000	**114**
	AIC	472	452	458	444	458	449	450	
	Dev (%)	2.8%	22.6%	12.8 %	28.1%	17.3 %	26.9%	29.2%	
Akkermansiaceae_asv1	*p*	n.s.	n.s.	n.s.	n.s.	n.s.	0.025	0.023	**108**
	AIC	523	524	523	522	524	520	522	
	Dev (%)	11.6%	2.2%	7.4%	10.3%	8.5%	6.4%	16.4%	
Erysipelotrichaceae_asv3	*p*	n.s.	0.000	0.001	0.000	0.006	0.000	0.000	**45**
	AIC	546	513	531	515	539	515	517	
	Dev (%)	12.8%	29.0%	25.9 %	29.4%	15.7 %	31.6%	36.3%	
Erysipelotrichaceae_asv4	*p*	0.005	0.000	0.000	0.000	0.012	0.000	0.000	**52**
	AIC	574	541	559	540	577	543	538	
	Dev (%)	23.1%	33.7%	30.4 %	35.6%	12.5 %	34.3%	44.2%	
Prevotellaceae_asv5	*p*	n.s.	n.s.	0.004	n.s.	0.021	0.021	0.006	**77**
	AIC	514	509	506	506	507	502	505	
	Dev (%)	0.2%	5.4%	7.0%	13.6%	7.3%	16.5%	19.3%	
Bacteroidaceae_asv7	*p*	0.000	0.000	n.s.	0.000	0.000	0.000	0.000	**111**
	AIC	401	395	417	389	401	397	394	
	Dev (%)	19.8%	22.5%	17.1 %	32.6%	23.9 %	22.7%	33.1%	
Lachnospiraceae_asv8	*p*	n.s.	0.000	0.000	0.000	0.000	0.000	0.000	**111**

ToD12	GAM	Prot	Carb	Fat	P x C	P x F	C x F	P x C X F	N data points
	AIC	393	378	377	370	379	372	376	
	Dev (%)	10.0%	14.5%	14.2 %	24.0%	14.2 %	19.6%	25.9%	
Lachnospiraceae_asv9	*p*	n.s.	0.018	n.s.	0.043	n.s.	n.s.	n.s.	**52**
	AIC	592	588	592	589	594	590	598	
	Dev (%)	2.5%	4.9%	1.7%	5.5%	1.9%	5.1%	9.6%	
Lachnospiraceae_asv10	*p*	n.s.	n.s.	0.015	n.s.	0.049	n.s.	n.s.	**90**
	AIC	533	532	528	534	530	530	535	
	Dev (%)	2.0%	1.3%	5.2%	1.5%	5.3%	5.2%	12.2%	
Lachnospiraceae_asv11	*p*	n.s.	0.033	n.s.	n.s.	n.s.	n.s.	n.s.	**97**
	AIC	495	494	497	493	495	496	501	
	Dev (%)	7.1%	4.0%	8.1%	13.7%	13.5 %	4.1%	11.5%	
Lactobacillaceae_asv12	*p*	0.003	n.s.	0.019	0.006	0.001	0.007	0.003	**109**
	AIC	394	399	396	396	391	392	395	
	Dev (%)	10.5%	15.1%	11.2 %	10.1%	13.9 %	16.0%	20.6%	
Lactobacillaceae_asv13	*p*	n.s.	n.s.	0.001	n.s.	n.s.	0.022	0.000	**57**
	AIC	514	517	498	514	511	505	502	
	Dev (%)	3.5%	3.4%	26.3 %	9.8%	12.3 %	19.3%	24.4%	
Rikenellaceae_asv15	*p*	0.000	n.s.	0.001	0.000	0.000	0.019	0.000	**113**
	AIC	360	370	361	341	351	361	348	
	Dev (%)	10.6%	8.4%	9.8%	25.6%	20.0 %	18.0%	30.3%	
Rikenellaceae_asv16	*p*	0.000	n.s.	0.012	0.000	0.000	0.009	0.006	**107**
	AIC	459	475	469	458	455	468	467	
	Dev (%)	13.5%	0.3%	5.5%	15.8%	18.0 %	8.2%	19.2%	
Lachnospiraceae_asv17	*p*	n.s.	n.s.	n.s.	n.s.	n.s.	n.s.	n.s.	**91**
	AIC	485	485	483	486	484	485	494	
	Dev (%)	0.5%	0.5%	2.1%	6.5%	2.8%	2.1%	6.5%	
Desulfovibrionaceae_asv 18	*p*	n.s.	n.s.	0.014	n.s.	n.s.	n.s.	0.048	**112**
	AIC	298	293	287	297	292	292	297	
	Dev (%)	0.9%	11.9%	16.0 %	7.4%	10.7 %	12.4%	14.7%	
Rikenellaceae_asv20	*p*	n.s.	0.000	n.s.	0.001	n.s.	0.002	0.004	**113**
	AIC	335	324	331	323	333	326	328	
	Dev (%)	3.6%	10.8%	7.4%	12.9%	9.1%	10.8%	20.0%	
Marinifilaceae_asv21	*p*	n.s.	n.s.	n.s.	n.s.	n.s.	n.s.	n.s.	**87**
	AIC	513	511	509	512	511	512	515	
	Dev (%)	0.0%	2.0%	5.2%	2.8%	6.6%	5.4%	11.3%	
Lachnospiraceae_asv22	*p*	n.s.	n.s.	n.s.	n.s.	n.s.	n.s.	n.s.	**94**

ToD12	GAM	Prot	Carb	Fat	P x C	P x F	C x F	P x C X F	N data points
	AIC	502	500	502	502	503	502	507	
	Dev (%)	2.7%	4.0%	1.5%	6.9%	1.9%	3.6%	10.4%	
Desulfovibrionaceae_asv25	*p*	n.s.	0.001	n.s.	0.004	n.s.	0.004	n.s.	**113**
	AIC	262	255	261	257	262	257	265	
	Dev (%)	5.0%	9.4%	5.9%	9.4%	7.2%	9.4%	14.0%	
Muribaculaceae_asv26	*p*	n.s.	0.001	0.013	0.003	0.033	0.014	0.007	**111**
	AIC	325	315	316	316	315	313	317	
	Dev (%)	0.7%	9.3%	11.6 %	9.9%	17.0 %	17.3%	20.1%	
Muribaculaceae_asv28	*p*	n.s.	n.s.	0.038	0.041	n.s.	n.s.	0.029	**88**
	AIC	453	454	446	445	449	453	450	
	Dev (%)	1.0%	0.5%	15.9 %	17.7%	9.6%	3.5%	16.7%	
Lachnospiraceae_asv29	*p*	0.020	0.025	n.s.	0.025	n.s.	0.048	n.s.	**75**
	AIC	524	522	526	518	526	523	528	
	Dev (%)	4.7%	7.2%	10.3 %	18.6%	4.7%	8.2%	15.3%	
Lachnospiraceae_asv30	*p*	0.000	0.000	0.000	0.000	0.000	0.000	0.000	**81**
	AIC	512	499	511	495	492	496	494	
	Dev (%)	15.5%	24.6%	17.1 %	31.7%	31.0 %	27.7%	37.2%	
Lachnospiraceae_asv31	*p*	0.000	0.039	n.s.	0.001	0.005	0.033	0.002	**87**
	AIC	471	483	482	474	472	478	476	
	Dev (%)	14.5%	3.8%	7.4%	12.5%	18.5 %	13.2%	21.5%	
Lachnospiraceae_asv33	*p*	0.013	n.s.	0.007	0.041	0.017	0.024	n.s.	**54**
	AIC	559	565	564	563	560	566	576	
	Dev (%)	20.8%	14.6%	6.4%	18.1%	19.5 %	6.5%	9.8%	
Rikenellaceae_asv34	*p*	n.s.	0.003	0.000	0.015	0.002	0.001	0.001	**113**
	AIC	260	249	241	252	245	244	247	
	Dev (%)	1.4%	11.4%	17.9 %	11.0%	17.3 %	19.2%	23.2%	
Lachnospiraceae_asv35	*p*	n.s.	0.007	n.s.	0.010	n.s.	0.008	n.s.	**86**
	AIC	494	488	492	490	497	489	496	
	Dev (%)	4.2%	8.5%	11.4 %	7.9%	3.1%	8.3%	14.3%	
Muribaculaceae_asv36	*p*	n.s.	n.s.	n.s.	n.s.	n.s.	n.s.	n.s.	**108**
	AIC	398	398	397	399	399	399	398	
	Dev (%)	0.0%	0.0%	2.1%	3.4%	2.0%	0.8%	13.4%	
Tannerellaceae_asv37	*p*	0.003	0.000	n.s.	0.000	0.012	0.001	0.001	**89**
	AIC	426	430	436	416	436	430	427	
	Dev (%)	21.3%	10.6%	12.7 %	22.3%	7.6%	12.3%	25.1%	

ToD12	GAM	Prot	Carb	Fat	P x C	P x F	C x F	P x C X F	N data points
Lachnospiraceae_asv39	*p*	0.013	n.s.	n.s.	0.032	0.044	n.s.	n.s.	**102**
	AIC	420	422	426	421	422	422	425	
	Dev (%)	5.3%	3.8%	0.2%	6.0%	5.5%	6.2%	13.8%	
Rikenellaceae_asv40	*p*	n.s.	0.000	0.000	0.000	0.000	0.000	0.000	**96**
	AIC	458	417	431	411	439	411	409	
	Dev (%)	2.8%	31.4%	32.3 %	35.8%	20.9 %	39.2%	44.2%	
Rikenellaceae_asv41	*p*	0.049	0.000	0.018	0.019	n.s.	0.001	0.008	**86**
	AIC	470	462	465	464	471	462	468	
	Dev (%)	6.7%	11.5%	19.8 %	17.5%	8.6%	12.7%	18.8%	
Lachnospiraceae_asv42	*p*	n.s.	n.s.	n.s.	n.s.	n.s.	n.s.	0.032	**100**
	AIC	428	430	432	428	431	431	428	
	Dev (%)	5.5%	2.9%	0.0%	15.6%	5.0%	6.6%	17.0%	
Bacteroidaceae_asv43	*p*	n.s.	0.003	0.006	0.000	0.004	0.003	0.001	**105**
	AIC	415	405	408	391	408	403	403	
	Dev (%)	2.3%	13.0%	8.6%	22.4%	9.8%	16.5%	23.7%	
Desulfovibrionaceae_asv 44	*p*	n.s.	n.s.	0.000	0.012	0.037	0.000	0.000	**40**
	AIC	471	470	448	462	468	445	457	
	Dev (%)	5.4%	10.9%	30.0 %	20.5%	13.3 %	33.8%	27.3%	
Muribaculaceae_asv47	*p*	n.s.	0.000	0.000	0.000	0.000	0.000	0.000	**42**
	AIC	449	430	417	431	416	413	418	
	Dev (%)	5.2%	20.7%	29.1 %	22.0%	32.9 %	34.5%	36.7%	
Lachnospiraceae_asv48	*p*	n.s.	n.s.	0.050	n.s.	n.s.	n.s.	n.s.	**110**
	AIC	375	374	372	375	373	373	377	
	Dev (%)	0.5%	6.6%	4.0%	6.9%	4.6%	7.9%	12.6%	
Lachnospiraceae_asv49	*p*	0.001	0.000	n.s.	0.000	0.014	0.000	0.000	**88**
	AIC	482	475	498	471	485	473	475	
	Dev (%)	14.4%	18.8%	5.7%	26.8%	15.5 %	23.7%	28.6%	
Oscillospiraceae_asv50	*p*	0.008	n.s.	n.s.	0.030	0.030	n.s.	n.s.	**107**
	AIC	347	347	351	349	349	351	356	
	Dev (%)	6.2%	15.2%	4.8%	6.2%	6.3%	8.7%	11.8%	
Lachnospiraceae_asv51	*p*	n.s.	n.s.	n.s.	n.s.	n.s.	n.s.	n.s.	**106**
	AIC	401	398	398	400	400	397	401	
	Dev (%)	0.6%	3.0%	4.8%	3.0%	5.9%	10.1%	13.6%	
Lachnospiraceae_asv52	*p*	n.s.	0.013	n.s.	0.031	n.s.	n.s.	n.s.	**110**
	AIC	354	348	351	349	352	347	354	
	Dev (%)	0.2%	5.3%	4.4%	6.1%	5.6%	12.8%	13.1%	
Muribaculaceae_asv53	*p*	n.s.	0.000	0.000	0.000	0.000	0.000	0.000	**38**

ToD12	GAM	Prot	Carb	Fat	P x C	P x F	C x F	P x C X F	N data points
	AIC	436	417	406	414	404	400	401	
	Dev (%)	10.2%	20.9%	29.0 %	30.9%	33.5 %	36.0%	39.0%	
Muribaculaceae_asv54	*p*	n.s.	0.036	0.001	0.000	0.000	0.001	0.000	**108**
	AIC	371	368	364	348	362	355	352	
	Dev (%)	5.9%	12.4%	10.5 %	23.5%	13.4 %	24.7%	30.0%	
Lachnospiraceae_asv55	*p*	n.s.	0.000	0.039	0.000	0.037	0.001	0.000	**56**
	AIC	556	539	549	532	552	535	539	
	Dev (%)	0.1%	14.5%	10.0 %	21.6%	5.8%	23.3%	25.8%	
Muribaculaceae_asv56	*p*	0.002	0.038	0.000	0.000	0.000	0.000	0.000	**62**
	AIC	426	433	410	391	403	400	388	
	Dev (%)	18.7%	15.3%	33.2 %	41.6%	29.9 %	38.4%	45.7%	
Lachnospiraceae_asv57	*p*	n.s.	n.s.	n.s.	0.025	n.s.	n.s.	n.s.	**97**
	AIC	422	421	423	418	424	422	427	
	Dev (%)	0.6%	7.3%	5.7%	6.5%	0.7%	3.0%	10.5%	
Rikenellaceae_asv59	*p*	n.s.	n.s.	n.s.	0.001	0.027	n.s.	n.s.	**94**
	AIC	445	447	447	437	445	447	448	
	Dev (%)	10.1%	2.7%	3.2%	12.6%	6.3%	4.3%	15.1%	
Oscillospiraceae_asv61	*p*	n.s.	n.s.	0.037	0.004	0.008	n.s.	0.036	**113**
	AIC	233	235	229	227	229	231	234	
	Dev (%)	3.2%	1.7%	10.9 %	9.7%	8.2%	11.2%	15.4%	
Bacteroidaceae_asv63	*p*	n.s.	n.s.	n.s.	0.022	n.s.	0.004	0.012	**85**
	AIC	409	410	408	402	409	396	405	
	Dev (%)	13.1%	5.9%	12.8 %	16.3%	5.1%	24.6%	19.8%	
Lachnospiraceae_asv64	*p*	0.000	0.021	n.s.	0.000	0.000	0.011	0.001	**108**
	AIC	342	349	355	342	341	344	345	
	Dev (%)	13.8%	15.2%	4.8%	15.3%	16.2 %	21.0%	22.7%	
Muribaculaceae_asv65	*p*	n.s.	n.s.	n.s.	n.s.	n.s.	n.s.	n.s.	**64**
	AIC	461	459	460	460	462	458	467	
	Dev (%)	0.1%	1.9%	0.6%	3.1%	0.7%	4.1%	8.9%	
Lachnospiraceae_asv67	*p*	0.000	0.000	0.004	0.000	0.000	0.000	0.000	**102**
	AIC	380	375	390	367	372	374	366	
	Dev (%)	20.5%	22.9%	16.7 %	34.0%	27.9 %	27.9%	37.9%	
Lachnospiraceae_asv68	*p*	0.000	0.028	0.000	0.000	0.000	0.000	0.000	**54**
	AIC	456	465	438	430	431	445	429	
	Dev (%)	11.4%	4.2%	32.4 %	33.5%	29.9 %	23.1%	38.9%	

ToD12	GAM	Prot	Carb	Fat	P x C	P x F	C x F	P x C X F	N data points
Oscillospiraceae_asv71	*p*	n.s.	0.001	0.000	0.001	0.000	0.000	0.000	**90**
	AIC	443	429	421	429	422	422	426	
	Dev (%)	2.0%	12.9%	20.2 %	14.8%	23.2 %	21.1%	26.2%	
Muribaculaceae_asv72	*p*	n.s.	n.s.	0.039	n.s.	0.033	n.s.	0.023	**108**
	AIC	307	310	303	309	299	301	305	
	Dev (%)	2.2%	0.0%	7.8%	2.7%	17.0 %	15.9%	17.4%	
Muribaculaceae_asv73	*p*	n.s.	0.002	n.s.	0.004	n.s.	0.010	0.002	**47**
	AIC	444	436	443	431	441	438	433	
	Dev (%)	3.3%	8.0%	3.0%	16.7%	11.2 %	8.0%	22.1%	
Erysipelotrichaceae_asv74	*p*	n.s.	n.s.	n.s.	n.s.	n.s.	n.s.	0.011	**81**
	AIC	467	464	467	462	468	458	461	
	Dev (%)	0.2%	3.7%	1.1%	15.8%	1.2%	15.2%	18.1%	
Muribaculaceae_asv75	*p*	0.001	n.s.	0.001	0.009	0.001	0.026	0.000	**71**
	AIC	389	399	386	390	383	392	384	
	Dev (%)	13.5%	5.3%	20.9 %	17.7%	23.1 %	17.8%	28.1%	
Ruminococcaceae_asv76	*p*	n.s.	n.s.	n.s.	n.s.	n.s.	n.s.	n.s.	**106**
	AIC	361	363	359	363	360	361	370	
	Dev (%)	1.2%	0.0%	3.3%	1.9%	4.3%	3.7%	7.9%	
Streptococcaceae_asv79	*p*	0.000	n.s.	0.010	0.000	0.000	0.024	0.000	**89**
	AIC	395	434	422	378	391	422	385	
	Dev (%)	36.5%	0.2%	17.2 %	40.4%	32.9 %	20.7%	43.6%	
Oscillospiraceae_asv80	*p*	n.s.	0.015	n.s.	n.s.	n.s.	0.049	n.s.	**102**
	AIC	367	362	367	364	369	364	372	
	Dev (%)	1.2%	5.4%	2.7%	5.5%	1.7%	5.5%	10.1%	
Lachnospiraceae_asv82	*p*	n.s.	n.s.	0.007	0.016	n.s.	n.s.	n.s.	**42**
	AIC	459	461	449	456	458	457	461	
	Dev (%)	10.8%	2.0%	17.8 %	7.2%	11.5 %	10.9%	14.4%	
Marinifilaceae_asv83	*p*	n.s.	0.010	0.004	0.003	0.013	0.004	0.030	**104**
	AIC	366	359	358	356	359	357	363	
	Dev (%)	0.4%	5.8%	7.3%	10.4%	7.5%	9.4%	15.8%	
Lachnospiraceae_asv84	*p*	n.s.	n.s.	n.s.	n.s.	n.s.	n.s.	n.s.	**61**
	AIC	453	453	448	454	455	454	459	
	Dev (%)	0.0%	0.4%	13.8 %	5.3%	0.3%	0.8%	8.5%	
Oscillospiraceae_asv85	*p*	n.s.	0.001	0.022	0.000	0.008	0.000	0.021	**97**
	AIC	404	392	394	387	396	390	399	

ToD12	GAM	Prot	Carb	Fat	P x C	P x F	C x F	P x C X F	N data points
	Dev (%)	0.1%	10.1%	14.1 %	15.0%	8.4%	13.3%	16.6%	
Lachnospiraceae_asv86	*p*	n.s.	n.s.	0.015	n.s.	n.s.	0.048	n.s.	**80**
	AIC	450	450	444	451	446	446	457	
	Dev (%)	0.1%	0.4%	5.2%	0.8%	5.2%	5.3%	7.2%	
Deferribacteraceae_asv88	*p*	n.s.	n.s.	n.s.	n.s.	n.s.	n.s.	n.s.	**81**
	AIC	447	446	447	446	448	448	450	
	Dev (%)	0.4%	0.6%	0.5%	7.1%	0.8%	0.8%	10.6%	
Lachnospiraceae_asv90	*p*	0.000	0.000	0.016	0.000	0.000	0.000	0.000	**112**
	AIC	240	240	254	233	237	241	240	
	Dev (%)	19.6%	18.9%	10.3 %	24.9%	24.1 %	21.3%	29.4%	
Lachnospiraceae_asv94	*p*	n.s.	n.s.	0.039	n.s.	0.034	n.s.	n.s.	**95**
	AIC	419	422	417	419	417	419	427	
	Dev (%)	2.5%	0.1%	3.8%	4.1%	5.9%	4.1%	9.4%	
Lachnospiraceae_asv95	*p*	n.s.	n.s.	0.002	0.049	0.005	0.010	n.s.	**40**
	AIC	480	482	474	479	474	476	484	
	Dev (%)	5.9%	0.9%	7.9%	5.3%	9.3%	8.0%	12.9%	
Oscillospiraceae_asv96	*p*	n.s.	0.011	0.026	0.037	0.043	n.s.	n.s.	**94**
	AIC	412	407	406	409	408	407	414	
	Dev (%)	2.0%	5.7%	8.5%	5.8%	7.5%	11.1%	12.8%	
Peptostreptococcaceae_asv98	*p*	n.s.	n.s.	n.s.	n.s.	n.s.	n.s.	n.s.	**90**
	AIC	440	443	444	442	442	444	450	
	Dev (%)	3.0%	1.4%	0.0%	4.4%	3.0%	3.8%	8.2%	
Lachnospiraceae_asv99	*p*	n.s.	n.s.	n.s.	n.s.	n.s.	n.s.	n.s.	**48**
	AIC	494	491	492	489	494	490	495	
	Dev (%)	0.0%	4.0%	1.7%	13.8%	1.7%	8.3%	12.5%	
Lachnospiraceae_asv100	*p*	n.s.	0.047	0.000	0.006	0.000	0.002	0.008	**47**
	AIC	473	468	459	461	460	460	467	
	Dev (%)	1.3%	7.2%	12.5 %	15.3%	13.3 %	15.2%	18.8%	
Lachnospiraceae_asv101	*p*	0.013	0.003	0.000	0.000	0.000	0.000	0.000	**89**
	AIC	422	424	396	392	404	410	393	
	Dev (%)	16.4%	7.8%	37.1 %	36.4%	27.8 %	25.1%	39.0%	
Rikenellaceae_asv102	*p*	n.s.	0.000	0.025	0.000	0.045	0.002	0.000	**74**
	AIC	440	434	438	426	441	433	431	
	Dev (%)	17.7%	11.5%	14.1 %	18.6%	9.0%	16.4%	24.9%	
Lachnospiraceae_asv103	*p*	n.s.	0.001	0.000	0.004	0.000	0.000	0.005	**69**
	AIC	473	466	458	467	459	457	466	

ToD12	GAM	Prot	Carb	Fat	P x C	P x F	C x F	P x C X F	N data points
	Dev (%)	11.2%	8.9%	14.5 %	9.6%	15.5 %	17.0%	21.4%	
Lachnospiraceae_asv104	*p*	0.027	n.s.	n.s.	n.s.	n.s.	n.s.	n.s.	**76**
	AIC	434	437	439	435	435	437	444	
	Dev (%)	4.7%	3.5%	1.2%	5.9%	6.6%	4.8%	9.0%	
Lachnospiraceae_asv107	*p*	n.s.	n.s.	n.s.	n.s.	n.s.	n.s.	n.s.	**50**
	AIC	478	478	476	477	474	478	487	
	Dev (%)	0.7%	0.8%	3.0%	3.0%	12.7 %	2.7%	6.4%	
Lachnospiraceae_asv108	*p*	n.s.	0.000	0.000	0.000	0.000	0.000	0.000	**91**
	AIC	415	392	393	381	397	385	387	
	Dev (%)	0.0%	19.1%	22.2 %	29.7%	16.2 %	25.4%	32.4%	
Lachnospiraceae_asv109	*p*	n.s.	n.s.	n.s.	n.s.	n.s.	n.s.	0.030	**80**
	AIC	415	413	410	415	413	412	412	
	Dev (%)	0.3%	9.5%	6.9%	8.2%	8.1%	10.6%	15.8%	
Muribaculaceae_asv111	*p*	n.s.	0.008	n.s.	0.003	n.s.	0.040	0.029	**84**
	AIC	367	357	364	356	367	358	363	
	Dev (%)	0.0%	9.6%	9.9%	10.4%	1.7%	12.1%	15.9%	
Muribaculaceae_asv112	*p*	n.s.	0.024	n.s.	n.s.	n.s.	0.014	n.s.	**89**
	AIC	414	413	417	414	416	411	422	
	Dev (%)	3.0%	4.5%	0.5%	5.1%	3.4%	7.4%	9.8%	
Oscillospiraceae_asv113	*p*	0.000	0.000	n.s.	0.000	0.000	0.005	0.003	**106**
	AIC	288	293	304	286	288	294	297	
	Dev (%)	15.7%	11.6%	4.9%	18.4%	16.8 %	14.9%	20.8%	
Lachnospiraceae_asv114	*p*	0.024	0.000	n.s.	0.000	0.009	0.000	0.000	**66**
	AIC	419	396	426	398	417	396	399	
	Dev (%)	12.1%	25.9%	3.3%	26.0%	12.6 %	28.8%	33.0%	
Lachnospiraceae_asv116	*p*	0.000	0.001	0.023	0.000	0.000	0.000	0.000	**74**
	AIC	335	418	427	338	331	392	342	
	Dev (%)	59.8%	17.1%	8.5%	58.0%	64.2 %	39.8%	61.4%	
Muribaculaceae_asv117	*p*	n.s.	n.s.	n.s.	n.s.	n.s.	n.s.	n.s.	**110**
	AIC	255	255	254	257	256	256	268	
	Dev (%)	0.1%	0.0%	1.3%	0.1%	1.3%	1.4%	2.7%	
Lachnospiraceae_asv118	*p*	0.000	0.015	n.s.	0.000	0.000	0.002	0.000	**77**
	AIC	395	418	418	397	392	406	398	
	Dev (%)	22.7%	5.2%	12.6 %	22.7%	25.6 %	20.8%	31.1%	
Lachnospiraceae_asv120	*p*	n.s.	n.s.	0.007	n.s.	0.027	n.s.	n.s.	**51**
	AIC	438	435	431	435	433	432	437	

ToD12	GAM	Prot	Carb	Fat	P x C	P x F	C x F	P x C X F	N data points
	Dev (%)	0.1%	5.3%	6.3%	6.0%	6.3%	9.8%	14.9%	
Lachnospiraceae_asv121	*p*	n.s.	n.s.	n.s.	n.s.	n.s.	n.s.	n.s.	**45**
	AIC	430	429	428	431	430	429	435	
	Dev (%)	2.5%	3.1%	2.6%	3.8%	2.6%	4.4%	9.9%	
Lachnospiraceae_asv122	*p*	n.s.	0.000	0.021	0.001	n.s.	0.001	0.018	**72**
	AIC	448	434	443	432	444	435	442	
	Dev (%)	0.0%	11.3%	4.6%	15.4%	4.7%	12.1%	18.6%	
Lachnospiraceae_asv124	*p*	n.s.	n.s.	n.s.	n.s.	n.s.	n.s.	n.s.	**41**
	AIC	475	474	474	475	476	475	482	
	Dev (%)	0.2%	0.9%	0.8%	2.0%	0.7%	3.3%	7.3%	
Lachnospiraceae_asv130	*p*	0.005	n.s.	n.s.	0.045	n.s.	n.s.	0.029	**71**
	AIC	441	449	448	441	443	450	445	
	Dev (%)	6.7%	0.1%	2.0%	10.8%	8.5%	1.7%	15.9%	
Lachnospiraceae_asv131	*p*	0.003	0.000	0.001	0.000	0.000	0.000	0.000	**58**
	AIC	451	432	443	434	438	431	441	
	Dev (%)	7.6%	21.6%	15.2 %	21.8%	19.6 %	23.7%	26.5%	
Oscillospiraceae_asv132	*p*	n.s.	n.s.	n.s.	n.s.	n.s.	n.s.	n.s.	**38**
	AIC	428	429	430	426	430	430	433	
	Dev (%)	1.1%	1.3%	0.0%	13.2%	1.1%	1.0%	11.7%	
Lachnospiraceae_asv133	*p*	0.001	0.012	n.s.	0.001	0.000	0.002	0.001	**62**
	AIC	439	448	453	435	440	444	439	
	Dev (%)	13.1%	5.5%	1.9%	22.2%	13.2 %	10.4%	24.3%	
Lachnospiraceae_asv135	*p*	n.s.	0.000	n.s.	0.000	n.s.	0.001	0.003	**62**
	AIC	444	424	443	425	441	425	434	
	Dev (%)	3.5%	17.5%	3.1%	18.4%	11.1 %	26.0%	22.5%	
Lachnospiraceae_ Eubacterium_asv137	*p*	0.014	n.s.	0.001	n.s.	0.015	0.001	0.000	**52**
	AIC	444	450	431	443	440	428	431	
	Dev (%)	5.3%	1.5%	24.0 %	11.8%	11.7 %	25.3%	26.9%	
Lachnospiraceae_asv138	*p*	n.s.	n.s.	n.s.	n.s.	n.s.	n.s.	n.s.	**50**
	AIC	445	446	447	446	446	448	455	
	Dev (%)	2.1%	1.3%	0.1%	2.1%	2.3%	1.5%	6.9%	
Oscillospiraceae_asv140	*p*	0.010	n.s.	0.015	0.012	0.006	n.s.	0.009	**76**
	AIC	411	419	411	414	406	417	414	
	Dev (%)	11.3%	2.4%	10.4 %	7.7%	20.7 %	9.7%	18.5%	
Eubacterium_asv141	*p*	n.s.	n.s.	n.s.	n.s.	n.s.	n.s.	n.s.	**66**
	AIC	411	414	412	413	412	413	420	
	Dev (%)	1.4%	6.7%	0.4%	1.5%	4.2%	6.9%	7.1%	

ToD12	GAM	Prot	Carb	Fat	P x C	P x F	C x F	P x C X F	N data points
Lachnospiraceae_asv142	*p*	n.s.	0.011	n.s.	n.s.	n.s.	0.037	n.s.	**88**
	AIC	400	400	406	401	404	402	405	
	Dev (%)	8.7%	5.7%	0.4%	10.3%	5.6%	5.8%	14.4%	
Muribaculaceae_asv144	*p*	n.s.	0.028	n.s.	n.s.	n.s.	0.040	n.s.	**72**
	AIC	388	383	388	385	390	384	394	
	Dev (%)	0.2%	4.3%	0.1%	4.8%	0.2%	5.6%	9.4%	
Lachnospiraceae_asv145	*p*	0.011	n.s.	0.019	n.s.	0.030	0.016	0.002	**47**
	AIC	440	450	440	447	440	438	439	
	Dev (%)	10.9%	0.8%	13.8 %	7.5%	17.0 %	21.7%	21.5%	
Peptococcaceae_asv146	*p*	0.020	0.002	n.s.	0.008	n.s.	0.010	0.005	**99**
	AIC	329	325	333	325	330	325	329	
	Dev (%)	9.8%	12.7%	7.8%	16.1%	12.6 %	16.3%	20.2%	
Oscillospiraceae_asv147	*p*	0.000	0.004	n.s.	0.000	0.000	0.007	0.000	**56**
	AIC	405	428	430	412	409	421	414	
	Dev (%)	25.6%	7.2%	7.4%	21.0%	26.3 %	19.7%	28.7%	
Lachnospiraceae_asv152	*p*	n.s.	0.000	0.000	0.000	0.000	0.000	0.000	**95**
	AIC	374	350	336	336	341	341	335	
	Dev (%)	1.4%	25.2%	35.7 %	38.3%	30.7 %	29.4%	38.3%	
Lachnospiraceae_asv154	*p*	0.034	0.024	0.014	0.000	n.s.	0.014	0.000	**66**
	AIC	422	419	415	406	420	412	410	
	Dev (%)	4.0%	8.3%	16.8 %	20.1%	10.5 %	19.7%	24.7%	
Ruminococcaceae_asv155	*p*	0.030	n.s.	n.s.	n.s.	n.s.	n.s.	n.s.	**53**
	AIC	442	443	446	443	443	445	450	
	Dev (%)	4.1%	8.4%	0.5%	12.6%	4.9%	11.6%	10.5%	
Lachnospiraceae_asv157	*p*	n.s.	0.007	0.022	0.001	0.020	0.014	0.030	**78**
	AIC	435	423	424	423	429	422	430	
	Dev (%)	0.0%	12.8%	16.2 %	11.5%	6.8%	16.2%	17.5%	
Lachnospiraceae_asv158	*p*	n.s.	0.011	n.s.	0.034	n.s.	0.037	n.s.	**98**
	AIC	351	347	352	349	353	349	361	
	Dev (%)	9.3%	5.7%	7.9%	5.9%	2.2%	5.8%	7.5%	
Lachnospiraceae_asv159	*p*	0.007	n.s.	0.001	n.s.	0.003	n.s.	0.000	**50**
	AIC	446	452	434	446	435	444	431	
	Dev (%)	6.4%	0.8%	23.9 %	16.8%	22.0 %	15.9%	28.4%	
Oscillospiraceae_asv161	*p*	0.011	n.s.	n.s.	n.s.	0.014	n.s.	0.018	**55**
	AIC	428	433	435	428	430	434	431	
	Dev (%)	8.5%	4.4%	2.7%	14.5%	7.4%	6.2%	17.9%	

ToD12	GAM	Prot	Carb	Fat	P x C	P x F	C x F	P x C X F	N data points
Lachnospiraceae_asv162	*p*	n.s.	n.s.	n.s.	0.013	0.032	n.s.	0.035	**39**
	AIC	446	448	444	442	444	447	445	
	Dev (%)	3.0%	0.9%	11.8 %	7.5%	6.0%	3.5%	17.1%	
Lachnospiraceae_asv165	*p*	0.001	0.000	0.004	0.000	0.000	0.000	0.000	**55**
	AIC	340	315	342	317	329	312	316	
	Dev (%)	8.9%	28.2%	7.3%	28.4%	20.6 %	34.2%	36.1%	
Lachnospiraceae_asv169	*p*	0.000	0.016	n.s.	0.000	0.001	n.s.	0.010	**95**
	AIC	330	342	342	333	332	341	341	
	Dev (%)	15.2%	5.1%	6.9%	13.9%	14.8 %	11.9%	18.3%	
Ruminococcaceae_asv174	*p*	n.s.	0.007	0.011	0.028	n.s.	0.021	0.021	**60**
	AIC	417	405	408	409	410	407	413	
	Dev (%)	1.2%	17.9%	10.7 %	11.6%	11.3 %	13.9%	16.6%	
Lachnospiraceae_asv176	*p*	0.000	n.s.	n.s.	0.001	0.004	n.s.	0.003	**49**
	AIC	404	416	412	406	405	413	408	
	Dev (%)	12.1%	2.7%	7.4%	12.1%	15.4 %	11.9%	20.8%	
Lachnospiraceae_asv177	*p*	n.s.	0.010	n.s.	0.028	n.s.	0.016	n.s.	**38**
	AIC	430	427	434	429	432	428	438	
	Dev (%)	3.3%	5.8%	0.0%	6.3%	3.3%	7.1%	10.1%	
Desulfovibrionaceae_asv180	*p*	0.001	n.s.	n.s.	0.002	0.001	n.s.	0.010	**104**
	AIC	286	299	296	286	287	297	292	
	Dev (%)	10.4%	0.3%	4.2%	12.6%	11.8 %	5.0%	18.2%	
Lachnospiraceae_asv185	*p*	n.s.	n.s.	n.s.	n.s.	n.s.	n.s.	0.030	**55**
	AIC	442	439	442	439	441	439	442	
	Dev (%)	3.0%	9.6%	4.6%	12.1%	14.3 %	14.3%	17.6%	
Oscillospiraceae_asv186	*p*	n.s.	0.017	n.s.	n.s.	0.045	0.033	n.s.	**72**
	AIC	388	384	386	386	386	385	393	
	Dev (%)	1.9%	5.0%	4.6%	5.1%	5.4%	6.0%	11.3%	
Bacteroidaceae_asv187	*p*	n.s.	n.s.	0.024	n.s.	n.s.	0.038	n.s.	**65**
	AIC	355	355	350	356	351	351	361	
	Dev (%)	0.0%	0.5%	4.5%	3.2%	8.4%	5.7%	8.9%	
Rikenellaceae_asv188	*p*	n.s.	n.s.	n.s.	n.s.	n.s.	n.s.	n.s.	**78**
	AIC	292	295	293	294	292	294	301	
	Dev (%)	2.8%	0.2%	1.8%	3.1%	4.3%	7.3%	8.9%	
Lachnospiraceae_asv191	*p*	0.018	0.006	n.s.	0.010	0.024	0.018	0.036	**67**
	AIC	387	386	390	386	384	387	390	

ToD12	GAM	Prot	Carb	Fat	P x C	P x F	C x F	P x C X F	N data points
	Dev (%)	5.4%	6.6%	2.6%	7.9%	11.1 %	7.0%	15.4%	
Oscillospiraceae_asv201	*p*	n.s.	n.s.	0.041	n.s.	n.s.	n.s.	n.s.	**38**
	AIC	411	412	404	412	410	410	410	
	Dev (%)	1.2%	0.2%	14.4 %	1.2%	6.7%	7.4%	14.5%	
Lachnospiraceae_asv202	*p*	0.000	0.000	0.036	0.000	0.000	0.000	0.001	**41**
	AIC	412	413	419	409	414	408	415	
	Dev (%)	13.5%	12.5%	16.0 %	17.3%	13.5 %	20.9%	23.0%	
Eggerthellaceae_asv203	*p*	0.007	0.008	0.013	0.014	0.001	0.005	0.005	**54**
	AIC	301	299	299	299	294	299	299	
	Dev (%)	6.4%	9.0%	11.1 %	10.6%	13.9 %	10.2%	19.7%	
Lachnospiraceae_asv204	*p*	0.009	n.s.	0.002	0.000	n.s.	n.s.	0.000	**52**
	AIC	400	403	389	383	400	399	386	
	Dev (%)	6.0%	3.0%	23.7 %	28.2%	10.4 %	17.8%	27.8%	
Lachnospiraceae_asv205	*p*	n.s.	n.s.	n.s.	n.s.	n.s.	n.s.	n.s.	**60**
	AIC	410	412	411	412	408	413	418	
	Dev (%)	3.8%	2.2%	4.8%	3.8%	10.2 %	2.5%	10.3%	
Oscillospiraceae_asv206	*p*	0.006	n.s.	n.s.	0.006	0.006	n.s.	n.s.	**55**
	AIC	372	382	384	376	376	383	388	
	Dev (%)	13.9%	2.5%	1.2%	8.8%	8.9%	2.7%	11.2%	
Lachnospiraceae_asv208	*p*	n.s.	n.s.	n.s.	n.s.	n.s.	n.s.	n.s.	**56**
	AIC	429	427	429	427	431	429	436	
	Dev (%)	0.4%	1.8%	5.0%	4.2%	0.6%	1.8%	8.6%	
Lachnospiraceae_asv211	*p*	0.042	n.s.	n.s.	n.s.	n.s.	n.s.	n.s.	**84**
	AIC	335	338	336	337	334	335	338	
	Dev (%)	3.7%	1.2%	3.7%	11.7%	9.0%	6.5%	14.4%	
Oscillospiraceae_asv212	*p*	0.000	n.s.	n.s.	0.000	0.000	n.s.	0.011	**58**
	AIC	376	394	395	377	378	395	390	
	Dev (%)	20.4%	2.5%	2.5%	17.4%	17.0 %	3.5%	18.1%	
Lachnospiraceae_asv214	*p*	0.000	n.s.	0.035	0.000	0.000	n.s.	0.002	**47**
	AIC	392	411	403	391	392	403	397	
	Dev (%)	15.2%	0.8%	8.2%	17.6%	16.9 %	12.9%	24.2%	
Lachnospiraceae_asv215	*p*	n.s.	n.s.	n.s.	0.011	n.s.	n.s.	0.009	**41**
	AIC	368	367	372	364	370	373	365	
	Dev (%)	3.5%	17.4%	0.3%	7.9%	3.5%	3.0%	18.5%	
Peptococcaceae_asv218	*p*	n.s.	n.s.	n.s.	n.s.	0.029	n.s.	0.028	**91**
	AIC	324	329	323	327	322	327	325	

ToD12	GAM	Prot	Carb	Fat	P x C	P x F	C x F	P x C X F	N data points
	Dev (%)	6.3%	0.7%	8.8%	3.9%	9.5%	3.9%	16.2%	
Lachnospiraceae_asv223	*p*	0.002	0.042	0.000	0.000	0.000	0.000	0.000	**68**
	AIC	382	384	374	356	366	359	350	
	Dev (%)	8.6%	13.8%	15.0 %	28.8%	22.2 %	33.1%	40.4%	
Oscillospiraceae_asv231	*p*	0.000	0.000	0.010	0.000	0.000	0.003	0.000	**58**
	AIC	365	366	371	362	362	367	364	
	Dev (%)	13.5%	12.6%	11.1 %	17.4%	17.4 %	15.9%	25.4%	
Muribaculaceae_asv232	*p*	n.s.	n.s.	n.s.	0.000	n.s.	0.020	0.005	**59**
	AIC	355	351	353	344	354	352	349	
	Dev (%)	3.9%	15.8%	15.4 %	13.1%	8.5%	6.8%	19.8%	
Gastranaerophilales_ asv236	*p*	n.s.	n.s.	n.s.	0.003	n.s.	n.s.	n.s.	**41**
	AIC	317	315	315	308	315	314	319	
	Dev (%)	1.8%	3.3%	3.8%	10.2%	5.0%	15.0%	12.5%	
Lachnospiraceae_asv237	*p*	n.s.	0.000	0.001	0.000	0.017	0.001	0.000	**40**
	AIC	422	409	410	398	410	404	397	
	Dev (%)	0.0%	11.2%	9.7%	27.7%	16.0 %	19.8%	30.3%	
Lachnospiraceae_asv238	*p*	0.014	n.s.	n.s.	0.003	0.005	n.s.	n.s.	**44**
	AIC	382	393	393	384	385	394	397	
	Dev (%)	16.1%	0.6%	0.3%	9.9%	9.3%	1.4%	10.2%	
Bacilli_asv240	*p*	n.s.	n.s.	n.s.	n.s.	n.s.	n.s.	0.041	**40**
	AIC	343	340	340	342	341	341	341	
	Dev (%)	0.6%	2.9%	2.9%	2.9%	6.2%	4.2%	15.1%	
Lachnospiraceae_asv241	*p*	n.s.	n.s.	n.s.	n.s.	n.s.	n.s.	n.s.	**39**
	AIC	383	382	384	382	385	383	388	
	Dev (%)	5.5%	3.3%	0.1%	5.9%	0.8%	5.6%	10.8%	
Lachnospiraceae_asv243	*p*	n.s.	n.s.	n.s.	n.s.	n.s.	n.s.	n.s.	**75**
	AIC	372	370	373	372	366	370	374	
	Dev (%)	3.9%	3.4%	1.4%	3.4%	15.7 %	6.9%	12.9%	
Oscillospiraceae_asv246	*p*	n.s.	n.s.	0.030	n.s.	n.s.	n.s.	n.s.	**58**
	AIC	337	336	333	335	335	335	344	
	Dev (%)	0.4%	2.0%	4.1%	4.3%	4.3%	4.5%	8.6%	
Lachnospiraceae_asv250	*p*	n.s.	n.s.	n.s.	n.s.	n.s.	n.s.	n.s.	**50**
	AIC	360	358	358	360	361	356	366	
	Dev (%)	0.0%	1.3%	3.3%	1.9%	2.8%	11.7%	8.9%	
Lachnospiraceae_asv252	*p*	0.000	0.004	n.s.	0.000	0.000	0.002	0.000	**54**
	AIC	365	396	401	368	367	391	378	

ToD12	GAM	Prot	Carb	Fat	P x C	P x F	C x F	P x C X F	N data points
	Dev (%)	30.3%	7.2%	8.8%	29.0%	29.6 %	15.1%	31.5%	
Lachnospiraceae_asv254	*p*	n.s.	n.s.	n.s.	n.s.	n.s.	n.s.	n.s.	**58**
	AIC	380	379	376	380	380	376	379	
	Dev (%)	0.4%	6.5%	6.2%	2.2%	4.7%	11.2%	15.6%	
Ruminococcaceae_asv257	*p*	n.s.	n.s.	n.s.	n.s.	n.s.	n.s.	n.s.	**76**
	AIC	324	325	325	326	326	327	333	
	Dev (%)	0.7%	0.0%	8.3%	0.8%	0.8%	0.1%	6.8%	
Lachnospiraceae_asv262	*p*	n.s.	n.s.	n.s.	n.s.	n.s.	n.s.	n.s.	**40**
	AIC	341	340	335	342	341	338	341	
	Dev (%)	0.2%	1.3%	15.1 %	1.3%	2.2%	10.8%	13.2%	
Oscillospirales_asv269	*p*	n.s.	n.s.	0.000	n.s.	0.000	0.000	0.000	**44**
	AIC	322	320	301	322	299	302	305	
	Dev (%)	1.2%	3.3%	24.0 %	3.3%	20.7 %	18.7%	26.2%	
Lachnospiraceae_asv272	*p*	n.s.	n.s.	0.002	0.009	0.005	0.003	0.006	**59**
	AIC	341	340	330	335	329	333	334	
	Dev (%)	1.5%	2.6%	12.3 %	8.1%	15.4 %	10.1%	19.5%	
Ruminococcaceae_asv276	*p*	0.000	0.010	n.s.	0.000	0.003	0.013	0.015	**50**
	AIC	324	336	340	328	326	336	337	
	Dev (%)	16.2%	5.8%	3.8%	13.8%	17.9 %	7.5%	17.4%	
Gastranaerophilales_asv279	*p*	n.s.	0.007	0.000	0.005	0.000	0.000	0.001	**64**
	AIC	338	325	318	328	320	318	322	
	Dev (%)	0.0%	15.8%	16.0 %	10.1%	16.2 %	17.5%	24.1%	
Oscillospiraceae_asv283	*p*	0.007	n.s.	0.047	0.012	n.s.	n.s.	n.s.	**42**
	AIC	304	305	305	305	305	306	311	
	Dev (%)	6.3%	9.2%	8.4%	7.6%	9.5%	10.5%	13.6%	
Anaerovoracaceae_Eubacterium_asv289	*p*	n.s.	n.s.	n.s.	n.s.	n.s.	n.s.	n.s.	**58**
	AIC	256	256	258	257	255	258	266	
	Dev (%)	4.8%	2.1%	0.5%	8.1%	13.1 %	2.1%	6.7%	
Lachnospiraceae_asv292	*p*	0.025	n.s.	0.045	0.044	0.007	n.s.	n.s.	**42**
	AIC	318	322	318	314	315	319	323	
	Dev (%)	4.4%	0.8%	5.2%	14.4%	8.5%	7.7%	13.8%	
Lachnospiraceae_asv296	*p*	0.000	0.004	n.s.	0.000	0.000	0.002	0.000	**39**
	AIC	336	350	364	338	338	354	342	
	Dev (%)	24.1%	22.5%	1.2%	24.5%	25.0 %	10.6%	28.7%	

ToD12	GAM	Prot	Carb	Fat	P x C	P x F	C x F	P x C X F	N data points
Ruminococcaceae_asv301	*p*	n.s.	n.s.	n.s.	n.s.	n.s.	n.s.	n.s.	**38**
	AIC	262	262	260	260	261	257	264	
	Dev (%)	3.7%	4.4%	6.0%	9.5%	6.5%	15.2%	15.5%	
Oscillospiraceae_asv305	*p*	0.041	n.s.	0.026	n.s.	n.s.	n.s.	0.009	**45**
	AIC	303	305	297	305	302	304	300	
	Dev (%)	3.7%	1.6%	17.0 %	3.8%	8.5%	8.5%	18.4%	
Butyricicoccaceae_asv318	*p*	0.000	0.000	0.000	0.000	0.000	0.000	0.000	**49**
	AIC	265	239	256	243	248	239	243	
	Dev (%)	10.8%	30.3%	23.6 %	29.8%	24.7 %	32.1%	35.9%	
Anaerovoracaceae_asv320	*p*	0.046	0.000	0.002	0.000	0.003	0.000	0.000	**61**
	AIC	272	255	263	256	263	254	258	
	Dev (%)	5.3%	20.0%	13.4 %	21.7%	15.3 %	24.5%	26.6%	
Bacilli_asv336	*p*	n.s.	n.s.	n.s.	n.s.	n.s.	n.s.	n.s.	**43**
	AIC	277	276	276	278	277	277	283	
	Dev (%)	0.6%	1.6%	2.4%	1.7%	4.0%	6.1%	8.5%	

Supplementary Table 7-9. GAM statistics for Figure 3-11 ToD18.
Dev = deviance explained, n.s. = p value >0.05

ToD18	GAM	Prot	Carb	Fat	P x C	P x F	C x F	P x C X F	N data points
InvSimpson	*p*	n.s.	n.s.	n.s.	n.s.	n.s.	n.s.	n.s.	**112**
	AIC	821	828	827	826	826	828	831	
	Dev (%)	11.0%	0.0%	1.0%	4.3%	4.1%	3.9%	10.4%	
Observed	*p*	n.s.	n.s.	n.s.	n.s.	n.s.	n.s.	n.s.	**112**
	AIC	1,046	1,045	1,046	1,046	1,048	1,047	1,057	
	Dev (%)	0.0%	1.5%	0.2%	2.0%	0.2%	1.5%	4.5%	
Shannon	*p*	n.s.	n.s.	n.s.	n.s.	n.s.	n.s.	n.s.	**112**
	AIC	77	82	80	81	80	82	86	
	Dev (%)	9.4%	0.0%	3.2%	2.9%	4.7%	4.5%	9.8%	
Verrucomicrobiota	*p*	n.s.	0.005	0.003	0.000	n.s.	0.000	0.000	**112**
	AIC	488	476	474	468	486	469	472	
	Dev (%)	4.7%	20.7%	23.7 %	27.6%	10.2 %	20.2%	27.3%	
Actinobacteriota	*p*	n.s.	0.000	0.000	0.000	0.001	0.000	0.000	**112**
	AIC	648	623	606	619	628	613	600	

	Dev (%)	0.2%	20.6%	39.1 %	24.8%	20.9 %	33.7%	43.6%	
Firmicutes	*p*	0.021	n.s.	n.s.	n.s.	n.s.	n.s.	0.035	**112**
	AIC	1,151	1,157	1,156	1,151	1,153	1,151	1,154	
	Dev (%)	4.7%	0.6%	1.9%	7.5%	10.2 %	11.9%	15.7%	
Desulfobacterota	*p*	n.s.	n.s.	0.000	n.s.	0.048	0.004	0.000	**112**
	AIC	527	529	506	529	522	513	506	
	Dev (%)	3.0%	1.0%	27.4 %	5.4%	11.7 %	21.3%	30.3%	
Bacteroidota	*p*	0.001	n.s.	n.s.	0.000	0.026	n.s.	0.005	**112**
	AIC	978	988	988	972	978	988	980	
	Dev (%)	9.6%	0.6%	1.1%	16.2%	17.5 %	6.5%	20.0%	
Deferribacterota	*p*	n.s.	n.s.	n.s.	n.s.	n.s.	n.s.	n.s.	**112**
	AIC	431	430	430	432	432	432	437	
	Dev (%)	0.0%	0.9%	0.3%	0.8%	0.3%	1.1%	9.7%	
Proteobacteria	*p*	0.043	0.011	0.000	0.000	0.000	0.001	0.000	**112**
	AIC	497	492	487	476	483	486	483	
	Dev (%)	3.7%	8.6%	12.1 %	23.8%	16.5 %	14.7%	26.6%	
Cyanobacteria	*p*	n.s.	0.000	0.002	0.000	0.001	0.000	0.000	**112**
	AIC	476	463	471	441	461	462	442	
	Dev (%)	5.7%	14.8%	8.1%	34.0%	26.6 %	16.6%	38.8%	
Akkermansiaceae_asv1	*p*	n.s.	0.005	0.003	0.000	n.s.	0.000	0.000	**106**
	AIC	488	476	474	468	486	469	472	
	Dev (%)	4.7%	20.7%	23.7 %	27.6%	10.2 %	20.2%	27.3%	
Erysipelotrichaceae_asv3	*p*	n.s.	0.002	0.000	0.003	n.s.	0.025	0.000	**44**
	AIC	535	525	512	517	529	524	510	
	Dev (%)	0.5%	8.8%	27.5 %	25.6%	10.2 %	14.9%	31.6%	
Erysipelotrichaceae_asv4	*p*	n.s.	0.000	0.001	0.000	0.019	0.000	0.000	**68**
	AIC	564	540	547	536	558	540	535	
	Dev (%)	5.3%	22.1%	25.9 %	30.3%	12.4 %	25.8%	35.5%	
Prevotellaceae_asv5	*p*	n.s.	n.s.	n.s.	n.s.	n.s.	n.s.	0.021	**62**
	AIC	500	497	499	494	500	497	496	
	Dev (%)	4.5%	5.5%	1.4%	15.3%	2.5%	8.3%	16.9%	
Bacteroidaceae_asv7	*p*	n.s.	0.000	n.s.	0.013	n.s.	0.002	0.006	**106**
	AIC	429	423	434	424	431	425	427	
	Dev (%)	8.2%	10.8%	1.0%	15.0%	9.8%	11.0%	19.6%	
Lachnospiraceae_asv8	*p*	n.s.	0.001	0.000	0.000	0.000	0.000	0.000	**106**
	AIC	416	410	394	391	390	396	387	
	Dev (%)	6.1%	9.5%	26.4 %	25.5%	25.7 %	21.9%	36.6%	

Lachnospiraceae_asv9	*p*	0.049	0.030	n.s.	0.034	n.s.	n.s.	n.s.	**52**
	AIC	573	571	575	572	575	573	580	
	Dev (%)	3.5%	5.6%	9.9%	6.0%	3.6%	6.2%	11.1%	
Lachnospiraceae_asv10	*p*	n.s.	n.s.	n.s.	0.029	n.s.	0.050	0.016	**87**
	AIC	519	513	516	509	514	516	514	
	Dev (%)	4.3%	13.6%	5.1%	18.0%	13.0 %	5.4%	19.3%	
Lachnospiraceae_asv11	*p*	n.s.	n.s.	n.s.	n.s.	n.s.	n.s.	n.s.	**97**
	AIC	494	489	493	491	494	492	499	
	Dev (%)	4.3%	7.1%	0.7%	9.2%	1.4%	8.4%	10.7%	
Lactobacillaceae_asv12	*p*	0.000	n.s.	n.s.	0.000	0.001	n.s.	0.000	**106**
	AIC	373	388	388	367	369	388	368	
	Dev (%)	13.9%	2.0%	0.7%	21.8%	22.5 %	6.6%	27.8%	
Lactobacillaceae_asv13	*p*	0.016	0.032	0.024	0.029	n.s.	0.020	0.001	**55**
	AIC	467	469	466	467	468	463	463	
	Dev (%)	7.6%	7.2%	16.8 %	10.8%	11.0 %	17.2%	22.7%	
Rikenellaceae_asv15	*p*	0.024	0.001	0.005	0.000	0.000	0.002	0.000	**111**
	AIC	344	329	338	311	326	331	314	
	Dev (%)	4.5%	25.5%	11.1 %	32.9%	24.0 %	19.9%	36.5%	
Rikenellaceae_asv16	*p*	0.000	n.s.	0.016	0.000	0.000	n.s.	0.000	**108**
	AIC	419	458	449	402	411	453	408	
	Dev (%)	29.2%	10.1%	10.2 %	41.0%	35.6 %	9.5%	44.6%	
Lachnospiraceae_asv17	*p*	n.s.	n.s.	0.006	n.s.	n.s.	0.041	0.021	**81**
	AIC	485	481	478	479	477	478	480	
	Dev (%)	0.4%	4.8%	6.6%	9.8%	16.7 %	9.6%	17.4%	
Desulfovibrionaceae_asv 18	*p*	n.s.	0.000	0.021	0.000	0.012	0.000	0.000	**112**
	AIC	286	246	276	248	279	254	260	
	Dev (%)	0.3%	37.0%	18.9 %	30.4%	7.8%	26.4%	31.5%	
Rikenellaceae_asv20	*p*	n.s.	0.000	0.017	0.000	n.s.	0.000	0.000	**111**
	AIC	327	310	319	304	323	311	306	
	Dev (%)	5.1%	16.2%	19.8 %	27.5%	10.8 %	17.1%	30.4%	
Marinifilaceae_asv21	*p*	n.s.	n.s.	n.s.	n.s.	n.s.	n.s.	n.s.	**72**
	AIC	536	537	537	537	538	539	548	
	Dev (%)	0.7%	0.3%	0.0%	1.9%	0.7%	0.4%	4.8%	
Lachnospiraceae_asv22	*p*	n.s.	n.s.	n.s.	n.s.	n.s.	n.s.	n.s.	**90**
	AIC	489	493	492	492	489	494	498	
	Dev (%)	6.8%	0.1%	2.1%	3.1%	10.9 %	5.4%	9.3%	

Desulfovibrionaceae_asv25	*p*	n.s.	0.015	0.000	n.s.	n.s.	n.s.	0.009	**111**
	AIC	320	315	298	317	320	316	314	
	Dev (%)	1.3%	5.3%	29.2%	5.3%	6.5%	9.9%	18.8%	
Muribaculaceae_asv26	*p*	n.s.	0.000	0.019	0.000	0.008	0.000	0.000	**112**
	AIC	287	264	279	266	282	259	269	
	Dev (%)	2.9%	21.0%	19.6%	21.2%	9.4%	33.1%	28.1%	
Muribaculaceae_asv28	*p*	n.s.	n.s.	n.s.	n.s.	n.s.	n.s.	0.010	**86**
	AIC	416	416	415	418	414	418	413	
	Dev (%)	3.2%	10.9%	11.4%	6.1%	10.8%	5.1%	18.6%	
Lachnospiraceae_asv29	*p*	n.s.	n.s.	n.s.	0.000	n.s.	n.s.	0.000	**77**
	AIC	514	512	509	495	513	511	498	
	Dev (%)	4.9%	6.3%	16.7%	28.7%	13.8%	16.3%	26.8%	
Lachnospiraceae_asv30	*p*	n.s.	n.s.	0.008	0.011	n.s.	n.s.	0.027	**81**
	AIC	513	510	509	501	507	509	511	
	Dev (%)	2.4%	10.4%	6.3%	20.4%	14.2%	15.2%	18.1%	
Lachnospiraceae_asv31	*p*	0.000	0.000	n.s.	0.000	0.000	n.s.	0.000	**95**
	AIC	418	421	437	419	419	439	424	
	Dev (%)	19.8%	29.5%	8.2%	21.5%	21.2%	8.1%	26.9%	
Muribaculaceae_asv32	*p*	0.005	n.s.	0.033	n.s.	0.012	n.s.	0.021	**57**
	AIC	419	424	423	420	416	423	422	
	Dev (%)	7.0%	3.0%	4.1%	11.9%	13.3%	5.0%	18.3%	
Lachnospiraceae_asv33	*p*	n.s.	0.002	0.000	0.000	0.000	0.000	0.000	**71**
	AIC	543	532	518	520	511	517	515	
	Dev (%)	4.0%	11.9%	21.9%	28.6%	33.5%	23.9%	34.8%	
Rikenellaceae_asv34	*p*	n.s.	0.000	0.000	0.000	0.000	0.000	0.000	**111**
	AIC	243	219	227	218	229	217	226	
	Dev (%)	1.1%	24.9%	13.9%	27.5%	14.5%	24.8%	27.3%	
Lachnospiraceae_asv35	*p*	n.s.	0.009	n.s.	0.045	n.s.	0.009	0.024	**97**
	AIC	435	429	433	431	438	427	434	
	Dev (%)	5.6%	10.0%	13.6%	10.5%	5.2%	14.3%	17.1%	
Muribaculaceae_asv36	*p*	n.s.	n.s.	n.s.	n.s.	n.s.	n.s.	n.s.	**109**
	AIC	362	361	360	363	358	362	363	
	Dev (%)	0.0%	0.8%	2.3%	2.0%	10.6%	1.4%	12.6%	
Tannerellaceae_asv37	*p*	n.s.	0.000	0.004	0.000	0.004	0.000	0.000	**96**
	AIC	441	409	425	384	432	409	396	
	Dev (%)	0.8%	25.0%	22.7%	46.8%	9.8%	29.1%	42.6%	
Lachnospiraceae_asv39	*p*	0.005	0.020	n.s.	0.025	0.048	n.s.	0.036	**92**

	AIC	438	437	442	437	437	439	443	
	Dev (%)	7.1%	9.3%	5.0%	11.2%	12.7 %	10.8%	15.6%	
Rikenellaceae_asv40	*p*	n.s.	0.000	0.000	0.000	0.000	0.000	0.000	**99**
	AIC	429	363	401	358	399	359	357	
	Dev (%)	5.3%	49.4%	34.1 %	53.9%	32.4 %	50.0%	56.8%	
Rikenellaceae_asv41	*p*	n.s.	0.008	0.033	0.044	n.s.	0.016	0.016	**94**
	AIC	436	433	436	431	436	434	435	
	Dev (%)	5.5%	6.2%	4.1%	13.9%	8.2%	7.3%	17.5%	
Lachnospiraceae_asv42	*p*	0.003	n.s.	n.s.	0.014	0.006	n.s.	n.s.	**108**
	AIC	387	393	395	389	388	395	395	
	Dev (%)	8.0%	3.6%	1.2%	8.4%	8.9%	3.0%	14.5%	
Bacteroidaceae_asv43	*p*	n.s.	n.s.	n.s.	0.044	n.s.	n.s.	n.s.	**102**
	AIC	416	410	415	411	416	414	417	
	Dev (%)	1.0%	16.3%	1.2%	7.2%	2.3%	8.3%	12.7%	
Desulfovibrionaceae_asv 44	*p*	n.s.	0.001	0.001	0.002	0.002	0.001	0.000	**52**
	AIC	488	477	475	476	477	465	470	
	Dev (%)	0.0%	8.9%	10.8 %	11.1%	10.5 %	24.9%	25.6%	
Lactobacillaceae_asv46	*p*	n.s.	n.s.	0.013	n.s.	n.s.	0.024	0.002	**50**
	AIC	432	428	422	427	430	420	420	
	Dev (%)	0.4%	5.5%	11.2 %	13.3%	8.6%	18.6%	22.4%	
Muribaculaceae_asv47	*p*	0.040	0.000	0.000	0.000	0.000	0.000	0.000	**38**
	AIC	425	400	396	403	398	380	392	
	Dev (%)	17.9%	29.0%	33.9 %	28.8%	29.2 %	44.3%	41.1%	
Lachnospiraceae_asv48	*p*	n.s.	n.s.	n.s.	n.s.	n.s.	n.s.	n.s.	**108**
	AIC	363	364	363	362	363	364	369	
	Dev (%)	1.5%	0.5%	1.8%	3.9%	2.7%	4.9%	9.6%	
Lachnospiraceae_asv49	*p*	0.007	0.000	n.s.	0.000	0.031	0.000	0.001	**79**
	AIC	486	470	488	472	487	471	480	
	Dev (%)	6.4%	18.7%	9.0%	19.0%	8.4%	19.3%	23.5%	
Oscillospiraceae_asv50	*p*	n.s.	0.011	0.050	0.003	n.s.	0.023	0.007	**112**
	AIC	176	166	171	167	173	165	169	
	Dev (%)	1.1%	13.5%	6.9%	10.1%	4.9%	15.5%	19.4%	
Lachnospiraceae_asv51	*p*	n.s.	n.s.	n.s.	n.s.	n.s.	n.s.	n.s.	**106**
	AIC	380	381	380	382	381	382	388	
	Dev (%)	0.9%	0.5%	4.7%	1.0%	1.7%	1.0%	7.7%	
Lachnospiraceae_asv52	*p*	n.s.	n.s.	n.s.	n.s.	n.s.	n.s.	n.s.	**110**
	AIC	302	303	297	305	300	301	304	

	Dev (%)	2.3%	3.6%	7.4%	0.6%	9.9%	7.0%	12.4%	
Muribaculaceae_asv54	*p*	0.011	0.012	0.001	0.000	0.000	0.002	0.000	**106**
	AIC	359	363	353	338	346	351	344	
	Dev (%)	11.7%	5.6%	15.2 %	27.2%	25.0 %	21.3%	31.1%	
Lachnospiraceae_asv55	*p*	n.s.	0.000	0.003	0.004	0.012	0.006	0.005	**66**
	AIC	523	502	516	507	518	515	516	
	Dev (%)	3.5%	29.9%	7.6%	24.3%	7.8%	10.1%	20.0%	
Muribaculaceae_asv56	*p*	0.001	0.034	n.s.	0.000	0.002	0.009	0.000	**72**
	AIC	397	405	404	378	391	394	382	
	Dev (%)	10.1%	4.0%	7.4%	26.0%	23.9 %	20.7%	32.3%	
Lachnospiraceae_asv57	*p*	n.s.	n.s.	n.s.	n.s.	n.s.	n.s.	n.s.	**90**
	AIC	442	444	441	443	441	442	448	
	Dev (%)	2.1%	0.0%	3.1%	4.9%	4.9%	4.1%	10.7%	
Rikenellaceae_asv59	*p*	n.s.	0.001	n.s.	0.000	n.s.	0.010	0.003	**105**
	AIC	398	388	395	380	396	386	389	
	Dev (%)	1.0%	9.6%	4.8%	17.2%	4.7%	16.6%	21.3%	
Oscillospiraceae_asv61	*p*	n.s.	n.s.	n.s.	n.s.	n.s.	n.s.	n.s.	**112**
	AIC	190	189	192	190	193	192	199	
	Dev (%)	3.3%	5.5%	0.4%	7.1%	3.9%	3.4%	7.7%	
Bacteroidaceae_asv63	*p*	n.s.	n.s.	n.s.	n.s.	n.s.	n.s.	n.s.	**88**
	AIC	378	378	370	380	379	377	387	
	Dev (%)	0.4%	0.0%	15.0 %	0.4%	4.8%	7.1%	6.2%	
Lachnospiraceae_asv64	*p*	0.027	n.s.	n.s.	n.s.	n.s.	n.s.	n.s.	**110**
	AIC	282	282	286	282	284	284	289	
	Dev (%)	4.4%	5.2%	0.8%	7.1%	5.0%	5.4%	11.8%	
Muribaculaceae_asv65	*p*	n.s.	0.010	n.s.	0.013	n.s.	0.035	n.s.	**75**
	AIC	426	419	424	419	426	421	426	
	Dev (%)	1.0%	5.9%	1.6%	7.6%	2.4%	6.0%	13.0%	
Lactobacillaceae_asv66	*p*	n.s.	0.005	0.000	0.000	0.000	0.000	0.000	**42**
	AIC	400	394	364	386	369	360	361	
	Dev (%)	2.0%	7.0%	30.8 %	14.7%	31.0 %	37.1%	39.8%	
Lachnospiraceae_asv67	*p*	0.000	0.000	0.019	0.000	0.000	0.000	0.000	**106**
	AIC	336	337	366	329	339	341	339	
	Dev (%)	34.9%	36.5%	12.7 %	35.5%	29.6 %	33.1%	38.0%	
Lachnospiraceae_asv68	*p*	n.s.	0.010	n.s.	0.006	n.s.	n.s.	0.006	**55**
	AIC	428	418	425	414	426	421	419	
	Dev (%)	0.7%	11.2%	5.8%	17.8%	5.6%	11.0%	21.4%	

Rikenellaceae_asv70	*p*	n.s.	n.s.	n.s.	n.s.	n.s.	n.s.	n.s.	**40**
	AIC	501	501	501	503	503	503	515	
	Dev (%)	0.9%	0.1%	0.0%	0.1%	0.0%	0.2%	2.2%	
Oscillospiraceae_asv71	*p*	n.s.	0.000	0.023	0.001	0.026	0.001	0.015	**98**
	AIC	398	386	392	387	394	386	393	
	Dev (%)	1.0%	11.1%	7.3%	11.4%	6.5%	12.2%	17.6%	
Muribaculaceae_asv72	*p*	n.s.	n.s.	n.s.	n.s.	n.s.	n.s.	n.s.	**110**
	AIC	265	265	264	267	266	266	272	
	Dev (%)	0.0%	0.1%	0.3%	0.1%	0.6%	0.4%	8.4%	
Muribaculaceae_asv73	*p*	n.s.	0.000	0.013	0.000	n.s.	0.000	0.000	**38**
	AIC	378	359	369	359	375	360	361	
	Dev (%)	3.7%	18.9%	20.8 %	21.6%	14.1 %	19.5%	27.1%	
Erysipelotrichaceae_asv74	*p*	n.s.	n.s.	n.s.	0.039	n.s.	n.s.	0.003	**89**
	AIC	447	444	449	439	449	443	438	
	Dev (%)	2.4%	6.1%	0.1%	17.8%	3.7%	12.1%	21.3%	
Muribaculaceae_asv75	*p*	0.000	0.002	n.s.	0.000	0.000	0.003	0.000	**74**
	AIC	347	359	376	338	351	359	345	
	Dev (%)	31.6%	24.7%	1.7%	38.5%	21.6 %	22.5%	35.5%	
Ruminococcaceae_asv76	*p*	n.s.	n.s.	0.002	n.s.	0.009	0.029	0.009	**110**
	AIC	307	301	298	302	300	296	300	
	Dev (%)	0.1%	10.5%	8.2%	11.4%	8.4%	15.1%	18.8%	
Lachnospiraceae_asv78	*p*	n.s.	n.s.	n.s.	n.s.	n.s.	n.s.	n.s.	**54**
	AIC	506	506	504	508	506	505	514	
	Dev (%)	0.0%	0.2%	1.6%	0.2%	1.6%	2.7%	7.0%	
Streptococcaceae_asv79	*p*	0.000	0.011	n.s.	0.000	0.000	0.029	0.000	**83**
	AIC	347	402	408	335	341	403	338	
	Dev (%)	45.3%	21.6%	6.7%	53.7%	48.8 %	16.0%	56.6%	
Oscillospiraceae_asv80	*p*	n.s.	0.001	0.019	0.023	0.018	0.013	0.018	**107**
	AIC	317	298	308	305	310	304	311	
	Dev (%)	0.1%	23.8%	10.6 %	14.7%	7.1%	18.7%	17.3%	
Lachnospiraceae_asv82	*p*	n.s.	0.009	0.038	0.043	n.s.	n.s.	n.s.	**48**
	AIC	451	439	447	442	449	442	451	
	Dev (%)	0.6%	15.4%	3.9%	18.3%	4.3%	17.0%	15.4%	
Marinifilaceae_asv83	*p*	n.s.	0.000	0.000	0.000	0.002	0.000	0.000	**111**
	AIC	281	260	266	253	267	257	258	
	Dev (%)	0.2%	16.6%	12.3 %	23.4%	13.5 %	20.5%	29.7%	
Lachnospiraceae_asv84	*p*	n.s.	n.s.	n.s.	n.s.	n.s.	n.s.	n.s.	**52**

	AIC	441	441	440	440	442	439	441	
	Dev (%)	0.2%	3.3%	1.8%	10.1%	1.2%	8.3%	15.0%	
Oscillospiraceae_asv85	*p*	n.s.	0.000	n.s.	0.002	n.s.	0.002	0.020	**91**
	AIC	412	401	410	403	410	403	410	
	Dev (%)	2.0%	11.1%	5.1%	11.2%	10.1 %	11.2%	17.0%	
Lachnospiraceae_asv86	*p*	0.029	n.s.	n.s.	n.s.	0.040	n.s.	0.007	**84**
	AIC	407	410	413	410	403	412	406	
	Dev (%)	7.8%	12.0%	2.5%	7.5%	17.9 %	7.4%	19.3%	
Bacteroidaceae_asv87	*p*	0.000	0.000	0.003	0.000	0.000	0.000	0.000	**58**
	AIC	413	433	454	418	418	423	419	
	Dev (%)	44.4%	33.3%	13.0 %	39.3%	39.4 %	39.7%	43.6%	
Deferribacteraceae_asv88	*p*	n.s.	n.s.	n.s.	n.s.	n.s.	n.s.	n.s.	**89**
	AIC	431	430	430	432	432	432	437	
	Dev (%)	0.0%	0.9%	0.3%	0.8%	0.3%	1.1%	9.7%	
Lachnospiraceae_asv90	*p*	n.s.	0.000	0.000	0.000	0.000	0.000	0.000	**110**
	AIC	283	254	265	253	268	256	256	
	Dev (%)	8.9%	35.9%	26.0 %	35.1%	22.3 %	29.7%	36.3%	
Muribaculaceae_asv91	*p*	n.s.	0.000	0.005	0.000	0.019	0.000	0.000	**43**
	AIC	424	408	416	403	418	408	408	
	Dev (%)	0.0%	13.6%	6.9%	18.4%	7.1%	15.0%	25.0%	
Lachnospiraceae_asv94	*p*	n.s.	n.s.	n.s.	n.s.	n.s.	n.s.	n.s.	**96**
	AIC	391	390	391	392	393	392	401	
	Dev (%)	0.8%	2.1%	0.0%	1.9%	0.5%	1.3%	5.9%	
Oscillospiraceae_asv96	*p*	0.002	0.001	n.s.	0.001	0.010	0.004	0.002	**88**
	AIC	401	395	409	395	399	397	400	
	Dev (%)	8.7%	14.6%	2.3%	17.3%	13.9 %	15.8%	21.9%	
Peptostreptococcaceae_asv98	*p*	0.001	0.001	n.s.	0.000	0.004	0.001	0.000	**93**
	AIC	398	399	408	391	397	391	394	
	Dev (%)	15.2%	12.9%	10.5 %	27.2%	23.5 %	25.8%	27.5%	
Lachnospiraceae_asv99	*p*	n.s.	n.s.	n.s.	n.s.	n.s.	n.s.	n.s.	**49**
	AIC	470	471	467	464	469	472	473	
	Dev (%)	1.5%	0.4%	11.7 %	16.7%	8.5%	1.3%	11.8%	
Lachnospiraceae_asv100	*p*	n.s.	0.001	0.000	0.001	0.000	0.000	0.000	**55**
	AIC	444	430	425	424	421	422	418	
	Dev (%)	4.0%	15.0%	17.3 %	27.5%	27.6 %	21.8%	32.8%	
Lachnospiraceae_asv101	*p*	0.002	n.s.	0.021	0.000	0.000	n.s.	0.000	**91**

	AIC	367	376	371	349	364	372	356	
	Dev (%)	11.5%	9.5%	9.9%	25.7%	14.8 %	13.3%	29.7%	
Rikenellaceae_asv102	*p*	n.s.	n.s.	n.s.	n.s.	n.s.	n.s.	n.s.	**63**
	AIC	460	464	464	462	465	466	470	
	Dev (%)	14.3%	0.8%	1.1%	4.3%	2.2%	2.4%	9.7%	
Lachnospiraceae_asv103	*p*	n.s.	n.s.	n.s.	0.010	0.034	n.s.	0.000	**76**
	AIC	426	424	428	417	420	425	414	
	Dev (%)	5.7%	11.4%	3.7%	18.7%	17.5 %	8.1%	25.3%	
Lachnospiraceae_asv104	*p*	0.002	0.007	0.029	0.005	0.003	n.s.	0.009	**84**
	AIC	396	398	399	395	391	399	400	
	Dev (%)	11.2%	9.9%	11.0 %	14.8%	21.2 %	13.7%	18.9%	
Lachnospiraceae_asv107	*p*	n.s.	n.s.	n.s.	n.s.	n.s.	n.s.	n.s.	**60**
	AIC	452	449	452	453	452	452	457	
	Dev (%)	0.9%	5.4%	6.6%	2.8%	2.2%	3.1%	10.3%	
Lachnospiraceae_asv108	*p*	n.s.	0.000	0.000	0.000	0.000	0.000	0.000	**90**
	AIC	393	364	368	353	370	355	353	
	Dev (%)	0.9%	23.9%	20.5 %	34.3%	22.1 %	32.2%	39.4%	
Lachnospiraceae_asv109	*p*	n.s.	n.s.	n.s.	n.s.	n.s.	n.s.	n.s.	**83**
	AIC	387	385	387	386	389	387	396	
	Dev (%)	7.0%	7.9%	0.4%	13.9%	0.5%	10.1%	8.4%	
Muribaculaceae_asv111	*p*	n.s.	0.002	0.001	0.000	0.001	0.001	0.000	**88**
	AIC	348	338	339	324	338	335	327	
	Dev (%)	2.3%	11.5%	9.7%	22.3%	12.7 %	16.0%	29.5%	
Muribaculaceae_asv112	*p*	n.s.	n.s.	n.s.	n.s.	n.s.	n.s.	n.s.	**78**
	AIC	421	424	423	426	423	424	430	
	Dev (%)	4.4%	0.4%	2.1%	0.5%	6.2%	2.4%	9.4%	
Oscillospiraceae_asv113	*p*	n.s.	0.032	n.s.	n.s.	n.s.	n.s.	n.s.	**107**
	AIC	297	290	296	296	299	298	306	
	Dev (%)	6.6%	17.6%	8.7%	12.4%	3.1%	6.6%	8.3%	
Lachnospiraceae_asv114	*p*	n.s.	0.000	n.s.	0.000	n.s.	0.001	0.002	**51**
	AIC	393	375	390	374	388	377	382	
	Dev (%)	0.2%	15.7%	2.8%	17.4%	10.6 %	15.6%	21.6%	
Ruminococcaceae_asv115	*p*	n.s.	n.s.	n.s.	n.s.	n.s.	n.s.	n.s.	**38**
	AIC	455	453	454	454	456	455	460	
	Dev (%)	0.1%	4.3%	1.2%	6.6%	1.3%	4.6%	9.4%	
Lachnospiraceae_asv116	*p*	0.000	0.000	n.s.	0.000	0.000	0.000	0.000	**71**
	AIC	357	403	420	358	355	387	355	

	Dev (%)	46.2%	27.0%	10.9 %	46.7%	48.1 %	36.5%	54.3%	
Muribaculaceae_asv117	*p*	n.s.	n.s.	n.s.	n.s.	n.s.	n.s.	n.s.	**107**
	AIC	248	246	247	249	249	248	258	
	Dev (%)	0.3%	3.4%	1.9%	3.5%	1.2%	5.0%	5.4%	
Lachnospiraceae_asv118	*p*	0.000	n.s.	0.038	0.003	0.000	0.009	0.015	**84**
	AIC	384	396	393	386	380	390	391	
	Dev (%)	11.3%	1.2%	3.9%	12.1%	15.9 %	8.3%	19.1%	
Lachnospiraceae_asv120	*p*	n.s.	0.002	n.s.	0.001	n.s.	0.018	0.002	**58**
	AIC	423	413	420	411	421	411	411	
	Dev (%)	0.1%	8.8%	3.3%	12.3%	4.1%	16.8%	22.4%	
Lachnospiraceae_asv121	*p*	n.s.	n.s.	n.s.	n.s.	n.s.	n.s.	n.s.	**43**
	AIC	365	367	368	365	367	369	377	
	Dev (%)	2.2%	0.3%	0.1%	4.3%	2.3%	0.3%	6.5%	
Lachnospiraceae_asv122	*p*	n.s.	0.006	0.008	0.013	0.028	0.005	n.s.	**66**
	AIC	394	386	387	387	389	386	397	
	Dev (%)	0.1%	6.7%	6.3%	7.6%	6.4%	9.1%	11.1%	
Lachnospiraceae_asv124	*p*	n.s.	n.s.	n.s.	n.s.	n.s.	n.s.	n.s.	**59**
	AIC	453	451	452	454	453	446	453	
	Dev (%)	0.3%	10.1%	1.7%	8.3%	3.6%	14.5%	15.0%	
Lachnospiraceae_asv130	*p*	n.s.	n.s.	n.s.	n.s.	n.s.	n.s.	n.s.	**73**
	AIC	421	420	419	421	421	420	430	
	Dev (%)	0.6%	1.7%	2.5%	2.4%	2.6%	3.0%	6.9%	
Lachnospiraceae_asv131	*p*	0.005	0.000	0.001	0.000	0.000	0.000	0.000	**80**
	AIC	430	390	420	392	420	390	393	
	Dev (%)	7.9%	35.6%	22.7 %	35.6%	18.7 %	37.8%	42.5%	
Oscillospiraceae_asv132	*p*	n.s.	n.s.	n.s.	n.s.	n.s.	n.s.	n.s.	**61**
	AIC	447	446	447	446	449	448	456	
	Dev (%)	0.3%	1.5%	7.8%	2.9%	0.4%	1.5%	6.4%	
Lachnospiraceae_asv133	*p*	0.011	0.010	0.032	0.012	0.002	0.009	n.s.	**74**
	AIC	412	412	409	411	407	411	418	
	Dev (%)	5.7%	5.8%	14.5 %	7.8%	11.1 %	8.3%	13.8%	
Muribaculaceae_asv134	*p*	n.s.	n.s.	n.s.	n.s.	n.s.	n.s.	n.s.	**56**
	AIC	398	400	399	400	399	400	409	
	Dev (%)	1.9%	0.1%	1.1%	2.1%	3.2%	1.7%	6.3%	
Lachnospiraceae_asv135	*p*	0.008	0.000	n.s.	0.000	0.025	0.000	0.000	**80**
	AIC	405	394	414	397	412	394	400	
	Dev (%)	18.6%	20.9%	6.5%	21.6%	8.2%	27.3%	26.6%	

Lachnospiraceae_ Eubacterium_asv137	*p*	0.002	n.s.	0.024	0.000	0.000	0.000	0.000	**61**
	AIC	445	448	447	428	439	431	423	
	Dev (%)	8.8%	8.0%	7.9%	26.9%	14.9 %	27.4%	34.7%	
Lachnospiraceae_asv138	*p*	0.034	0.037	n.s.	0.049	n.s.	n.s.	n.s.	**62**
	AIC	420	420	424	420	421	422	431	
	Dev (%)	4.0%	3.9%	0.4%	5.4%	4.3%	3.9%	7.7%	
Oscillospiraceae_asv140	*p*	0.000	0.000	0.006	0.000	0.000	0.000	0.000	**87**
	AIC	388	388	390	383	389	383	384	
	Dev (%)	13.9%	14.2%	20.9 %	19.2%	14.5 %	23.5%	27.9%	
Eubacterium_asv141	*p*	n.s.	0.000	0.029	0.000	n.s.	0.001	0.002	**68**
	AIC	398	381	391	382	395	377	389	
	Dev (%)	2.2%	16.2%	12.0 %	16.4%	12.7 %	28.2%	21.9%	
Lachnospiraceae_asv142	*p*	n.s.	0.039	n.s.	n.s.	n.s.	n.s.	0.011	**96**
	AIC	381	373	379	376	376	375	374	
	Dev (%)	0.0%	8.9%	1.6%	9.9%	9.8%	9.5%	18.4%	
Sutterellaceae_asv143	*p*	n.s.	n.s.	n.s.	n.s.	n.s.	n.s.	n.s.	**38**
	AIC	332	335	333	334	333	336	340	
	Dev (%)	3.7%	0.0%	3.6%	2.2%	5.2%	2.7%	8.9%	
Muribaculaceae_asv144	*p*	n.s.	n.s.	n.s.	n.s.	n.s.	n.s.	n.s.	**84**
	AIC	347	345	346	346	348	347	359	
	Dev (%)	2.7%	1.7%	3.0%	2.1%	2.1%	1.7%	3.5%	
Peptococcaceae_asv146	*p*	n.s.	0.000	0.009	0.000	0.019	0.000	0.000	**96**
	AIC	342	318	335	319	334	319	323	
	Dev (%)	2.3%	21.5%	9.2%	24.1%	14.9 %	22.5%	29.4%	
Oscillospiraceae_asv147	*p*	0.000	0.001	n.s.	0.001	0.004	0.012	0.004	**81**
	AIC	391	391	399	388	387	392	394	
	Dev (%)	11.0%	10.3%	11.3 %	15.2%	22.5 %	13.6%	20.4%	
Lachnospiraceae_asv152	*p*	0.031	0.000	0.001	0.000	0.000	0.000	0.000	**108**
	AIC	277	250	267	249	262	246	254	
	Dev (%)	7.0%	29.2%	17.1 %	32.6%	23.8 %	37.1%	34.3%	
Lachnospiraceae_asv154	*p*	n.s.	0.049	n.s.	n.s.	n.s.	n.s.	0.028	**84**
	AIC	409	402	406	402	407	405	405	
	Dev (%)	0.3%	9.7%	2.9%	11.4%	6.6%	8.8%	16.7%	
Ruminococcaceae_asv155	*p*	0.020	n.s.	n.s.	n.s.	0.040	n.s.	n.s.	**61**
	AIC	412	417	416	413	413	418	420	
	Dev (%)	4.9%	1.0%	1.1%	5.3%	5.7%	1.1%	11.7%	

Lachnospiraceae_asv157	*p*	n.s.	n.s.	n.s.	n.s.	n.s.	n.s.	n.s.	**91**
	AIC	373	375	374	373	374	372	380	
	Dev (%)	1.9%	0.1%	4.6%	3.2%	2.2%	12.6%	9.4%	
Lachnospiraceae_asv158	*p*	n.s.	n.s.	n.s.	n.s.	n.s.	n.s.	n.s.	**99**
	AIC	315	316	316	317	316	316	325	
	Dev (%)	2.4%	0.9%	0.6%	1.1%	5.3%	2.4%	7.0%	
Lachnospiraceae_asv159	*p*	n.s.	n.s.	0.010	n.s.	n.s.	n.s.	0.048	**60**
	AIC	424	424	410	425	424	421	421	
	Dev (%)	0.0%	0.2%	20.9 %	0.4%	4.7%	11.8%	16.0%	
Oscillospiraceae_asv161	*p*	0.004	n.s.	n.s.	0.014	0.009	n.s.	n.s.	**81**
	AIC	396	404	402	398	397	404	406	
	Dev (%)	7.4%	1.0%	10.8 %	7.5%	8.4%	6.0%	13.2%	
Oscillospiraceae_asv163	*p*	0.036	0.006	n.s.	0.015	0.040	0.022	n.s.	**61**
	AIC	424	421	422	422	424	423	431	
	Dev (%)	3.9%	6.6%	12.0 %	7.4%	5.7%	6.8%	10.9%	
Lachnospiraceae_asv165	*p*	0.000	0.000	0.016	0.000	0.000	0.000	0.000	**62**
	AIC	271	249	283	246	262	251	254	
	Dev (%)	17.6%	32.3%	13.8 %	35.3%	25.4 %	32.7%	39.1%	
Clostridiaceae_asv167	*p*	0.000	n.s.	n.s.	0.004	0.003	n.s.	0.000	**47**
	AIC	454	463	466	453	450	464	449	
	Dev (%)	11.3%	5.2%	0.9%	16.7%	20.2 %	5.6%	26.3%	
Muribaculaceae_asv168	*p*	n.s.	0.007	n.s.	0.019	n.s.	0.025	n.s.	**43**
	AIC	388	386	393	388	384	388	396	
	Dev (%)	10.6%	6.4%	0.5%	7.0%	18.9 %	6.5%	11.3%	
Lachnospiraceae_asv169	*p*	0.000	0.002	0.034	0.000	0.000	0.006	0.001	**100**
	AIC	290	306	307	291	292	300	301	
	Dev (%)	23.8%	8.5%	12.3 %	21.3%	22.1 %	19.4%	23.8%	
Ruminococcaceae_asv174	*p*	n.s.	n.s.	n.s.	n.s.	n.s.	0.009	0.038	**77**
	AIC	381	375	380	377	379	366	378	
	Dev (%)	0.1%	7.4%	1.3%	8.7%	12.4 %	22.2%	15.5%	
Lachnospiraceae_asv176	*p*	0.005	0.004	n.s.	0.002	0.008	0.025	0.009	**63**
	AIC	381	383	390	381	384	381	384	
	Dev (%)	10.0%	7.1%	2.9%	10.7%	8.6%	15.7%	18.8%	
Lachnospiraceae_asv179	*p*	0.006	0.000	0.031	0.000	0.013	0.000	0.000	**48**
	AIC	385	366	390	341	386	368	352	
	Dev (%)	20.5%	31.0%	15.5 %	47.3%	20.8 %	31.5%	43.8%	
Desulfovibrionaceae_	*p*	0.000	0.027	0.034	0.002	0.000	0.001	0.000	**106**

asv180									
	AIC	268	275	275	267	266	264	265	
	Dev (%)	12.9%	9.6%	9.3%	16.9%	15.6 %	20.9%	26.3%	
Lachnospiraceae_asv181	*p*	0.027	0.048	n.s.	0.000	n.s.	n.s.	0.000	**65**
	AIC	453	452	455	433	455	451	423	
	Dev (%)	4.4%	6.1%	11.7 %	24.5%	4.4%	11.4%	36.2%	
Lachnospiraceae_asv185	*p*	n.s.	n.s.	n.s.	n.s.	n.s.	n.s.	n.s.	**63**
	AIC	429	432	432	431	429	432	434	
	Dev (%)	3.8%	0.8%	0.2%	3.2%	6.9%	2.5%	12.0%	
Oscillospiraceae_asv186	*p*	0.003	0.000	0.000	0.005	0.000	0.001	0.000	**81**
	AIC	360	361	354	358	347	354	350	
	Dev (%)	13.7%	10.7%	21.7 %	21.4%	30.1 %	22.9%	30.7%	
Bacteroidaceae_asv187	*p*	n.s.	0.007	0.015	0.016	0.036	0.012	0.009	**79**
	AIC	300	289	294	291	293	288	295	
	Dev (%)	3.0%	16.9%	8.9%	20.0%	14.4 %	22.0%	20.6%	
Rikenellaceae_asv188	*p*	n.s.	n.s.	n.s.	n.s.	n.s.	n.s.	n.s.	**92**
	AIC	246	245	251	248	250	247	255	
	Dev (%)	12.2%	9.9%	7.7%	7.5%	3.6%	9.5%	11.5%	
Lachnospiraceae_asv190	*p*	n.s.	n.s.	n.s.	n.s.	n.s.	n.s.	n.s.	**38**
	AIC	409	409	409	411	410	411	414	
	Dev (%)	0.2%	4.1%	0.1%	0.3%	3.7%	0.6%	11.2%	
Lachnospiraceae_asv191	*p*	0.010	0.002	0.001	0.006	0.001	0.000	0.001	**87**
	AIC	329	320	323	319	315	319	320	
	Dev (%)	5.9%	18.2%	10.6 %	23.6%	23.1 %	15.3%	24.8%	
Lachnospiraceae_asv193	*p*	n.s.	n.s.	n.s.	n.s.	n.s.	n.s.	n.s.	**40**
	AIC	385	385	385	387	385	383	392	
	Dev (%)	1.4%	2.6%	2.4%	4.3%	5.8%	11.4%	10.4%	
Rikenellaceae_asv194	*p*	n.s.	n.s.	n.s.	n.s.	n.s.	n.s.	n.s.	**58**
	AIC	308	311	310	309	309	312	318	
	Dev (%)	2.8%	0.0%	1.0%	3.4%	3.6%	1.1%	8.5%	
Ruminococcaceae_asv196	*p*	n.s.	n.s.	n.s.	n.s.	n.s.	n.s.	n.s.	**38**
	AIC	405	403	405	406	407	405	412	
	Dev (%)	0.6%	4.1%	0.8%	4.8%	1.3%	5.5%	8.9%	
Oscillospiraceae_asv201	*p*	n.s.	n.s.	n.s.	n.s.	n.s.	n.s.	n.s.	**48**
	AIC	403	401	403	403	405	399	402	
	Dev (%)	1.2%	3.2%	0.2%	2.8%	0.7%	11.0%	14.6%	
Lachnospiraceae_asv202	*p*	n.s.	0.001	n.s.	0.001	0.021	0.001	0.023	**66**

	AIC	398	386	390	386	392	386	394	
	Dev (%)	0.0%	9.9%	13.3 %	11.9%	6.9%	11.9%	16.7%	
Eggerthellaceae_asv203	*p*	n.s.	n.s.	n.s.	n.s.	0.027	n.s.	n.s.	**48**
	AIC	309	315	315	317	304	317	319	
	Dev (%)	10.5%	0.1%	3.9%	2.0%	19.6 %	0.1%	11.1%	
Lachnospiraceae_asv204	*p*	0.040	0.024	n.s.	0.038	n.s.	n.s.	0.042	**63**
	AIC	366	365	364	365	367	360	368	
	Dev (%)	3.8%	4.8%	11.3 %	5.8%	5.5%	15.0%	15.2%	
Lachnospiraceae_asv205	*p*	n.s.	0.000	n.s.	0.000	0.037	0.000	0.000	**76**
	AIC	394	372	392	374	392	374	381	
	Dev (%)	3.0%	20.4%	11.7 %	20.6%	6.7%	20.4%	25.2%	
Oscillospiraceae_asv206	*p*	n.s.	n.s.	n.s.	n.s.	n.s.	n.s.	n.s.	**83**
	AIC	345	346	349	347	347	348	354	
	Dev (%)	17.2%	4.2%	1.2%	5.4%	6.2%	4.9%	10.6%	
Lachnospiraceae_asv208	*p*	n.s.	n.s.	n.s.	n.s.	n.s.	n.s.	n.s.	**62**
	AIC	398	395	397	395	398	397	399	
	Dev (%)	0.1%	3.1%	1.1%	4.7%	5.2%	3.2%	13.0%	
Lachnospiraceae_asv211	*p*	0.009	0.016	0.010	0.001	0.007	n.s.	0.002	**97**
	AIC	280	281	280	271	278	285	280	
	Dev (%)	16.1%	19.1%	21.1 %	26.4%	21.9 %	10.9%	23.9%	
Oscillospiraceae_asv212	*p*	0.011	0.021	n.s.	0.006	0.011	n.s.	0.050	**79**
	AIC	370	375	374	372	373	374	378	
	Dev (%)	11.4%	4.7%	12.9 %	9.0%	8.6%	10.5%	14.8%	
Lachnospiraceae_asv213	*p*	0.002	n.s.	0.003	0.000	0.000	n.s.	0.003	**64**
	AIC	431	440	433	422	422	433	430	
	Dev (%)	8.6%	1.5%	7.6%	17.3%	17.1 %	14.1%	22.1%	
Lachnospiraceae_asv214	*p*	0.000	0.013	0.035	0.002	0.000	0.000	0.003	**47**
	AIC	373	380	378	374	371	372	376	
	Dev (%)	11.2%	5.5%	14.2 %	12.4%	14.6 %	14.1%	21.0%	
Lachnospiraceae_asv215	*p*	0.032	0.003	n.s.	0.000	0.003	0.004	0.001	**41**
	AIC	345	340	342	323	340	340	335	
	Dev (%)	4.1%	8.0%	14.2 %	22.3%	10.1 %	9.6%	24.2%	
Peptococcaceae_asv218	*p*	n.s.	0.036	n.s.	n.s.	n.s.	n.s.	n.s.	**97**
	AIC	297	293	295	296	297	295	302	
	Dev (%)	2.8%	7.9%	6.3%	10.6%	5.5%	9.6%	11.9%	
Peptostreptococcaceae_ asv219	*p*	0.011	0.001	n.s.	0.002	0.002	0.002	0.000	**51**
	AIC	416	403	421	403	403	403	401	

	Dev (%)	5.7%	20.0%	1.7%	24.9%	22.3 %	23.7%	29.0%	
Lachnospiraceae_asv221	*p*	0.032	0.000	0.043	0.001	0.012	0.001	0.001	**49**
	AIC	415	397	413	400	412	399	406	
	Dev (%)	4.1%	19.9%	6.8%	20.2%	7.8%	21.4%	23.5%	
Lachnospiraceae_asv223	*p*	0.002	0.044	n.s.	0.000	0.003	n.s.	0.000	**60**
	AIC	350	360	360	334	349	358	338	
	Dev (%)	12.8%	3.6%	4.8%	24.6%	16.1 %	11.0%	31.2%	
Eggerthellaceae_asv230	*p*	n.s.	n.s.	n.s.	0.021	n.s.	n.s.	0.012	**57**
	AIC	327	330	326	320	328	332	324	
	Dev (%)	4.9%	1.9%	12.5 %	18.0%	11.8 %	1.9%	19.9%	
Oscillospiraceae_asv231	*p*	0.011	0.001	n.s.	0.002	n.s.	0.002	0.008	**76**
	AIC	350	350	355	351	353	352	355	
	Dev (%)	18.4%	10.4%	12.9 %	10.7%	17.6 %	10.5%	19.0%	
Muribaculaceae_asv232	*p*	0.018	0.029	0.004	0.000	0.003	0.022	0.000	**84**
	AIC	308	306	304	291	297	303	293	
	Dev (%)	5.0%	9.0%	8.1%	23.3%	19.1 %	14.3%	28.3%	
Muribaculaceae_asv235	*p*	0.016	n.s.	n.s.	0.026	0.029	n.s.	n.s.	**39**
	AIC	258	263	266	260	260	264	271	
	Dev (%)	6.7%	2.4%	0.4%	6.5%	6.3%	3.0%	9.7%	
Lachnospiraceae_asv237	*p*	n.s.	0.004	0.008	0.022	0.005	0.002	0.000	**45**
	AIC	372	365	363	362	359	363	357	
	Dev (%)	2.7%	7.5%	11.4 %	17.8%	18.0 %	11.0%	25.3%	
Lachnospiraceae_asv238	*p*	0.001	n.s.	n.s.	0.012	0.002	n.s.	0.020	**61**
	AIC	352	361	359	352	352	360	358	
	Dev (%)	9.6%	9.7%	4.6%	21.1%	11.3 %	4.3%	17.1%	
Lachnospiraceae_asv239	*p*	0.000	0.001	0.015	0.000	0.000	0.013	0.001	**42**
	AIC	308	320	321	311	310	318	315	
	Dev (%)	26.0%	9.6%	10.9 %	19.8%	21.6 %	17.3%	24.6%	
Lachnospiraceae_asv241	*p*	n.s.	0.000	n.s.	0.000	n.s.	0.000	0.001	**53**
	AIC	350	339	355	341	351	332	338	
	Dev (%)	5.5%	13.4%	0.4%	13.6%	8.1%	22.9%	26.3%	
Oscillospiraceae_asv242	*p*	n.s.	n.s.	0.028	0.013	n.s.	n.s.	0.006	**46**
	AIC	355	350	351	343	353	347	347	
	Dev (%)	0.7%	7.1%	4.3%	21.7%	4.9%	14.9%	19.8%	
Lachnospiraceae_asv243	*p*	n.s.	n.s.	0.003	n.s.	0.010	0.016	0.022	**75**
	AIC	337	336	328	338	330	325	332	
	Dev (%)	0.7%	4.4%	8.0%	7.0%	8.1%	18.4%	18.8%	

Oscillospiraceae_asv246	*p*	0.014	0.021	n.s.	0.020	n.s.	n.s.	0.018	**86**
	AIC	300	301	306	301	302	303	301	
	Dev (%)	5.4%	4.8%	0.4%	6.9%	5.8%	4.8%	17.3%	
Lachnospiraceae_asv250	*p*	n.s.	n.s.	n.s.	n.s.	0.040	0.041	n.s.	**64**
	AIC	357	356	361	355	352	356	363	
	Dev (%)	8.9%	9.0%	0.0%	17.4%	19.7 %	5.7%	11.5%	
Lachnospiraceae_asv254	*p*	n.s.	0.007	0.001	n.s.	0.006	0.005	0.012	**72**
	AIC	329	324	312	324	317	322	325	
	Dev (%)	3.3%	6.5%	23.2 %	12.5%	23.7 %	9.3%	18.1%	
Ruminococcaceae_asv257	*p*	n.s.	n.s.	n.s.	n.s.	n.s.	n.s.	n.s.	**90**
	AIC	312	312	314	313	314	307	320	
	Dev (%)	1.9%	2.8%	0.2%	3.1%	1.9%	16.8%	8.9%	
Oscillospiraceae_asv261	*p*	n.s.	n.s.	n.s.	n.s.	n.s.	n.s.	n.s.	**53**
	AIC	370	366	367	370	369	366	370	
	Dev (%)	0.0%	7.8%	4.5%	4.6%	7.5%	12.0%	14.2%	
Lachnospiraceae_asv262	*p*	n.s.	n.s.	n.s.	n.s.	n.s.	n.s.	n.s.	**45**
	AIC	352	352	352	354	353	353	363	
	Dev (%)	6.4%	1.6%	2.1%	1.6%	2.4%	2.6%	6.0%	
Oscillospiraceae_asv267	*p*	0.027	0.029	n.s.	n.s.	n.s.	0.023	n.s.	**43**
	AIC	208	212	217	213	215	211	222	
	Dev (%)	18.7%	4.3%	0.3%	5.0%	4.0%	6.7%	9.2%	
Oscillospirales_asv269	*p*	n.s.	n.s.	0.046	0.010	n.s.	0.034	0.007	**50**
	AIC	303	301	303	294	300	302	299	
	Dev (%)	6.8%	10.9%	3.6%	17.1%	11.5 %	6.0%	19.2%	
Rhodospirillales_asv270	*p*	n.s.	0.008	n.s.	0.004	n.s.	0.046	0.000	**43**
	AIC	295	286	292	281	292	288	276	
	Dev (%)	2.0%	10.3%	4.9%	18.0%	8.4%	11.7%	27.5%	
Lachnospiraceae_asv272	*p*	n.s.	0.016	0.002	0.004	0.001	0.001	0.007	**76**
	AIC	320	315	306	311	308	308	313	
	Dev (%)	0.6%	5.2%	15.3 %	9.6%	12.3 %	12.2%	19.5%	
Ruminococcaceae_asv276	*p*	0.007	n.s.	n.s.	0.007	0.007	n.s.	n.s.	**53**
	AIC	290	300	302	296	296	302	306	
	Dev (%)	20.7%	4.4%	3.3%	8.6%	8.6%	7.0%	12.1%	
Gastranaerophilales_asv279	*p*	n.s.	0.000	0.000	0.000	0.002	0.000	0.000	**74**
	AIC	322	310	314	299	308	307	301	

	Dev (%)	5.9%	14.0%	11.1 %	23.3%	21.8 %	17.7%	31.5%	
Oscillospiraceae_asv283	*p*	n.s.	n.s.	n.s.	n.s.	n.s.	n.s.	n.s.	**66**
	AIC	310	313	310	311	311	312	320	
	Dev (%)	10.7%	0.1%	4.5%	3.0%	4.2%	6.9%	7.9%	
Muribaculaceae_asv286	*p*	n.s.	0.016	0.001	0.001	0.002	0.003	0.022	**45**
	AIC	210	205	201	200	201	201	207	
	Dev (%)	1.7%	5.2%	9.1%	11.6%	10.8 %	10.3%	16.8%	
Anaerovoracaceae_ Eubacterium_asv289	*p*	0.000	n.s.	0.027	0.000	0.000	0.005	0.000	**57**
	AIC	223	243	240	226	220	233	224	
	Dev (%)	20.9%	7.4%	9.6%	22.1%	23.2 %	18.4%	30.4%	
Ruminococcaceae_asv290	*p*	0.028	0.013	n.s.	n.s.	n.s.	0.030	0.032	**62**
	AIC	274	272	278	273	274	273	275	
	Dev (%)	4.3%	5.5%	0.8%	12.0%	8.7%	6.2%	15.9%	
Lachnospiraceae_asv292	*p*	n.s.	0.002	n.s.	0.002	n.s.	0.015	0.001	**49**
	AIC	303	297	302	288	301	298	292	
	Dev (%)	4.7%	8.2%	4.1%	20.6%	9.7%	9.5%	23.6%	
Lachnospiraceae_asv296	*p*	0.000	0.009	n.s.	0.000	0.000	0.010	0.000	**58**
	AIC	335	355	366	335	329	352	343	
	Dev (%)	25.0%	17.8%	2.6%	31.4%	37.1 %	22.6%	31.4%	
Lachnospiraceae_asv299	*p*	n.s.	n.s.	n.s.	n.s.	n.s.	n.s.	n.s.	**50**
	AIC	301	303	301	303	303	302	310	
	Dev (%)	2.6%	1.0%	8.4%	2.6%	2.6%	9.4%	8.1%	
Ruminococcaceae_asv301	*p*	n.s.	n.s.	n.s.	n.s.	n.s.	n.s.	n.s.	**47**
	AIC	272	275	275	273	274	269	277	
	Dev (%)	4.3%	0.7%	3.5%	5.9%	6.1%	15.6%	12.3%	
Clostridia_asv303	*p*	0.025	0.010	0.002	0.007	0.000	0.005	0.005	**47**
	AIC	291	286	286	281	282	282	287	
	Dev (%)	5.7%	12.4%	9.6%	20.8%	14.2 %	18.0%	21.5%	
Oscillospiraceae_asv305	*p*	0.019	n.s.	n.s.	n.s.	n.s.	n.s.	0.025	**71**
	AIC	322	323	321	323	319	323	323	
	Dev (%)	4.9%	5.4%	7.0%	6.4%	12.5 %	9.9%	16.5%	
Lachnospiraceae_asv312	*p*	0.029	n.s.	n.s.	n.s.	n.s.	n.s.	n.s.	**59**
	AIC	285	294	293	291	292	295	299	
	Dev (%)	18.5%	0.3%	4.7%	5.1%	4.1%	1.1%	10.1%	
Butyricicoccaceae_asv318	*p*	0.001	0.000	0.002	0.000	0.001	0.000	0.000	**58**

	AIC	254	246	259	245	254	243	245	
	Dev (%)	26.1%	22.7%	15.0 %	25.2%	20.0 %	29.2%	32.6%	
Rikenellaceae_asv319	*p*	0.016	n.s.	0.001	0.004	0.000	0.016	0.001	**39**
	AIC	271	275	259	260	255	263	261	
	Dev (%)	5.2%	1.3%	23.1 %	23.4%	28.6 %	19.0%	26.0%	
Anaerovoracaceae_asv320	*p*	n.s.	0.000	0.004	0.000	n.s.	0.000	0.000	**71**
	AIC	244	212	232	210	243	223	217	
	Dev (%)	5.9%	36.0%	23.0 %	35.8%	8.7%	21.4%	34.3%	
Lachnospiraceae_asv325	*p*	0.000	n.s.	n.s.	0.000	0.005	n.s.	0.002	**43**
	AIC	280	295	297	282	282	299	285	
	Dev (%)	15.7%	9.2%	0.1%	14.2%	17.3 %	0.6%	22.1%	

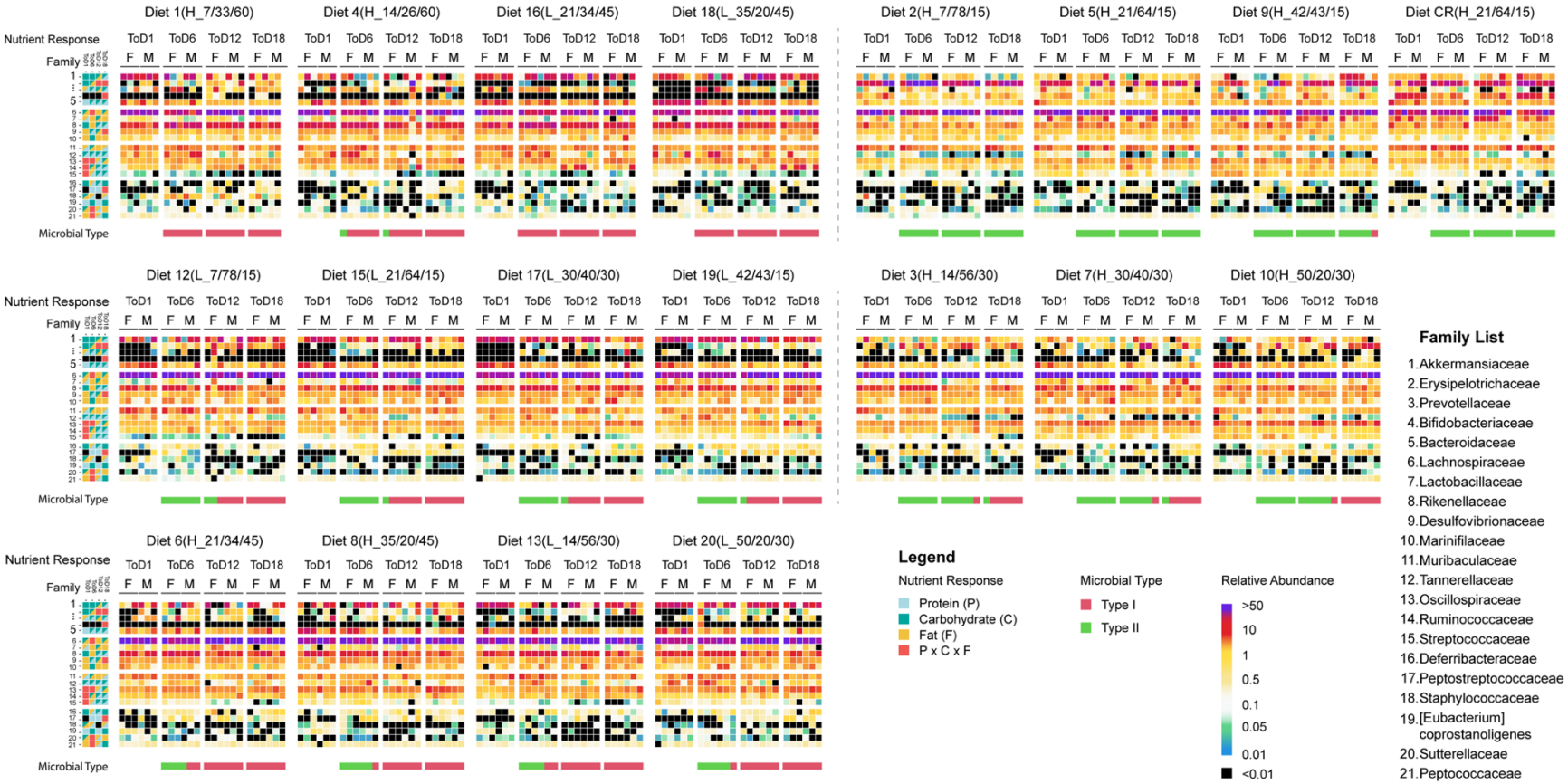

Supplementary Figure 7-17. The relative abundance of microbes in associate with nutrient response change and microbial type shift over age at family level.

In each panel, the first 4 columns are the best model fit resulted from the GAM modelling at each timepoints. From left to right are ToD1, ToD6, ToD12 and ToD18. The number on the left are the family listed in the legend. Color indicates best model fit to a single nutrient (single colored squares), an interaction of two nutrients (diagonally splitted coloured squares) or the interaction of all three nutrients (red colored single square). Full model statistics are in appendix. The rest of the columns are the heatmap of relative abundance of these family in each diet. In each diet, the samples were arranged by first by time on diet then by the mice gender. The missing samples that were under detection threshold were shown as black. The bottom row in each panel is the microbial community type. Each bar represents 6 mice in each diet at each timepoint. Color indicates the community types, type I (red) and type II (green). The size of the bar indicates the number of mice under specific community type (See also Figure 3-9). The position of the bar does not correlates to the individual mouse showing the relative abundance above.

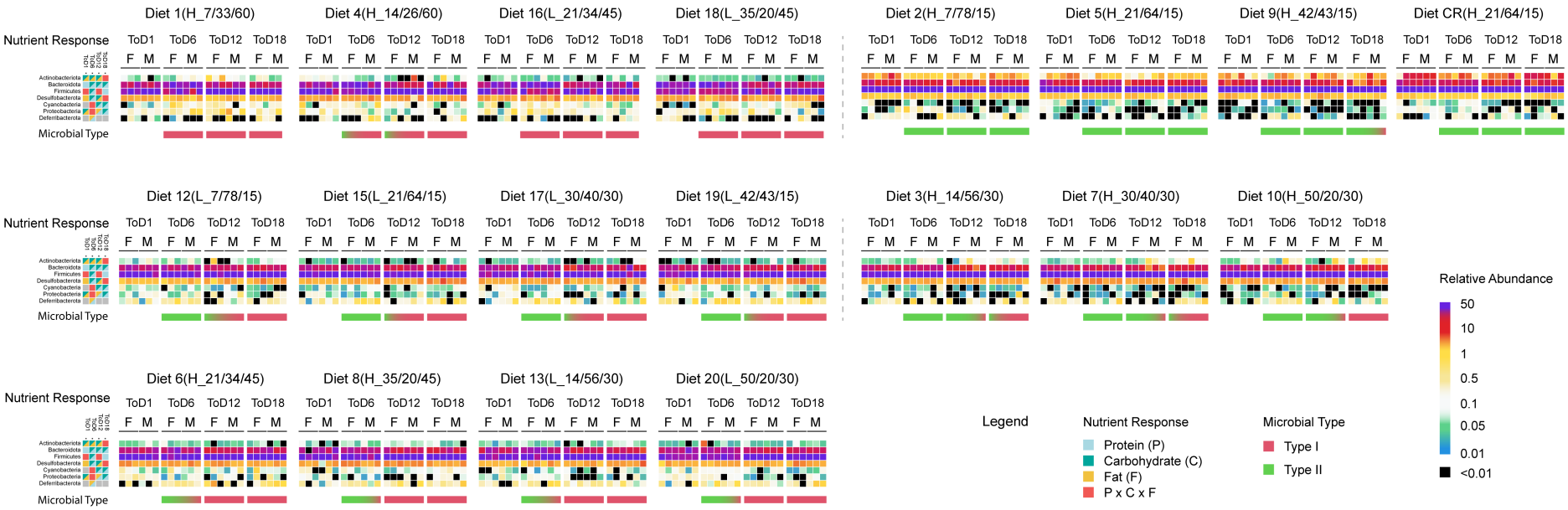

Supplementary Figure 7-18. The relative abundance of microbes in associate with nutrient response change and microbial type shift over age at phylum level.

In each panel, the first 4 columns are the best model fit resulted from the GAM modelling at each timepoints. From left to right are ToD1, ToD6, ToD12 and ToD18. The number on the left are the family listed in the legend. Color indicates best model fit to a single nutrient (single colored squares), an interaction of two nutrients (diagonally splitted coloured squares) or the interaction of all three nutrients (red colored single square). Full model statistics are in appendix. The rest of the columns are the heatmap of relative abundance of these family in each diet. In each diet, the samples were arranged by first by time on diet then by the mice gender. The missing samples that were under detection threshold were shown as black. The bottom row in each panel is the microbial community type. Each bar represents 6 mice in each diet at each timepoint. Color indicates the community types, type I (red) and type II (green). The size of the bar indicates the number of mice under specific community type (See also Figure 3-9). The position of the bar does not correlates to the individual mouse showing the relative abundance above.

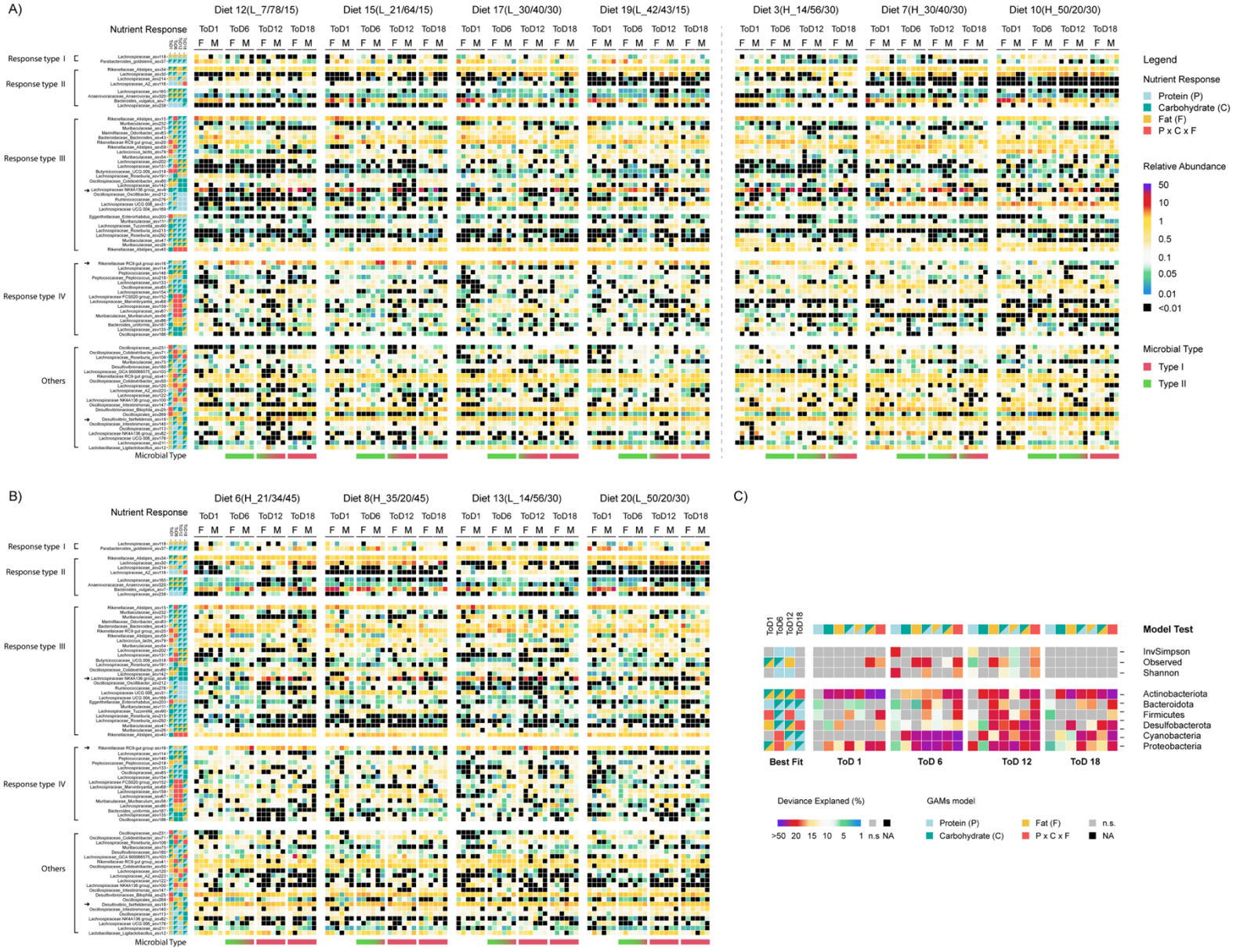
A)
Diet 12(L_7/78/15)
Diet 15(L_21/64/15)
Diet 17(L_30/40/30)
Diet 19(L_42/43/15)
Diet 3(H_14/56/30)
Diet 7(H_30/40/30)
Diet 10(H_50/20/30)
Nutrient Response
ToD1 ToD6 ToD12 ToD18
F M
Response type I
Response type II
Response type III
Response type IV
Others
Microbial Type
B)
Diet 6(H_21/34/45)
Diet 8(H_35/20/45)
Diet 13(L_14/56/30)
Diet 20(L_50/20/30)
C)
Legend
Nutrient Response
Protein (P)
Carbohydrate (C)
Fat (F)
P x C x F
Relative Abundance
50
10
1
0.5
0.1
0.05
0.01
<0.01
Microbial Type
Type I
Type II
Model Test
InvSimpson
Observed
Shannon
Actinobacteriota
Bacteroidota
Firmicutes
Desulfobacterota
Cyanobacteria
Proteobacteria
Best Fit
ToD 1
ToD 6
ToD 12
ToD 18
Deviance Explaned (%)
>50 20 15 10 5 1 n.s NA
GAMs model
Protein (P)
Carbohydrate (C)
Fat (F)
P x C x F
n.s.
NA

Supplementary Figure 7-19. GAM nutrients response at ASV level with corresponding to ASV relative abundance the microbial community shift for drifters.

A) and B) are the heatmaps of relative abundance of the consistent responders in diets with microbial drift during aging. The first 4 columns are nutrient response of the consistent responders over time. The rest of the columns are the relative abundance of these ASVs in each diet. In each diets, the samples were arranged by first by time on diet then by the mice gender. The missing samples were left blank. A)Diets with microbial drift started after 6mo on diet. B) Diets with microbial drift start before 6mo on diet. C) Alpha diversity and taxa at phylum level show difference in nutrient response over time. Column 1-4 were the best model determined for the alpha diversity and each phylum using the combination of lowest AIC values and highest deviance explained. The rest of the columns were the % deviance explained by dietary nutrient dimensions. From left to right panels are time on diet for 1mo, 6mo, 12mo and 18mo. Within each panel, each column represents one nutrient dimension, from left to right are, protein, carbohydrate, fat, interaction between two of the macronutrients and the interaction among all three nutrients. The arrow indicates taxa that were selected for microbial types from core microbiome analysis.

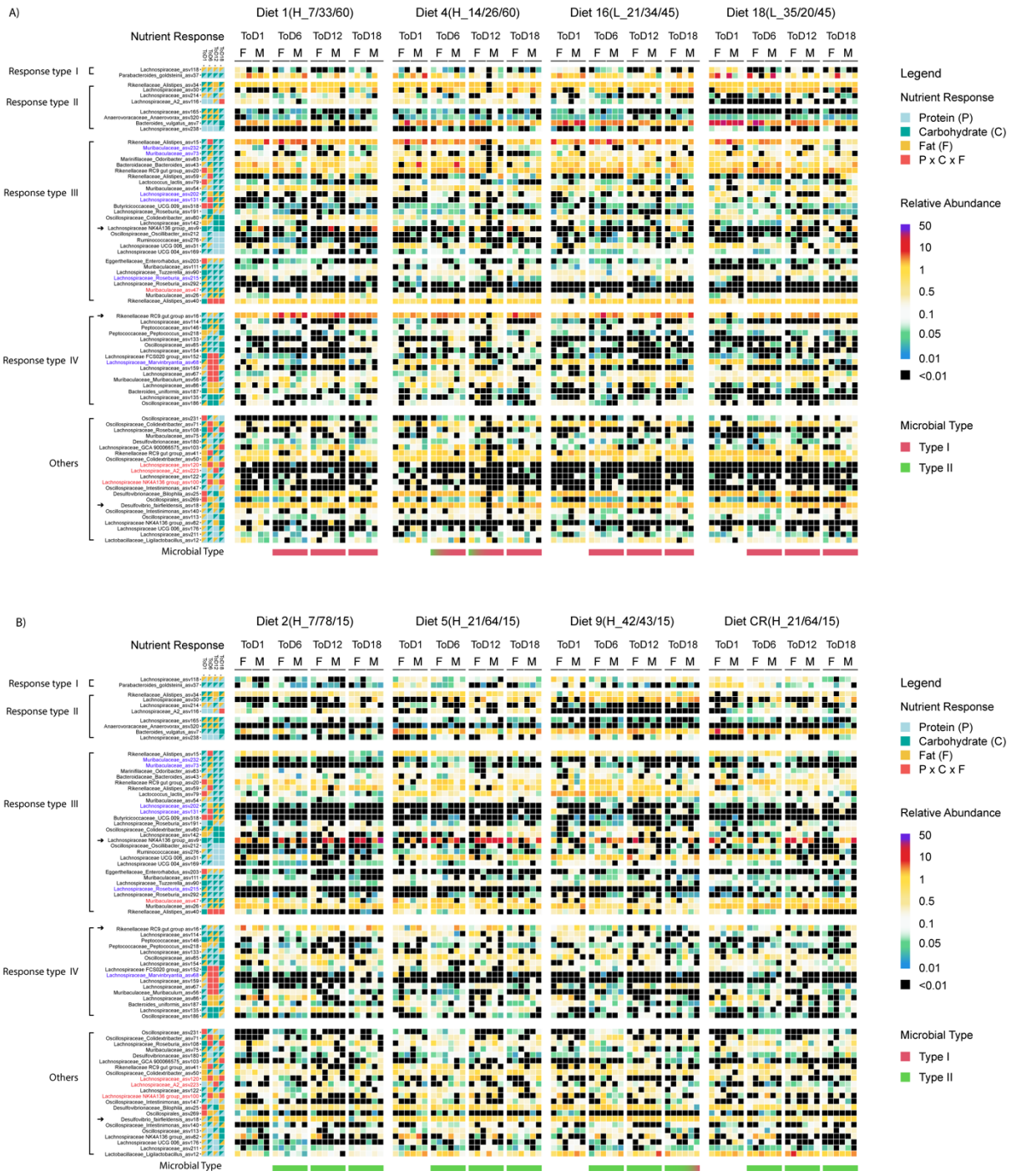

Supplementary Figure 7-20. GAM nutrients response at ASV level with corresponding to ASV relative abundance the microbial community shift for non-drifters.

A) Microbial type 1 diets. B) Microbial type 2 diets. The first 4 columns were nutrient response of the consistent responders over time. The rest of the columns were the relative abundance of these ASVs in each diet. In each diet, the samples were arranged by first by time on diet then by the mice gender. The missing samples were left blank. The arrow indicates taxa that were selected for microbial types from core microbiome analysis.

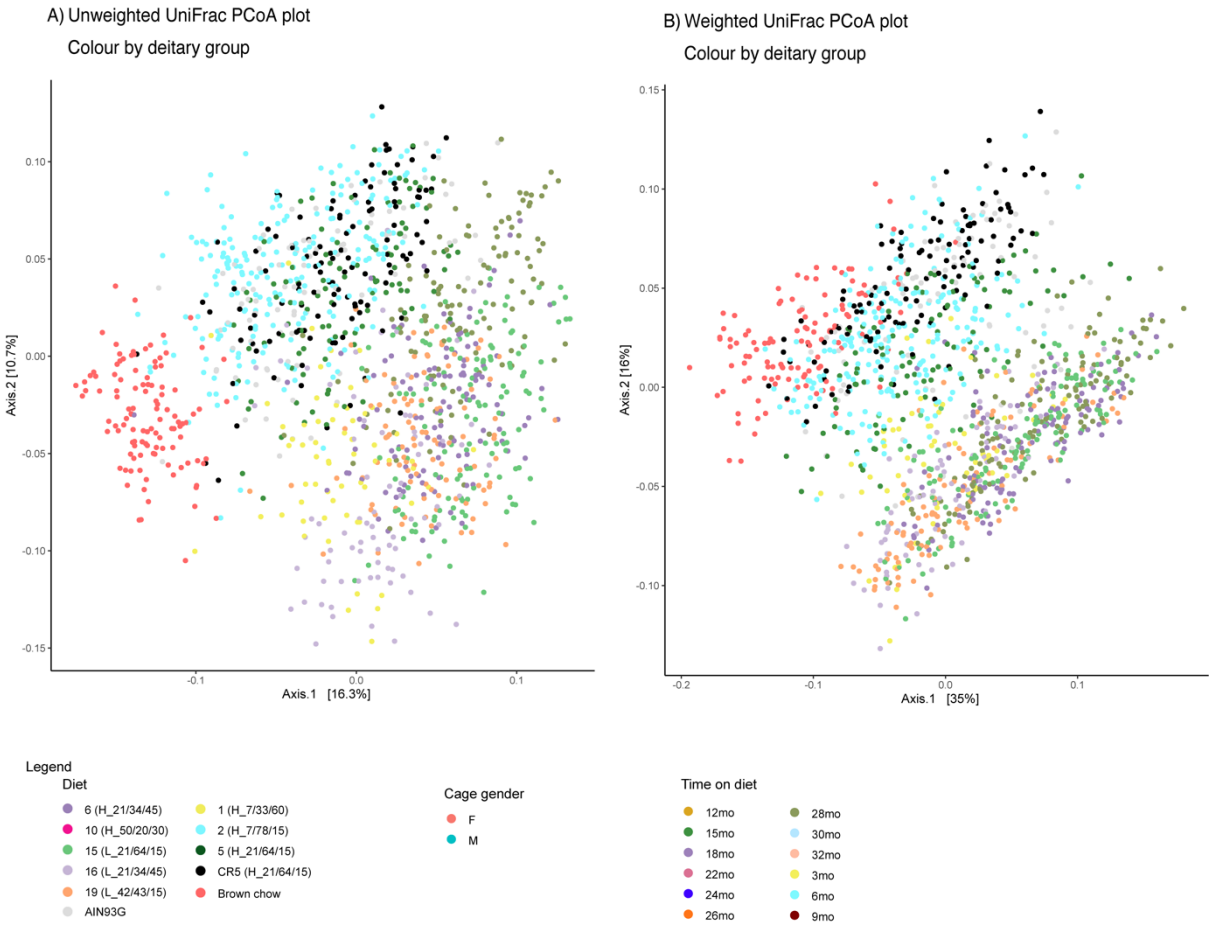

Supplementary Figure 7-21. PCoA plot of beta-diversity of all samples in Chapter 4. A)Unweighted UniFrac distance; B)Weighted UniFrac distance. Color by diet (sample n = 1,526, mice n = 36)

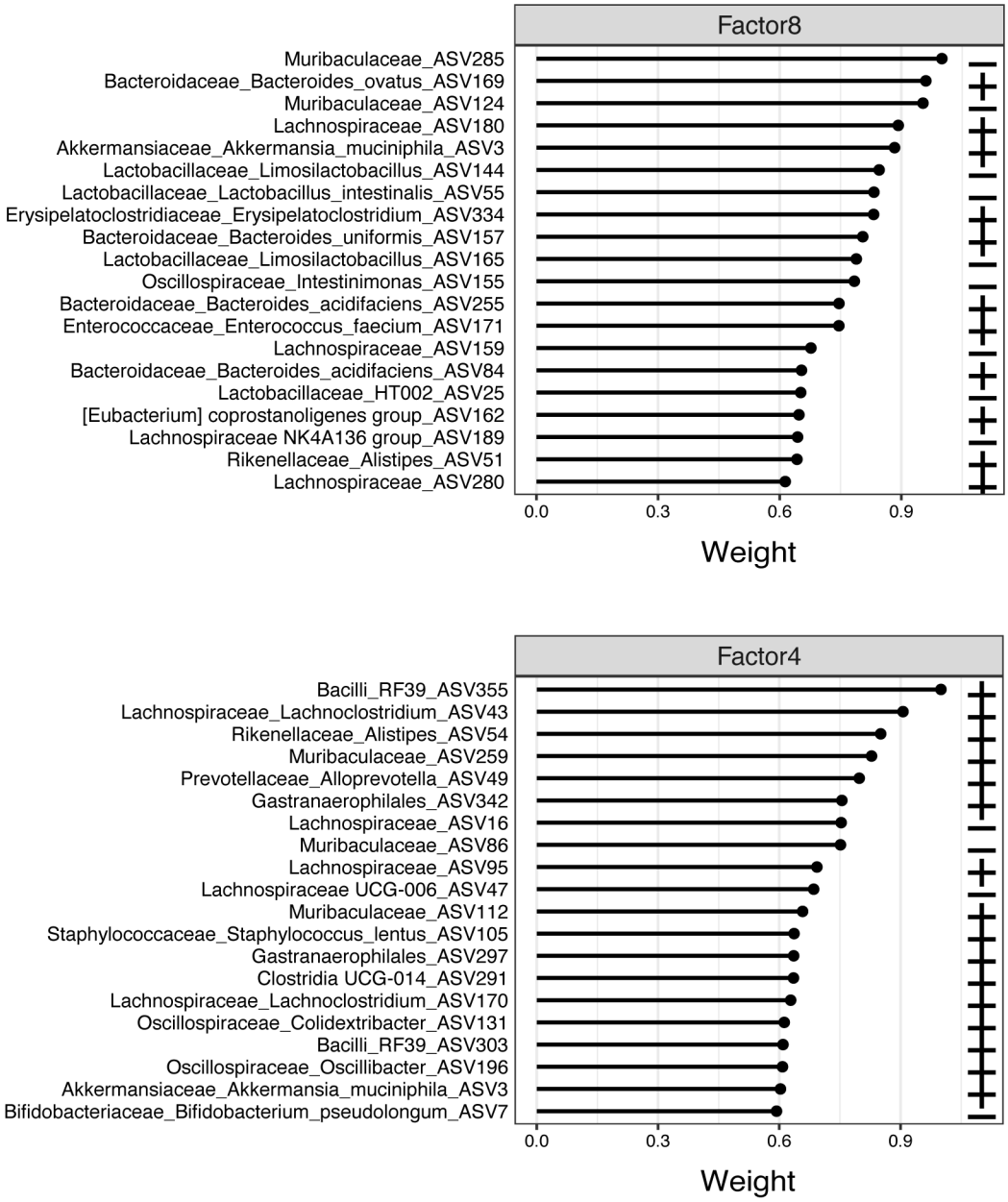

Supplementary Figure 7-22. Top 20 weighted ASVs in factor 4 and factor 8 from MOFA+ analysis grouped by diet in Chapter 4.

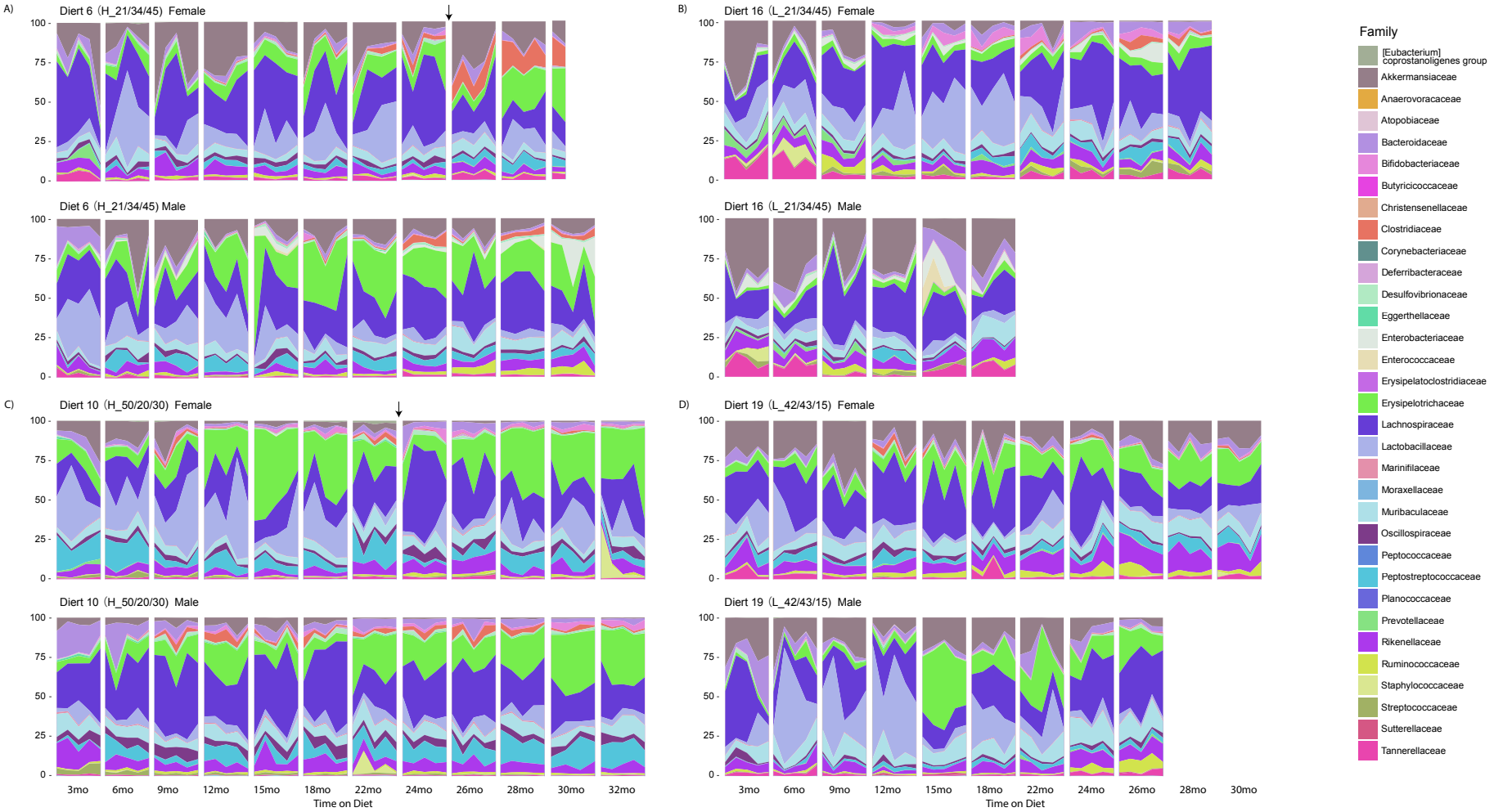

Supplementary Figure 7-23. Taxa plot at family level for Diet 6, 10, 16 and 19 in Chapter 4.
A) Diet 6; B) Diet 16; C) Diet 10 and D) Diet 19. For each diet, the top panel is female and bottom panel is male. Each small rectangle represents 2-5 pieces of faeces collected at each time window. The arrow indicates switch of mouse.

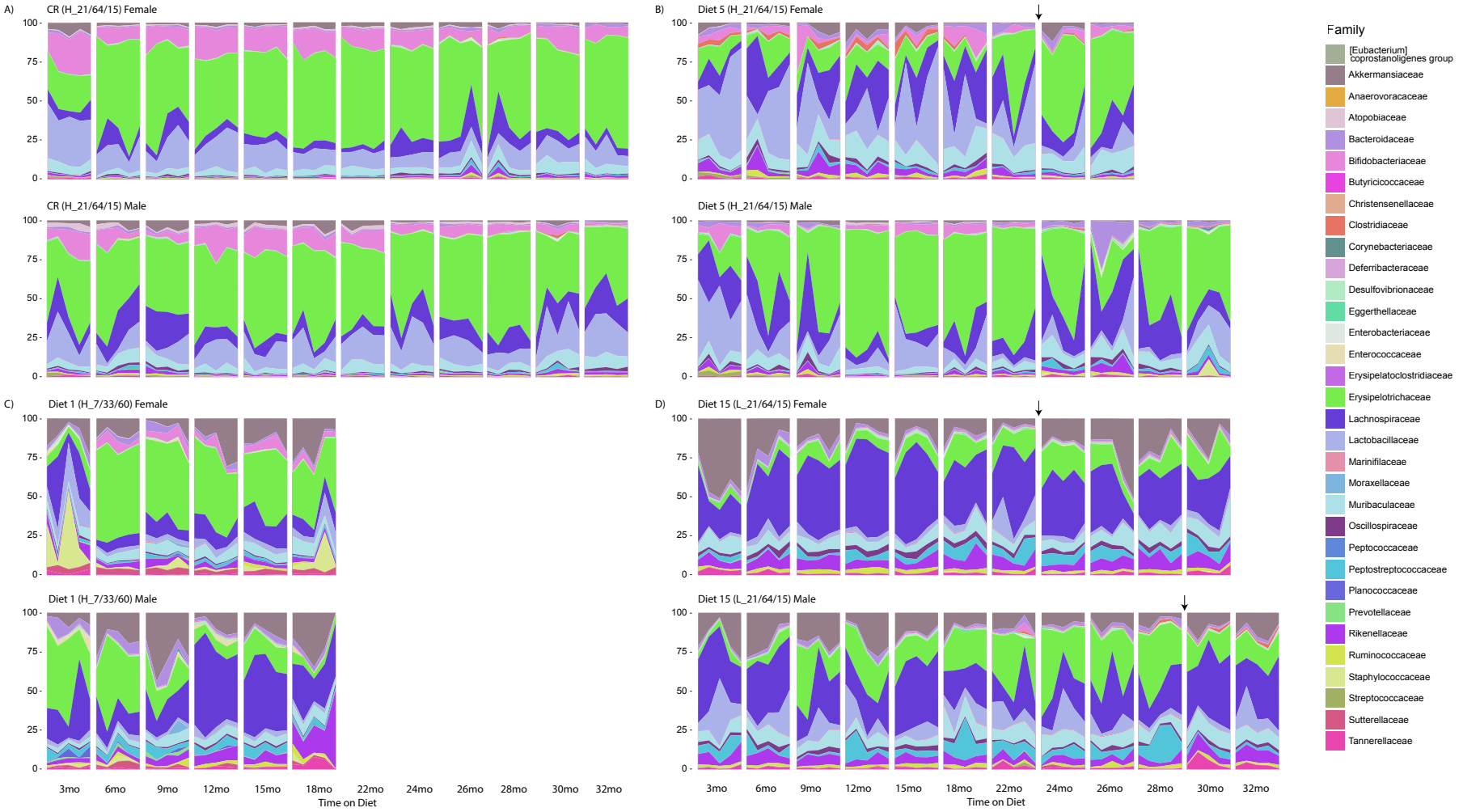

Supplementary Figure 7-24. Taxa plot at family level for Diet 1, 5, 15 and the caloric restriction diet in Chapter 4.
A) Caloric restriction diet; B) Diet 5; C) Diet 1 and D) Diet 15. For each diet, the top panel is female and the bottom panel is male. Each small rectangle represents 2-5 pieces of faeces collected at each time window. The arrow indicates the switch of mouse.

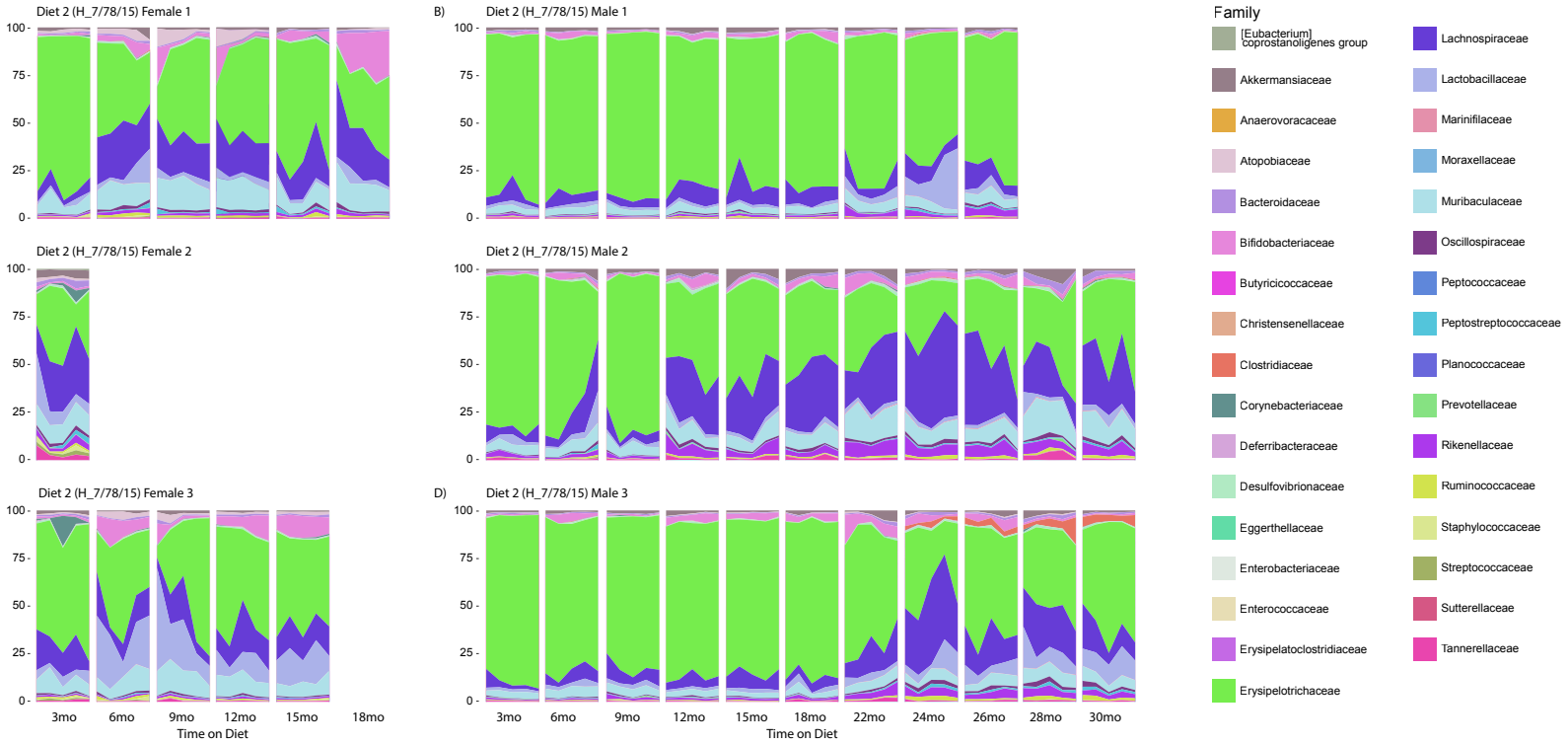

Supplementary Figure 7-25. Taxa plot at family level for Diet 2 in Chapter 4.
A) Female cage and B) Male cage. For each gender, each panel represents 1 mouse. Each small rectangle represents 2-5 pieces of faeces collected at each time window. The arrow indicates the switch of mouse.

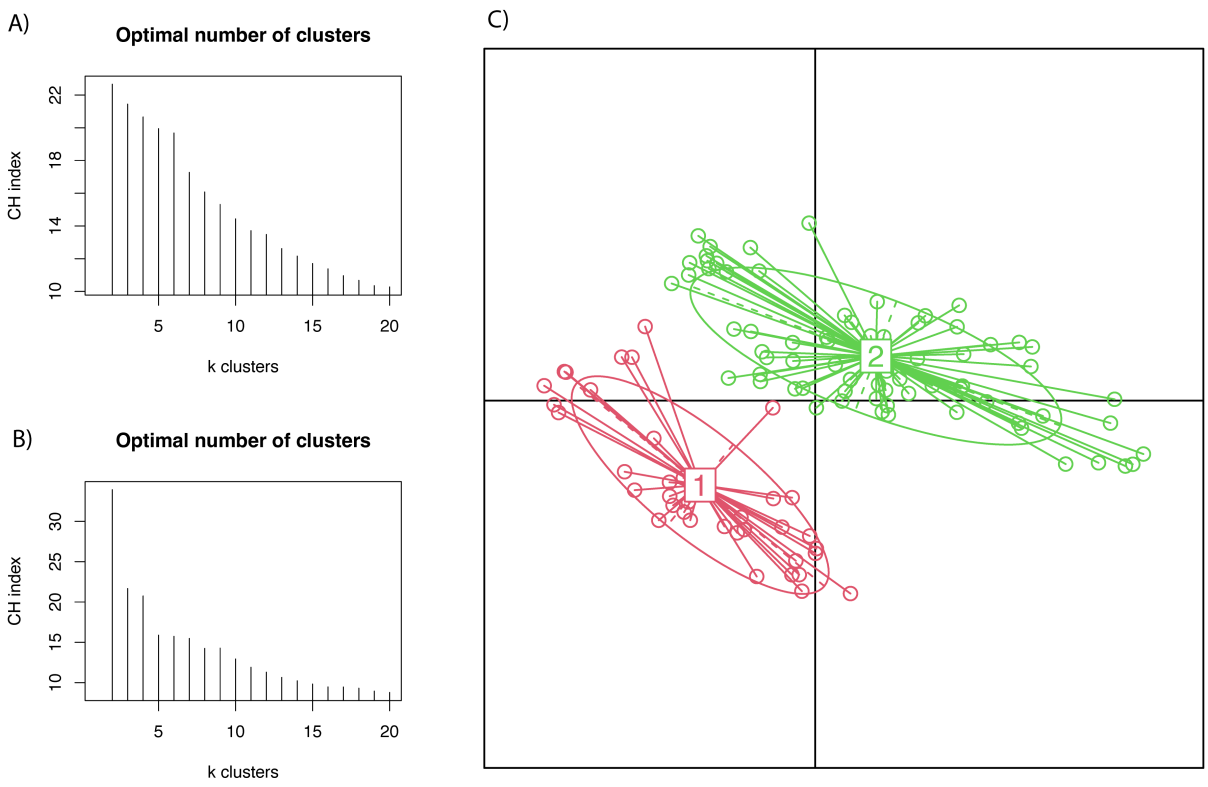

Supplementary Figure 7-26. PAM cluster based on Bray-Curtis dissimilarity at ASV level and weight UniFrac distance in Chapter 4.
The number of clusters was determined based on the Calinski-Harabasz (CH) index (maximum value) for A) Bray-Curtis dissimilarity distance and C) weighted UniFrac. D) PAM cluster with optimal number of clusters (k=2) using unweighted UniFrac distance.

Supplementary Table 7-10. Sample allocation for diet 1, diet 4 and diet AIN93G in Chapter 4.

Diet	Cluster	3mo	6mo	9mo	12mo	15mo	18mo	22mo	24mo	26mo	28mo	30mo	F	M
1	1	10	3	5	5	5	4	-	-	-	-	-	6	26
	3	-	7	5	5	5	6	-	-	-	-	-	24	4
5	1	2	-	1	-	-	-	1	5	4	4	3	2	18
	3	8	14	9	10	10	10	9	5	6	1	2	47	37
AIN93G	1	-	3	-	-	-	1	4	1	3	-	-	7	5
	3	10	12	10	10	10	12	5	4	2	-	-	35	40

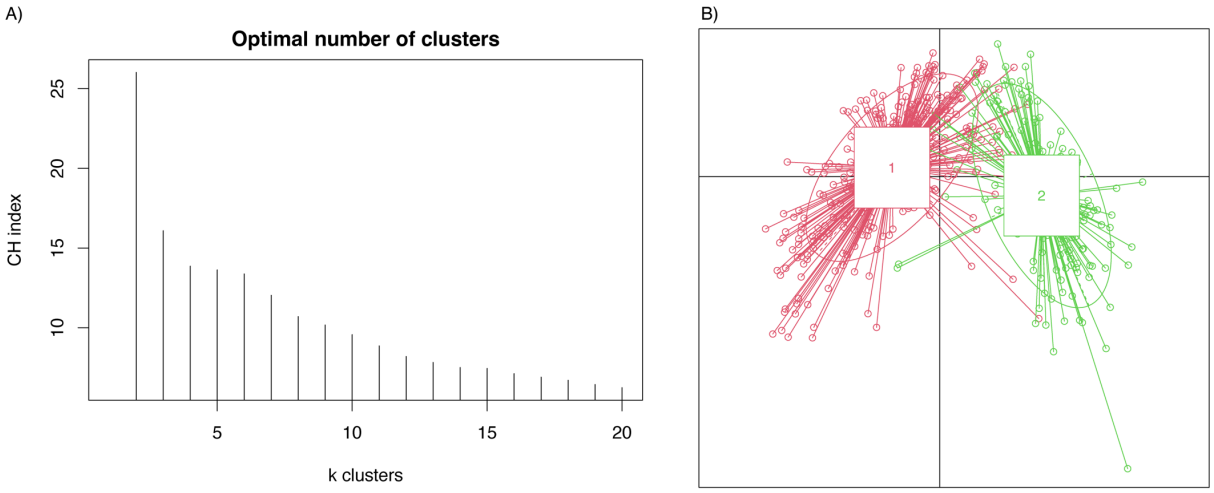

Supplementary Figure 7-27. PAM cluster based on Bray-Curtis dissimilarity at ASV level for all samples in Chapter 3.

A) The number of clusters was determined based on the Calinski-Harabasz (CH) index (maximum value). B) PAM cluster with optimal number of clusters (k=2) using bray-curtis distance.

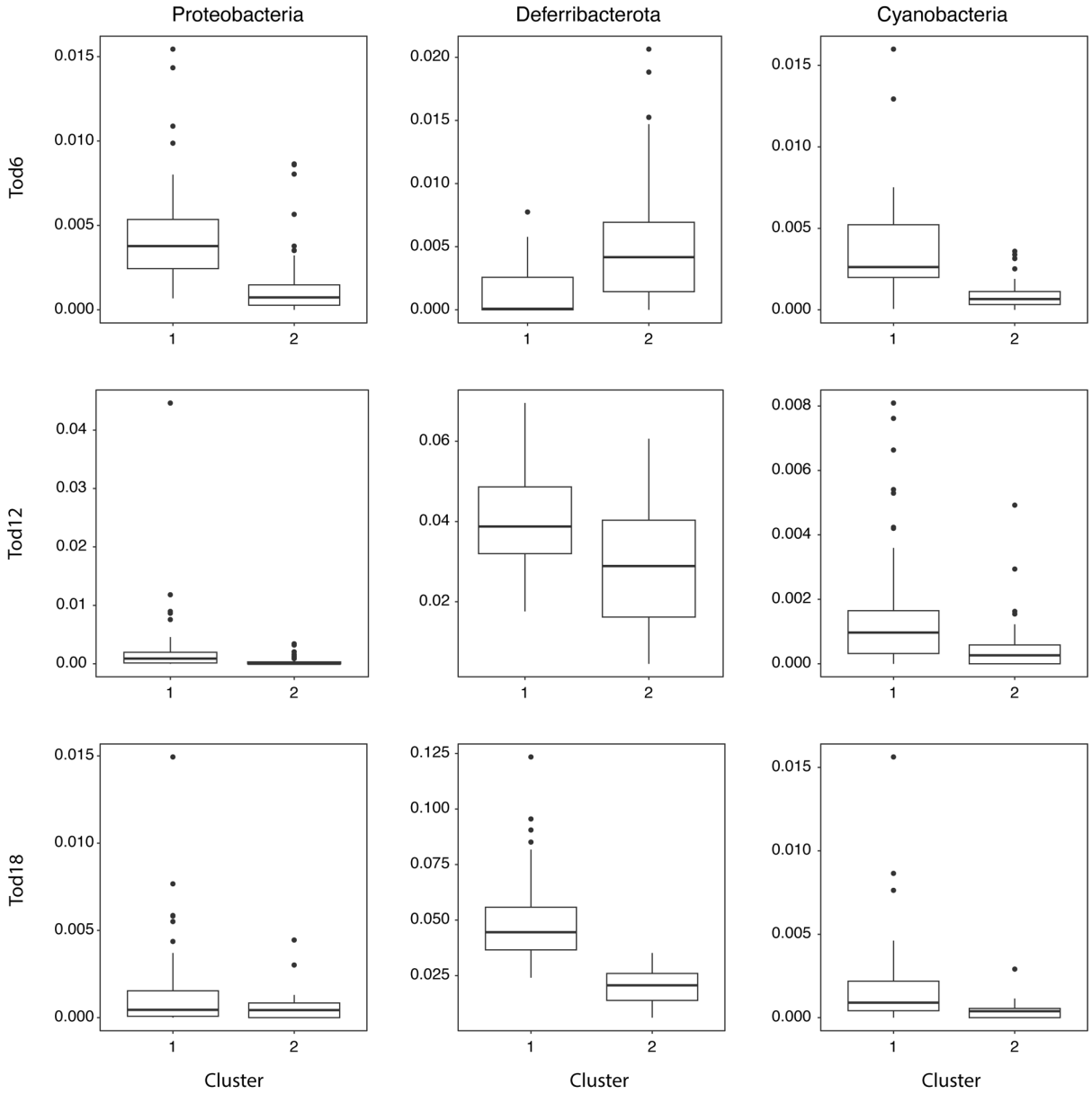

Supplementary Figure 7-28. Relative abundance of minority phylum in EP clusters in Chapter 3.

From top to bottom are experimental group ToD6, ToD12 and ToD18.

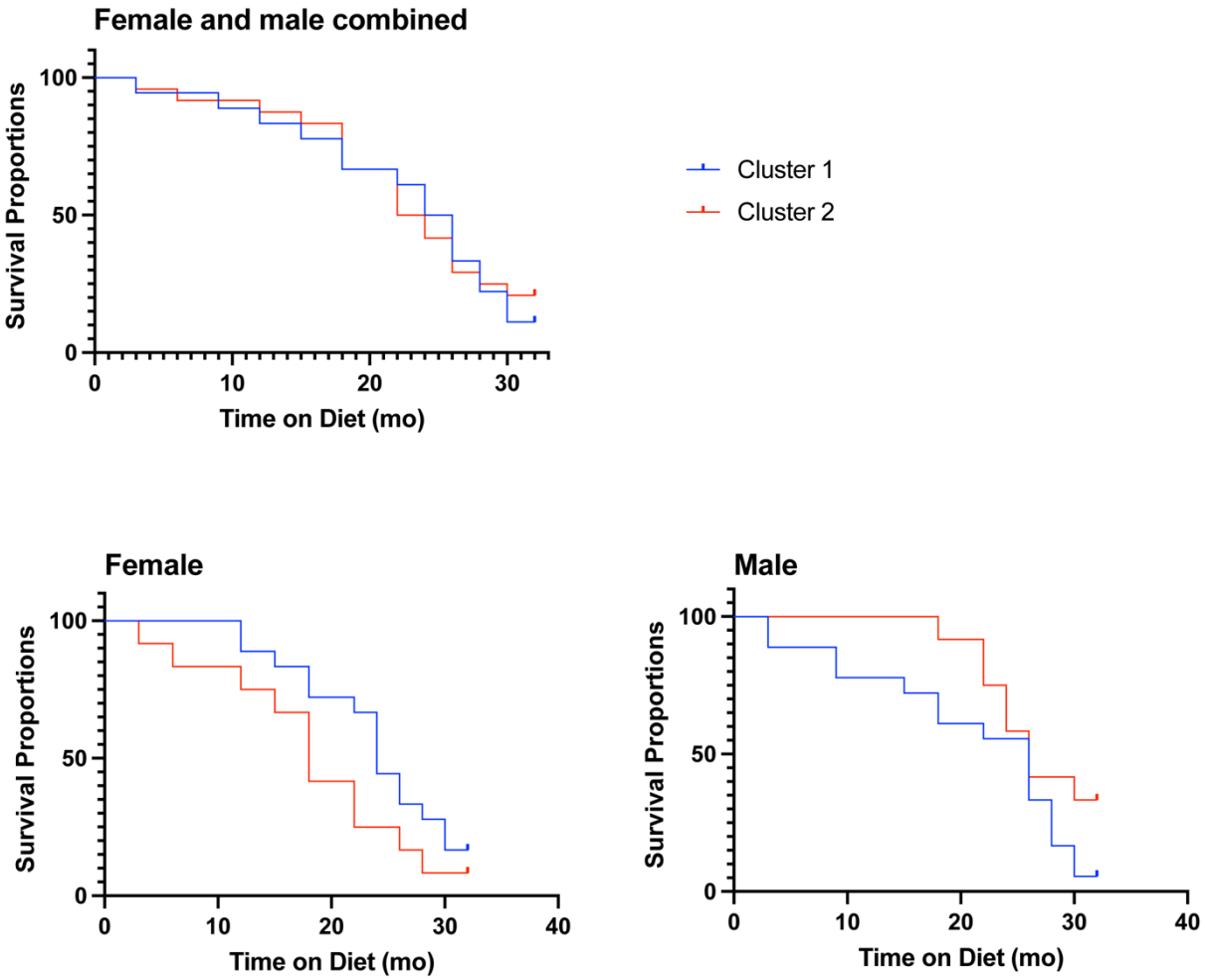

Supplementary Figure 7-29. Survival proportions for the mice used in microbial analysis. Top left: survival ratio for both females and males combined. Bottom left: survival ratio for females only. Bottom right: survival ratio for males only.

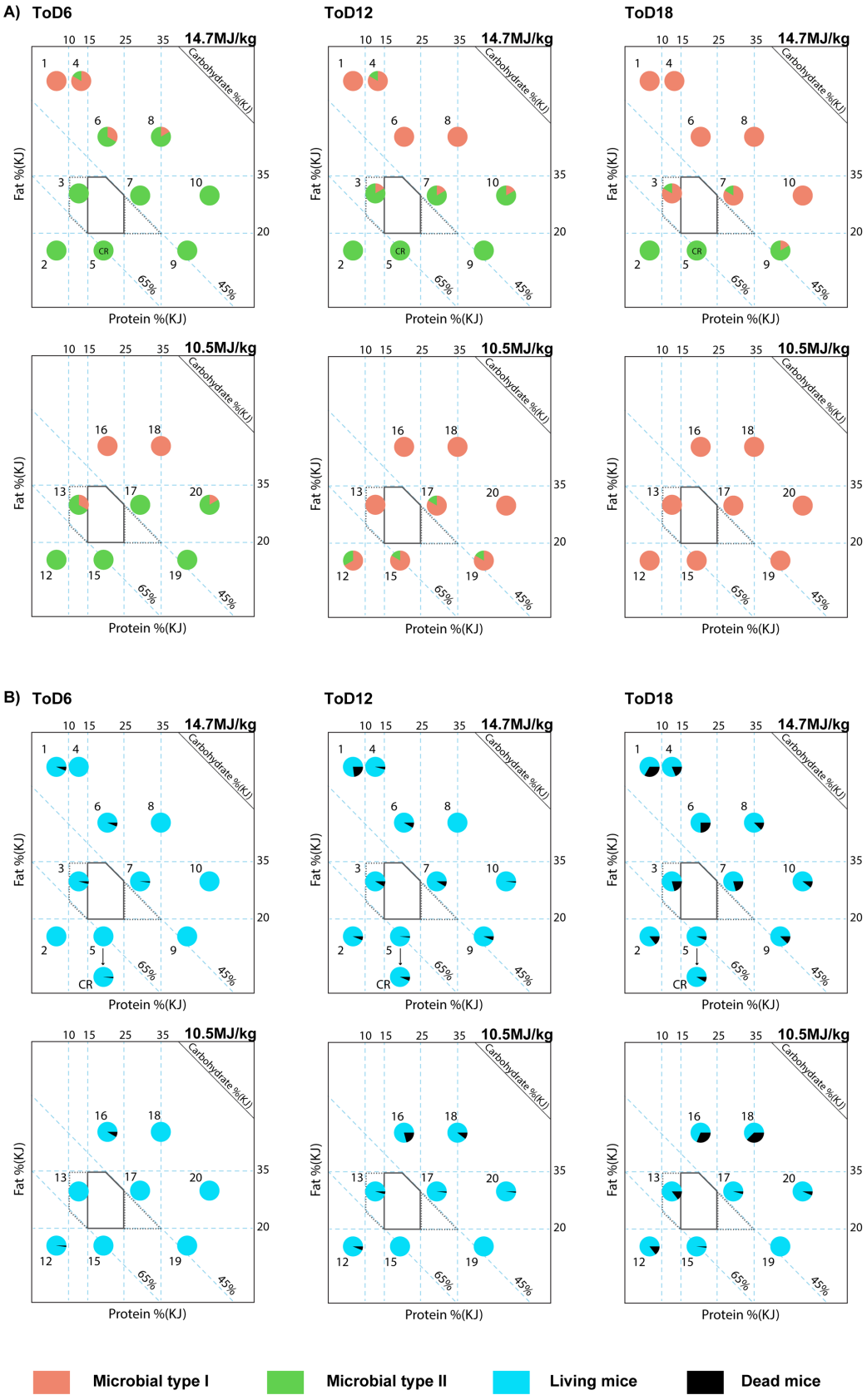

Supplementary Figure 7-30. Association between the microbial type transition and the mice lifespan.

A) Microbial type transition using data from Chapter 3. Each cycle represents 6 mice of equal gender. B) Mice lifespan using data from the global longevity study from Chapter 4. Each cycle represent 48 mice of each equal gender.

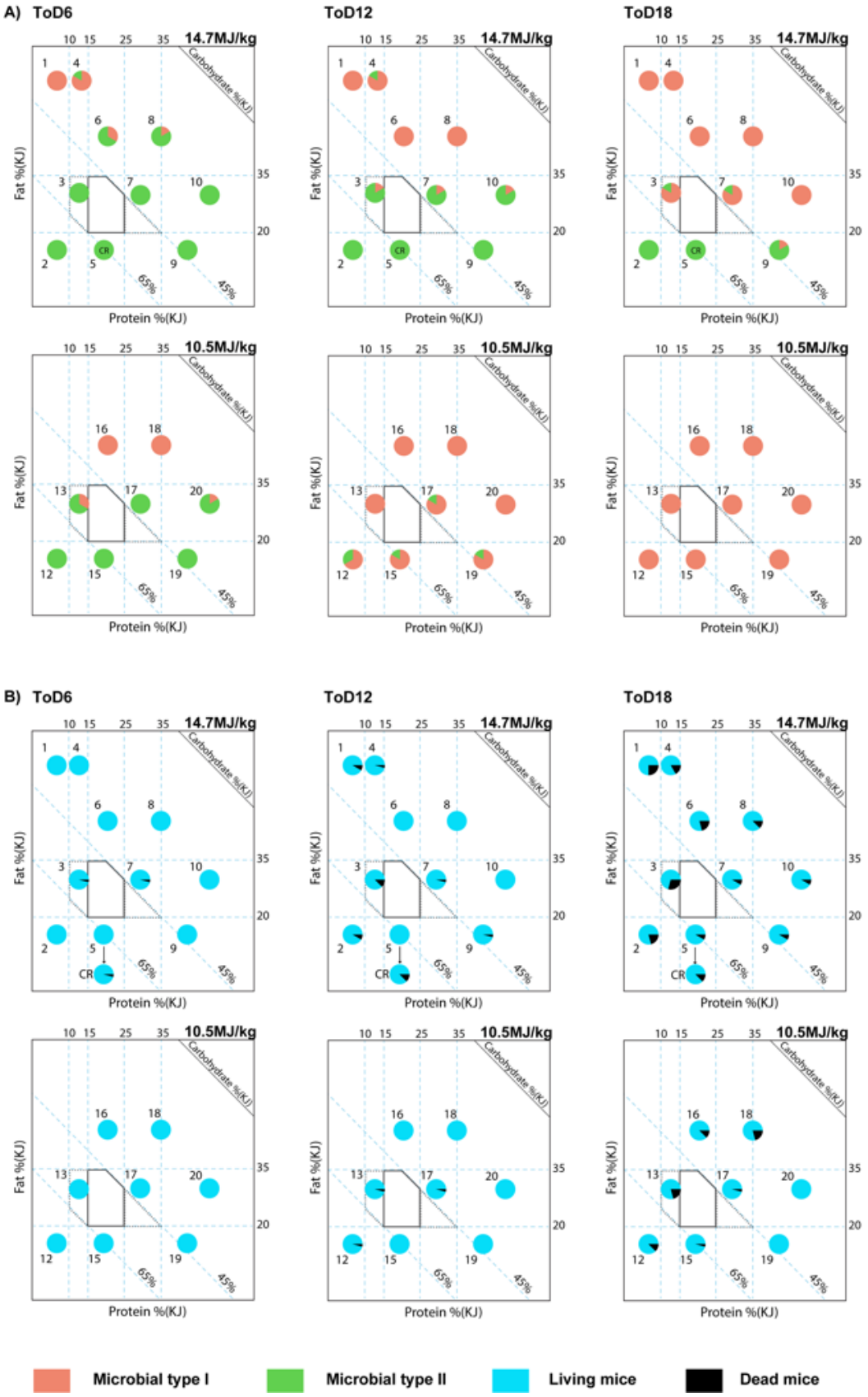

Supplementary Figure 7-31. Association between the microbial type transition and the mice lifespan in females.

A) Microbial type transition using data from Chapter 3. Each cycle represents 6 mice of equal gender. B) Female mice's lifespan using data from the global longevity study from Chapter 4. Each cycle represent 24 of female mice.

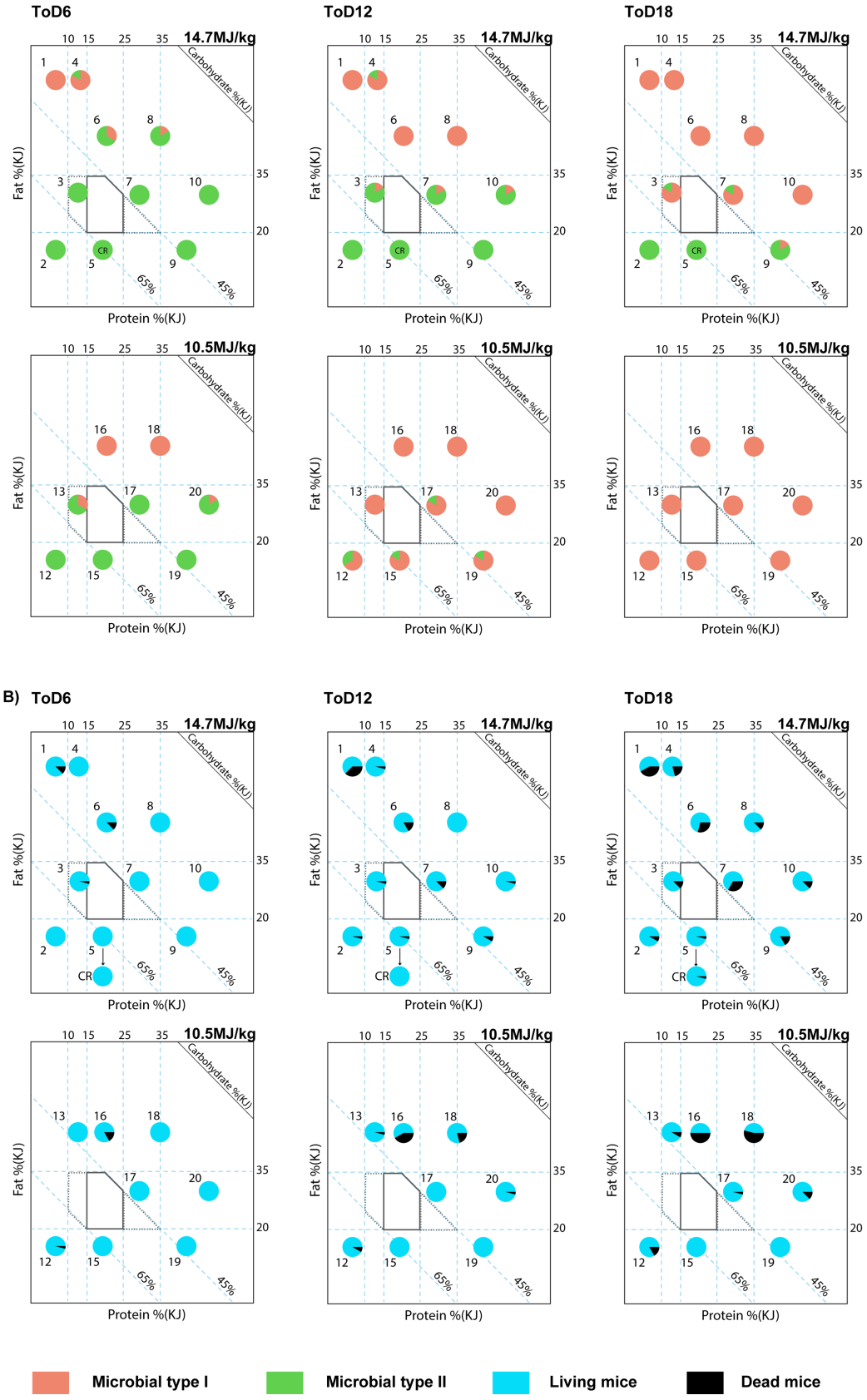

Supplementary Figure 7-32. Association between the microbial type transition and the mice lifespan in males.

A) Microbial type transition using data from Chapter 3. Each cycle represents 6 mice of equal gender. B) Male mice's lifespan using data from the global longevity study from Chapter 4. Each cycle represent 24 of male mice.

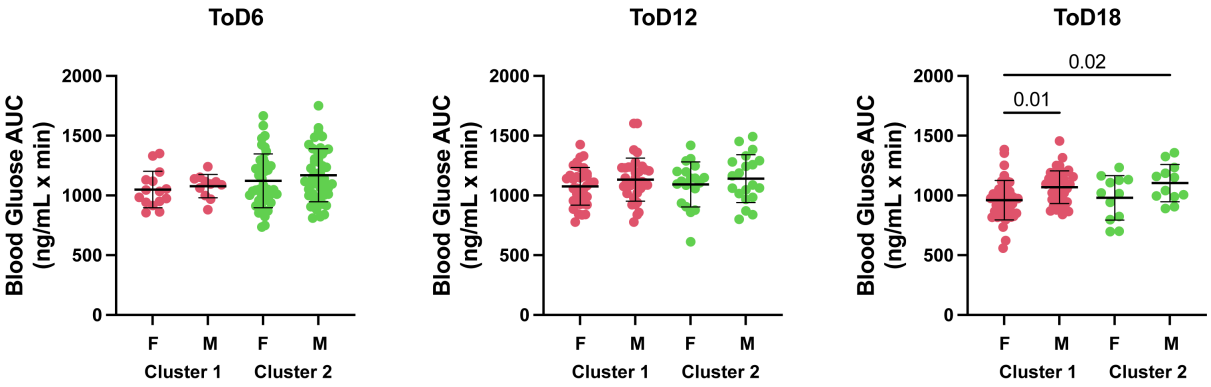

Supplementary Figure 7-33. Blood glucose level (AUC) for mice in Chapter 3.
Mice were grouped according to microbial types and gender. Significance was determined by one-way ANOVA followed by pair-wise comparison.

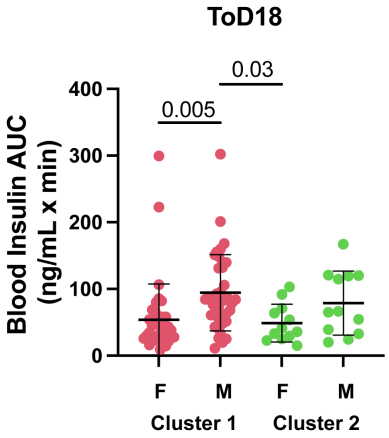

Supplementary Figure 7-34. Blood insulin level (AUC) for mice in Chapter 3.
Mice were grouped according to microbial types and gender. Significance was determined by one-way ANOVA followed by pair-wise comparison.

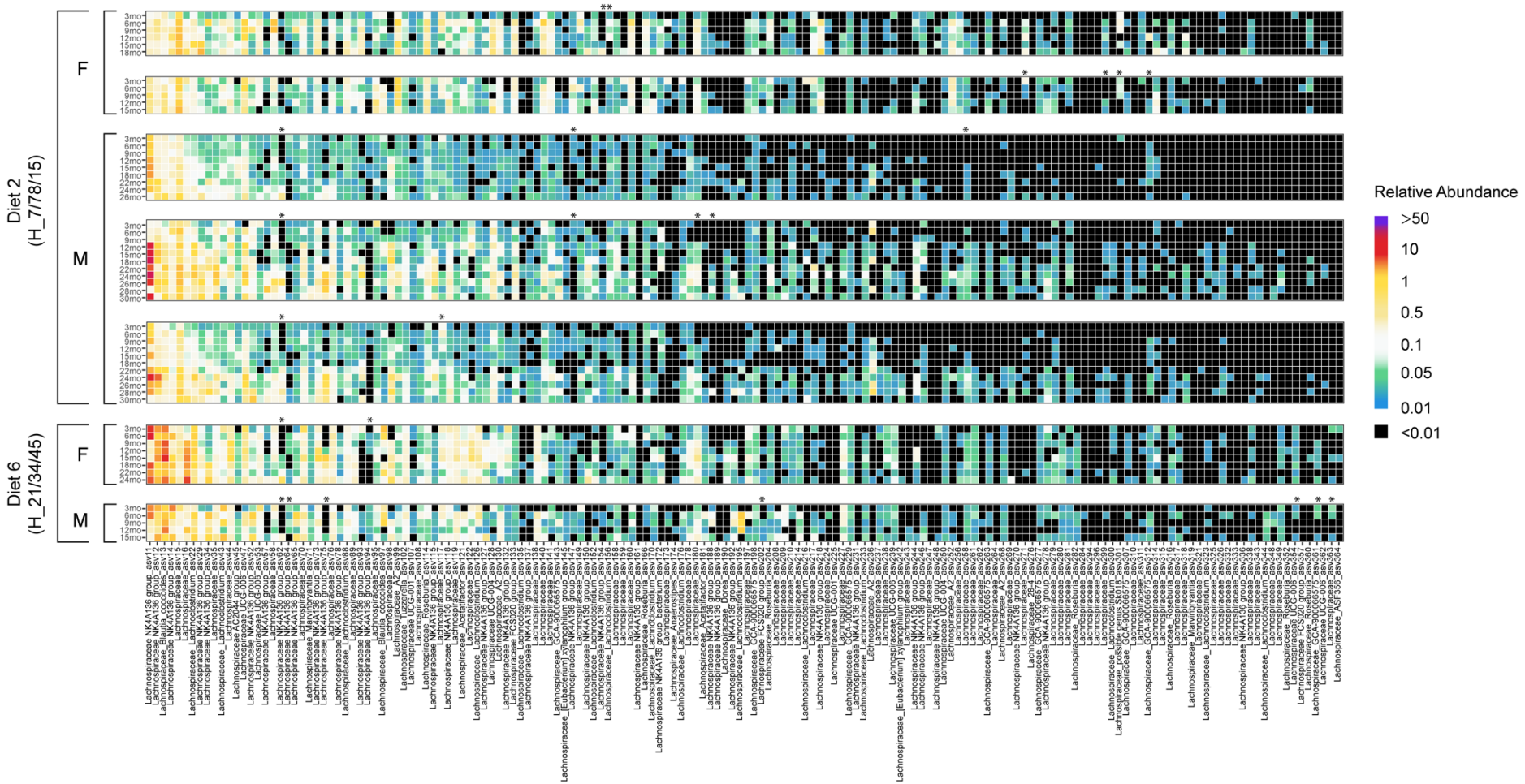

Supplementary Figure 7-35. Heatmap of mean relative abundance of all Lachnospiraceae ASVs as per timepoint per mouse for Diet 2 and Diet 6 in Chapter 4.

Each row presents one mouse and the pairs of presence and absence of ASVs were marked as * for each gender in each diet. The x-axis is each Lachnospiraceae ASVs and the y-axis is time on diet.

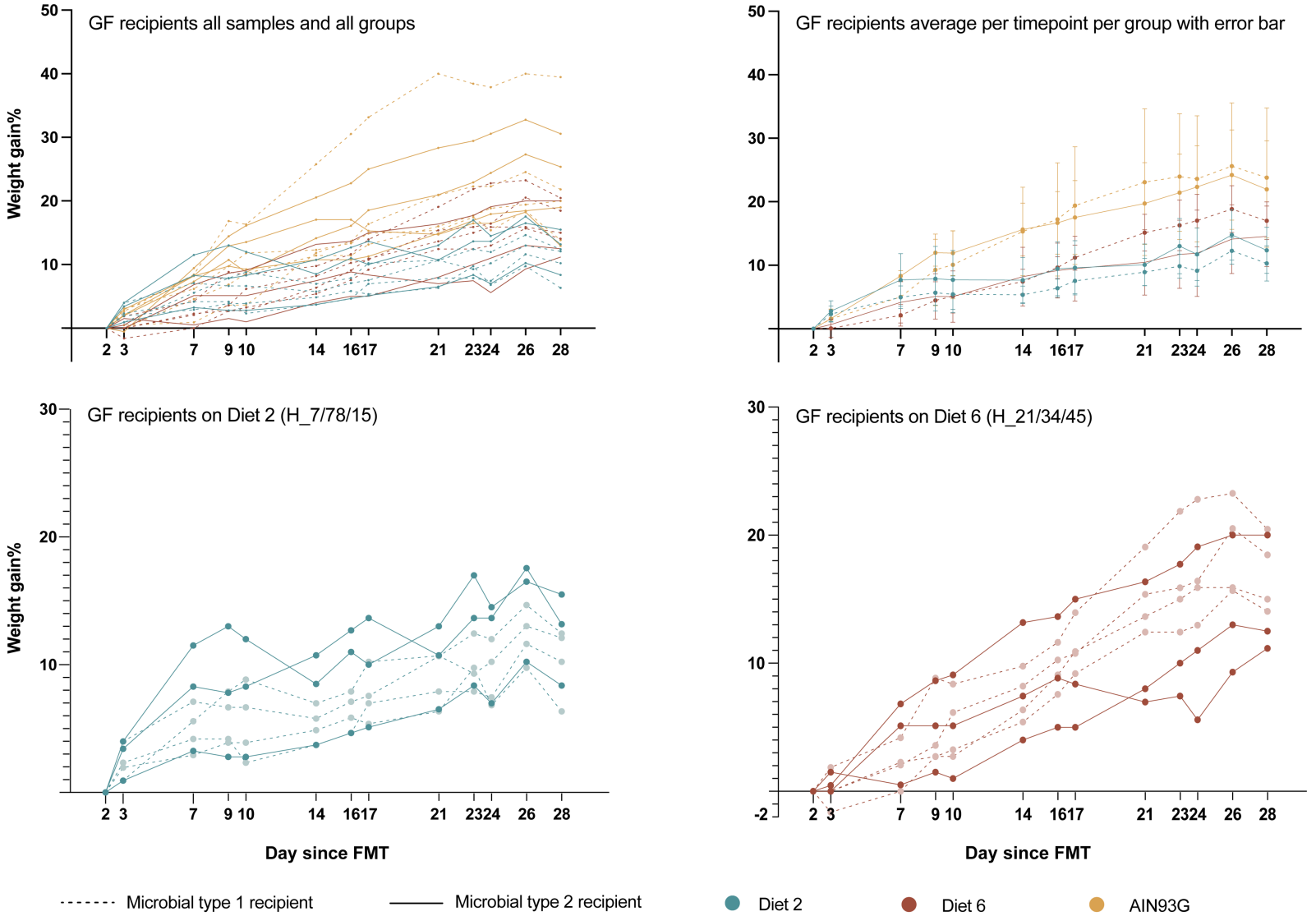

Supplementary Figure 7-36. Percentage body weight gain after FMT in Chapter 5.

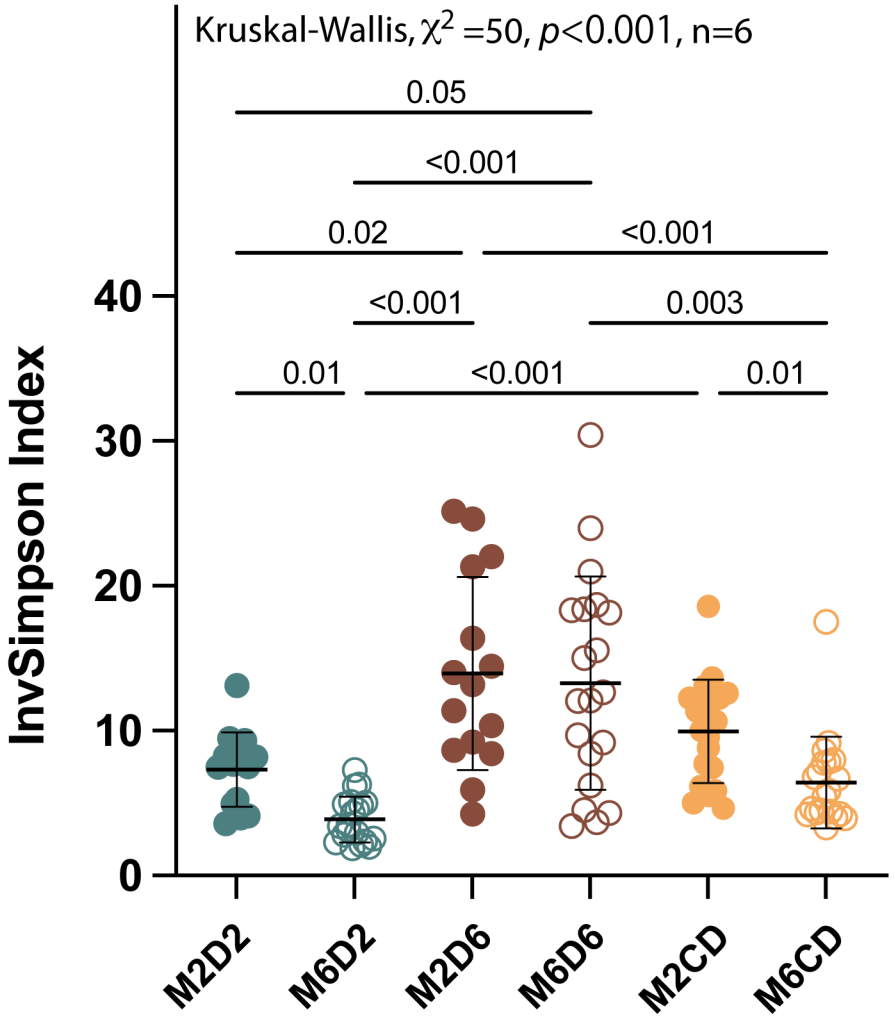

Supplementary Figure 7-37. With-in samples inverse Simpson index all recipient mice. The significance was determined using the Kruskal-Wallis test, followed by pairwise comparisons with the Wilcoxon test and correction for multiple comparisons using the Benjamini-Hochberg procedure. All timepoints were combined together for each treatment group.

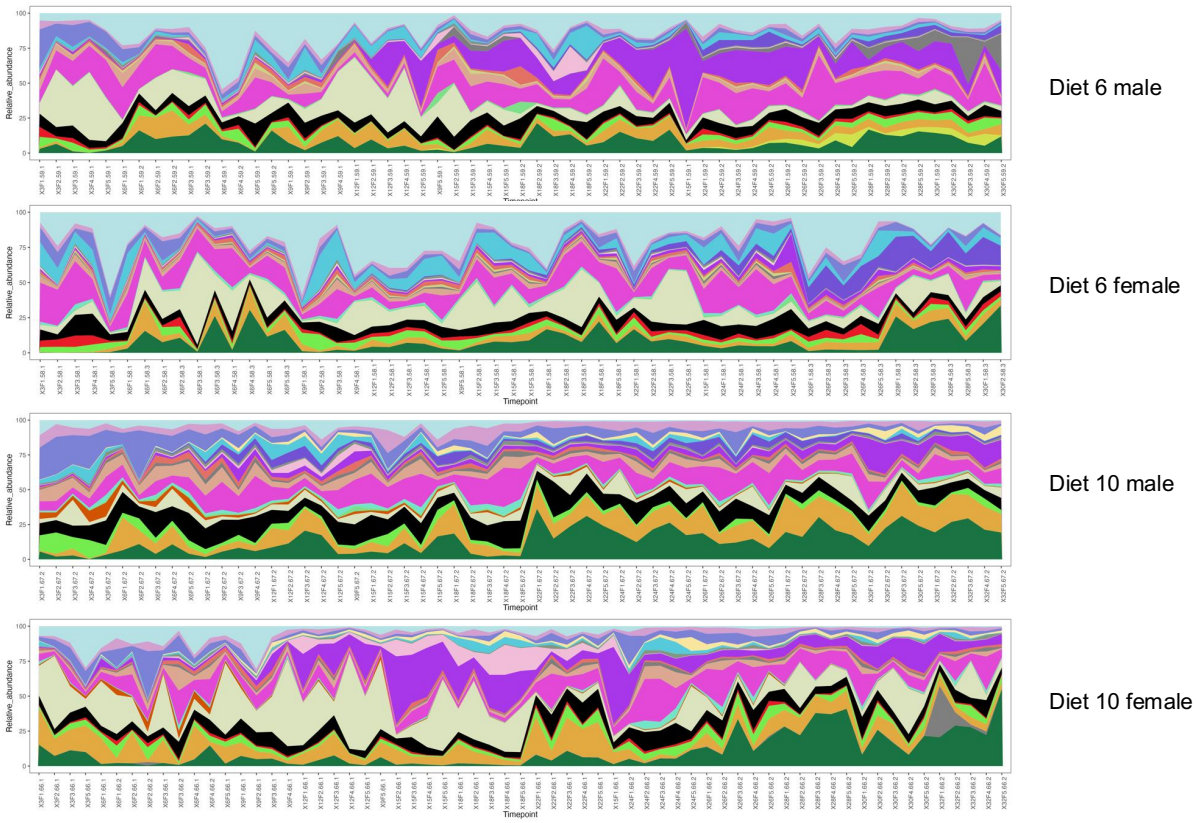

Supplementary Figure 7-38. Stagger plot of the top 20 taxa at the genus level for 4 mice in Chapter 4.

Y-axis indicates the relative abundance, and x-axis indicates the collection time. The color of the genus was the same as Figure 5-9.

8 Reference

Agrawal, A., J. Tay, G.-E. Yang, S. Agrawal and S. Gupta (2010). "Age-associated epigenetic modifications in human DNA increase its immunogenicity." Aging (Albany NY) **2**(2): 93.

Amarya, S., K. Singh and M. Sabharwal (2014). "Health consequences of obesity in the elderly." Journal of Clinical Gerontology and Geriatrics **5**(3): 63-67.

Anstey, K., L. Stankov and S. Lord (1993). "Primary aging, secondary aging, and intelligence." Psychology and Aging **8**(4): 562.

Argelaguet, R., D. Arnol, D. Bredikhin, Y. Deloro, B. Velten, J. C. Marioni and O. Stegle (2020). "MOFA+: a statistical framework for comprehensive integration of multi-modal single-cell data." Genome biology **21**(1): 1-17.

Argelaguet, R., B. Velten, D. Arnol, S. Dietrich, T. Zenz, J. C. Marioni, F. Buettner, W. Huber and O. Stegle (2018). "Multi-Omics Factor Analysis—a framework for unsupervised integration of multi-omics data sets." Molecular systems biology **14**(6): e8124.

Arumugam, M., J. Raes, E. Pelletier, D. Le Paslier, T. Yamada, D. R. Mende, G. R. Fernandes, J. Tap, T. Bruls and J.-M. Batto (2011). "Enterotypes of the human gut microbiome." nature **473**(7346): 174-180.

Bäckhed, F., H. Ding, T. Wang, L. V. Hooper, G. Y. Koh, A. Nagy, C. F. Semenkovich and J. I. Gordon (2004). "The gut microbiota as an environmental factor that regulates fat storage." Proceedings of the national academy of sciences **101**(44): 15718-15723.

Bäckhed, F., J. Roswall, Y. Peng, Q. Feng, H. Jia, P. Kovatcheva-Datchary, Y. Li, Y. Xia, H. Xie and H. Zhong (2015). "Dynamics and stabilization of the human gut microbiome during the first year of life." Cell host & microbe **17**(5): 690-703.

Beyhan, Y. E. and M. R. Yıldız (2023). "Microbiota and parasite relationship." Diagnostic Microbiology and Infectious Disease **106**(4): 115954.

Binyamin, D., N. Werbner, M. Nuriel-Ohayon, A. Uzan, H. Mor, A. Abbas, O. Ziv, R. Teperino, R. Gutman and O. Koren (2020). "The aging mouse microbiome has obesogenic characteristics." Genome Medicine **12**(1): 1-9.

Blumberg, R. and F. Powrie (2012). "Microbiota, disease, and back to health: a metastable journey." Science translational medicine **4**(137): 137rv137-137rv137.

Bodenhofer, U., E. Bonatesta, C. Horejš-Kainrath and S. Hochreiter (2015). "msa: an R package for multiple sequence alignment." Bioinformatics **31**(24): 3997-3999.

Bordenstein, S. R. and K. R. Theis (2015). "Host biology in light of the microbiome: ten principles of holobionts and hologenomes." PLoS biology **13**(8): e1002226.
Borsom, E. M., K. Conn, C. R. Keefe, C. Herman, G. M. Orsini, A. H. Hirsch, M. Palma Avila, G. Testo, S. A. Jaramillo and E. Bolyen (2023). "Predicting neurodegenerative disease using Prepathology gut microbiota composition: a longitudinal study in mice modeling Alzheimer's disease pathologies." Microbiology Spectrum **11**(2): e03458-03422.
Boyce, J. M. and G. Shone (2006). "Effects of ageing on smell and taste: This article is part of a series on ageing edited by Professor Chris Bulpitt." Postgraduate medical journal **82**(966): 239-241.
Brucker, R. M. and S. R. Bordenstein (2013). "The hologenomic basis of speciation: gut bacteria cause hybrid lethality in the genus Nasonia." Science **341**(6146): 667-669.
Brunt, V. E., A. G. Casso, R. A. Gioscia-Ryan, Z. J. Sapinsley, B. P. Ziemba, Z. S. Clayton, A. E. Bazzoni, N. S. VanDongen, J. J. Richey and D. A. Hutton (2021). "Gut microbiome-derived metabolite trimethylamine N-oxide induces aortic stiffening and increases systolic blood pressure with aging in mice and humans." Hypertension **78**(2): 499-511.
Brunt, V. E., R. A. Gioscia-Ryan, J. J. Richey, M. C. Zigler, L. M. Cuevas, A. Gonzalez, Y. Vázquez-Baeza, M. L. Battson, A. T. Smithson and A. D. Gilley (2019). "Suppression of the gut microbiome ameliorates age-related arterial dysfunction and oxidative stress in mice." The Journal of physiology **597**(9): 2361-2378.
Callahan, B. J., P. J. McMurdie, M. J. Rosen, A. W. Han, A. J. A. Johnson and S. P. Holmes (2016). "DADA2: High-resolution sample inference from Illumina amplicon data." Nature methods **13**(7): 581-583.
Cao, Y. G., S. Bae, J. Villarreal, M. Moy, E. Chun, M. Michaud, J. K. Lang, J. N. Glickman, L. Lobel and W. S. Garrett (2022). "Faecalibaculum rodentium remodels retinoic acid signaling to govern eosinophil-dependent intestinal epithelial homeostasis." Cell Host Microbe **30**(9): 1295-1310.e1298.
Çavdar, G., T. Papich and E. P. Ryan (2019). "Microbiome, Breastfeeding and Public Health Policy in the United States: The Case for Dietary Fiber." Nutr Metab Insights **12**: 1178638819869597.
Chang, W. K., D. VanInsberghe and L. Kelly (2020). "Topological analysis reveals state transitions in human gut and marine bacterial communities." npj Biofilms and Microbiomes **6**(1): 41.

Chen, Y., H. Wang, W. Lu, T. Wu, W. Yuan, J. Zhu, Y. K. Lee, J. Zhao, H. Zhang and W. Chen (2022). "Human gut microbiome aging clocks based on taxonomic and functional signatures through multi-view learning." Gut Microbes **14**(1): 2025016.

Chu, C., T. Li, L. Yu, Y. Li, M. Li, M. Guo, J. Zhao, Q. Zhai, F. Tian and W. Chen (2023). "A Low-Protein, High-Carbohydrate Diet Exerts a Neuroprotective Effect on Mice with 1-Methyl-4-phenyl-1, 2, 3, 6-tetrahydropyridine-Induced Parkinson's Disease by Regulating the Microbiota-Metabolite–Brain Axis and Fibroblast Growth Factor 21." Journal of Agricultural and Food Chemistry.

Claesson, M. J., I. B. Jeffery, S. Conde, S. E. Power, E. M. O'connor, S. Cusack, H. Harris, M. Coakley, B. Lakshminarayanan and O. O'sullivan (2012). "Gut microbiota composition correlates with diet and health in the elderly." Nature **488**(7410): 178-184.

Costea, P. I., F. Hildebrand, M. Arumugam, F. Bäckhed, M. J. Blaser, F. D. Bushman, W. M. De Vos, S. D. Ehrlich, C. M. Fraser and M. Hattori (2018). "Enterotypes in the landscape of gut microbial community composition." Nature microbiology **3**(1): 8-16.

Cox, N. J., R. C. Bowyer, M. Ni Lochlainn, P. M. Wells, H. C. Roberts and C. J. Steves (2021). "The composition of the gut microbiome differs among community dwelling older people with good and poor appetite." Journal of cachexia, sarcopenia and muscle **12**(2): 368-377.

D'Amato, A., L. Di Cesare Mannelli, E. Lucarini, A. L. Man, G. Le Gall, J. J. Branca, C. Ghelardini, A. Amedei, E. Bertelli and M. Regoli (2020). "Faecal microbiota transplant from aged donor mice affects spatial learning and memory via modulating hippocampal synaptic plasticity-and neurotransmission-related proteins in young recipients." Microbiome **8**(1): 1-19.

Dangin, M., C. Guillet, C. Garcia-Rodenas, P. Gachon, C. Bouteloup-Demange, K. Reiffers-Magnani, J. Fauquant, O. Ballèvre and B. Beaufrère (2003). "The rate of protein digestion affects protein gain differently during aging in humans." The Journal of physiology **549**(2): 635-644.

David, L. A., C. F. Maurice, R. N. Carmody, D. B. Gootenberg, J. E. Button, B. E. Wolfe, A. V. Ling, A. S. Devlin, Y. Varma and M. A. Fischbach (2014). "Diet rapidly and reproducibly alters the human gut microbiome." Nature **505**(7484): 559-563.

de la Cuesta-Zuluaga, J., S. T. Kelley, Y. Chen, J. S. Escobar, N. T. Mueller, R. E. Ley, D. McDonald, S. Huang, A. D. Swafford and R. Knight (2019). "Age-and sex-dependent patterns of gut microbial diversity in human adults." Msystems **4**(4): 10.1128/msystems. 00261-00219.

Demontiero, O., C. Vidal and G. Duque (2012). "Aging and bone loss: new insights for the clinician." Therapeutic advances in musculoskeletal disease **4**(2): 61-76.

Dubal, D. B., L. Broestl and K. Worden (2012). "Sex and gonadal hormones in mouse models of Alzheimer's disease: what is relevant to the human condition?" Biology of sex differences **3**: 1-17.

Dutta, S. and P. Sengupta (2016). "Men and mice: relating their ages." Life sciences **152**: 244-248.

Elderman, M., B. Sovran, F. Hugenholtz, K. Graversen, M. Huijskes, E. Houtsma, C. Belzer, M. Boekschoten, P. De Vos and J. Dekker (2017). "The effect of age on the intestinal mucus thickness, microbiota composition and immunity in relation to sex in mice." PloS one **12**(9): e0184274.

Elyahu, Y., I. Hekselman, I. Eizenberg-Magar, O. Berner, I. Strominger, M. Schiller, K. Mittal, A. Nemirovsky, E. Eremenko and A. Vital (2019). "Aging promotes reorganization of the CD4 T cell landscape toward extreme regulatory and effector phenotypes." Science advances **5**(8): eaaw8330.

Faizan, U. and A. S. Rouster (2020). "Nutrition and hydration requirements in children and adults."

Fan, Y. and O. Pedersen (2021). "Gut microbiota in human metabolic health and disease." Nature Reviews Microbiology **19**(1): 55-71.

Ferland, G., B. Tuchweber, A. Perea and I. Yousef (1989). "Effect of aging and dietary restriction on bile acid metabolism in rats." Lipids **24**(10): 842-848.

Fernandes, A. D., J. Macklaim, T. Linn, G. Reid and G. Gloor (2013). "ANOVA-like differential gene expression analysis of single-organism and meta-RNA-seq." PLoS one **8**(7): e67019.

Ferretti, P., E. Pasolli, A. Tett, F. Asnicar, V. Gorfer, S. Fedi, F. Armanini, D. T. Truong, S. Manara and M. Zolfo (2018). "Mother-to-infant microbial transmission from different body sites shapes the developing infant gut microbiome." Cell host & microbe **24**(1): 133-145. e135.

Flint, H. J., K. P. Scott, S. H. Duncan, P. Louis and E. Forano (2012). "Microbial degradation of complex carbohydrates in the gut." Gut microbes **3**(4): 289-306.

Flurkey, K., J. M. Currer and D. Harrison (2007). Mouse models in aging research. The mouse in biomedical research, Elsevier**:** 637-672.

Franceschi, C., P. Garagnani, P. Parini, C. Giuliani and A. Santoro (2018). "Inflammaging: a new immune–metabolic viewpoint for age-related diseases." Nature Reviews Endocrinology **14**(10): 576-590.

Fransen, F., A. A. Van Beek, T. Borghuis, S. E. Aidy, F. Hugenholtz, C. van der Gaast–de Jongh, H. F. Savelkoul, M. I. De Jonge, M. V. Boekschoten and H. Smidt (2017). "Aged gut microbiota contributes to systemical inflammaging after transfer to germ-free mice." Frontiers in immunology **8**: 1385.

Fransen, F., A. A. van Beek, T. Borghuis, B. Meijer, F. Hugenholtz, C. van der Gaast-de Jongh, H. F. Savelkoul, M. I. de Jonge, M. M. Faas and M. V. Boekschoten (2017). "The impact of gut microbiota on gender-specific differences in immunity." Frontiers in immunology **8**: 754.

Fredrickson, A. and G. Stephanopoulos (1981). "Microbial competition." Science **213**(4511): 972-979.

Ghisolfi, J. (2003). "Dietary fibre and prebiotics in infant formulas." Proc Nutr Soc **62**(1): 183-185.

Ghosh, T. S., F. Shanahan and P. W. O'Toole (2022). "The gut microbiome as a modulator of healthy ageing." Nature Reviews Gastroenterology & Hepatology **19**(9): 565-584.

Ghoul, M. and S. Mitri (2016). "The ecology and evolution of microbial competition." Trends in microbiology **24**(10): 833-845.

Glöckner, F. O., P. Yilmaz, C. Quast, J. Gerken, A. Beccati, A. Ciuprina, G. Bruns, P. Yarza, J. Peplies and R. Westram (2017). "25 years of serving the community with ribosomal RNA gene reference databases and tools." Journal of biotechnology **261**: 169-176.

Gomez de Agüero, M., S. C. Ganal-Vonarburg, T. Fuhrer, S. Rupp, Y. Uchimura, H. Li, A. Steinert, M. Heikenwalder, S. Hapfelmeier and U. Sauer (2016). "The maternal microbiota drives early postnatal innate immune development." Science **351**(6279): 1296-1302.

Guittar, J., A. Shade and E. Litchman (2019). "Trait-based community assembly and succession of the infant gut microbiome." Nature communications **10**(1): 512.

Guo, J., C. Ren, X. Han, W. Huang, Y. You and J. Zhan (2021). "Role of IgA in the early-life establishment of the gut microbiota and immunity: Implications for constructing a healthy start." Gut Microbes **13**(1): 1908101.

Hapfelmeier, S., M. A. Lawson, E. Slack, J. K. Kirundi, M. Stoel, M. Heikenwalder, J. Cahenzli, Y. Velykoredko, M. L. Balmer and K. Endt (2010). "Reversible microbial colonization of germ-free mice reveals the dynamics of IgA immune responses." Science **328**(5986): 1705-1709.

Health, A. I. o. and Welfare (2021). Older Australians. Canberra, AIHW.
Health, A. I. o. and Welfare (2023). Overweight and obesity. Canberra, AIHW.
Hildebrand, F., T. L. A. Nguyen, B. Brinkman, R. G. Yunta, B. Cauwe, P. Vandenabeele, A. Liston and J. Raes (2013). "Inflammation-associated enterotypes, host genotype, cage and inter-individual effects drive gut microbiota variation in common laboratory mice." Genome biology **14**: 1-15.
Hill, M. O. and H. G. Gauch Jr (1980). "Detrended correspondence analysis: an improved ordination technique." Vegetatio **42**(1-3): 47-58.
Holloszy, J. O. (2000). The biology of aging. Mayo Clinic Proceedings, Elsevier.
Holmes, A. J., Y. V. Chew, F. Colakoglu, J. B. Cliff, E. Klaassens, M. N. Read, S. M. Solon-Biet, A. C. McMahon, V. C. Cogger, K. Ruohonen, D. Raubenheimer, D. G. Le Couteur and S. J. Simpson (2017). "Diet-Microbiome Interactions in Health Are Controlled by Intestinal Nitrogen Source Constraints." Cell Metab **25**(1): 140-151.
Hou, Q., J. Huang, L. Zhao, X. Pan, C. Liao, Q. Jiang, J. Lei, F. Guo, J. Cui and Y. Guo (2023). "Dietary genistein increases microbiota-derived short chain fatty acid levels, modulates homeostasis of the aging gut, and extends healthspan and lifespan." Pharmacological Research **188**: 106676.
Hrncir, T., R. Stepankova, H. Kozakova, T. Hudcovic and H. Tlaskalova-Hogenova (2008). "Gut microbiota and lipopolysaccharide content of the diet influence development of regulatory T cells: studies in germ-free mice." BMC Immunology **9**(1): 65.
Huang, X.-Z., L.-B. Zhu, Z.-R. Li and J. Lin (2013). "Bacterial colonization and intestinal mucosal barrier development." World journal of clinical pediatrics **2**(4): 46.
Issa, J.-P. (2003). "Age-related epigenetic changes and the immune system." Clinical Immunology **109**(1): 103-108.
Janeway, C., P. Travers, M. Walport and M. Shlomchik (2001). Immunobiology: the immune system in health and disease, Garland Pub. New York.
Janiak, M. C., M. J. Montague, C. I. Villamil, M. K. Stock, A. E. Trujillo, A. N. DePasquale, J. D. Orkin, S. E. Bauman Surratt, O. Gonzalez and M. L. Platt (2021). "Age and sex-associated variation in the multi-site microbiome of an entire social group of free-ranging rhesus macaques." Microbiome **9**(1): 1-17.
Jin, J., X. Yang, H. Gong and X. Li (2023). "Time-and Gender-Dependent Alterations in Mice during the Aging Process." International Journal of Molecular Sciences **24**(16): 12790.
Johnson, A. J., P. Vangay, G. A. Al-Ghalith, B. M. Hillmann, T. L. Ward, R. R. Shields-Cutler, A. D. Kim, A. K. Shmagel, A. N. Syed, S. Personalized Microbiome Class, J. Walter,

R. Menon, K. Koecher and D. Knights (2019). "Daily Sampling Reveals Personalized Diet-Microbiome Associations in Humans." Cell Host Microbe **25**(6): 789-802 e785.
Kaklamani, V. G., A. Linos, E. Kaklamani, I. Markaki, Y. Koumantaki and C. S. Mantzoros (1999). "Dietary fat and carbohydrates are independently associated with circulating insulin-like growth factor 1 and insulin-like growth factor–binding protein 3 concentrations in healthy adults." Journal of Clinical Oncology **17**(10): 3291-3298.
Kanehisa, M. and S. Goto (2000). "KEGG: kyoto encyclopedia of genes and genomes." Nucleic acids research **28**(1): 27-30.
Ke, S., S. J. Mitchell, M. R. MacArthur, A. E. Kane, D. A. Sinclair, E. M. Venable, K. S. Chadaideh, R. N. Carmody, F. Grodstein and J. R. Mitchell (2021). "Gut microbiota predicts healthy late-life aging in male mice." Nutrients **13**(09): 3290.
Kim, H.-J., C. M. Moon, J. L. Kang and E.-M. Park (2021). "Aging effects on the diurnal patterns of gut microbial composition in male and female mice." The Korean Journal of Physiology & Pharmacology: Official Journal of the Korean Physiological Society and the Korean Society of Pharmacology **25**(6): 575-583.
Kirkwood, T. B. (1977). "Evolution of ageing." Nature **270**(5635): 301-304.
Kirkwood, T. B. and R. Holliday (1979). "The evolution of ageing and longevity." Proceedings of the Royal Society of London. Series B. Biological Sciences **205**(1161): 531-546.
Knights, D., T. L. Ward, C. E. McKinlay, H. Miller, A. Gonzalez, D. McDonald and R. Knight (2014). "Rethinking “enterotypes”." Cell host & microbe **16**(4): 433-437.
Koay, Y. C., Y.-C. Chen, J. A. Wali, A. W. Luk, M. Li, H. Doma, R. Reimark, M. T. Zaldivia, H. T. Habtom and A. E. Franks (2021). "Plasma levels of trimethylamine-N-oxide can be increased with ‘healthy’and ‘unhealthy’diets and do not correlate with the extent of atherosclerosis but with plaque instability." Cardiovascular research **117**(2): 435-449.
Koay, Y. C., J. A. Wali, A. W. Luk, L. Macia, V. C. Cogger, T. J. Pulpitel, D. Wahl, S. M. Solon-Biet, A. Holmes and S. J. Simpson (2019). "Ingestion of resistant starch by mice markedly increases microbiome-derived metabolites." The FASEB Journal **33**(7): 8033-8042.
Koenig, J. E., A. Spor, N. Scalfone, A. D. Fricker, J. Stombaugh, R. Knight, L. T. Angenent and R. E. Ley (2011). "Succession of microbial consortia in the developing infant gut microbiome." Proceedings of the National Academy of Sciences **108**(supplement_1): 4578-4585.
Kundu, P., H. U. Lee, I. Garcia-Perez, E. X. Y. Tay, H. Kim, L. E. Faylon, K. A. Martin, R. Purbojati, D. I. Drautz-Moses and S. Ghosh (2019). "Neurogenesis and prolongevity

signaling in young germ-free mice transplanted with the gut microbiota of old mice." Science translational medicine **11**(518): eaau4760.
Lahti, L. and S. Shetty (2018). "Introduction to the microbiome R package." Preprint at https://microbiome. github. io/tutorials.
Lamberts, S. W., A. W. Van den Beld and A.-J. Van Der Lely (1997). "The endocrinology of aging." Science **278**(5337): 419-424.
Langille, M. G., C. J. Meehan, J. E. Koenig, A. S. Dhanani, R. A. Rose, S. E. Howlett and R. G. Beiko (2014). "Microbial shifts in the aging mouse gut." Microbiome **2**: 1-12.
Lee, G., H. Lee, J. Hong, S. H. Lee and B. H. Jung (2016). "Quantitative profiling of bile acids in rat bile using ultrahigh-performance liquid chromatography–orbitrap mass spectrometry: Alteration of the bile acid composition with aging." Journal of Chromatography B **1031**: 37-49.
Legendre, P. and M. J. Anderson (1999). "Distance-based redundancy analysis: testing multispecies responses in multifactorial ecological experiments." Ecological monographs **69**(1): 1-24.
Legendre, P. and E. D. Gallagher (2001). "Ecologically meaningful transformations for ordination of species data." Oecologia **129**: 271-280.
Lehallier, B., D. Gate, N. Schaum, T. Nanasi, S. E. Lee, H. Yousef, P. Moran Losada, D. Berdnik, A. Keller and J. Verghese (2019). "Undulating changes in human plasma proteome profiles across the lifespan." Nature medicine **25**(12): 1843-1850.
Leite, G., M. Pimentel, G. M. Barlow, C. Chang, A. Hosseini, J. Wang, G. Parodi, R. Sedighi, A. Rezaie and R. Mathur (2021). "Age and the aging process significantly alter the small bowel microbiome." Cell Reports **36**(13).
Leiter, E. H., F. Premdas, D. E. Harrison and L. G. Lipson (1988). "Aging and glucose homeostasis in C57BL/6J male mice." The FASEB journal **2**(12): 2807-2811.
Lesker, T. R., A. C. Durairaj, E. J. Gálvez, I. Lagkouvardos, J. F. Baines, T. Clavel, A. Sczyrba, A. C. McHardy and T. Strowig (2020). "An integrated metagenome catalog reveals new insights into the murine gut microbiome." Cell Reports **30**(9): 2909-2922. e2906.
Ley, R. E., F. Bäckhed, P. Turnbaugh, C. A. Lozupone, R. D. Knight and J. I. Gordon (2005). "Obesity alters gut microbial ecology." Proceedings of the national academy of sciences **102**(31): 11070-11075.
Li, W., J. E. Cerise, Y. Yang and H. Han (2017). "Application of t-SNE to human genetic data." Journal of bioinformatics and computational biology **15**(04): 1750017.

Liguori, I., G. Russo, F. Curcio, G. Bulli, L. Aran, D. Della-Morte, G. Gargiulo, G. Testa, F. Cacciatore and D. Bonaduce (2018). "Oxidative stress, aging, and diseases." Clinical interventions in aging: 757-772.

Ma, J., Y. Hong, N. Zheng, G. Xie, Y. Lyu, Y. Gu, C. Xi, L. Chen, G. Wu and Y. Li (2020). "Gut microbiota remodeling reverses aging-associated inflammation and dysregulation of systemic bile acid homeostasis in mice sex-specifically." Gut Microbes **11**(5): 1450-1474.

Magne, F., M. Gotteland, L. Gauthier, A. Zazueta, S. Pesoa, P. Navarrete and R. Balamurugan (2020). "The firmicutes/bacteroidetes ratio: a relevant marker of gut dysbiosis in obese patients?" Nutrients **12**(5): 1474.

Maric, I., J.-P. Krieger, P. van der Velden, S. Börchers, M. Asker, M. Vujicic, I. Wernstedt Asterholm and K. P. Skibicka (2022). "Sex and species differences in the development of diet-induced obesity and metabolic disturbances in rodents." Frontiers in nutrition **9**: 828522.

Marmentini, C., G. M. Soares, G. A. Bronczek, S. Piovan, C. E. Mareze-Costa, E. M. Carneiro, A. C. Boschero and M. A. Kurauti (2021). "Aging reduces insulin clearance in mice." Frontiers in endocrinology **12**: 679492.

McClanahan, F., J. C. Riches, S. Miller, W. P. Day, E. Kotsiou, D. Neuberg, C. M. Croce, M. Capasso and J. G. Gribben (2015). "Mechanisms of PD-L1/PD-1–mediated CD8 T-cell dysfunction in the context of aging-related immune defects in the Eμ-TCL1 CLL mouse model." Blood, The Journal of the American Society of Hematology **126**(2): 212-221.

McMurdie, P. J. and S. Holmes (2013). "phyloseq: an R package for reproducible interactive analysis and graphics of microbiome census data." PloS one **8**(4): e61217.

McNeil, N. (1984). "The contribution of the large intestine to energy supplies in man." The American journal of clinical nutrition **39**(2): 338-342.

Milan, A., R. D'Souza, S. Pundir, C. Pileggi, M. Barnett, J. Markworth, D. Cameron-Smith and C. Mitchell (2015). "Older adults have delayed amino acid absorption after a high protein mixed breakfast meal." The journal of nutrition, health & aging **19**(8): 839-845.

Mogilenko, D. A., O. Shpynov, P. S. Andhey, L. Arthur, A. Swain, E. Esaulova, S. Brioschi, I. Shchukina, M. Kerndl and M. Bambouskova (2021). "Comprehensive profiling of an aging immune system reveals clonal GZMK+ CD8+ T cells as conserved hallmark of inflammaging." Immunity **54**(1): 99-115. e112.

Moorefield, E. C., S. F. Andres, R. E. Blue, L. Van Landeghem, A. T. Mah, M. A. Santoro and S. Ding (2017). "Aging effects on intestinal homeostasis associated with expansion and dysfunction of intestinal epithelial stem cells." Aging (Albany NY) **9**(8): 1898.

Morley, J. E. (2001). "Decreased food intake with aging." The Journals of Gerontology Series A: Biological Sciences and Medical Sciences **56**(suppl_2): 81-88.
Nakanishi, Y., R. Nozu, M. Ueno, K. Hioki, C. Ishii, S. Murakami, K. Suzuki, Y. Ka, T. Ogura and A. Ito (2020). "Longitudinal analyses reveal that aging-related alterations in the intestinal environment lead to gut dysbiosis with the potential to induce obesity."
Niess, J. H., F. Leithäuser, G. Adler and J. r. Reimann (2008). "Commensal gut flora drives the expansion of proinflammatory CD4 T cells in the colonic lamina propria under normal and inflammatory conditions." The Journal of Immunology **180**(1): 559-568.
Ochman, H., S. Elwyn and N. A. Moran (1999). "Calibrating bacterial evolution." Proceedings of the National Academy of Sciences **96**(22): 12638-12643.
Oh, Y. S., E.-H. Seo, Y.-S. Lee, S. C. Cho, H. S. Jung, S. C. Park and H.-S. Jun (2016). "Increase of calcium sensing receptor expression is related to compensatory insulin secretion during aging in mice." PloS one **11**(7): e0159689.
Ohwaki, M., N. Yasutake, H. Yasui and R. Ogura (1977). "A comparative study on the humoral immune responses in germ-free and conventional mice." Immunology **32**(1): 43-48.
Oksanen, J., F. G. Blanchet, M. Friendly, R. Kindt, P. Legendre, D. McGlinn, P. R. Minchin, R. O'hara, G. L. Simpson and P. Solymos (2019). "Package 'vegan'." Community ecology package, version **2**(9).
Oksanen, J. and P. R. Minchin (1997). "Instability of ordination results under changes in input data order: explanations and remedies." Journal of Vegetation Science **8**(3): 447-454.
Onorati, A., A. P. Havas, B. Lin, J. Rajagopal, P. Sen, P. D. Adams and Z. Dou (2022). "Upregulation of PD-L1 in Senescence and Aging." Molecular and Cellular Biology **42**(10): e00171-00122.
Östman, S., C. Rask, A. E. Wold, S. Hultkrantz and E. Telemo (2006). "Impaired regulatory T cell function in germ-free mice." European journal of immunology **36**(9): 2336-2346.
Ostrem Loss, E., J. Thompson, P. L. K. Cheung, Y. Qian and O. S. Venturelli (2023). "Carbohydrate complexity limits microbial growth and reduces the sensitivity of human gut communities to perturbations." Nature ecology & evolution **7**(1): 127-142.
Otsuka, R., Y. Kato, Y. Nishita, C. Tange, M. Tomida, M. Nakamoto, T. Imai, F. Ando and H. Shimokata (2016). "Age-related changes in energy intake and weight in community-dwelling middle-aged and elderly Japanese." The journal of nutrition, health & aging **20**: 383-390.

Pang, S., X. Chen, Z. Lu, L. Meng, Y. Huang, X. Yu, L. Huang, P. Ye, X. Chen, J. Liang, T. Peng, W. Luo and S. Wang (2023). "Longevity of centenarians is reflected by the gut microbiome with youth-associated signatures." Nature Aging **3**(4): 436-449.
Papanicolas, L. E., J. M. Choo, Y. Wang, L. E. Leong, S. P. Costello, D. L. Gordon, S. L. Wesselingh and G. B. Rogers (2019). "Bacterial viability in faecal transplants: which bacteria survive?" EBioMedicine **41**: 509-516.
Paradis, E., J. Claude and K. Strimmer (2004). "APE: analyses of phylogenetics and evolution in R language." Bioinformatics **20**(2): 289-290.
Parker, A., S. Romano, R. Ansorge, A. Aboelnour, G. Le Gall, G. M. Savva, M. G. Pontifex, A. Telatin, D. Baker and E. Jones (2022). "Fecal microbiota transfer between young and aged mice reverses hallmarks of the aging gut, eye, and brain." Microbiome **10**(1): 1-25.
Pataky, M. W., W. F. Young and K. S. Nair (2021). Hormonal and metabolic changes of aging and the influence of lifestyle modifications. Mayo Clinic Proceedings, Elsevier.
Platzer, A. (2013). "Visualization of SNPs with t-SNE." PloS one **8**(2): e56883.
Prattichizzo, F., V. De Nigris, R. Spiga, E. Mancuso, L. La Sala, R. Antonicelli, R. Testa, A. D. Procopio, F. Olivieri and A. Ceriello (2018). "Inflammageing and metaflammation: the yin and yang of type 2 diabetes." Ageing research reviews **41**: 1-17.
Priyadarshini, M., K. U. Kotlo, P. K. Dudeja and B. T. Layden (2018). "Role of short chain fatty acid receptors in intestinal physiology and pathophysiology." Comprehensive Physiology **8**(3): 1091.
Qiao, C.-M., Y. Zhou, W. Quan, X.-Y. Ma, L.-P. Zhao, Y. Shi, H. Hong, J. Wu, G.-Y. Niu and Y.-N. Chen (2023). "Fecal Microbiota Transplantation from Aged Mice Render Recipient Mice Resistant to MPTP-Induced Nigrostriatal Degeneration Via a Neurogenesis-Dependent but Inflammation-Independent Manner." Neurotherapeutics **20**(5): 1405-1426.
Qiu, Y., J. Yu, X. Ji, H. Yu, M. Xue, F. Zhang, Y. Li and Z. Bao (2022). "Ileal FXR-FGF15/19 signaling activation improves skeletal muscle loss in aged mice." Mechanisms of Ageing and Development **202**: 111630.
R Core Team, R. (2013). "R: A language and environment for statistical computing."
Rampelli, S., M. Candela, S. Turroni, E. Biagi, S. Collino, C. Franceschi, P. W. O'Toole and P. Brigidi (2013). "Functional metagenomic profiling of intestinal microbiome in extreme ageing." Aging **5**(12): 902-912.
Rasheed, A. and K. J. Rayner (2021). "Macrophage responses to environmental stimuli during homeostasis and disease." Endocrine Reviews **42**(4): 407-435.

Raubenheimer, D. and S. J. Simpson (2016). "Nutritional Ecology and Human Health." Annu Rev Nutr **36**: 603-626.
Raubenheimer, D. and S. J. Simpson (2016). "Nutritional ecology and human health." Annual review of nutrition **36**: 603-626.
Rautava, S. and E. Isolauri (2002). "The development of gut immune responses and gut microbiota: effects of probiotics in prevention and treatment of allergic disease." Current issues in intestinal microbiology **3**(1): 15-22.
Ridaura, V. K., J. J. Faith, F. E. Rey, J. Cheng, A. E. Duncan, A. L. Kau, N. W. Griffin, V. Lombard, B. Henrissat and J. R. Bain (2013). "Gut microbiota from twins discordant for obesity modulate metabolism in mice." Science **341**(6150): 1241214.
Rio-Aige, K., I. Azagra-Boronat, M. Castell, M. Selma-Royo, M. C. Collado, M. J. Rodríguez-Lagunas and F. J. Pérez-Cano (2021). "The breast milk immunoglobulinome." Nutrients **13**(6): 1810.
Risely, A., K. Wilhelm, T. Clutton-Brock, M. B. Manser and S. Sommer (2021). "Diurnal oscillations in gut bacterial load and composition eclipse seasonal and lifetime dynamics in wild meerkats." Nature communications **12**(1): 6017.
Rocha, D., A. Caldas, L. Oliveira, J. Bressan and H. Hermsdorff (2016). "Saturated fatty acids trigger TLR4-mediated inflammatory response." Atherosclerosis **244**: 211-215.
Rossiello, F., D. Jurk, J. F. Passos and F. d'Adda di Fagagna (2022). "Telomere dysfunction in ageing and age-related diseases." Nature cell biology **24**(2): 135-147.
Roswall, J., L. M. Olsson, P. Kovatcheva-Datchary, S. Nilsson, V. Tremaroli, M.-C. Simon, P. Kiilerich, R. Akrami, M. Krämer and M. Uhlén (2021). "Developmental trajectory of the healthy human gut microbiota during the first 5 years of life." Cell host & microbe **29**(5): 765-776. e763.
Roth, G. S. (1979). "Hormone action during aging: alterations and mechanisms." Mechanisms of Ageing and Development **9**(5-6): 497-514.
Rowland, I., G. Gibson, A. Heinken, K. Scott, J. Swann, I. Thiele and K. Tuohy (2018). "Gut microbiota functions: metabolism of nutrients and other food components." European Journal of Nutrition **57**(1): 1-24.
Saito, T., H. Nishikawa, H. Wada, Y. Nagano, D. Sugiyama, K. Atarashi, Y. Maeda, M. Hamaguchi, N. Ohkura and E. Sato (2016). "Two FOXP3+ CD4+ T cell subpopulations distinctly control the prognosis of colorectal cancers." Nature medicine **22**(6): 679-684.
Sayin, S. I., A. Wahlström, J. Felin, S. Jäntti, H.-U. Marschall, K. Bamberg, B. Angelin, T. Hyötyläinen, M. Orešič and F. Bäckhed (2013). "Gut microbiota regulates bile acid

metabolism by reducing the levels of tauro-beta-muricholic acid, a naturally occurring FXR antagonist." Cell metabolism **17**(2): 225-235.
Schirmer, M., S. P. Smeekens, H. Vlamakis, M. Jaeger, M. Oosting, E. A. Franzosa, R. Ter Horst, T. Jansen, L. Jacobs and M. J. Bonder (2016). "Linking the human gut microbiome to inflammatory cytokine production capacity." Cell **167**(4): 1125-1136. e1128.
Schliep, K. P. (2011). "phangorn: phylogenetic analysis in R." Bioinformatics **27**(4): 592-593.
Schmitt, V., L. Rink and P. Uciechowski (2013). "The Th17/Treg balance is disturbed during aging." Experimental gerontology **48**(12): 1379-1386.
Shafquat, A., R. Joice, S. L. Simmons and C. Huttenhower (2014). "Functional and phylogenetic assembly of microbial communities in the human microbiome." Trends in microbiology **22**(5): 261-266.
Simpson, S. and D. Raubenheimer (1997). "Geometric analysis of macronutrient selection in the rat." Appetite **28**(3): 201-213.
Simpson, S. J. and D. Raubenheimer (2005). "Obesity: the protein leverage hypothesis." obesity reviews **6**(2): 133-142.
Solon-Biet, S. M., A. C. McMahon, J. W. O. Ballard, K. Ruohonen, L. E. Wu, V. C. Cogger, A. Warren, X. Huang, N. Pichaud and R. G. Melvin (2014). "The ratio of macronutrients, not caloric intake, dictates cardiometabolic health, aging, and longevity in ad libitum-fed mice." Cell metabolism **19**(3): 418-430.
Sonnenburg, E. D., H. Zheng, P. Joglekar, S. K. Higginbottom, S. J. Firbank, D. N. Bolam and J. L. Sonnenburg (2010). "Specificity of polysaccharide use in intestinal bacteroides species determines diet-induced microbiota alterations." Cell **141**(7): 1241-1252.
Sovran, B., F. Hugenholtz, M. Elderman, A. A. Van Beek, K. Graversen, M. Huijskes, M. V. Boekschoten, H. F. Savelkoul, P. De Vos and J. Dekker (2019). "Age-associated impairment of the mucus barrier function is associated with profound changes in microbiota and immunity." Scientific reports **9**(1): 1-13.
Starke, S., D. M. Harris, J. Zimmermann, S. Schuchardt, M. Oumari, D. Frank, C. Bang, P. Rosenstiel, S. Schreiber and N. Frey (2023). "Amino acid auxotrophies in human gut bacteria are linked to higher microbiome diversity and long-term stability." The ISME Journal: 1-11.
Statistics, A. B. o. (2017). Patient Experiences in Australia. A. B. o. Statistics. Canberra, ABS.
Statistics, A. B. o. (2018). Disability, Ageing and Carers, Australia: Summary of Findings A. B. o. Statistics, ABS.

Suzuki, K., B. Meek, Y. Doi, M. Muramatsu, T. Chiba, T. Honjo and S. Fagarasan (2004). "Aberrant expansion of segmented filamentous bacteria in IgA-deficient gut." Proceedings of the National Academy of Sciences **101**(7): 1981-1986.

Templeman, N. M., S. Flibotte, J. H. Chik, S. Sinha, G. E. Lim, L. J. Foster, C. Nislow and J. D. Johnson (2017). "Reduced circulating insulin enhances insulin sensitivity in old mice and extends lifespan." Cell reports **20**(2): 451-463.

Thaiss, C. A., S. Itav, D. Rothschild, M. T. Meijer, M. Levy, C. Moresi, L. Dohnalová, S. Braverman, S. Rozin and S. Malitsky (2016). "Persistent microbiome alterations modulate the rate of post-dieting weight regain." Nature **540**(7634): 544-551.

Thaiss, C. A., D. Zeevi, M. Levy, G. Zilberman-Schapira, J. Suez, A. C. Tengeler, L. Abramson, M. N. Katz, T. Korem and N. Zmora (2014). "Transkingdom control of microbiota diurnal oscillations promotes metabolic homeostasis." Cell **159**(3): 514-529.

Tharanathan, M. and R. Tharanathan (2001). "Resistant starch in wheat-based products: isolation and characterisation." Journal of Cereal Science **34**(1): 73-84.

Tomassen, M. M., C. Govers, A. P. Vos and N. J. de Wit (2023). "Dietary fat induced chylomicron-mediated LPS translocation in a bicameral Caco-2cell model." Lipids in Health and Disease **22**(1): 4.

Tremblay, S., N. M. L. Côté, G. Grenier, G. Duclos-Lasnier, L.-C. Fortier, S. Ilangumaran and A. Menendez (2017). "Ileal antimicrobial peptide expression is dysregulated in old age." Immunity & Ageing **14**(1): 1-5.

Turnbaugh, P. J., R. E. Ley, M. Hamady, C. M. Fraser-Liggett, R. Knight and J. I. Gordon (2007). "The human microbiome project." Nature **449**(7164): 804-810.

Turnbaugh, P. J., R. E. Ley, M. A. Mahowald, V. Magrini, E. R. Mardis and J. I. Gordon (2006). "An obesity-associated gut microbiome with increased capacity for energy harvest." nature **444**(7122): 1027-1031.

Uitto, J. (1986). "Connective tissue biochemistry of the aging dermis: age-related alterations in collagen and elastin." Dermatologic clinics **4**(3): 433-446.

van Muijlwijk, G. H., G. van Mierlo, P. W. Jansen, M. Vermeulen, N. M. Bleumink-Pluym, N. W. Palm, J. P. van Putten and M. R. de Zoete (2021). "Identification of Allobaculum mucolyticum as a novel human intestinal mucin degrader." Gut Microbes **13**(1): 1966278.

Vatanen, T., K. S. Jabbar, T. Ruohtula, J. Honkanen, J. Avila-Pacheco, H. Siljander, M. Stražar, S. Oikarinen, H. Hyöty and J. Ilonen (2022). "Mobile genetic elements from the maternal microbiome shape infant gut microbial assembly and metabolism." Cell **185**(26): 4921-4936. e4915.

Vera-Ponce de Leon, A., M. G. Schneider, B. C. Jahnes, V. Sadowski, L. A. Camuy-Vélez, J. Duan and Z. L. Sabree (2022). "Genetic drift and host-adaptive features likely underlie the cladogenesis of insect-associated Lachnospiraceae." Genome Biology and Evolution **14**(6): evac086.

Wali, J. A., A. J. Milner, A. W. Luk, T. J. Pulpitel, T. Dodgson, H. J. Facey, D. Wahl, M. A. Kebede, A. M. Senior and M. A. Sullivan (2021). "Impact of dietary carbohydrate type and protein–carbohydrate interaction on metabolic health." Nature Metabolism **3**(6): 810-828.

Wang, J., M. Linnenbrink, S. Künzel, R. Fernandes, M.-J. Nadeau, P. Rosenstiel and J. F. Baines (2014). "Dietary history contributes to enterotype-like clustering and functional metagenomic content in the intestinal microbiome of wild mice." Proceedings of the National Academy of Sciences **111**(26): E2703-E2710.

Wang, J., J. Qie, D. Zhu, X. Zhang, Q. Zhang, Y. Xu, Y. Wang, K. Mi, Y. Pei and Y. Liu (2022). "The landscape in the gut microbiome of long-lived families reveals new insights on longevity and aging–relevant neural and immune function." Gut Microbes **14**(1): 2107288.

Wang, Y., J. Tang, Q. Lv, Y. Tan, X. Dong, H. Liu, N. Zhao, Z. He, Y. Kou and Y. Tan (2022). "Establishment and resilience of transplanted gut microbiota in aged mice." Iscience **25**(1): 103654.

Wang, Y., Z. Zhang, B. Liu, C. Zhang, J. Zhao, X. Li and L. Chen (2022). "A study on the method and effect of the construction of a humanized mouse model of fecal microbiota transplantation." Frontiers in Microbiology **13**: 1031758.

Wickham, H., W. Chang and M. H. Wickham (2016). "Package 'ggplot2'." Create elegant data visualisations using the grammar of graphics. Version **2**(1): 1-189.

Wilmanski, T., C. Diener, N. Rappaport, S. Patwardhan, J. Wiedrick, J. Lapidus, J. C. Earls, A. Zimmer, G. Glusman and M. Robinson (2021). "Gut microbiome pattern reflects healthy ageing and predicts survival in humans." Nature metabolism **3**(2): 274-286.

Wood, S. N., N. Pya and B. Säfken (2016). "Smoothing parameter and model selection for general smooth models." Journal of the American Statistical Association **111**(516): 1548-1563.

Wu, C.-S., S. D. V. Muthyala, C. Klemashevich, A. U. Ufondu, R. Menon, Z. Chen, S. Devaraj, A. Jayaraman and Y. Sun (2021). "Age-dependent remodeling of gut microbiome and host serum metabolome in mice." Aging (albany NY) **13**(5): 6330.

Wu, G. D., J. Chen, C. Hoffmann, K. Bittinger, Y.-Y. Chen, S. A. Keilbaugh, M. Bewtra, D. Knights, W. A. Walters and R. Knight (2011). "Linking long-term dietary patterns with gut microbial enterotypes." Science **334**(6052): 105-108.

Wu, G. D., J. Chen, C. Hoffmann, K. Bittinger, Y. Y. Chen, S. A. Keilbaugh, M. Bewtra, D. Knights, W. A. Walters, R. Knight, R. Sinha, E. Gilroy, K. Gupta, R. Baldassano, L. Nessel, H. Li, F. D. Bushman and J. D. Lewis (2011). "Linking long-term dietary patterns with gut microbial enterotypes." Science **334**(6052): 105-108.

Yamamura, K. (1999). "Transformation using (x+ 0.5) to stabilize the variance of populations." Population Ecology **41**(3): 229-234.

Yang, C., J. Mai, X. Cao, A. Burberry, F. Cominelli and L. Zhang (2023). "ggpicrust2: an R package for PICRUSt2 predicted functional profile analysis and visualization." Bioinformatics **39**(8): btad470.

Yatsunenko, T., F. E. Rey, M. J. Manary, I. Trehan, M. G. Dominguez-Bello, M. Contreras, M. Magris, G. Hidalgo, R. N. Baldassano and A. P. Anokhin (2012). "Human gut microbiome viewed across age and geography." nature **486**(7402): 222-227.

You, X., U. C. Dadwal, M. E. Lenburg, M. A. Kacena and J. F. Charles (2022). "Murine gut microbiome meta-analysis reveals alterations in carbohydrate metabolism in response to aging." Msystems **7**(2): e01248-01221.

Zagato, E., C. Pozzi, A. Bertocchi, T. Schioppa, F. Saccheri, S. Guglietta, B. Fosso, L. Melocchi, G. Nizzoli and J. Troisi (2020). "Endogenous murine microbiota member Faecalibaculum rodentium and its human homologue protect from intestinal tumour growth." Nature microbiology **5**(3): 511-524.

Zeng, X., X. Xing, M. Gupta, F. C. Keber, J. G. Lopez, Y.-C. J. Lee, A. Roichman, L. Wang, M. D. Neinast and M. S. Donia (2022). "Gut bacterial nutrient preferences quantified in vivo." Cell **185**(18): 3441-3456. e3419.

Zhang, X., H. Zhong, Y. Li, Z. Shi, H. Ren, Z. Zhang, X. Zhou, S. Tang, X. Han and Y. Lin (2021). "Sex-and age-related trajectories of the adult human gut microbiota shared across populations of different ethnicities." Nature Aging **1**(1): 87-100.

Zhu, K., A. Devine, A. Suleska, C. Tan, C. Toh, D. Kerr and R. Prince (2010). "Adequacy and change in nutrient and food intakes with aging in a seven-year cohort study in elderly women." The journal of nutrition, health & aging **14**: 723-729.